

Transfer of Tritium in the Environment after Accidental Releases from Nuclear Facilities

*Report of Working Group 7
Tritium Accidents
of EMRAS II Topical Heading
Approaches for Assessing
Emergency Situations*

*Environmental Modelling for
Radiation Safety (EMRAS II) Programme*



IAEA

International Atomic Energy Agency

IAEA SAFETY STANDARDS AND RELATED PUBLICATIONS

IAEA SAFETY STANDARDS

Under the terms of Article III of its Statute, the IAEA is authorized to establish or adopt standards of safety for protection of health and minimization of danger to life and property, and to provide for the application of these standards.

The publications by means of which the IAEA establishes standards are issued in the **IAEA Safety Standards Series**. This series covers nuclear safety, radiation safety, transport safety and waste safety. The publication categories in the series are **Safety Fundamentals**, **Safety Requirements** and **Safety Guides**.

Information on the IAEA's safety standards programme is available at the IAEA Internet site

<http://www-ns.iaea.org/standards/>

The site provides the texts in English of published and draft safety standards. The texts of safety standards issued in Arabic, Chinese, French, Russian and Spanish, the IAEA Safety Glossary and a status report for safety standards under development are also available. For further information, please contact the IAEA at PO Box 100, 1400 Vienna, Austria.

All users of IAEA safety standards are invited to inform the IAEA of experience in their use (e.g. as a basis for national regulations, for safety reviews and for training courses) for the purpose of ensuring that they continue to meet users' needs. Information may be provided via the IAEA Internet site or by post, as above, or by email to Official.Mail@iaea.org.

RELATED PUBLICATIONS

The IAEA provides for the application of the standards and, under the terms of Articles III and VIII.C of its Statute, makes available and fosters the exchange of information relating to peaceful nuclear activities and serves as an intermediary among its Member States for this purpose.

Reports on safety and protection in nuclear activities are issued as **Safety Reports**, which provide practical examples and detailed methods that can be used in support of the safety standards.

Other safety related IAEA publications are issued as **Radiological Assessment Reports**, the International Nuclear Safety Group's **INSAG Reports**, **Technical Reports** and **TECDOCs**. The IAEA also issues reports on radiological accidents, training manuals and practical manuals, and other special safety related publications.

Security related publications are issued in the **IAEA Nuclear Security Series**.

The **IAEA Nuclear Energy Series** consists of reports designed to encourage and assist research on, and development and practical application of, nuclear energy for peaceful uses. The information is presented in guides, reports on the status of technology and advances, and best practices for peaceful uses of nuclear energy. The series complements the IAEA's safety standards, and provides detailed guidance, experience, good practices and examples in the areas of nuclear power, the nuclear fuel cycle, radioactive waste management and decommissioning.

TRANSFER OF TRITIUM IN THE
ENVIRONMENT AFTER ACCIDENTAL
RELEASES FROM NUCLEAR FACILITIES

The following States are Members of the International Atomic Energy Agency:

AFGHANISTAN	GHANA	PAKISTAN
ALBANIA	GREECE	PALAU
ALGERIA	GUATEMALA	PANAMA
ANGOLA	HAITI	PAPUA NEW GUINEA
ARGENTINA	HOLY SEE	PARAGUAY
ARMENIA	HONDURAS	PERU
AUSTRALIA	HUNGARY	PHILIPPINES
AUSTRIA	ICELAND	POLAND
AZERBAIJAN	INDIA	PORTUGAL
BAHAMAS	INDONESIA	QATAR
BAHRAIN	IRAN, ISLAMIC REPUBLIC OF	REPUBLIC OF MOLDOVA
BANGLADESH	IRAQ	ROMANIA
BELARUS	IRELAND	RUSSIAN FEDERATION
BELGIUM	ISRAEL	RWANDA
BELIZE	ITALY	SAN MARINO
BENIN	JAMAICA	SAUDI ARABIA
BOLIVIA	JAPAN	SENEGAL
BOSNIA AND HERZEGOVINA	JORDAN	SERBIA
BOTSWANA	KAZAKHSTAN	SEYCHELLES
BRAZIL	KENYA	SIERRA LEONE
BRUNEI DARUSSALAM	KOREA, REPUBLIC OF	SINGAPORE
BULGARIA	KUWAIT	SLOVAKIA
BURKINA FASO	KYRGYZSTAN	SLOVENIA
BURUNDI	LAO PEOPLE'S DEMOCRATIC REPUBLIC	SOUTH AFRICA
CAMBODIA	LATVIA	SPAIN
CAMEROON	LEBANON	SRI LANKA
CANADA	LESOTHO	SUDAN
CENTRAL AFRICAN REPUBLIC	LIBERIA	SWAZILAND
CHAD	LIBYA	SWEDEN
CHILE	LIECHTENSTEIN	SWITZERLAND
CHINA	LITHUANIA	SYRIAN ARAB REPUBLIC
COLOMBIA	LUXEMBOURG	TAJIKISTAN
CONGO	MADAGASCAR	THAILAND
COSTA RICA	MALAWI	THE FORMER YUGOSLAV REPUBLIC OF MACEDONIA
CÔTE D'IVOIRE	MALAYSIA	TOGO
CROATIA	MALI	TRINIDAD AND TOBAGO
CUBA	MALTA	TUNISIA
CYPRUS	MARSHALL ISLANDS	TURKEY
CZECH REPUBLIC	MAURITANIA	UGANDA
DEMOCRATIC REPUBLIC OF THE CONGO	MAURITIUS	UKRAINE
DENMARK	MEXICO	UNITED ARAB EMIRATES
DOMINICA	MONACO	UNITED KINGDOM OF GREAT BRITAIN AND NORTHERN IRELAND
DOMINICAN REPUBLIC	MONGOLIA	UNITED REPUBLIC OF TANZANIA
ECUADOR	MONTENEGRO	UNITED STATES OF AMERICA
EGYPT	MOROCCO	URUGUAY
EL SALVADOR	MOZAMBIQUE	UZBEKISTAN
ERITREA	MYANMAR	VENEZUELA
ESTONIA	NAMIBIA	VIET NAM
ETHIOPIA	NEPAL	YEMEN
FIJI	NETHERLANDS	ZAMBIA
FINLAND	NEW ZEALAND	ZIMBABWE
FRANCE	NICARAGUA	
GABON	NIGER	
GEORGIA	NIGERIA	
GERMANY	NORWAY	
	OMAN	

The Agency's Statute was approved on 23 October 1956 by the Conference on the Statute of the IAEA held at United Nations Headquarters, New York; it entered into force on 29 July 1957. The Headquarters of the Agency are situated in Vienna. Its principal objective is "to accelerate and enlarge the contribution of atomic energy to peace, health and prosperity throughout the world".

TRANSFER OF TRITIUM IN THE
ENVIRONMENT AFTER ACCIDENTAL
RELEASES FROM NUCLEAR FACILITIES

REPORT OF WORKING GROUP 7
TRITIUM ACCIDENTS
OF EMRAS II TOPICAL HEADING
APPROACHES FOR ASSESSING EMERGENCY SITUATIONS

ENVIRONMENTAL MODELLING FOR
RADIATION SAFETY (EMRAS II) PROGRAMME

COPYRIGHT NOTICE

All IAEA scientific and technical publications are protected by the terms of the Universal Copyright Convention as adopted in 1952 (Berne) and as revised in 1972 (Paris). The copyright has since been extended by the World Intellectual Property Organization (Geneva) to include electronic and virtual intellectual property. Permission to use whole or parts of texts contained in IAEA publications in printed or electronic form must be obtained and is usually subject to royalty agreements. Proposals for non-commercial reproductions and translations are welcomed and considered on a case-by-case basis. Enquiries should be addressed to the IAEA Publishing Section at:

Marketing and Sales Unit, Publishing Section
International Atomic Energy Agency
Vienna International Centre
PO Box 100
1400 Vienna, Austria
fax: +43 1 2600 29302
tel.: +43 1 2600 22417
email: sales.publications@iaea.org
<http://www.iaea.org/books>

For further information on this publication, please contact:

Radiation Safety and Monitoring Section
International Atomic Energy Agency
Vienna International Centre
PO Box 100
1400 Vienna, Austria
Email: Official.Mail@iaea.org

© IAEA, 2014
Printed by the IAEA in Austria
July 2014

IAEA Library Cataloguing in Publication Data

Transfer of tritium in the environment after accidental releases from nuclear facilities : report of Working Group 7 Tritium Accidents of EMRAS II Topical Heading Approaches for Assessing Emergency Situations. — Vienna : International Atomic Energy Agency, 2014. p. ; 30 cm. — (IAEA-TECDOC series, ISSN 1011-4289 ; no. 1738)
ISBN 978-92-0-102814-3
Includes bibliographical references.

1. Radioisotopes — Migration — Mathematical models. 2. Nuclear facilities — Accidents. 3. Tritium — Environmental aspects. 4. Radiation — Safety measures. I. International Atomic Energy Agency. II. Series.

FOREWORD

Environmental assessment models are used for evaluating the radiological impact of actual and potential releases of radionuclides to the environment. They are essential tools for use in the regulatory control of routine discharges to the environment and also in planning measures to be taken in the event of accidental releases. They are also used for predicting the impact of releases which may occur far into the future, for example, from underground radioactive waste repositories. It is important to verify, to the extent possible, the reliability of the predictions of such models by a comparison with measured values in the environment or with predictions of other models.

The IAEA has been organizing programmes of international model testing since the 1980s. These programmes have contributed to a general improvement in models, in the transfer of data and in the capabilities of modellers in Member States. IAEA publications on this subject over the past three decades demonstrate the comprehensive nature of the programmes and record the associated advances which have been made.

From 2009 to 2011, the IAEA organized a programme entitled Environmental Modelling for Radiation Safety (EMRAS II), which concentrated on the improvement of environmental transfer models and the development of reference approaches to estimate the radiological impacts on humans, as well as on flora and fauna, arising from radionuclides in the environment.

Different aspects were addressed by nine working groups covering three themes: reference approaches for human dose assessment, reference approaches for biota dose assessment and approaches for assessing emergency situations. This publication describes the work of the Tritium Accidents Working Group.

The IAEA wishes to express its gratitude to all those who participated in the work of the EMRAS II programme and gratefully acknowledges the valuable contribution of D. Galeriu (Romania) and A. Melintescu (Romania). The IAEA officer responsible for this publication was V. Berkovskyy of the Division of Radiation, Transport and Waste Safety.

EDITORIAL NOTE

This publication has been prepared from the original material as submitted by the contributors and has not been edited by the editorial staff of the IAEA. The views expressed remain the responsibility of the contributors and do not necessarily represent the views of the IAEA or its Member States.

Neither the IAEA nor its Member States assume any responsibility for consequences which may arise from the use of this publication. This publication does not address questions of responsibility, legal or otherwise, for acts or omissions on the part of any person.

The use of particular designations of countries or territories does not imply any judgement by the publisher, the IAEA, as to the legal status of such countries or territories, of their authorities and institutions or of the delimitation of their boundaries.

The mention of names of specific companies or products (whether or not indicated as registered) does not imply any intention to infringe proprietary rights, nor should it be construed as an endorsement or recommendation on the part of the IAEA.

The IAEA has no responsibility for the persistence or accuracy of URLs for external or third party Internet web sites referred to in this publication and does not guarantee that any content on such web sites is, or will remain, accurate or appropriate.

CONTENTS

SUMMARY	1
1. INTRODUCTION.....	3
1.1. Background of the EMRAS II Programme	3
1.2. Background for EMRAS II Working Group 7: Tritium Accidents.....	3
1.3. Objectives.....	5
2. KEY MECHANISMS FOR TRITIUM TRANSFER IN THE TERRESTRIAL ENVIRONMENT.....	7
2.1. Overview	7
2.2. Tritiated gas (HT)	7
2.3. Tritiated water (HTO).....	7
2.4. HTO transfer from air to plant	8
2.4.1. Kinetics	8
2.4.2. Exchange velocity	9
2.4.3. Practical conclusions	10
2.5. HTO transfer from air to soil.....	10
2.6. HTO transfer from soil to plant	11
2.7. HTO transfer from air to rain and soil	12
2.8. Production of tritiated organic matter.....	13
2.9. Tritiated organic matter produced during the night.....	16
2.10. Animals	16
2.11. Conclusions	18
3. INTERACTION MATRICES AND ASSOCIATED PROCESSES FOR TERRESTRIAL PATHWAYS OF TRITIUM TRANSFER	21
3.1. Overview	21
3.2. Methodology	21
3.3. Interaction matrices of terrestrial pathways of tritium transfer	22
3.3.1. Assessment context	22
3.3.2. Biosphere system features	22
3.3.3. Conceptual model objects.....	22
3.3.4. Tritium interaction matrices	23
3.4. Descriptions of events and processes.....	23
3.4.1. Aerenchyma.....	23
3.4.2. Bioturbation	23
3.4.3. Capillary rise.....	28
3.4.4. Cropping loss (plants – animals).....	28
3.4.5. Death and decomposition	28
3.4.6. Deposition (wet and dry).....	28
3.4.7. Diffusion or diffusive exchange.....	28
3.4.8. Discharge from below (upwelling)	29
3.4.9. Erosion.....	29
3.4.10. Evaporation.....	29
3.4.11. Excretion.....	29
3.4.12. Exhalation (or expiration).....	30
3.4.13. Foliar uptake	30
3.4.14. Gas sorption	30

3.4.15.	Gross photosynthesis and growth	30
3.4.16.	H metabolism.....	30
3.4.17.	Infiltration.....	31
3.4.18.	Ingestion	31
3.4.19.	Inhalation.....	31
3.4.20.	Interception.....	31
3.4.21.	Irrigation.....	32
3.4.22.	Micro-organism metabolism and assimilation.....	32
3.4.23.	OBT formation.....	32
3.4.24.	Oxidation (HT to HTO).....	32
3.4.25.	Percolation.....	32
3.4.26.	Ploughing.....	32
3.4.27.	Precipitation.....	33
3.4.28.	Resuspension	33
3.4.29.	Root uptake.....	33
3.4.30.	Root respiration.....	33
3.4.31.	Surface run-off.....	33
3.4.32.	Translocation	33
3.4.33.	Transpiration.....	34
3.4.34.	Weathering.....	34
3.5.	Conclusions and way forward	34
4.	WASHOUT OF ATMOSPHERIC TRITIUM.....	35
4.1.	Overview	35
4.2.	Calculation of washout rate.....	35
4.3.	Washout rate from experimental data	37
4.3.1.	Washout by rain	37
4.3.2.	Washout for snow	39
4.3.3.	HTO deposition by fog.....	39
4.3.4.	Synthesis.....	39
4.4.	Detailed HTO models	42
4.4.1.	Generalized calculation of washout rate	42
4.4.2.	Modelling of the HTO concentration in rain water.....	42
4.4.3.	Potential effect of buildings.....	48
4.5.	Sensitivity of models	50
4.5.1.	Raindrop distribution.....	50
4.5.2.	Raindrop diameter.....	53
4.5.3.	Raindrop velocity.....	53
4.5.4.	Sensitivity of models.....	53
4.6.	Conclusion on washout rate	59
5.	HT AND HTO DRY DEPOSITION AND REEMISSION.....	61
5.1.	Overview	61
5.2.	Dry deposition of HTO and reemission	61
5.3.	Dry deposition of HT and reemission.....	65
5.4.	Conclusions	67

6.	HTO UPTAKE IN PLANTS AND OBT FORMATION DURING DAY LIGHT.....	69
6.1.	Overview	69
6.2.	Dynamics of HTO uptake in leaves.....	69
6.3.	Exchange velocity approach.....	71
6.4.	Modelling approaches for canopy conductance	74
6.5.	OBT formation during daytime	80
6.6.	OBT partition in plant parts	82
6.7.	Conclusions and recommendations	82
7.	OVERVIEW OF EXPERIMENTS ON TRITIUM TRANSFER FROM AIR TO PLANTS AND SUBSEQUENT CONVERSION TO OBT.....	83
7.1.	Overview	83
7.2.	Experiments in Germany: wheat, bean, potato.....	84
7.2.1.	Wheat.....	84
7.2.2.	Beans and potatoes.....	92
7.3.	Experiments in Japan: rice, soybean and tangerine	93
7.3.1.	Rice	93
7.3.2.	Soybeans.....	94
7.3.3.	Tangerine.....	96
7.4.	Experiments in Korea: rice, soybean, cabbage, radish	97
7.4.1.	Rice	97
7.4.2.	Soybean	98
7.4.3.	Radish.....	101
7.4.4.	Cabbage.....	101
7.5.	Experiments in Canada: cherry tomato.....	101
7.6.	Experiments in France: lettuce	106
7.7.	Dependence of TLI of rice on duration of exposure.....	107
7.8.	Uptake of HTO at night and leaf resistance	107
7.9.	Preliminary conclusions following review of the experimental data	109
8.	REVIEW OF SOIL-PLANT TRITIUM TRANSFER	113
8.1.	Overview	113
8.2.	Approach to the role of soil moisture in the spatial variability of evapotranspiration.....	113
8.3.	Handling the spatial variability of evapotranspiration in hydrological models	114
8.4.	Complexity of the soil-plant-atmosphere system in the context of tritium transfer	115
8.5.	General overview of the soil-plant system.....	116
8.5.1.	Compartments of the soil-plant system.....	116
8.5.2.	Processes in the soil-plant system.....	116
8.6.	Interaction of the soil-plant system with the atmosphere: coupling of atmosphere to soil and three generations of land surface schemes	117
8.7.	Spatial variability of coupling as a basis for robust tritium modeling.....	118
8.8.	Overview of soil-plant tritium modules	118
8.8.1.	Processes in the soil-plant system.....	118
8.8.2.	Boundary conditions for HTO	118

8.9.	Land-atmosphere coupling and remarks on applicability of analysed models	118
8.10.	Overview of feedbacks in the soil-plant system.....	120
8.11.	Parameterization of dynamical feedback from roots: root growth.....	120
	8.11.1. Biomass Growth.....	120
	8.11.2. Root density profile.....	122
	8.11.3. Constraint on transpiration	123
8.12.	Respiration	123
9.	TRITIUM TRANSFER IN WHEAT EXPERIMENTS AND MODEL TESTS.....	125
9.1.	Overview	125
9.2.	Experiments and scenario definition.....	125
9.3.	Model results	128
9.4.	Statistical analysis of results for models acceptance	128
9.5.	Discussion of statistical analysis	135
9.6.	Conclusions	135
10.	TRITIUM TRANSFER IN FARM ANIMALS.....	136
10.1.	Overview	136
10.2.	Classic approach	137
10.3.	OBT biokinetic rates and basic models	140
10.4.	Derivation of the dynamic equation for a single organic compartment	142
10.5.	Analysis of simple models	144
10.6.	Complex models	146
10.7.	Quality assurance of models	149
10.8.	Final discussion	152
11.	DESCRIPTION OF A COMPLEX MODEL	155
11.1.	Overview	155
11.2.	Atmospheric model.....	155
11.3.	Soil model	156
11.4.	Vegetation model.....	156
11.5.	Conclusions	158
12.	TRITIUM IN THE AQUATIC FOOD CHAIN	159
12.1.	Overview	159
12.2.	Dynamics of organic tritium transfer in producers.....	160
	12.2.1. OBT dynamics in phytoplankton.....	160
	12.2.2. OBT dynamics in macrophytes.....	161
12.3.	Dynamics of organic tritium transfer in consumers	162
	12.3.1. OBT dynamics in zooplankton	165
	12.3.2. OBT dynamics in zoobenthos.....	165
	12.3.3. OBT dynamics in fish	166
12.4.	Dissolved organic tritium (DOT)	168
12.5.	Examples of modelling a typical fish using the AQUATRIT model	170

13.	QUALITY ASSURANCE OF DATA	173
13.1.	Overview	173
13.2.	Analytical issues	174
13.2.1.	Issues with the OBT analysis process	174
13.2.2.	HTO measurement	174
13.2.3.	OBT measurement	174
13.2.4.	Uncertainties	176
13.3.	Previous OBT inter-comparison programs	177
13.3.1.	Canada (Chalk River Laboratories, CRL)	177
13.3.2.	France (CETAMA)	180
13.3.3.	Japan (Akita University School of Medicine)	180
13.3.4.	UK (National Compliance and Assessment Service, NCAS)	183
13.4.	CRL's OBT experiment to evaluate the contribution of residual water	183
13.5.	Discussion	184
14.	QUALITY ASSURANCE OF MODELS	185
14.1.	Overview	185
14.2.	Quality assurance (QA) and sensitivity – uncertainty analysis (SU)	186
14.2.1.	Model development.....	188
14.2.2.	Model evaluation.....	190
14.3.	Sources of uncertainty.....	193
14.3.1.	Types of uncertainty.....	193
14.4.	Techniques to manage uncertainties	196
14.4.1.	Management of scenario uncertainty	197
14.4.2.	Management of model uncertainty	198
14.5.	Management of data/parameter uncertainty.....	198
14.6.	Management of subjective uncertainty	200
14.7.	Conclusions	201
15.	STATUS AND PERSPECTIVES OF ACCIDENTAL TRITIUM MODELLING.....	203
APPENDIX I.	INPUT DATA FOR MODELS OF FARM ANIMALS	205
APPENDIX II.	TRITIUM DYNAMICS IN AN AQUATIC ENVIRONMENT FOR TROPICAL ENVIRONMENTS.....	207
APPENDIX III.	DEFINITION OF ORGANICALLY BOUND TRITIUM (OBT)	231
REFERENCES.....		233
LIST OF ABBREVIATIONS.....		259
CONTRIBUTORS TO DRAFTING AND REVIEW.....		261
LIST OF PARTICIPANTS.....		263

SUMMARY

This report describes the work undertaken by Working Group 7 (WG7) of the IAEA's EMRAS II Programme and considers the conclusions drawn during EMRAS (Phase I) (2003–2007). Regarding the tritium (^3H) studies carried out during previous IAEA programme, the needs for a continuation of work were argued as follows:

- The need for a sound scientific basis to assess and evaluate the possible radiological impact arising from releases of tritium to the environment under accidental conditions;
- The analysis of new data sets and experiments that were performed to investigate the environmental behaviour of tritium under for a wide range of environmental conditions;
- To enable the exchange of experience and knowhow in modelling the transfer of tritium in the environment bearing in mind tritium releases from nuclear power plants, reprocessing plants and and possible future fusion reactors.

The most important topic for further studies was the development of a standard conceptual model and mathematical model to simulate the transfer of tritium in the environment following accidental releases, covering a wide range of environmental and weather conditions as well as seasonal peculiarities. The following processes are of particular interest:

- The formation of organically bound tritium (OBT) in plants during the night time, the transport of tritium within the plants to fruits and roots, the transfer of tritium from feed to meat, milk and eggs as well as the modification of tritium activity concentrations during processing and preparation of food;
- The washout of tritium by snow as well as the dry deposition of tritium to snow;
- Tritium behaviour in soils following the deposition from the atmosphere;
- Tritium and ^{14}C behaviour in the environment in the context of releases from waste disposal facilities;
- The uptake of tritiated water (HTO) by plants during day and night, under wet and dry conditions;
- The deposition of gaseous tritiated hydrogen (HT) to plants and soil and the conversion of HT to HTO;
- Differences in the environmental behaviour of tritiated against non-tritiated compounds (isotopic discrimination).

At the beginning of WG7 activities, a large number of participants elaborated a set of subtopics: processes contributing to tritium transfer, modelling attempts, uncertainty and quality assurance aspects. The final goal was to obtain a harmonized model for the aquatic and atmospheric releases, which is quality controlled and easy to apply in operational cases. Focus was given to address the large variability regarding the environmental and weather conditions when a tritium accident may potentially occur.

In Sections 2 and 3 of this report, the key mechanisms and interaction matrix for terrestrial pathways of tritium transfer are described. Section 4 addresses the dispersion of tritium in the atmosphere, including washout by rain and deposition to plants and soil. In Section 5, dry deposition of HT and HTO and the re-emission to the atmosphere is described and discussed and guidance is given on how to address these processes in assessment models. Section 6 addresses the HTO uptake by plants and the conversion to OBT during the day time and provides models to quantify these processes. In addition, Section 6 also discusses the

simplification of models as well as the availability of model parameters. An analysis of recently published experimental work as input for models to simulate the tritium transfer from air to plants and the subsequent synthesis of OBT is discussed in detail in Section 7. In Section 8, models to estimate the transfer of caesium from soil to plant transfer are described and the currently existing limitations of these models are discussed.

Experiments to study the tritium transfer to wheat are presented in Section 9, which enables a detailed process analyses and a database for further models tests.

The tritium transfer to animal food products (meat, milk and eggs) is described in detail in Section 10 and approaches to model are presented.

Section 11 addresses very detailed and complex models to simulate the atmosphere-plant-soil system, highlighting the challenges to find appropriate data sets for testing and validating such complex models. .

For tritium transfer in the aquatic food chain, the processes and related models are described in Section 12 together with examples of model application and robustness.

The main of goal of WG7's work was to develop a harmonized, robust model for practical applications. Aspects of the quality assurance of the input data and models are discussed in Sections 13 and 14.

The present status and needs are also summarized (Section 15) and further fields of activities are identified to improve the reliability and the application of models to asses tritium behavior in the environment and the resulting radiological impacts to people and the environment. There was broad consensus among the participants that the following processes require further efforts:

- Interception and uptake by plants of tritium that has been deposited during precipitation: by leaves;
- Transfer of tritium to bare and vegetated soil;
- Transfer from soil to plants – HTO: dynamics of the soil-plant-atmosphere complex;
- Reemission of tritiated water due to evapo-transpiration HTO as a secondary source;
- Transformation of OBT during the night;
- Oxidation of OBT in feed and food during processing and storage;
- The behaviour and the interaction of OBT with the organic matter in soil.

In the Appendices, useful information is given regarding the input data for farm animal models, tritium dynamics in tropical aquatic conditions and a detailed definition of OBT.

1. INTRODUCTION

1.1. BACKGROUND OF THE EMRAS II PROGRAMME

The IAEA organized a programme from 2009 to 2011 entitled Environmental Modelling for RADIATION SAFETY (EMRAS II), which concentrated on the improvement of environmental transfer models and the development of reference approaches to estimate the radiological impacts on humans, as well as on flora and fauna, arising from radionuclides in the environment.

The following topics were addressed in nine working groups:

Reference Approaches for Human Dose Assessment

- Working Group 1: Reference Methodologies for Controlling Discharges of Routine Releases
- Working Group 2: Reference Approaches to Modelling for Management and Remediation at NORM and Legacy Sites
- Working Group 3: Reference Models for Waste Disposal

Reference Approaches for Biota Dose Assessment

- Working Group 4: Biota Modelling
- Working Group 5: Wildlife Transfer Coefficient Handbook
- Working Group 6: Biota Dose Effects Modelling

Approaches for Assessing Emergency Situations

- Working Group 7: Tritium Accidents
- Working Group 8: Environmental Sensitivity
- Working Group 9: Urban Areas

The activities and the results achieved by the Working Groups are described in individual IAEA Technical Documents (IAEA-TECDOCs). This report describes the work of the Tritium Accidents Working Group.

1.2. BACKGROUND FOR EMRAS II WORKING GROUP 7: TRITIUM ACCIDENTS

Tritium is a weak beta emitter that is naturally present on earth but is also routinely released by almost all nuclear facilities (nuclear power plants, defence facilities, fusion facilities, fuel processing plants, etc). Some recent studies [1] have mentioned that the radiotoxicity of tritium might be underestimated, even though it remains one of the least radiotoxic nuclides, whatever its chemical form. Nevertheless, this has raised more concerns on how it could migrate in the environment and eventually affect people through the food chain.

Tritium has a complex behaviour once released into the environment. Being an isotope of hydrogen, its behaviour depends on its initial chemical form, its transformation from one form to another (in particular in its oxidised form as water) and on the weather and soil/aquatic conditions at the time of release. An overview of tritium occurrence, chemistry and physics, speciation, analytical techniques, separation and remediation was published recently [2]. With respect to its environmental behaviour, tritium is unique among radionuclides in a number of respects [3]:

- In aqueous systems, tritium moves as a non-reactive, non-absorbed constituent with the bulk water flow. Accordingly, the environmental transport of tritium is governed in large part by local and global hydrologic cycles.
- As a gas, tritium moves in response to its own vapour pressure gradient and can, under some circumstances, move against the water vapour flux.
- Tritium deposited from the atmosphere to soil and plants is readily recycled back to the atmosphere via evapotranspiration, forming a secondary airborne plume.
- The processes responsible for tritium transfer have time scales as short as minutes. Tritium can be rapidly taken up by organisms, but just as rapidly lost. As a result, tritium transfer is highly dependent on the environmental conditions prevailing at the time and place of release and the time of measurement.
- Tritium can be effectively incorporated into biological systems, including the human body, as organically bound tritium (OBT).
- Although tritium is three times heavier than hydrogen, it usually occurs as part of larger molecules. Therefore, isotopic effects, although present, are not important in environmental tritium transport, except in OBT formation.
- Tritium is transferred through the environment and through food chains without bioaccumulation in any compartment.

These unique features must be taken into account in understanding the environmental transport of tritium and in estimating the radiological consequences of releases into the environment. Many international programmes have considered the radiological aspects of tritium transfer into the environment, such as BIOMOVs II (BIOSpheric Model Validation Study) in 1991–1996¹, BIOMASS (BIOSphere Modelling and ASSESSment) in 1996–2001² and EMRAS I (Environmental Modelling for Radiation Safety) in 2003–2007³. In these programmes, the predictions of different environmental models were compared to assess the potential uncertainties and the level of confidence given by the codes. The outcomes of the EMRAS I programme are available in the form of a Summary report, to which all Working Group reports are appended on a CD-ROM⁴.

In EMRAS I, the Tritium and ¹⁴C Working Group made a first attempt to compare models for a hypothetical accidental release of tritium to the environment [4]. Nevertheless, the tritium community felt that further work in this area would be beneficial.

Tritium behaviour following an accidental release is of high interest for nuclear facilities with a large tritium inventory, and/or those for which the health impact on members of the public is not driven by other radionuclides. Among such facilities are heavy water power plants, fuel reprocessing plants, tritium defence facilities and fusion facilities such as ITER⁵.

The main goal of an increased knowledge of tritium environmental behaviour in accident situations is not only to get a (moderately) conservative assessment of the dose to members of the public, but also to prepare the conditions for the management of the emergency. For the

¹ See http://www.iaea.org/inis/collection/NCLCollectionStore/_Public/31/047/31047298.pdf

² See <http://www-ns.iaea.org/projects/emras/emras-publications.asp?s=8#1>

³ See <http://www-ns.iaea.org/projects/emras/>

⁴ See <http://www-ns.iaea.org/projects/emras/draft-reports.asp?s=8>

⁵ See <http://www.iter.org/>

latter, excessive conservatism has to be reduced in order not to propose too large or needless emergency actions.

In most cases, large potential accidents involve short duration releases to air whereas minor incidental releases may also involve liquid emissions. Thus both terrestrial and aquatic pathways have to be studied for all weather conditions for a better knowledge of tritium environmental behaviour and its impact.

The main differences between routine and accidental releases of tritium are generally the larger magnitude and shorter kinetics of accidental releases compared with annual routine releases. The kinetic effects of tritium environmental behaviour are a topic of further study.

1.3. OBJECTIVES

The EMRAS II WG7 “Tritium Accidents” addressed certain areas of interest related to accidental releases of tritium into the environment, and some key objectives were proposed:

- Developing a standard conceptual dynamic model for tritium dose assessment for acute releases to the atmosphere and water bodies, from the source to receptor.
- Agreeing on common sub-models for specific transfers or processes, based on an interdisciplinary approach involving the understanding of the processes and key parameters taken from recent research in life sciences. Quality assurance requires moderate conservatism.
- Defining the framework for an operational model (requirements for meteorological data, atmospheric transport, site specific data and so on).
- Achieving the capability to assimilate real measured data in the models.

It is especially important to focus on the uncertainties and sensitivities that are involved in modelling the behaviour of tritium in the environment after accidents. The dynamics of tritium in the terrestrial environment is the result of the complex interaction of a number of factors that are subject to hourly, daily and annual fluctuations. Due to the large uncertainties related to the environmental conditions at the time of an accidental release, predictions are unavoidably associated with considerable uncertainties. However, these inherent problems in tritium modelling are not clear to everyone; therefore, it was very important for the work to:

- Identify the main contributors to uncertainty;
- Identify the critical periods during the year when a release would result in the greatest exposure to tritium;
- Identify the important and sensitive parameters, having in mind the hourly, daily and annual variations in parameters/processes;
- Explore the practical difficulties in determining those parameters;
- Get an idea of the achievable reliability of tritium modelling under the conditions that hold at the time of the accident;
- Get a clear idea for the phases of a tritium accident the application of a tritium model is most desirable and useful.

A general concern is to get an adequate level of conservatism in the predictions of robust and proven models, using data that are easily accessible. Among the points to be assessed, the following topics are highlighted:

- The physical models associated with tritium accidental releases;
- The data needed to validate the models, including the quality of environmental tritium measurements, particularly for OBT.

The present report partially covers the needs that must be met to obtain a harmonised approach to developing a robust model to be applied in practice. The nuclear regulators and utilities prefer a transparent, simple model that is moderately conservative. It is a matter of present debate if this is possible in the near future and much effort is still needed.

2. KEY MECHANISMS FOR TRITIUM TRANSFER IN THE TERRESTRIAL ENVIRONMENT

2.1. OVERVIEW

It is not the purpose of this section to review the large volume of literature that describes the processes of tritium transport between the different compartments of the environment. However, this section deals with the key mechanisms and definitions for understanding tritium transfer and its fate in plants and animals.

Atmospheric transport and dispersion of tritium is similar to that for other radionuclides, except that HTO is re-emitted from vegetation and soil to air. Reemission may represent some tens of percent of the deposition and can be neglected in a first approach.

The reemitted material undergoes atmospheric dispersion over the course of many hours, and then this secondary exposure pathway becomes even less important.

In accident scenarios, tritium can be released as a gas (HT) or as tritiated water vapour (HTO).

2.2. TRITIATED GAS (HT)

It has to be noted that HT is not transferred to plants and has a low dry deposition velocity. Furthermore, it is not washed out by rain and has a low dose per unit intake by inhalation. Then the only pathway of interest is the chemical transformation by soil microorganisms of the small amount of HT deposited on the soil into tritiated water, and the following use of the water by plants.

In practice, it is necessary to release about 1 kg of HT to achieve a significant radiological impact, delivered over the course of some weeks. As this quantity is difficult to reach in any existing facility, the case of HT does not need to be developed here. Nevertheless, in a real accident, it is important to know the fraction of HT in the release, as this fraction will contribute a negligible amount to the total dose.

In the case of a pure HT release, the dose is of the order of a few percent (1–5%) of that imparted by an equivalent HTO release. The HT dose is mainly due to the soil- plant pathway, as the HT must first be transformed into tritiated water.

2.3. TRITIATED WATER (HTO)

The transport and exposure pathways for tritiated water are more complex than those for HT and operate on different time scales.

It is well-known that the main pathway for HTO exposure following an acute release is consumption of food with a high concentration of OBT.

Nevertheless, most models predict the instantaneous concentration in different compartments, which is useful for comparison to measurements but which often misses the second objective of the calculations, which is to propose efficient countermeasures. This is why it is useful to analyze in detail the different mechanisms, their times of occurrence and contributions to total dose.

During the accident, many mechanisms of transfer operate depending on many interconnected processes.

The first process is the direct transfer from air to leaves by exchange between air vapour and the free water of the leaves through the stomata and the cuticle. This transfer depends on the leaf area index (m^2 of leaves per m^2 of soil) and on the stomatal resistance, which characterizes the opening of the stomata.

The second pathway is the transfer from air to soil, which occurs by diffusion of air vapour through the soil surface. This is essentially a deposition process and can be modelled with a deposition velocity, which depends mainly on soil humidity.

To quantify these pathways, it is interesting to give some idea of the different water contents of the related compartments. The absolute humidity of air is of the order of $5\text{--}25 \text{ g m}^{-3}$. The quantity of water in 1 m^2 of vegetation covering the soil is between 500 and 5000 g m^{-2} , and the quantity of water released by transpiration is between 50 and $250 \text{ g h}^{-1} \text{ m}^{-2}$. It needs only a few hours to reach equilibrium between plant free water and air vapour. There is a flux from plant to air but also a diffusion mechanism from air to plant.

As a part of the free water coming from the soil, the equilibrium between air vapour and plant water is not 100%, but about 40% [5]. This shows that the turnover of the free water of the plant is rapid, on the order of a day.

2.4. HTO TRANSFER FROM AIR TO PLANT

Stomata are cellular structures that constitute doors through which pass the different gases (CO_2 , O_2 and water vapour) of photosynthetic exchange between air and the internal medium of the plant. The cuticle is a more or less impervious layer that covers the epidermis.

Stomata control the rate of transpiration. They are open when there is light and sufficient water coming from the soil and can be moderated by internal regulation (abscisic acid for water stress). Photosynthesis and transpiration will occur when fluxes of CO_2 and water are possible.

Photosynthetic transfer depends on many environmental factors such as light, temperature, and the relative humidity of air and soil, and on internal factors such as the number of stomata, their location, sugar concentration, age of the plant, etc. In practice, information on these factors is unlikely to be available at the moment of the accident.

2.4.1. Kinetics

In leaves, charge and discharge of HTO from air are fast phenomena. The plant concentration increases and decreases with a biological period of the order of an hour during the day. Tritium delabeling of plant tissue after exposure from the atmosphere is much slower in darkness than in the light, with the loss of HTO primarily depending on transpiration. During the night, many hours may be required for the tritium concentration in the plant to drop significantly.

In such conditions, the exact timing of the release is important, as most of the decrease phase will occur the following morning, in daytime conditions.

The activity of the leaves increases from zero at the beginning of the release to a maximum at the end, and comes back to the low level of soil water activity some hours later.

The main dose contribution from the air to plant free water to man pathway occurs during the first day for vegetables harvested that day (fresh garden vegetables).

2.4.2. Exchange velocity

From the mathematical point of view, deposition and reemission is modelled using a parameter called the exchange velocity” (m s^{-1}), which represents the flux of air that enters the leaves ($\text{Bq m}^{-2} \text{ s}^{-1}$) per unit air concentration (Bq m^{-3}).

If we suppose that the exchange velocity between the free water of the plant and air vapour remains the same in both charge and discharge phases, then the water-integrated concentration is less sensitive than the instantaneous concentration to the exchange rate. Photosynthetic production is bound to this integrated concentration, as is ingestion by man of HTO in vegetables. However, in practice, people do not harvest vegetables continuously, especially not during the night.

Water absorption by the leaves is fast during the day and slower during the night. Vapour exchanges occur mainly through the stomata, for which the mechanism is controlled by the internal pressure of by-stander cells. Nevertheless, the cuticle is not absolutely watertight, especially for young and old leaves.

Depending on the internal pressure, the stomata will be more or less open.

Key external factors that influence the state of the stomata are the relative humidity of the air (HR) and light levels.

- Moist air (HR = 80%) promotes the opening of the stomata whereas drier air (HR = 50%) closes them.
- Light also plays a direct role in the opening of the stomata. It causes a large increase (from 12 to 18 bars) in the osmotic pressure of guard cells; meanwhile, the pressure in the by-stander cells is about 15 bars. Based on current knowledge, the stomata guard cells accumulate potassium with the inverse transport of protons. This “proton pump” seems to be stimulated by light, especially in the blue part of the spectrum. At the same time, light produces adenosine tri-phosphate (ATP), which is the energy source for further biochemical transformations.

As an internal factor, abscissic acid plays a key role in controlling the opening of the stomata. In the case of water stress, the abscissic content increases considerably, which causes a quick closure of stomatal orifices. Abscissic acid acts as a hormone of distress and allows a vigorous response by the plants.

The exchange velocity is calculated as follows:

$$V_c = \frac{LAI}{r} \quad (1)$$

where:

- V_c is the water vapour exchange velocity between air and leaves (m s^{-1});
- LAI is the leaf area index at the moment of the release (dimensionless); and
- r is the stomatal resistance of the leaf surface (s m^{-1}).

The stomatal resistance of the leaf surface, r , has a value of 300 s m^{-1} as an average during the day when stomata are completely open and, 3000 s m^{-1} during the night when they are closed. Knowing the leaf area index of the different vegetable categories, one can estimate the exchange velocity of water vapour between air and leaves.

The concentration of free water in the leaves during the release is given by:

$$\frac{d A_l}{d t} = \frac{V_c C_w^{\text{sat}}}{m} (A_{\text{vap}} - A_l) \quad (2)$$

where:

- A_l is the activity of leaf free water (Bq m^{-3});
- A_{vap} is the activity of water vapour in air (Bq m^{-3});
- V_c is the water exchange velocity between air and leaves (m s^{-1});
- m is the quantity of water in leaves per m^2 of soil (kg m^{-2}); and
- C_w^{sat} is the quantity of water in air at saturation (kg m^{-3}).

C_w (which depends on temperature) and m (which is not very different from yield) can be easily evaluated. V_c is the most variable parameter. The half life of charge and discharge is then given by:

$$T_{1/2} = \frac{m \ln(2)}{V_c C_w^{\text{sat}} 3600} \quad (\text{in hours}) \quad (3)$$

m and V_c both depend on the leaf area index, so LAI does not appear to be an influential parameter. The half time is proportional to stomatal resistance, and decreases when air temperature increases.

Moreover, if the charge and discharge are rapid and conditions are constant, then the integrated activity of the free water is independent of the incorporation rate and equal to the integrated activity of air vapour at saturation, but the time of release can be much longer.

In practice, conditions do not remain constant for many hours. A physiological approach is needed to integrate stomata resistance and leaf area index. The best approach would be to evaluate stomata resistance from available data at the moment of the accident, if possible.

2.4.3. Practical conclusions

From the point of view of countermeasures, if there is no consumption of leafy or fruit vegetables in the 2 or 3 days immediately following the release, then this exposure pathway will be avoided.

The main significance of tritium contamination of the leaf free water is that the OBT built up during and after the release is more or less proportional to the integrated activity of the free water of the leaves. The integrated activity of air vapour at saturation can be used, in a first approximation, as an upper limit to the free water integrated activity.

2.5. HTO TRANSFER FROM AIR TO SOIL

A second pathway is the transfer from air to soil, which occurs by diffusion of air vapour through the surface. This is essentially a deposition process, and can be modelled with a deposition velocity that depends mainly on soil humidity. About half of the total deposition is

reemitted to the air after the end of the release. This value can be used to calculate inhalation doses from the reemitted plume. In practice, this question is of little interest.

A quantitative idea of this mechanism can be obtained from an assessment of the vapour exchange between air and soil in a temperate climate carried out in the environment of Dijon in France. 300 L y⁻¹ of air vapour is incorporated in the soil through deposition, compared to 700 L y⁻¹ of rain. Considering that the average air vapour content is 8 g m⁻³, this gives an average deposition velocity of air vapour of 1.2 × 10⁻³ m s⁻¹ (in the expected range of 10⁻³ to 10⁻² m s⁻¹). The average deposition of vapour in 1 hour is 0.03 to 0.3 kg h⁻¹ m⁻².

2.6. HTO TRANSFER FROM SOIL TO PLANT

At any given moment, the relative humidity of the soil is typically between 10 and 30%, corresponding to 50 and 150 kg m⁻² for the rooting zone (it can be more for deeper soils). This means that the soil water concentration will be, for a short release of 1 h, less than 0.1–1% of the air vapour concentration. This is small compared to air transfer, which is of some percent during the day. Nevertheless, the halftime in the soil is a few weeks instead of a few hours for free water in leaves. This means that doses from the soil pathway are not negligible when they are integrated over time. Considering the fast turnover of free water in the plant, equilibrium between plant and soil will be reached in 2 or 3 days. Then the plant free water concentration will decrease with the same halftime as the soil concentration.

From the point of view of countermeasures, the soil-plant pathway needs to be taken into account and assessed during the first week post-release, with help from environmental measurements.

From spring to autumn, evapotranspiration is of the order of some liters per square meter per day, compared to 50–150 L of water contained in the soil. The decrease of activity in temperate climates implies half-lives between 10 and 100 days. The longest period corresponds to the largest soil content and consequently, to the lowest concentration. Then the dose, which is a function of integrated activity, will not be very different from one case to another.

Evapotranspiration is the mechanism that reduces soil water activity. The concept of potential evapotranspiration (ETP), the water loss from a field crop that covers the soil completely and has an optimum supply of water from the soil) is used.

Homogenisation over the depth of the soil occurs because of hydraulic potential equilibrium related to root distribution and following rains. Then the daily rate of emission may be considered as the ratio of real evapotranspiration to the total quantity of water in the root zone.

The critical soil moisture content is defined as the quantity of stored soil moisture below which the plant starts to close its stomata.

Real evapotranspiration is equivalent to potential evapotranspiration when the humidity of soil is above a critical humidity, given by the relation [6]:

$$\theta_{ws} = (1 - p)(\theta_{fc} - \theta_{wp}) + \theta_{wp}, \text{ which can also be expressed as: } p = \frac{(\theta_{fc} - \theta_{ws})}{(\theta_{fc} - \theta_{wp})} \quad (4)$$

where:

- θ_{fc} is the humidity at field capacity (unitless, soil moisture suction = 0.1 bar);
- θ_{wp} is the humidity at the wilting point (unitless, soil moisture suction = 16 bars);
- θ_{ws} is the humidity at the critical point (unitless, closure of stomata depending on plant type and ETP); and
- p is the fraction of easily available soil water (unitless).

p values are indicated in Table 1 as a function of ETP. We can see that p decreases when potential evapotranspiration increases.

For soil humidity above θ_{ws} , real evapotranspiration is equivalent to ETP (if the plant entirely covers the surface). Below θ_{ws} , a reduction factor has to be applied and is given by the following equations:

$$\frac{ETR}{ETP} = R_{ws} = \inf\left(1, \frac{\theta_t - \theta_{wp}}{(\theta_{ws} - \theta_{wp})}\right) = \inf\left(1, \frac{\theta_t - \theta_{wp}}{(1-p)(\theta_{fc} - \theta_{wp})}\right) \quad (5)$$

where:

- θ_t is the soil humidity at time t (unitless)
- ETP is the potential evapotranspiration ($L\ m^{-2}$)
- ETR is the real evapotranspiration ($L\ m^{-2}$)

2.7. HTO TRANSFER FROM AIR TO RAIN AND SOIL

It is well-known that the tritium concentration in rain is lower (by up to a factor of 10) than the concentration in air moisture at ground level some distance (a few hundred meters) from the stack. Of course, near the stack, rainwater which falls through the plume can have a much higher concentration than air at ground level, depending on the height of the stack.

Many equations exist to define washout, tritium concentration in rain and deposition on the soil (see Section 4).

A washout rate equation depending on rainfall intensity was proposed by several authors.

TABLE 1. FRACTION OF EASILY AVAILABLE SOIL WATER–SOIL DEPLETION FACTOR

Crop group	ETP (mm d ⁻¹)									
	1	2	3	4	5	6	7	8	9	10
Leafy veg, strawberry, cabbage, onion	0.53	0.45	0.38	0.30	0.25	0.23	0.20	0.18	0.16	0.15
Clover, carrot, early banana, pepper	0.80	0.60	0.50	0.43	0.35	0.30	0.28	0.25	0.23	0.20
Grape, pea, potato, sunflower, tomato, water melon, grass	0.90	0.75	0.65	0.55	0.45	0.40	0.38	0.33	0.30	0.25
Citrus, groudnut, pineapple, alfalfa, cotton, cassava, sweet potato, grains	0.95	0.85	0.75	0.65	0.55	0.50	0.48	0.43	0.38	0.35
Olive, safflower, sorghum, soyabean, sugarcane	1.00	0.92	0.85	0.75	0.65	0.60	0.55	0.50	0.48	0.45

$$\lambda = a \times (\delta)^b \quad (6)$$

where:

a and b are empirical coefficients, nominally 10^{-5} and 0.73;
 δ is the precipitation intensity ($L h^{-1}$); and
 λ is the washout rate (s^{-1}).

Deposition is assumed to be proportional to the integrated air concentration in the column washed by the rain. Then:

$$F_{hto} = \lambda \iint C(z, t) dz dt \quad (7)$$

where:

λ is the washout rate (s^{-1});
 F_{hto} is the HTO deposition rate ($Bq m^{-2} s^{-1}$);
 C is the HTO concentration in air ($Bq m^{-3}$); and
 z is the height above the ground (m).

In practice, tritium concentration in rain does not depend strongly on rain intensity and seems to decrease slightly when the intensity increases ($b < 1$). So, deposition is more or less proportional to the total quantity of rain ($L m^{-2}$). Generally, the amount of rain falling in a given precipitation event in a temperate climate is of the order of some mm. This is small compared to the total quantity of water in the soil. A dilution factor of 10 to 100 applies in the transfer process from soil to plant. Finally, the tritium concentration in soil water will be about 2 orders of magnitude lower than the concentration in air moisture.

The tritium activity in leaves in the case of rain is not well known. One simple modelling approach consists in considering the time needed for evaporation to eliminate the water remaining on the leaves. Then the exposure period can be much longer than in dry conditions, but this is counterbalanced by the activity in rain, which is generally smaller than the activity in air vapour (except at the foot of the stack).

2.8. PRODUCTION OF TRITIATED ORGANIC MATTER

A part of HTO is incorporated in plant organic matter during photosynthesis. This tritium is called organically bound tritium (OBT). In practice it includes two very different types of bonds: tritium bound to carbon, which undergoes practically no decrease in concentration up to harvest (carbon-bound tritium or non-exchangeable (NE) OBT) and tritium bound to other elements (O, N, S), which exchanges easily with the hydrogen in free water in a few hours (E-OBT). Depending on the part of the vegetable eaten, the tritiated organic matter built from air water may be translocated in totality to the accumulation organ after flowering or shortly before. The influence of the date of the accident is then important in terms of the dose received from vegetables such as wheat or potatoes, which are stored and eaten over a long period. At some critical time of the year (e.g. in June for the European climate), the total dose may be significantly reduced by replacing the existing crop with a new one (if possible).

Deposition on the ground also contributes to the contamination of the plants by the root pathway and subsequent incorporation of tritium in organic material. The HTO concentration in soil is much smaller than that in air vapour, but the soil HTO has a much longer turnover and will lead to continuous production of OBT up to harvest. Rain may substantially increase deposition to soil and is a particular point to take into account.

The organic compounds of a plant are produced by photosynthesis transforming sunlight energy into chemical energy. The general reaction produces a C3 molecule (H-C-OH)₃ plus O₂ from CO₂ and H₂O. We can see that each carbon corresponds to a molecule of H₂O and may propose this equivalence as a basic approach to modeling OBT formation (in fact, only one H is carbon bound).

For a continuous, normal release, the average incorporation rate of tritium into organic matter can be calculated from the yield of dry matter at harvest divided by the duration of growth multiplied by 0.53, which corresponds to the proportion of H₂O in C3 molecules corrected by a discrimination factor of 0.95.

$$\tau_{inc} = 0,53 \frac{\tau_{dm}^{veg} Y}{86400 \Delta t_{growth}} \quad (8)$$

where:

- τ_{inc} is the incorporation rate of tritium into organic matter ($\text{kg}_{\text{water}} \text{m}_{\text{soil}}^{-2} \text{s}^{-1}$);
- 0.53 is the water equivalence of dry organic matter ($\text{kg}_{\text{water}} \text{kg}_{\text{dry plant}}^{-1}$);
- τ_{dm}^{veg} is the dry matter content in the vegetable ($\text{kg}_{\text{dry plant}} \text{kg}_{\text{fresh plant}}^{-1}$);
- Y is the yield at harvest ($\text{kg}_{\text{fresh plant}} \text{m}_{\text{soil}}^{-2}$);
- 86400 is a conversion factor (s d^{-1}); and
- Δt_{growth} is the growth duration of the vegetable (d).

This type of very simple approach does not discriminate between day and night and between cold, warm and hot weather. It should at least be corrected by the ratio of daylight hours per day, as there is no incorporation by light reactions during the night (dividing by about 0.6 for summertime). But, on the other hand, only one H is carbon-bound and corresponds to real OBT.

As the effect of temperature is relatively important for incorporation, it is useful to refine the equation to include this parameter. The simplest approach is then to consider the general case and to characterize the extreme cases.

As soon as the sun rises, photosynthetic mechanisms begin to operate. Light is then never the limiting factor of this process. As it is a chemical process, temperature plays an important role in the speed of the reactions. At the same time, respiration is minimal for temperatures around 20°C and increases for lower and higher temperatures. The net photosynthesis becomes zero when the temperature of the leaf reaches about 35°C. At low temperatures, net photosynthesis becomes positive above a given temperature depending on the crop considered. Values of 0°C, 5°C and 7.5°C are often used for grass, wheat and maize (depending on the geographical origin of the plant). The formation rate of organic material may be assumed proportional to temperature for temperatures between 10°C and 30°C.

A very useful concept for expressing heat units is “total degree days”: that is, the accumulated number of days (or sometimes hours) above the crop base temperature.

Considering that air temperature is an available parameter, and considering that in the general case the incorporation rate is proportional to temperature, then it is possible to modify the previous equation to introduce the temperature and total degree days in place of growth duration.

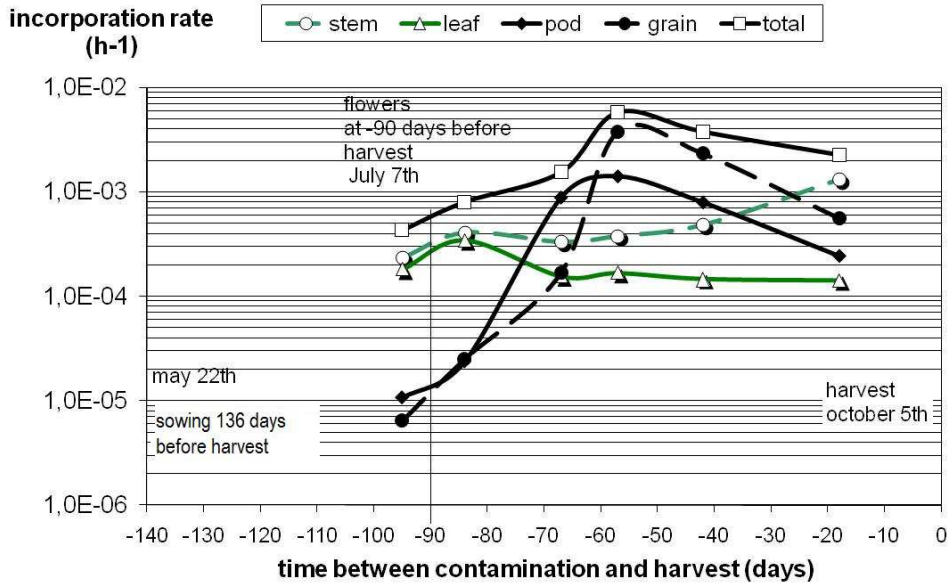


FIG. 1. Measured incorporation rate of tritium in soybean organic matter.

$$\tau_{inc} = 0.53 \frac{\tau_{dm}^{veg} Y (\theta - \theta_0)}{24 \cdot TDD_{harvest}} \quad (9)$$

where:

- τ_{inc} is the incorporation rate of tritium in organic matter ($\text{kg}_{\text{water}} \text{m}_{\text{soil}}^{-2} \text{s}^{-1}$);
- 0.53 is the water equivalence of dry organic matter ($\text{kg}_{\text{water}} \text{kg}_{\text{dryplant}}^{-1}$);
- τ_{dm}^{veg} is the dry matter content in the vegetable ($\text{kg}_{\text{dry plant}} \text{kg}_{\text{fresh plant}}^{-1}$);
- Y is the yield at harvest ($\text{kg}_{\text{fresh plant}} \text{m}_{\text{soil}}^{-2}$);
- 24 is a conversion factor (h d^{-1});
- θ is the average temperature during the accident and in the following hours ($^{\circ}\text{C}$);
- θ_0 is the crop base temperature ($^{\circ}\text{C}$); and
- $TDD_{harvest}$ is the total degree days above θ_0 (d°).

It is possible to free the incorporation rate from the surface dimension ($\text{m}_{\text{soil}}^{-2}$) by dividing it by the dry matter yield ($\text{kg}_{\text{dm}} \text{m}^{-2}$) to obtain a mass incorporation rate expressed in kg of water per kg of dry matter per hour.

This allows the activity integrated inside the whole plant to be calculated, which is useful for leafy vegetables but cannot be used for grains or fruits because the metabolism of these crops changes during growth and partitioning occurs between different organs of the plants.

Figure 1 shows the measured mass incorporation rate for soybeans from the IAEA EMRAS I WG2 soybean scenario [7]. It can be seen that the total incorporation rate reaches a maximum at the beginning of August, the best time for photosynthesis/temperature for a well-developed canopy. The incorporation rate remains relatively stable for leaves after blooming. Most of the incorporation to pods and grain is done by transfer from the leaves. This is typically plant dependant and a data base characterizing the physiology of the different plants eaten by the population is required to model the process.

These translocation mechanisms are important, as edible parts of the plants are generally accumulation organs in the form of grains, tubers or fruits. These organs will accumulate organic matter labelled through the air-plant and soil-plant pathways in great part. Generally, these edible parts contain more dry organic matter than leaves and will be eaten for quite a long time after harvest.

2.9. TRITIATED ORGANIC MATTER PRODUCED DURING THE NIGHT

Nighttime is a special case of OBT formation for which relatively large differences in models still exist. Some models do not take into account any incorporation of tritium at night because the plant stomata are closed and photosynthesis does not occur. Some other models make no difference between night and day, because some chemical reactions exist during the photosynthesis dark phase, because stomatal closure is not absolute and some transfer occurs through the cuticle, and, lastly, to adopt a “conservative approach”.

A few experimental studies show that some tritium incorporation occurs at night, but the OBT concentration reached seems to be lower than during the day. Many explanations may be given:

- It is clear that many chemical reactions exist during the night, and that some hydrogen is directly bound to carbon. Nevertheless, the temperature is lower during the night and this limits the speed of the chemical synthesis.
- The amount of tritiated organic matter formed during the night depends on the integrated concentration of free water in the plant. Because the exchange velocity between air and free water is smaller at night than during the day, the maximum concentration reached at the end of a nighttime release, and the integrated activity, is smaller. This can also be the case during the discharge phase, especially when exposure occurs at the end of the night.
- Enough tritiated water remains in the plant at the end of the night to be incorporated in the morning.
- The exchange of hydrogen and tritium in organic matter occurs quickly at night, and the measurement of exchangeable and non-exchangeable tritium is not so easy.

For all these reasons, it is recommended that the incorporation rate of tritium into plant organic matter at night be determined with the same equation as applies during the day, but using the night temperature and the nighttime value of the exchange velocity between air and plant free water.

2.10. ANIMALS

In this section, a quite complete overview of the dynamic models for tritium transfer to animal products is presented (see Section 10). The purpose here is to describe all the processes that apply after an accidental release.

In the case of an accidental release, animals will be exposed to tritium over a very short period, partly by inhalation but more importantly by the ingestion of grass if the animals are grazing. The product of interest is then milk, for both cows and sheep. The free water and exchangeable organic tritium of the grass, resulting from the air pathway, will be incorporated mainly within the first day and will follow the water cycle in the animal with a turnover of 2–4 days. So the milk of grazing animals will contain HTO from the air pathway with a maximum reached on the second or third day and a decrease over the following 2 or 3 weeks.

The animal will continue to incorporate tritiated organic matter via grass ingestion for the entire time of the pasture cycle (2–3 months), and also water and tritiated organic matter from the soil. This last pathway has a decay period of some weeks, so an equilibrium between soil, grass and animal will eventually be reached and the concentration of the milk water will be the concentration of the intake water.

Nowadays, animals do not often graze, but rather are fed grass that is grown remotely in industrial farming areas and shipped to the cattle. Animals are then protected against immediate contamination. The choice of uncontaminated grass is then an easy way to reduce contamination.

Here again, it is useful to consider separately tritiated water and tritiated organic molecules ingested by the animals. For dosimetric purposes, it is possible to assess the integrated activity of milk and meat from the global intake by the animals, using the transfer factors presented for normal conditions [8]. Nevertheless, this approach does not address the instantaneous activity of milk and meat, and is useful only if no countermeasures are applied.

The proposed model explicitly takes into account transfers from HTO in the diet to HTO and OBT in the product, and from OBT in the diet to HTO and OBT in the product. It is expressed in terms of transfer coefficients; the equilibrium activity concentrations of HTO and OBT in fresh weight animal products are given by:

$$CI_{afw}^{HTO} = F_{HH} \cdot II^{HTO} + F_{OH} \cdot II^{OBT} \quad (10)$$

$$CI_{afw}^{OBT} = F_{HO} \cdot II^{HTO} + F_{OO} \cdot II^{OBT} \quad (11)$$

where:

- CI is the integrated concentration in the product (Bq d kg⁻¹);
- F_{HH} is the transfer coefficient from HTO in diet to HTO in animal product (d kg⁻¹ FW);
- F_{HO} is the transfer coefficient from HTO in diet to OBT in animal product (d kg⁻¹ FW);
- F_{OH} is the transfer coefficient from OBT in diet to HTO in animal product (d kg⁻¹ FW);
- F_{OO} is the transfer coefficient from OBT in diet to OBT in animal product (d kg⁻¹ FW);
- II^{HTO} is the total animal intake of HTO (Bq); and
- II^{OBT} is the total animal intake of OBT (Bq).

The dose to man following ingestion of animal products is given by

$$H_{man} = (CI_{afw}^{HTO} \cdot DF_{HTO} + CI_{afw}^{OBT} \cdot DF_{OBT}) \cdot I_{man} \quad (12)$$

where:

- I_{man} is the daily intake of milk or meat by man; and
- H_{man} is the corresponding effective Dose.

In practice, as was seen in an intercomparison exercise undertaken by the Tritium and C-14 Working Group (herein referred to as the EMRAS I WG2) of the EMRAS I programme, milk and meat are not the major exposure pathways in case of an accident and do not need countermeasures for a release of up to 10 g of HTO [4]. One reason is probably that tritium concentrations in the animals are diluted by the large quantities of uncontaminated water that they drink; another is that the biological turnovers in the animals are relatively speedy.

2.11. CONCLUSIONS

Figure 2 illustrates the evolution of tritium activity in vegetables per square meter versus time following an accidental HTO release to the atmosphere, considering the two pathways (air and soil) and the two chemical forms (tritiated water and tritiated organic molecules). We can see that different mechanisms occur at different times, HTO contributing a big part of the dose in the short term and OBT at longer times. This effect is reinforced by the consumption of foods such as potatoes and grains, which are eaten for many months after harvest.

Figures 3 and 4 present some results of the EMRAS I WG2 intercomparison exercise for the dose 1 km downwind of a release of 10g of tritiated water [4]. All the different pathways contribute to the total dose, and are differently estimated by the different models and/or modellers. It is also interesting to note that the soil pathway seems to be as important as the air pathway.

The incorporation rate of H in organic material is the single most important parameter in determining dose following an accidental release of tritium to the atmosphere.

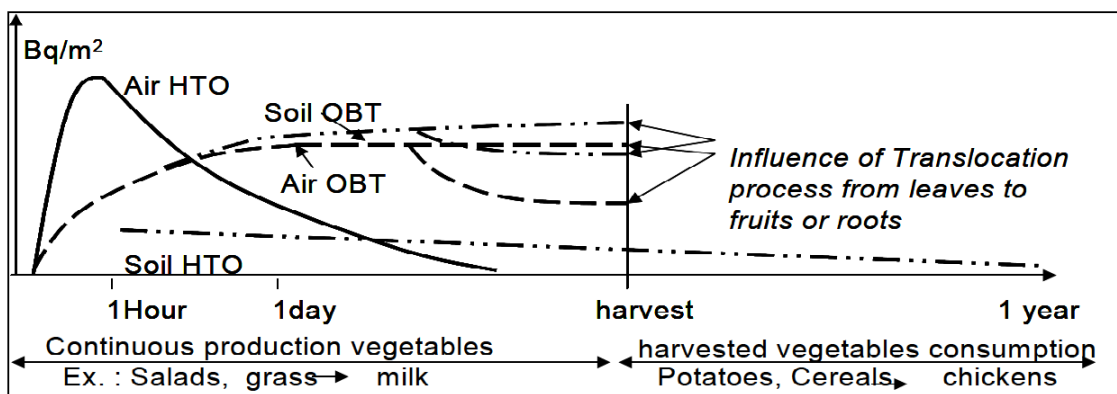


FIG. 2. Evolution of activities by different pathways.

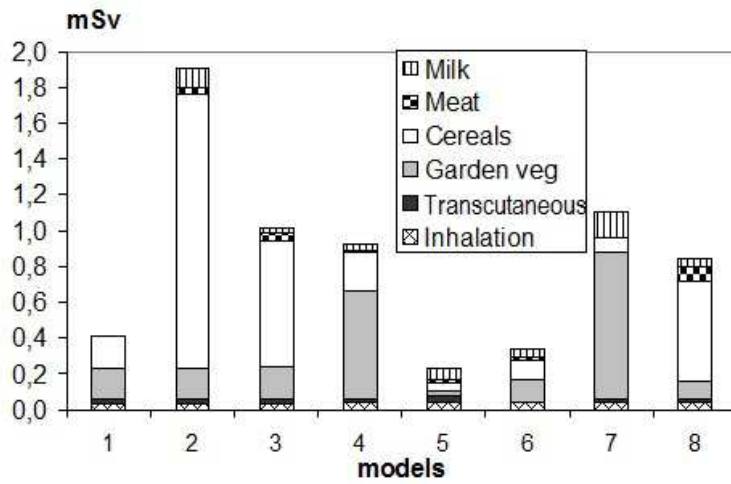


FIG. 3. Dose details by pathway (normalized air concentration) for a release on a sunny day.

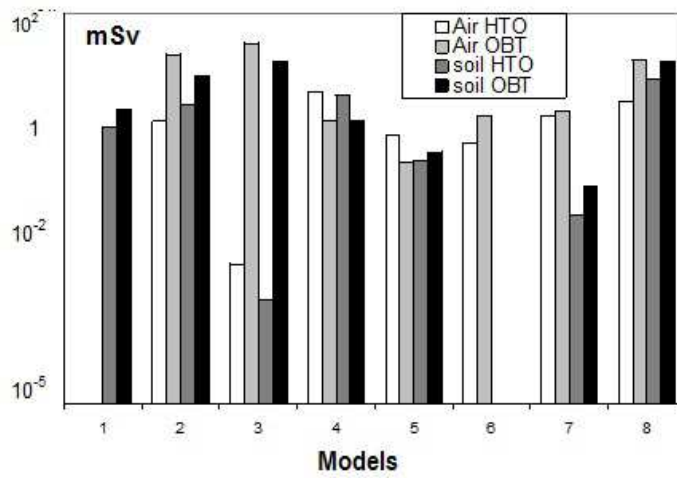


FIG. 4. Dose details by pathway and by the chemical nature of tritium.

3. INTERACTION MATRICES AND ASSOCIATED PROCESSES FOR TERRESTRIAL PATHWAYS OF TRITIUM TRANSFER

3.1. OVERVIEW

This section presents a preliminary analysis of the important features, events and processes (FEPs) that are relevant in modeling the behaviour of terrestrial agricultural systems in response to accidental releases and time-varying environmental conditions. Accidental release involves an emission lasting from a few minutes to less than 2 days. It is characterized by less than 1 g of tritium released at ground level (or less than 10 g of tritium released at stack level). The focus of the analysis is an aqueous and gaseous release of tritium into agricultural systems under various climates and agricultural practices.

FEPs are terms used to define the relevant scenarios, whereby:

- Features include the components of the site, such as soil and water bodies;
- Events include incidents that may occur on the system, such as climatic changes, agriculture practice, etc;
- Processes include those things that are ongoing, for example irrigation of agricultural land, percolation, etc.

For completeness, all participants were involved in this analysis in order to get a recognised generic list that takes into consideration all the potentially relevant FEPs of the system. It was necessary to audit the list so that modellers can more transparently explain their conceptual models for tritium. Indeed, they can compare and review which FEPs are considered in their model, and why, if applicable, certain FEPs have been disregarded.

Interaction matrices (IMs) have been developed from this analysis, forming the basis for conceptual models for the assessment of terrestrial pathways of tritium transfer.

3.2. METHODOLOGY

The methodology used for our analysis was already defined in several projects such as the BIOSpheric Model Validation Study (BIOMOVs II) [9, 10] and BIOPROTA [11]; the following steps are used to carry out the FEP audit and the subsequent conceptual model development:

- (1) Refine the FEP list from the generic list, by screening those that are relevant to the specific question that the model is supposed to address;
- (2) Choose a set of key conceptual model objects (CMOs), which make up the leading diagonal elements of the IM;
- (3) Go through all the off-diagonal elements (ODEs) to identify processes that affect transfer of tritium among those CMOs. This can be done in two steps:
 - (a) Consider each leading diagonal element in turn and how tritium might be transferred to other leading diagonal elements;
 - (b) Check that all the FEPs in the refined list are somewhere in the IM, or explain why the FEP is not included in the IM.
- (4) This process may identify redundant leading diagonal elements or the need to create new leading diagonal elements, such that step 3 may need to be repeated.

By doing so, we get a conceptual model: a non-quantitative description of components in the environment and the processes of tritium transfer between them.

The mathematical model development and the search for data to support parameter value choice then follows on from this FEPs analysis and conceptual model development. Where data gaps are highlighted, this may signal the need to go back and simplify the processes being modelled, or the need to instigate a research program.

3.3. INTERACTION MATRICES OF TERRESTRIAL PATHWAYS OF TRITIUM TRANSFER

3.3.1. Assessment context

The site context is any agricultural ecosystem. Differences between temperate or tropical ecosystems should be noted. The source could be in groundwater or in the atmosphere (in gaseous form). The current context assumes acute releases of tritium, which may occur in the form of HTO or HT.

3.3.2. Biosphere system features

Agricultural environments include living components (e.g. animals, plant materials) and non-living components (soil water, soil and canopy atmosphere). Climate impact is assessed for temperate and other climatic zones.

3.3.3. Conceptual model objects

The conceptual model objects (CMOs) that were identified and located in the IMs are described in Table 2.

It is considered that soil could be broken down into two layers: an upper layer (UL), which is subject to ploughing, and a lower layer (LL), which is not normally disturbed by human activity. Relevant soil features are similar for both layers.

Soil macrobiota, soil organic matter and mycorrhizae are not considered for inclusion as a CMO in the context of accidental release. We assume they all play a negligible role in our current acute release scenario. Soil microbes are not considered explicitly either, although they are responsible for the process of HT oxidation to HTO in the soil, in the case of an HT atmospheric release. Rather than including soil microbes as an explicit CMO, their presence is implicit in the inclusion of the process “Oxidation (HT to HTO)” in the soil layer interaction matrix (Table 3).

Tritium is readily incorporated in the form of tissue water (HTO) in biological organisms. This fraction is particularly important in plants, whose water content is 80–95% of fresh weight, depending on species and stage of development considered. In the model, the plant compartment is represented by a water compartment (including HTO) and a dry matter (including organic ³H) compartment in both belowground and aboveground plant material (Table 3). A distinction should be made between the foliar system and edible plant organs, which are intended for human or animal consumption (leaves, grains, fruit, root or tuber).

TABLE 2. CONCEPTUAL MODEL OBJECTS

Conceptual model object	Description
Source	Gas: tritiated water (HTO) and tritiated hydrogen (HT). Specific flux rates would need to be defined for a specific scenario. Water: Groundwater contaminated with HTO, used for irrigation and upwelling into soil of interest. Scenario specific flux rates would also need to be defined.
Soil water	Liquid water (HTO) in the soil pores. Agricultural soil (depth, texture, pH)
Soil gas	Tritiated water vapour in the soil pores
Plant canopy atmosphere	Within the canopy (with or without lateral air flow)
Belowground plant material	Liquid water (HTO) and dry matter (OBT) in roots.
Aboveground plant material	Liquid water (HTO) and dry matter (OBT) in leaves, stems, fruits and grains
Animal water	Liquid water (HTO) in the animal
Animal dry matter	Dry matter (OBT) of the animal
Sink	Anything outside the system of interest

3.3.4. Tritium interaction matrices

The interaction matrix that has been developed for a water source or a gas source scenario is given in Table 3. The two soil layers are considered further in Table 4, including how they interact with each other; the yellow boxes indicate the lower soil layer (LL) and the grey boxes indicate the upper soil layer (UL). The interaction matrix for animals is given in Table 5. Metabolic processes in animals are also described by considering the two compartments, water and dry matter, of the animal (Table 5). A general tritium interaction matrix for the terrestrial environment is given in Table 6.

3.4. DESCRIPTIONS OF EVENTS AND PROCESSES

In this section, descriptions of the events and processes within the interaction matrices are given, as well as how they relate to tritium behaviour in the biosphere.

3.4.1. Aerenchyma

Aerenchyma are inter-connected gas-filled pathways found in some plants, e.g. rice, which grows on water logged soils. They are a potential route of transport for water vapour from soil atmosphere to plant tissues.

3.4.2. Bioturbation

One of the agents of organic weathering, bioturbation is the disturbance of the soil or sediment by living organisms. It may include displacing soil by plant roots, digging by burrowing animals (such as ants or rodents), pushing sediment aside (such as in animal tracks), or eating and excreting sediment, as earthworms do. Bioturbation aids the penetration of air and water and loosens sediment to promote winnowing or washing (transportation).

TABLE 3. GAS OR WATER SOURCE INTERACTION MATRIX FOR H³

	A	B	C	D	E	F	G	H
1	SOURCE (Gas)		Wet deposition Sprinkler irrigation Interception by soil	Advection/diffusion			Wet input Interception by plant	
2		SOURCE (Water)	Irrigation (Infiltration) Upwelling Capillary rise				Interception of irrigation water	
3		Percolation	SOIL WATER	Diffusive exchange	Evaporation	Root uptake		Percolation to groundwater Surface run-off
4			Gas sorption Diffusive exchange	SOIL ATMOSPHERE	Diffusion	Root uptake	Aerenchyma	
5					CANOPY ATMOSPHERE		Foliar Uptake (HTO) Gross photosynthesis (OBT) Oxidation (HTtoHTO) (if HT gaseous release)	Free air
6				Root respiration		BELOWGROUND PLANT MATERIAL	Translocation (assuming root uptake)	Cropping loss
7					Transpiration Foliar respiration	Translocation	ABOVEGROUND PLANT MATERIAL	Cropping loss Weathering
8				Oxidation (HTtoHTO) (if HT gaseous release)				SINK

TABLE 4. SOIL LAYER INTERACTION MATRIX (WATER SOURCE)

	A	B	C	D	E	F
1	SOURCE (gas)				Wet deposition Sprinkler irrigation Interception by soil	Advection/diffusion
2		SOURCE (Water)	Upwelling		Infiltration (Irrigation)	
3		Percolation	SOIL WATER	Diffusive exchange	Capillary rise (HTO)	
4			Gas sorption	SOIL ATMOSPHERE		Diffusion/advection
5	Evaporation		Percolation		SOIL WATER	Diffusive exchange
6				Diffusion	Gas sorption	SOIL ATMOSPHERE

Yellow boxes indicate the lower soil layer (LL) and grey boxes indicate the upper soil layer (UL).

TABLE 5. TRITIUM INTERACTION MATRIX FOR ANIMALS

	A	B	C	D	E	F	G
1	ATMOSPHERE				Inhalation		
2		SOIL			Ingestion	Ingestion	
3			PLANT MATERIAL		Ingestion	Ingestion	
4		Excretion Death and decomposition	Excretion	ANIMAL	Translocation H metabolism		
5	Exhalation	Inhalation (burrowing animals)			WATER		Excretion
6						DRY MATTER	Excretion Death and decomposition
7							SINK

Animals are described by considering two compartments: water (HTO) and dry matter (OBT).

TABLE 6. A GENERAL TRITIUM INTERACTION MATRIX FOR THE TERRESTRIAL ENVIRONMENT

ATMOSPHERE	Deposition		Deposition and interception Gross photosynthesis	Gross photosynthesis		Inhalation		Dry deposition Precipitation Interception		
Evaporation Droplet production	WATER BODIES		Root uptake irrigation			Ingestion		Irrigation Recharge by surface waters	Release from solution	Recharge by surface waters
		VEGETATION (ABOVE - BELOWGROUND)				Ingestion				
Respiration Transpiration	Senescence and death		WATER						Root respiration	Biological weathering
Respiration Leaf fall Release of other organic compounds				DRY MATTER					Root respiration	Litterfall Senescence and death Biological weathering
	Excretion Death	Excretion			ANIMALS	Translocation H metabolism	Translocation			
Exhalation						WATER	OBT formation	Excretion	Inhalation (burrowing animals)	Excretion
							DRY MATTER			Excretion Death and decomposition
Evaporation	Groundwater recharge		Root uptake		Ingestion			SOIL WATER	Diffusive exchange	Surface run-off
Diffusion			Root uptake Transport in aerenchyma					Diffusive exchange	SOIL ATMOSPHERE	Diffusive exchange
Resuspension Diffusion	Desorption	External contamination Irrigation			Ingestion Bioturbation			Diffusion Advection Colloid transport	Diffusive exchange	Interface with geosphere

Processes in bold are of potential importance for tritium.

3.4.3. Capillary rise

Capillary rise is the upward movement of water through soil layers above the water table. This process arises as a result of capillary forces relating to evaporation and transpiration. Capillary rise is important in the overall water and nutrient dynamics in soil–crop systems and is a potential transport route of HTO from groundwater to the soil rooting zone.

3.4.4. Cropping loss (plants – animals)

Potentially, cropping provides an important removal process, at least for plants with rapid root uptake. Some models may conservatively ignore this process based on the assumption that radionuclides taken up into crops would eventually be returned to the same soil through a variety of processes (including plant senescence and degradation or animal excretion).

3.4.5. Death and decomposition

The death of animals or plants (e.g. plant roots) leads to the release of radionuclides to the immediate environment during decomposition. During plant senescence and decomposition, changes in the location and chemical form of tritium may occur (e.g. transfer from above ground to below ground storage organs during senescence or incorporation within detritivorous animals or decomposing micro-organisms).

3.4.6. Deposition (wet and dry)

HTO atmospheric deposition on vegetation and deposition on soil are determined similarly in the models, using a deposition velocity, an exchange coefficient (see diffusive exchange) or a net deposition modelled by constant transfer coefficients.

Deposition velocities for dry deposition are the following:

- HT dry deposition velocity to the soil surface is about $4 \times 10^{-5} - 4 \times 10^{-3} \text{ m s}^{-1}$;
- HTO dry deposition velocity to the soil surface is about $10^{-3} - 10^{-2} \text{ m s}^{-1}$.

The deposition velocities follow Fick's law and depend on soil composition, soil humidity, land cover, etc.

In the case of wet deposition during rain, we must emphasize that:

- HT solubility is very weak. Deposition is negligible
- HTO solubility is important. HTO is exchanged with H₂O in rain drops.

To estimate HTO wet deposition, the specific activity of rain water must be calculated using a washout rate or a washout coefficient

3.4.7. Diffusion or diffusive exchange

Diffusion is a physical process whereby material moves under the influence of a concentration gradient, resulting in a net flux from high to low concentration regions.

Water-air diffusive exchange can be a significant environmental transport pathway, notably in the soil-solution to soil-atmosphere phase.

Diffusive exchange may also include an exchange process between the net tritium in water from the soil surface and atmospheric water vapor. This exchange involves transport of tritiated water vapor to the surface and an exchange between tritiated water and light water [12–15], and implicitly takes into account the evaporation process [12]. The exchange rate is used in place of a deposition rate to estimate the contribution to ground contamination by dry deposition [12].

The mean value for the exchange velocity is 0.015 m s^{-1} [14].

Strictly speaking, this parameter depends on day-night variations (with higher values during the day than at night) and on the type of vegetation (which may provide additional resistance to the transfer of water vapor). It gradually decreases when exposure is prolonged [14, 15].

3.4.8. Discharge from below (upwelling)

In assessing the discharge of HTO in groundwater from below, the chemical processes associated with changes in redox conditions should be considered as groundwater migrates from sub-soil to surface soil.

3.4.9. Erosion

Erosion is the process of transporting solids (sediment, soil, rock and other particles) in the natural environment and depositing them elsewhere. Erosion is not a tritium specific issue. It should be included in models if the site context suggests that wind or surface run-off occurs. Erosion is distinguished from weathering, which is the process of chemical or physical breakdown of the minerals in the rocks, although the two processes may occur concurrently.

In general, given similar vegetation and ecosystems, areas with high-intensity precipitation, more frequent rainfall, more wind, or more storms are expected to have more erosion. Sediment with high sand or silt contents and areas with steep slopes erode more easily, as do areas with highly fractured or weathered rock. The porosity and permeability of the sediment or rock affect the speed with which water can percolate into the ground. If the water moves underground, less runoff is generated, reducing the amount of surface erosion. Sediments containing more clay tend to erode less than those with sand or silt.

3.4.10. Evaporation

Evaporation is the transfer of water from the ground directly to the atmosphere, including the transfer of tritium in the form of HTO. In some models, evaporation is treated in the equation describing deposition. When it is treated in a separate module, models include either constant transfer coefficients or a rate of reemission (i.e. the ratio of the amount of HTO re-emitted over time to the total quantity of HTO deposited, generally expressed in % per unit of time). Other models that rely on complex calculations of energy balances to estimate the flux of tritiated water vapour from soil require the determination of a large number of micro-meteorological parameters, including field measurements difficult to achieve.

3.4.11. Excretion

Excretion represents the process by which waste products of metabolism and other non-useful materials are eliminated from an organism. Models simulating tritium behavior in animals may differ in the value of the elimination rate of tritium from the animal.

3.4.12. Exhalation (or expiration)

Exhalation represents the loss of tritium from the animal gaseous phase to the external environment during breathing. Exhalation has a complementary relationship to inhalation; the cycling between these two processes defines respiration.

3.4.13. Foliar uptake

Foliar uptake is an important pathway to consider for atmospheric tritiated water uptake in the soil-plant system through leaf absorption. Tritium as tritiated hydrogen (HT) is not absorbed by vegetation because of its very low solubility in water.

The absorption of atmospheric tritiated water by leaves is based on the diffusion of vapour through the stomata. This diffusive process is controlled by weather conditions (temperature, humidity, light) and physiological characteristics of the plant (size and density of stomates, hormonal factors).

Stomatal resistance plays an important role as the plant is subjected to conditions of darkness or drought, leading to closure of the ostiole. Because of the different degrees of stomatal closure, an acute presence of ^3H in the plume when the latter passes above the plant during the day is likely to have a different radioecological impact on plants than if the plume passed during the night with the same ^3H concentration. Consequently, the determination of stomatal resistance is essential to estimate the incorporation of atmospheric HTO by leaves in response to an intermittent presence of the contaminated plume.

3.4.14. Gas sorption

Tritium in soil gas may dissolve in soil water.

3.4.15. Gross photosynthesis and growth

A fraction of tritium is incorporated into plant organic matter (OBT) through the process of photosynthesis following transport across the stomata. Absorption of HTO in irrigation water reaching plant leaves and subsequent incorporation into plant material by photosynthesis cannot be precluded.

Net photosynthesis results implicitly in the balance between synthesis of biomass (photosynthesis or gross primary production) and degradation of biomass (foliar respiration).

In models, the processes of formation and elimination of organic tritium in plants are described using transfer coefficients (constant or variable with environmental conditions) or by the use of plant growth curves. However, values of the parameters necessary for accurate prediction of transfers are rare, particularly for acute releases. The highly variable behaviour of tritium as a function of exposure duration, environmental parameters (humidity, plant water status, day / night timing of the release) means that a given experiment yields only parameter values specific to the conditions under which the experiment took place. Generalization to other conditions is difficult.

3.4.16. H metabolism

Hydrogen metabolism is the process whereby the organic hydrogen of food is metabolized within living organisms.

3.4.17. Infiltration

Infiltration is the process by which HTO present in contaminated rain or irrigation water enters soil. The infiltration rate of water in soil depends on several characteristics such as water supply (by rain or irrigation), type of vegetation covering the soil and soil depth. Its minimum value is given by the hydraulic conductivity of saturated soil.

The balance of infiltration, run-off and evaporation is determined by a number of factors including soil type, topography, climate and rate of input. For most controlled systems, run-off is likely to be negligible.

3.4.18. Ingestion

Ingestion is the incorporation of tritium into animals, micro-organisms or soil macro fauna as a result of food or water intake.

For tritium in animals, ingestion pathways may include ingestion of water and organic matter derived from plants in the field (pasture grass) and consumer products intended for animal feed (corn silage, hay, etc.). Another source of contamination may also be drinking water.

3.4.19. Inhalation

Inhalation is the incorporation of tritium water vapour as a result of breathing. See also Section 3.4.12.

In the case of atmospheric releases of short duration, most models consider the ingestion of food (mainly grass) and absorption by inhalation as the main routes of tritium incorporation in animals.

3.4.20. Interception

Interception by vegetation can be defined as the fraction of the wet deposit retained by plants covering the ground. Indeed, radionuclides dissolved in rain or in groundwater applied to plants via spray irrigation may be intercepted by plant aerial parts, thus preventing direct transport of water (and HTO) to the soil. Interception is a process that is accounted for in most current models. It is particularly important for direct contamination of crops such as green vegetables whose edible parts can directly intercept contamination. The interception efficiency depends more on the nature of the deposit, the plant species, the development stage and the biomass density of vegetation than on the radionuclide considered [16]. Chadwick and Chamberlain [17] and Chamberlain [18] described the relation between the interception fraction (f) and the vegetation biomass (χ_p , in kg FW.m⁻²) by the following equation:

$$f = 1 - \exp(-\mu \times \chi_p) \quad (13)$$

where μ (m² kg⁻¹) is the interception coefficient.

HTO in intercepted water may bind to plant material leading to surface contamination or be taken up through the stomata and incorporated into organic plant material. Alternatively, intercepted water and HTO may subsequently be deposited in soil as a result of plant run-off.

3.4.21. Irrigation

Irrigation represents the use of abstracted water (containing HTO) to supplement natural water supplies to agricultural crops. Irrigation may involve the spraying of water directly onto plants or the application to soils (surface soil or flood irrigation).

3.4.22. Micro-organism metabolism and assimilation

Micro-organisms play an important role in the environmental fate of many elements, with a multiplicity of physico-chemical and biological mechanisms affecting changes in mobility and speciation. Physico-chemical mechanisms of removal include adsorption and ion exchange.

Microbial activity may be particularly important for the gas scenario, whereby ^3H enters the soil in the form of HTO, HT or CH_3T . Tritiated hydrogen (HT) undergoes microbial oxidation when it enters the ground, and then behaves as tritiated water (HTO), being rapidly re-emitted to the atmosphere or transferred to deeper soil layers. We do not know about the fate of the CH_3T form and still less about any other organic forms. Some degree of assimilation of tritium into microbes may occur as a result of the CH_3T metabolic process.

Microbial activity is dependent on a number of factors including nutrient availability. Thus nutrient deficient soils may have a slower rate of microbially-induced speciation than nutrient-rich soils.

3.4.23. OBT formation

This process covers the formation of OBT from tritiated water present in the animal. This formation rate may have very different values in models. More generally, models may differ in their assumptions regarding the main mechanism for OBT formation: OBT intake or metabolic processes within the animal.

3.4.24. Oxidation (HT to HTO)

In all cases contamination of plants by tritium gas (HT) by direct oxidation of plant surfaces is very low and the processes are dominated by HT oxidation in soil (see Section 5.3). Due to the rapid oxidation of HT to HTO in soil, the mechanism of HT transfer from the environment to plants can be roughly associated with HT transfer from soil to plants.

3.4.25. Percolation

This is the process by which tritium in soil water moves downwards into deeper horizons. The losses by vertical migration may be described by using constant transfer coefficients or by classical equations of migration, or by a combination of both approaches.

3.4.26. Ploughing

This farming practice is used for initial cultivation of soil in preparation for sowing seed or planting. Its primary purpose is to turn over the upper layer of the soil, bringing fresh nutrients to the surface while burying weeds and the remains of previous crops, allowing them to break down. It also aerates the soil, and allows it to hold moisture better.

3.4.27. Precipitation

The rate of precipitation drives water flow from the soil surface to depth and acts to dilute HTO in groundwater. Precipitation of water may inhibit release of HTO in the gas phase.

3.4.28. Resuspension

This process represents the renewed suspension of insoluble particles after they have been precipitated.

3.4.29. Root uptake

Water absorption by roots of plants involves the transfer of tritium from the soil. Tritiated water generally follows the same biological pathways as water within plants. Tritiated water in the soil is absorbed and transported in the xylem by a movement of "mass flux" due to an energy gradient associated with the evaporation of water from the leaves. This route of exposure to tritium is highly dependent on the concentration and distribution of tritiated water in soil and soil characteristics (structure, texture, water content and so on). The transfer is also likely to be modulated by the plant species considered, its stage of development and the condition of its root system. In models, root uptake of HTO is generally assumed to be equal to foliar transpiration, taken into account by exchange rates determined from differences in humidity, or described using constant transfer coefficients. The root uptake of OBT is negligible because of the small pool of soil organic tritium. In general, in cultivated soils characterized by low humus content (1–5%), organically bound tritium is mostly negligible. However, in soils containing high humus content (organic matter content above 10%), the degradation of organic molecules may be a secondary source of tritium for plants, which remains however low. All available data indicate that soil is not a compartment where organic tritium accumulates, unlike what is observed for most other radionuclides. Photosynthesis is assumed to be the main process responsible for the incorporation of OBT in plants following sprinkler irrigation using contaminated water.

3.4.30. Root respiration

Respiration in root tissues may lead to the release of tritium in the form of HTO into the soil atmosphere.

3.4.31. Surface run-off

Surface runoff is the water flow that occurs when soil is infiltrated to full capacity and excess water from rain, melt water, or other sources flows over the land. This is a major component of the hydrologic cycle. It more commonly occurs in arid and semi-arid regions, in paved areas, or where rainfall intensities are high and the soil infiltration capacity is reduced because of surface sealing. Surface runoff causes erosion of the soil surface.

3.4.32. Translocation

In plants, translocation involves the transfer of tritium in the form of HTO from one part of a plant to another. It is a process taken into account in most current models.

In animals, translocation stands for the allocation of radioactive contamination in the water or dry matter pools of the different organs, once ingested by the animal.

3.4.33. Transpiration

Transpiration is a process similar to evaporation and occurs through stomata. It is the loss of water vapor from parts of plants, especially from leaves but also from stems, flowers and roots. The rate of transpiration is directly related to the degree of stomatal opening, and to the evaporative demand of the atmosphere surrounding the leaf. The amount of water lost by a plant depends on its size, along with surrounding light intensity, temperature, humidity and wind speed (all of which influence evaporative demand). Soil water supply and soil temperature can influence stomatal opening, and thus transpiration rate.

Conservative values of the average flow transpired by plants range from around 2×10^{-8} to $3 \times 10^{-8} \text{ m}^3 \text{ m}^{-2} \text{ s}^{-1}$ [19].

3.4.34. Weathering

Weathering is the breaking down of rocks, soils and minerals through direct contact with the atmosphere. Weathering occurs *in situ*, or “with no movement”, and thus should not be confused with erosion, which involves the movement of rocks and minerals by agents such as water, ice, wind, and gravity. Weathering involves the loss of tritium from the system. It can involve loss of superficial tritium from leaf surfaces or physical loss of tritium associated with surface soils as a result of atmospheric processes.

3.5. CONCLUSIONS AND WAY FORWARD

The interaction matrices presented here provide a list of FEPs against which models can be audited. They help to support information used in the wider case, and provide the modeller with an opportunity to clearly demonstrate which processes have been included in each model, and how, as well as justification for the exclusion of any processes from the model. Interaction matrices also provide a basis for comparison between models. FEPs have been applied here on the basis of our own understanding and modelling approaches.

4. WASHOUT OF ATMOSHERIC TRITIUM

4.1. OVERVIEW

Washout of HTO by precipitation is the principal process resulting in wet deposition. During precipitation, HTO that exists in the atmosphere dissolves into falling raindrops and is removed from the atmosphere. It can also be scavenged by all other atmospheric hydrometeors such as cloud and fog drops, and snow. HTO is consequently deposited to the ground. For wet removal, three steps are necessary. HTO must first be brought into the presence of condensed water. Then, HTO must be scavenged by the hydrometeors, and finally it needs to be delivered to the ground. Figure 5 shows the conceptual framework of wet deposition processes for aerosols and gases [20]. Washout is a reversible process. Once HTO is scavenged, raindrops can evaporate before reaching the ground.

Rainout refers to in-cloud scavenging by cloud droplets or ice crystals. *Washout* refers to below-cloud scavenging by precipitation. The traditional goal of HTO washout studies is to determine the washout ratio:

$$Wr = \frac{C_f}{C_g(1)} \quad (14)$$

and the washout coefficient (rate):

$$\Lambda = Wc = \frac{J}{HTO}, \text{ (s}^{-1}\text{)} \quad (15)$$

where:

\overline{HTO} is the amount of HTO in an air column with unit cross-sectional area (g cm^{-2});
J is the flux of liquid HTO at the ground surface ($\text{g cm}^{-2} \text{s}^{-1}$);
 C_f is the mass concentration of liquid HTO in the falling rain water (g cm^{-3}); and
 C_g is the concentration of vapour phase HTO in the drop's environment (g cm^{-3}) at 1 m reference height.

Rain concentrations are proportional to the vertical integral of tritium air concentration. In the case of gas scavenging, the factor of proportionality $\Lambda(x)$, otherwise called the washout coefficient or washout rate, is not constant throughout the plume as in the case of aerosols, but depends on the shape of the vertical tritium concentration profile, and hence on the distance from the source.

4.2. CALCULATION OF WASHOUT RATE

Washout rate (Λ) is usually defined by the Engelmann equation [21]:

$$F_{hto} = \Lambda \int C(z) dz \quad (16)$$

where:

Λ is the washout rate (s);
 F_{hto} is the HTO deposition rate ($\text{Bq m}^{-2} \text{s}^{-1}$);
C is the HTO concentration in air (Bq m^{-3}); and
z is the height above the ground (m).

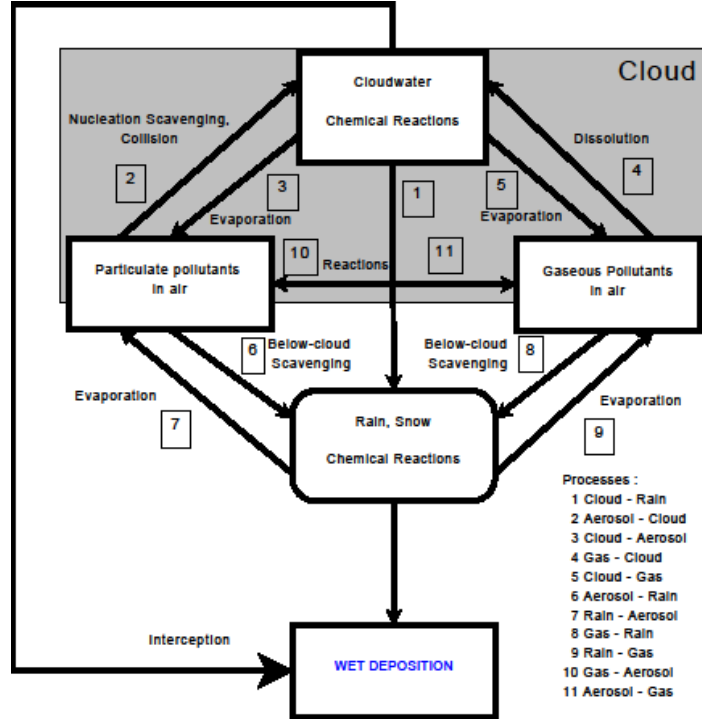


FIG. 5. Conceptual framework of wet deposition processes (taken from [20]).

The tritium deposition rate can be expressed as:

$$F_{hto} = C_p \times I_p \quad (17)$$

where:

I_p is the depth of falling precipitation collected over time (m s^{-1}); and
 C_p is the tritium concentration in precipitation (Bq m^{-3}).

$\int C(z)dz$ can be expressed by using a vertical tritium profile assumed to be Gaussian. In this case, the integral can be written as:

$$\int C(z)dz = \left(\frac{\pi}{2}\right)^{0.5} C_a \sigma_z e^{\left(\frac{H_{eff}^2}{2\sigma_z^2}\right)} \quad (18)$$

where:

C_a is the ground level tritium air concentration (Bq m^{-3}) at downwind distance x (m);
 σ_z is the vertical dispersion parameter; and
 H_{eff} is the effective release height (L).

The integral can also be expressed as:

$$\int C(z)dz = \chi_0 \times H_{eff} \quad (19)$$

where:

χ_0 is the atmospheric tritium concentration at ground level (Bq m⁻³).

The effective release height can be calculated using the dispersion equation [22]:

$$H_{eff} = \sum_s \frac{1}{\sqrt{2\pi}} \frac{Q}{\sigma_{ys} U_s} \frac{1}{\chi_{0,cal}} \quad (20)$$

where:

Q is the tritium release rate (Bq m⁻³);

σ_{ys} is the standard deviation of the tritium concentration distribution in the y direction (m);

U_s is the mean wind speed (m s⁻¹); and

$\chi_{0,cal}$ is the mean concentration (Bq m⁻³) calculated from the ground-level formula [23].

The subscript s refers to the atmospheric stability.

Therefore, washout can be expressed as:

$$\Lambda = \frac{C_p \times I_p}{\chi_0 \times H_{eff}} \quad (21)$$

The washout rate can also be derived by field experiments measuring the depletion of the air concentration, χ as function of time.

$$\Lambda = \frac{1}{t} \ln \left[\frac{\chi(t=0)}{\chi(t)} \right] = \frac{\text{removal rate per unit volume and time}}{\text{HTO concentration per unit volume}} \quad (22)$$

where:

Λ is the washout rate (s);

t is the duration of rainfall or the sampling period (s); and

χ is the HTO concentration in the atmosphere (Bq m⁻³).

4.3. WASHOUT RATE FROM EXPERIMENTAL DATA

Washout rate has been calculated from experimental data by several authors, especially for rain but also for snow.

4.3.1. Washout by rain

In the state of Michigan (USA), tritium release from the Cook Nuclear Plant was studied by analyzing tritium vapour concentrations in samples of precipitation, air-conditioning condensate, surface water and well water. Tritium deposition by precipitation scavenging was determined from the tritium activity collected in rain water samples. Samples of atmospheric water vapor were also collected to determine the ground-level tritium concentration required for the washout coefficient [24]. Water vapour samples were collected far from the site to serve as a baseline for environmental tritium levels. The washout rate varied from $2.4 \times 10^{-5} - 1.5 \times 10^{-4} \text{ s}^{-1}$, with a mean value of $(9.2 \pm 8.4) \times 10^{-5} \text{ s}^{-1}$ for 15 data points.

In Fukui Prefecture (Japan), the washout rate was computed from available data on tritium concentrations in water vapour and rainwater for the years 1986–1992 in the Tsuruga area [25]. Rain water was sampled and measured monthly. The rainfall intensity observed was 2 mm h^{-1} . Samples of water vapour at ground level were collected continuously and analyzed monthly. The washout rate varied from $1.3 \times 10^{-5} - 1.6 \times 10^{-4} \text{ s}^{-1}$, with a mean value of $(7.3 \pm 4.1) \times 10^{-5} \text{ s}^{-1}$ for 29 data points.

In a different area of Japan, at Tokai village (Ibaraki Prefecture), the yearly average tritium deposition was calculated and compared [26] with observed data by using the following equation:

$$D = A \frac{N}{2\pi x} \sum q_{imt} \frac{\Lambda_t}{U_m} \quad (23)$$

with:

$$\Lambda = a \delta^b \quad (24)$$

where:

- D is the tritium deposition (Bq m^{-2});
- A is the tritium activity emitted (Bq);
- N is the number of wind direction sectors;
- x is the distance from the emitter (m);
- q_{imt} is the frequency of precipitation (where i is the wind direction sector and m is the wind speed level);
- t is precipitation intensity level;
- U_m is the wind speed (m s^{-1});
- Λ is the washout rate (s^{-1});
- a is a proportionality constant (m^{-1});
- δ is the precipitation intensity (m s^{-1}); and
- b is the power exponent.

Comparison of observed and calculated tritium deposition implied a proportionality constant of $8.2 \times 10^{-1} \text{ mm}^{-1}$; thus $\Lambda = 2.3 \times 10^{-4} \text{ s}^{-1}$ for a rainfall of 1 mm h^{-1} .

In the same way, rain water was collected and the tritium concentration determined at the Karlsruhe Nuclear Research Center (KfK) in 1982, 1983 and 1984 [27]. The proportionality constant used was $9.4 \times 10^{-2} \text{ mm}^{-1}$, leading to $\Lambda = 2.6 \times 10^{-5} \text{ s}^{-1}$ for a rainfall of 1 mm h^{-1} .

Weekly concentrations of tritium in air and in rain water were measured in the vicinity of the Savannah River Plant (South Carolina, USA) [28]. Experimental data and calculation of the height of the radioactive cloud for the observed meteorological conditions (81 m) allowed washout to be calculated. The authors concluded that a washout rate of $3.6 \times 10^{-4} \text{ s}^{-1}$ is a good estimate for a rainfall of 4 mm h^{-1} .

More recently, around the Paks Nuclear Power Plant (Hungary), rainwater was collected and analyzed for tritium [29]. Based on emission and meteorological data, a reversible washout model [30] was used to calculate the tritium concentrations, which were then compared with measured values. Washout rate were calculated only for samples above background levels and varied from $8.2 \times 10^{-6} - 1.9 \times 10^{-4} \text{ s}^{-1}$, with a mean value of $5.5 \times 10^{-5} \text{ s}^{-1}$.

In order to study the kinetics and mechanisms of HTO exchange between vapour and drops, experiments using a device for generating drops of specific size, a flight gap with known HTO concentration and a drop collector were performed [31]. In laboratory conditions, for a drop radius of 0.02 cm , the washout rate was $1.4 \times 10^{-4} \text{ s}^{-1}$.

In order to study HTO washout by rain,, an experimental project (Project 654) was performed [32]. Tritium was released through a stack 30 m high. Meteorological conditions such as wind speed, wind direction, air temperature and relative humidity were recorded at a weather station. During the experiments, rain characteristics such as rain intensity and drop size distribution were also recorded, together with the dependence of the fall rate of the drops on their diameter. The source parameters were measured and the volumetric activity of HT and HTO were known. The HTO activity was measured in the rainwater of 10 samplers that were installed downwind in a $\pm 45^\circ$ sector. The washout rate varied from $12.4 \times 10^{-5} - 18 \times 10^{-4} \text{ s}^{-1}$, with a mean value of $(14.5 \pm 2.1) \times 10^{-5} \text{ s}^{-1}$ for 4 data points.

4.3.2. Washout for snow

Based on data collected following an accidental release of HTO to the atmosphere from a reactor at Chalk River Laboratories in January 1991, the washout coefficient of HTO by falling snow was calculated [33]. Dispersion of the atmospheric plume was modelling using a simple Gaussian model in order to calculate the total amount of tritium deposited to the snow pack over the release period. This quantity was compared with the observed value to obtain a washout rate for snow of $(2.1 \pm 1.0) \times 10^{-5} \text{ s}^{-1}$. A literature review disclosed that washout rates for snow are scarce. A semi-empirical value of $2.6 \times 10^{-5} \text{ s}^{-1}$ has been reported for a snowfall rate of 1 mm.g^{-1} [34].

The diffusion and persistence of HTO in the snow pack was also observed [35]. In conditions of cold weather and dry snow, the diffusion coefficient lies in the range of $1 - 2 \times 10^{-10} \text{ m}^2 \text{ s}^{-1}$. This is an order of magnitude lower than diffusion in water, but an order of magnitude higher than self-diffusion in ice. In spring, when the snow melts, about 70 % of the initial fallout remains.

4.3.3. HTO deposition by fog

To the best of our knowledge, there are no experimental results on HTO deposition in foggy conditions, but some general considerations can be made. The properties of radiation and coastal fog are given in Table 7 [36].

A preliminary assessment of deposition in foggy conditions has been reported [37] using data for chemical pollutants. Minimum and maximum deposition velocities were recommended as a function of fog flux (Table 8). Typical fog fluxes are given in Table 9.

For cultivated land, typical values of the fog flux are near 0.05 mm h^{-1} . The dependency of droplet HTO concentration on drop radius [38] (Figure 6) can be used to estimate HTO deposition.

Figure 6 shows that the concentration in fog droplets is very close to that in air moisture. Deposition by fog is 2–3 times larger than that for rain of the same intensity.

4.3.4. Synthesis

Figure 7 shows a compilation of washout values from the literature. These values are computed from experimental work or based on models that take account of field measurements. The washout rate varies from $1.3 \times 10^{-5} - 3.6 \times 10^{-4} \text{ s}^{-1}$, with a mean value of $(9.2 \pm 5.8) \times 10^{-5} \text{ s}^{-1}$ for 54 data points. Much of the variation can be attributed to different tritium release characteristics and meteorological conditions.

In Table 10 some washout rates for different rainfall rates and different distances from the release source are given.

TABLE 7. CHARACTERISTICS OF COASTAL-ADVECTION AND RADIATION FOG [36]

Fog parameters at ground level	Radiation (inland) fog	Advection (coastal) fog
Average drop diameter	10 μm	20 μm
Typical drop size range	5–35 μm	7–65 μm
Liquid water content	110 mg m^{-3}	170 mg m^{-3}
Droplet concentration	200 cm^{-3}	40 cm^{-3}
Vertical depth of fog:		
Typical	100 m	200 m
Severe	300 m	600 m
Horizontal visibility	100 m	300 m
Nuclei:		
Size	0.08–0.8 μm	0.5 μm and greater
Type	Combustion products	Chlorides and nitrates

TABLE 8. DEPOSITION VELOCITY FOR FOG

Fog flux (mm h^{-1})	0.01	0.05	0.10	0.50	1.00	2.00
V_d (low) (cm s^{-1})	1	3	7	35	70	140
V_d (high) (cm s^{-1})	3	14	28	140	280	560

TABLE 9. FOG FLUX ON TYPICAL SURFACES

Flux	Soil	Snow	Water	Grass	Closed forest	Forest edge
F_{low} (mm h^{-1})	0.01	0.01	0.01	0.01	0.1	0.5
F_{high} (mm h^{-1})	0.05	0.05	0.1	0.1	0.5	2.

TABLE 10. WASHOUT RATES FOR DIFFERENT DISTANCES FROM THE RELEASE POINT FOR A RAINFALL RATE OF 0.6 MM H^{-1}

Distance from release (m)	Λ (s^{-1})
400	2.60×10^{-5}
800	1.86×10^{-5}

TABLE 11. PROPOSED WASHOUT RATES ACCORDING TO THE TYPE OF PRECIPITATION IN SIMPLE AND ROBUST HTO MODELS

Precipitation	Intensity (mm h^{-1})	Washout (s^{-1})
Drizzle-fog	all	no data
Light rain	$\leq 2.5 \text{ mm h}^{-1}$	$< 2.5 \times 10^{-4}$
Moderate rain	$2.6\text{-}7.6 \text{ mm h}^{-1}$	3.6×10^{-4}
Heavy rain	$> 7.6 \text{ mm h}^{-1}$	1.0×10^{-3}
Snow	all	2.2×10^{-6}

In addition to rain and snow, some types of liquid (sleet), solid (hail) or mixed precipitation can lead to wet deposition. Several precipitation classifications exist, but considering that existing experimental values are scarce, the simplest classification is proposed. According to the American Meteorology Society, precipitation may be classified as follows:

- **Drizzle-fog:** drops are generally less than 0.5 mm in diameter, and are very numerous;
- **Light rain:** the rate of fall varies between a trace and 2.5 mm h⁻¹, with the maximum rate of fall being no more than 0.25 mm in 6 minutes;
- **Moderate rain:** the rate of fall varies from 2.6 to 7.6 mm h⁻¹, with the maximum rate of fall being no more than 0.76 cm in 6 minutes;
- **Heavy rain:** over 7.6 mm h⁻¹ or more than 0.76 mm in 6 minutes;
- **Snow:** precipitation in the form of crystalline water ice of all sizes.

According to the experimental data, Table 11 gives an average value of the washout rate for each of these precipitation types.

4.4. DETAILED HTO MODELS

4.4.1. Generalized calculation of washout rate

Washout rate as a function of rainfall intensity is calculated using Eq. (24) by several authors (Figure 8). For a rainfall rate of 1 mm.h⁻¹, the washout rates given by Eq. (24) vary from $2.6 \times 10^{-5} - 2.27 \times 10^{-4} \text{ s}^{-1}$, which is in good agreement with the washout rate calculated from experimental data. The recommended values in 2002 were $a=6.10^5$ and $b=0.73$ [39].

4.4.2. Modelling of the HTO concentration in rain water

Several models are used to compute the wet deposition of tritium. The simplest model is based on a simple equation, $C_{rain} = \alpha C_a$. A sophisticated model, i.e. an Eulerian Stationary model, was developed by Atanassov and Galeriu [40].

Comparison between the simplest model results with the experimental data showed that the value $\alpha=0.4$ provides the best description of the averaged experimental data. At the same time, the value of α varies with wind speed; for speeds of 3 m s⁻¹, $\alpha = 0.35$, whereas for speeds of 6 m s⁻¹, $\alpha = 0.45$ [41].

4.4.2.1. Hales model

In order to calculate wet removal of pollutants from Gaussian plumes, basic linear equations and computational approaches were proposed by Hales [42]. The approach takes the form of a set of analytical equations that correspond to five kinds of Gaussian plume formulations: standard bivariate-normal point-source plumes, line-source plumes, unrestricted instantaneous puffs, and point-source plumes and puffs that experience reflection from inversion layers aloft. These equations represent the concentration of scavenged pollutants in falling raindrops and are similar in complexity to their associated gas-phase plume equations. They are strictly linear, thus allowing superposition of wet-deposition contributions by multiple plumes. Numerical solution and analytical approximation are given but up to now there is no direct application for tritium (HTO). The equation for gaseous pollutant scavenging from point-source plumes is based on the concept of the gas scavenging model developed by Chamberlain and Eggleton [22]:

$$\frac{dc(a, z)}{dz} = \frac{3K_y(a)}{v_z(a)a} [y_{AB} - H'c(a, z)] \quad (25)$$

where:

- C is the pollutant concentration with respect to height in a raindrop falling through a plume (Bq m^{-3});
- a is the raindrop's radius (m);
- H' is a solubility parameter ($\text{m}^{-3} \text{mol}^{-1}$);
- Y_{AB} is the mixing ratio of the pollutant in air ($\text{mol}_{\text{pollutant}} \text{mol}_{\text{air}}^{-1}$);
- V_z is the raindrop's vertical velocity (m s^{-1}); and
- k_y is an overall mass-transfer coefficient that can be estimated on the basis of physical properties.

The transfer of the pollutant to the drop from the gas phase is driven by the difference between the bulk gas concentration and the concentration at the drop surface:

$$c_{rain}(z) = \frac{4\pi n_0}{3\delta} \int_0^\infty a^3 n(a) v_z(a) c(a, z) da \quad (26)$$

where:

- n_0 is the total number of raindrops in a volumetric space (m^{-3});
- $n(a)$ is the associated probability density function for raindrops of size a (m^{-1}); and
- δ is the rain flux (m s^{-1}).

The wet-deposition flux of the pollutant approaching the surface at $z=s$ follows directly from the rain flux: $\text{Flux}_s = \delta C_{rain}(s)$ ($\text{Bq m}^{-2} \text{s}^{-1}$).

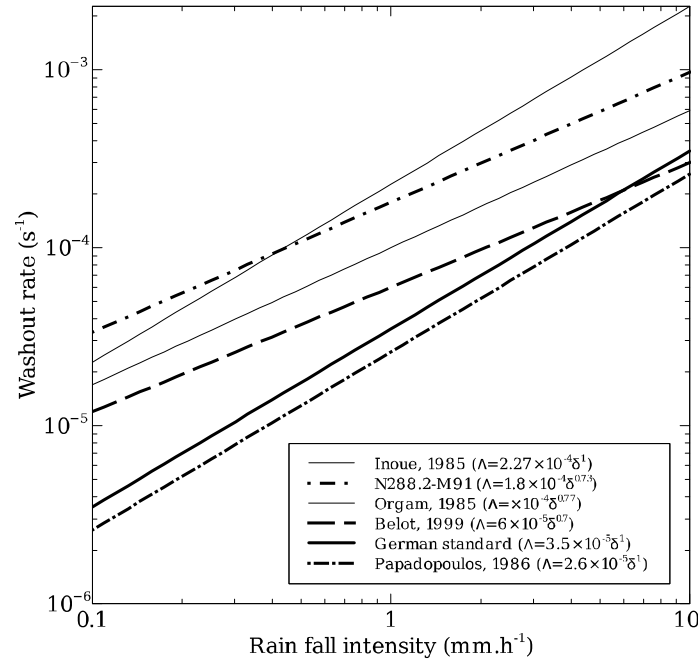


FIG. 8. Washout rate as a function of rainfall intensity according to several authors.

For a plume with a bivariate-normal distribution, the vertical distribution of the gas-phase pollutant can be integrated in a straightforward way [42]; the distribution is:

$$y_{AB} = \frac{QF}{2\pi\sigma_y\sigma_z u} \exp\left(-\frac{y^2}{2\sigma_y^2}\right) \left\{ \exp\left[-\frac{(z-h)^2}{2\sigma_z^2}\right] + \exp\left[\frac{(z+h)^2}{2\sigma_z^2}\right] \right\} + y_{AB|Bkg} \quad (27)$$

where:

- Q is the pollutant emission rate ($\text{m}^3 \text{s}^{-1}$);
- F is the plume depletion factor, which varies between 0 and 1 (dimensionless);
- σ_y, σ_z are, respectively, the horizontal and vertical dispersion parameters (m);
- u is the mean wind speed (m s^{-1});
- h is the emission height (m);
- y and z denote vertical and crosswind position (mL); and
- $y_{AB|Bkg}$ is a spatially invariant background mixing ratio ($\text{mol}_{\text{pollutant}} \text{mol}_{\text{air}}^{-1}$).

Combining the equation for the pollutant concentration in a raindrop with the equation for the mixing ratio of the pollutant in air and integrating with respect to z :

$$c(a, z) = -\frac{\alpha}{2\sqrt{2\pi}H'} \exp\left(-\frac{y^2}{2\sigma_y^2}\right) \left\langle \exp\left(\frac{\sigma_z^2 \zeta^2}{2}\right) \left\{ \exp[-\zeta(z-h)] \text{erfc}(\beta_1) + \exp[-\zeta+h] \text{erfc}(\beta_2) \right\} \right\rangle + \frac{y_{AB|Bkg}}{H'} \quad (28)$$

where:

- $\alpha = (QF\zeta)/(\sigma_y u)$ (dimensionless);
- $\beta_1 = (-\zeta\sigma_z^2 + z - h)/\sqrt{2\sigma_z^2}$ (dimensionless);
- $\beta_2 = (-\zeta\sigma_z^2 + z + h)/\sqrt{2\sigma_z^2}$ (dimensionless);
- $\zeta = [3K_y(a)H']/[v_z(a)a]$ (L^{-1}).

Hales proposed other equations for computer solution using single-precision arithmetic for large plume spreads with rapid mass-transfer rates. To compute concentrations in bulk deposited rain water, integration must be made over the total drop size spectrum or a suitable approximation thereof.

4.4.2.2. Project #654 model

The study performed at the Russian Federal Nuclear Center by Alexey Golubev under Project #654 of the International Science and Technology Center funded by the U.S. Government and the European Union proposed a model of HTO concentration in raindrops. It was based on the molecular flow of condensation which passes on to the liquid phase (J_+) and on the molecular flow of evaporation which passes on to the gas phase (J). The variation of HTO concentration in the drop is described by:

$$V_{drop} \frac{dC_{drop}(t)}{dt} = f \cdot S_{drop} \quad (29)$$

where:

$$f = \alpha \cdot \sqrt{\frac{RT}{2\pi\mu}} \cdot (C_{air} - \gamma \cdot m \cdot C_{drop}) \quad (30)$$

where:

- V_{drop} is the drop volume (m^3);
 S_{drop} is the area of the drop surface (m^2);
 R is the universal gas constant ($R = 8.314 \text{ J mol}^{-1} \text{ K}^{-1}$);
 α is the condensation factor depending on environmental conditions as well as on the water's aggregative state (dimensionless);
 C_{air} is the HTO concentration in the surrounding air (Bq m^{-3});
 γ is the $\text{H}_2\text{O}/\text{HTO}$ isotopic separation factor at 20°C ($\gamma=0.9$) (dimensionless);
 C_{drop} is the HTO concentration in the liquid drop, which is in equilibrium with the vapour (Bq m^{-3});
 m is the percentage of saturated moisture in air ($m_{water} m_{air}^{-1}$);
 T is the air temperature (K); and
 μ is the molecular mass (kg mol^{-1}).

The rate at which the concentration varies depends on the difference of flow densities of HTO molecules directed into the drop and out of the drop. The variation in HTO concentrations due to the change in the total number of molecules in the drop (condensation or evaporation) is taken into account by the third equation of the system.

The full system of equations describing the variations in the HTO concentration in the drop has the form:

$$\begin{cases}
 \frac{\rho_w}{6} \frac{dD^3}{dt} = D^2 (J_+ - J_-) \\
 C_w \rho_w \frac{1}{6D^2} \frac{d(D^3 T_{drop})}{dt} = \beta [T_{air}(L) - T_{drop}] + \lambda (J_+ - J_-) \\
 \frac{d\hat{n}^{HTO}}{dt} = \frac{6}{D(t)} \left(V_+^{HTO} \cdot n^{HTO}(L) - V_-^{HTO} \cdot \gamma \cdot \left(\frac{\hat{n}^{H_2O}}{\hat{n}^{H_2O}} \right) \cdot \hat{n}^{HTO} \right) - \frac{n^*}{3D(t)} \cdot \frac{dD}{dt}
 \end{cases} \quad (31)$$

where:

$$\begin{aligned}
 J_+ &= \alpha \cdot \mu \cdot p(T_{air}(L)) \cdot \psi(L) / \sqrt{2\pi \cdot \mu \cdot RT_{air}(L)} \\
 J_- &= \alpha \cdot \mu \cdot p(T_{drop}) / \sqrt{2\pi \cdot \mu \cdot RT_{drop}} \\
 C_{air} &\equiv n^{HTO} \\
 C_{drop} &\equiv \hat{n}^{HTO} \\
 n^* &= (\hat{n}^{HTO} - \hat{n}^{H_2O}) = const \\
 V_+^{HTO} &= 4\alpha \sqrt{RT_{air}(L) / 2\pi \cdot \mu^{HTO}} \\
 V_-^{HTO} &= 4\alpha \sqrt{RT_{drop}(L) / 2\pi \cdot \mu^{HTO}}
 \end{aligned} \quad (32)$$

where:

- D_{drop} is the drop diameter (m);
 α is the fraction of molecules that pass on to the liquid phase (the probability of passing from the gas phase to the liquid phase) on encountering the drop surface (dimensionless); $(1-\alpha)$ is the fraction of reflected molecules;

$p(T_{air}), p(T_{drop})$ are the saturated vapour pressures of H₂O at the temperatures of the atmosphere (T_{air}) and the drop (T_{drop}) (taking into account the curvature of the drop surface) (Pa);

ψ is the relative humidity of the atmosphere (dimensionless);

L is drop trajectory (m);

C_w is the heat capacity of the liquid phase (J K⁻¹ kg⁻¹);

ρ_w is the density of the liquid phase (kg m⁻³);

λ is the condensation heat (evaporation) (J kg⁻¹);

β is the heat transfer factor (dimensionless);

\tilde{n} relates to the saturated vapours “produced” by the liquid phase (dimensionless); and

\hat{n} relates to the liquid phase proper (dimensionless).

For full completion, this system must be supplemented with the dependences $\psi = \psi(L)$ and $T_{air} = T_{air}(L)$ or some model allowing determination of these dependences.

The specific activity of rainwater falling onto the soil surface is described by the equation [41]:

$$C = \frac{\int_0^{\infty} C_{drop}(D_{drop}) \cdot \frac{\pi}{6} \cdot D_{drop}^3 \cdot F'(D_{drop}) dD_{drop}}{\int_0^{\infty} \frac{\pi}{6} \cdot D_{drop}^3 \cdot F'(D_{drop}) dD_{drop}} \quad (33)$$

where:

C is the specific activity of rainwater (Bq kg⁻¹);

$C_{drop}(D_{drop})$ is the specific activity of a rain drop of diameter D_{drop} falling onto the soil surface (Bq m⁻³);

$F'(D_{drop})$ is the fraction of drops ranging in size from D_{drop} to $(D_{drop} + dD_{drop})$ (dimensionless).

The function $F'(D_{drop})$ represents the derivative of the empirical Best formula:

$$F'(D_{drop}) = \left(\frac{D_{drop}}{A} \right)^n \cdot \frac{n}{D_{drop}} \cdot \exp \left(- \left(\frac{D_{drop}}{A} \right)^n \right) \quad (34)$$

where $n=2.25$ and A is a parameter depending on rain intensity [43].

The vertical velocity of raindrops as a function of their size, $V_{\perp}(D_{drop})$, is described by the following empirical relationship:

$$V_{\perp}(D_{drop}) = 4.874 \cdot D_{drop} \cdot \exp(-0.195 \cdot D_{drop}) \quad (35)$$

Adding the horizontal component of velocity $\vec{V}_{\perp} = \vec{V}_{\perp}(t)$, whose direction and magnitude coincide with the instantaneous values of the wind velocity, we obtain the equations of motion for drops of size D_{drop} s in the atmosphere. Integration of these equations determines the trajectory of the drop.

In summary, the model presented here is the further development of the model described in [41] and allows the exchange of HTO molecules between drops of fixed volume and atmospheric moisture.

This model was compared with experimental data. The Gaussian model was used to calculate atmospheric dispersion.

Compared to the simplest model ($\alpha=0.4=\text{const}$), the model described above yields higher values of the washout coefficient in the vicinity of the source and at long distances from it. The explicit introduction of wind velocity and a better choice of formula for the drop velocity explain the differences between the predictions of this model and those of the Belot model.

4.4.2.3. Eulerian model

An attempt to generalize washout modelling was done recently [40] in a collaboration between IFIN-HH and Bulgarian researchers. A numerical Eulerian model that describes washout independent of dispersion was developed:

$$\frac{dC}{dt} = \frac{6K}{\alpha d} (\alpha C_g - C) \quad (36)$$

Here, following [44], the mass of gaseous and liquid HTO is expressed in terms of the concentration instead of the mole-fraction. In Eq. (36), t (T) is the time, C is the concentration of the liquid phase (mol m^{-3}), C_g is the concentration of gas phase HTO in the drop's environment (mol m^{-3}), and d is the drop diameter (m). K is the overall mass-transfer coefficient and is calculated using a semi-empirical expression, also known as the Froessling equation:

$$K = k_y = \frac{D_g}{d} (2 + 0.6 \text{Re}^{1/2} \text{Sc}^{1/3}) = \frac{D_g}{d} \left[2 + 0.6 \left(\frac{d v}{\nu} \right)^{1/2} \left(\frac{\nu}{D_g} \right)^{1/3} \right] \quad (37)$$

α is a dimensionless coefficient, constant with respect to C but dependent on temperature, Henry's Law constant and the universal gas constant, and on the density and molecular weight of water:

$$\alpha = \frac{T}{H} R \frac{\rho}{M} \quad (38)$$

The domain of the model is between the soil surface and the level H_{rain} from which the drops start their fall. A uniform vertical grid is defined. At the top level ($H_{\text{rain}} = z(N)$), the model assumes the liquid HTO in the raindrops is in equilibrium with the surrounding gaseous HTO. Eq. (36) is applied layer by layer downward, separately for all drop size intervals. If all parameters in the equation are assumed constant within a grid layer, an analytic solution can be found for the time t taken by the drop in passing through the grid layer.

This time is determined for each drop diameter d in layer i by using an accepted formula for the fall velocity of the drop. The concentration $C(d,i)$, calculated for this drop after it has spent time t in the i -th layer, is used as the initial condition for the next layer. The calculations for the last layer, the layer above the ground, give the spectral mass concentration of liquid HTO in raindrops at the surface $C(d,1)$.

$$C(t) = C_0 e^{-\frac{6K}{\alpha d}} + \alpha C_g \left[1 - e^{-\frac{6K}{\alpha d}(t-t_0)} \right] \quad (39)$$

A sensitivity analysis of the Eulerian model shows that the washout process is influenced most significantly by rainfall parameters and air temperature. The vertical profile of HTO in the atmosphere must be considered for non-Gaussian dispersion. The sensitivity of the washout rate or ratio varies from less than 1% to 70%. Atanassov and Galeriu [40] conclude that the influence of the rain parameters and the temperature on the washout process is significant. Contemporary weather radars are able to provide information about cloud and raindrop distributions in space and time, their spectra and movements (sometimes raindrops may even move upward). A substantial reformulation of the modelling approach will be necessary to incorporate this information.

4.4.3. Potential effect of buildings

Recently, unexpectedly high tritium concentrations have been reported in precipitation, surface water and ground water near reactors. The US nuclear power industry has focused on characterizing the type and extent of the on-site recapture of airborne tritium released after monitoring in the plant vent radiation monitoring system. The need to understand on-site atmospheric deposition is described elsewhere [45]. The CANDU Owners Group is interested in “Atmospheric Deposition of Tritium at Nuclear Power Plants”. The interest in the topic is caused by past misunderstanding of the role of buildings on the concentration field of the pollutant. For the flow of air in the presence of a building, we must consider the regions of roof recirculation, high turbulence, roof wake and building wake recirculation. The plume emitted from the stack will be influenced by the wind flow in these regions (Figure 9).

A modified Gaussian model was used with enhanced dispersion and low emission height, but the approach did not reproduce the experimental data. The PRIME algorithm [46] represents a more advanced approach with more details on enhanced plume dispersion coefficients due to the turbulent wake and reduced plume rise caused by a combination of descending streamlines in the lee of the building and increased entrainment in the wake. PRIME tended to underestimate the overall maximum concentrations when the ratio of stack height (h) to building height (H) was in the mid range of the ratios tested (i.e, h/H = 1.30 and 1.46).

A comprehensive wind-tunnel dataset (US Environmental Protection Agency) on dispersion behind model rectangular buildings, which was compiled by Thompson [47] for non-buoyant emissions, is of special interest. The PRIME algorithm (included in AERMOD-USA), the Danish atmospheric transport model OLM, and a computational fluid dynamics model (MISKAM) have been compared [48] (Figure 10). Thompson [47] presents contour plots of the so-called building amplification factor (BAF), which is determined by comparing concentrations in two situations: a situation where a building is located near a stack, and a reference situation without a building. For both situations, the maximum ground level concentration is determined. The ratio between these two concentrations is the BAF, and its value depends on the height and position of the stack relative to the building.

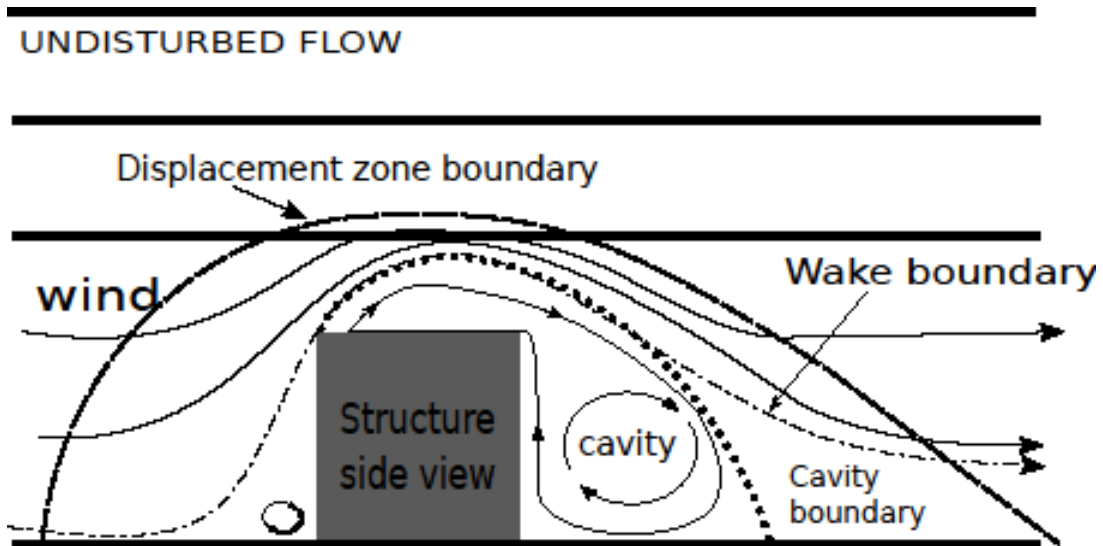


FIG. 9. Flow and turbulence in the presence of a building (taken from [49]).

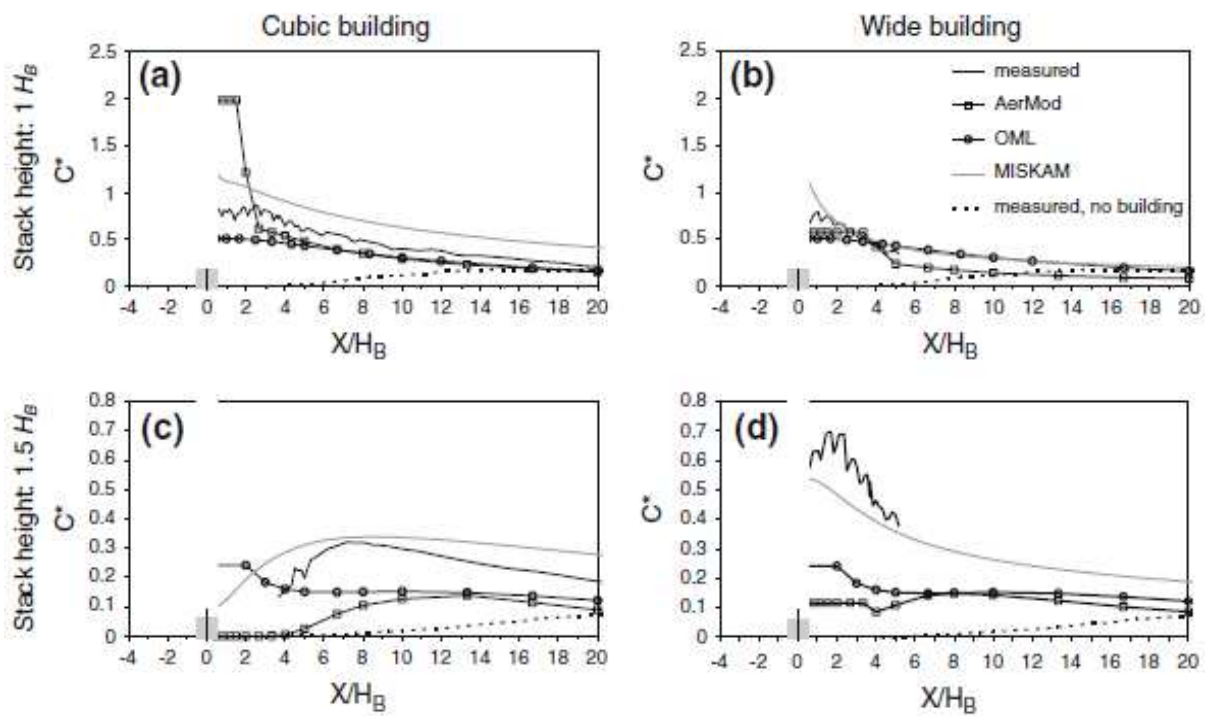


FIG. 10. Along-wind normalized concentration profiles at ground level for four scenarios (as measured, and as modeled by AERMOD/PRIME, standard OML and MISKAM). For reference, measured concentrations for the case without building are included. The horizontal axis refers to the distance from the stack in units of building height. Note that the vertical scale differs between the top row and the bottom row (taken from [48]).

Thompson's studies of BAF allowed him to conclude that the "good engineering practice" 2.5-times rule (according to which a stack height of 2.5 building heights is sufficient to ensure building effects are negligible) is inadequate for wide buildings. Furthermore, the results indicated that, even with a distance between stack and building of ten times building height (HB), the building still has a significant effect on maximum concentrations. It has been demonstrated that with a stack height equal to HB, measured results are not very sensitive to the building width, but for a stack height of 1.5HB, building width does have a substantial influence on results. The measured maximum ground-level concentration for the widest building is more than twice that for the cubic building.

The simulation of atmospheric dispersion is usually conducted with two types of models [50]: Fast Approximate Models (FAM) and Fully Computational Models (FCM). FAM models are mainly empirical models [51] based on extensive field and wind tunnel studies. As a result, their application is recommended for, or sometimes limited to, the type of topography on which they are based. On the other hand, FCM models are based on the numerical solution of the momentum, energy and mass transport equations. They can be applied to almost all types of topographies, but their applicability is limited by the computational power and time that they require. In general, the choice of model depends on its practical purpose (in relation to dispersion modelling), on the level of spatial/temporal detail and scientific understanding involved, and on the detail and accuracy of the available meteorological and topographical input data [52]. Computational Fluid Dynamics and Lagrangean/ Eulerian dispersion models have been combined [53] and this hybrid method shows best results for concentration profiles near buildings.

4.5. SENSITIVITY OF MODELS

In any model, the time required for raindrops to pass through the plume has to be calculated. This quantity depends on the size of the raindrops in question. In fact, the raindrop size distribution is the most important parameter in determining the time of passage, and can lead to high discrepancies in the HTO drop concentration if it is not characterized correctly.

4.5.1. Raindrop distribution

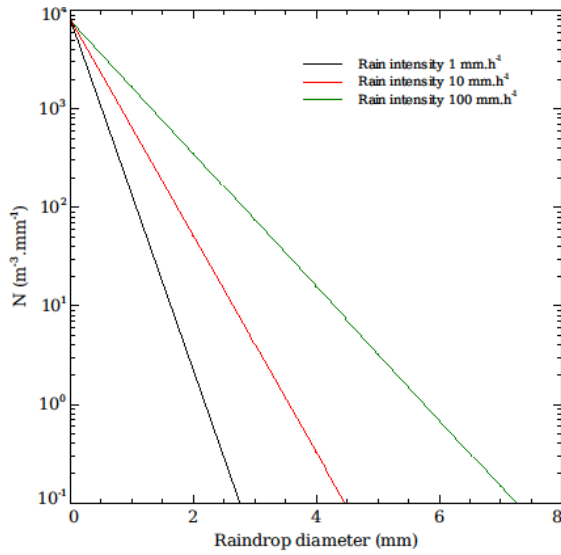
Raindrop size distributions are the end points for all cloud physical processes, cloud dynamical processes and interactions that affect the formation and growth of liquid precipitation. In addition, the raindrop distributions, once formed, can interact with the essential dynamics of the clouds.

The number and size of raindrops within a unit volume is described by the number concentration, $N(D)$ (number $m^{-3} mm^{-1}$), also called the rain drop size distribution (DSD).

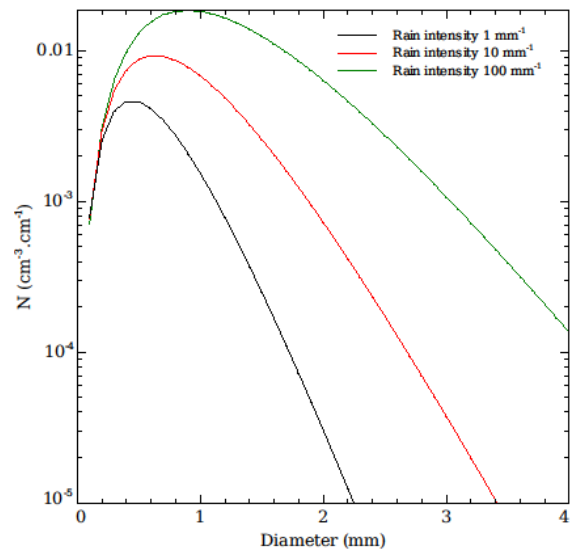
In recent work, the raindrop size distribution is usually described by a Gamma function [54], differing from the classical distribution of Marshall and Palmer [55]. Figure 11 shows the distribution of raindrop sizes according to Marshall and Palmer for three rainfall intensities: 1, 10 and 100 $mm h^{-1}$. These distributions were developed for mid-latitude stratiform rain, and lead to an overestimation of the number of smallest drops.

Willis [56] proposed the Gamma function for the drop size distribution, as shown in Figure 11. Feingold and Levin [57] assumed that raindrop sizes were log-normally distributed, as shown in Figure 12 for three rainfall intensities. Table 12 shows equations for the Marshall-Palmer, gamma and log-normal distributions.

Statistical raindrop distributions are numerous and well known. However, studies of HTO washout are not usually accompanied by information on drop size distribution, but only on the intensity of the rain.



Marshall-Palmer



Willis

FIG. 11. Marshall Palmer and Willis (gamma) distribution functions for modeling drop size distribution.

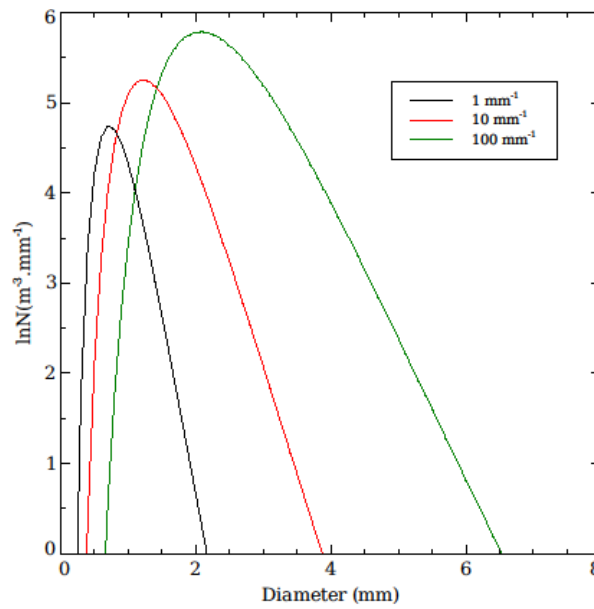


FIG. 12. Lognormal distribution function for modelling drop size distribution.

TABLE 12. PARAMETERS FOR THE MARSHALL-PALMER, LOG-NORMAL AND GAMMA RAINDROP SIZE DISTRIBUTIONS

Marshall and Palmer [55]	Log-normal [57]	Gamma [56]
$N_D = N_0 e^{-\Lambda D}$	$N_D = \frac{N_T}{\sqrt{2\pi} \cdot D \cdot \log \sigma} e^{-\frac{(\log D - \log D_{gm})^2}{2 \log^2 \sigma}}$	$N_D = N_G D^{2.50} e^{-\Lambda D}$
$N_0 = 8000 \text{ m}^{-3} \text{ mm}^{-1}$	$N = 172 R^{0.22} \text{ m}^{-3}$	$N_G = \frac{6.36 \times 10 M}{D_0^4} \left(\frac{1}{D_0} \right)^{2.50}$
$\Lambda = 4.1 \cdot R^{-0.21} \text{ mm}^{-1}$	$D_r = 0.72 R^{0.23} \text{ mm}$	$\Lambda = \frac{5.57}{D_0} \text{ mm}^{-1}$
–	$\sigma = (1.43 - 3.0) \times 10^{-4} R$	$D_0 = 1.57 M^{0.168} \text{ mm}$
–	–	$M = 0.062 R^{0.913} \text{ g} \cdot \text{m}^{-3}$

Notes:

- N_D is the drop size distribution (number of drops $\text{m}^{-3} \text{ mm}^{-1}$);
- R is rainfall intensity (mm h^{-1});
- D_{gm} is the geometric mean of drop diameter (mm); and
- D_0 is the volume median diameter (mm).

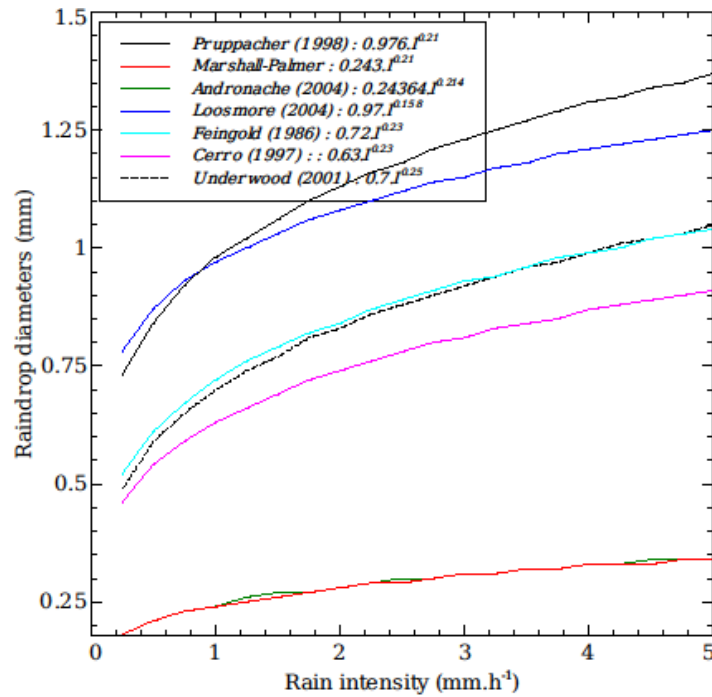


FIG. 13. Evolution of the representative diameter as a function of rain intensity according to different authors.

4.5.2. Raindrop diameter

Raindrop diameter is often described as a function of rain intensity. There exist several equations to calculate the representative diameter of raindrops. The most current form is $D_r = \alpha j^\beta$. In the literature, α ranges between 0.243 and 0.97 and β between 0.15 and 0.25. Figure 13 shows some parameterizations for the representative diameters of raindrops, D_r , as a function of rain intensity j according to Andronache [58], Cerro et al. [59], Feingold and Levin [57], Loosmore and Cederwall [60], Marshall and Palmer [55], Pruppacher and Klett [61], and Underwood [62]. Figure 13 shows that there is a range of a factor of 4 between the diameters computed by these authors.

4.5.3. Raindrop velocity

Raindrop velocity can be computed as a function of diameter. The Stokes formula cannot be used for the terminal velocity due to the size of falling raindrops, which have a diameter bigger than 20 μ m.

$$v = \sqrt{\frac{4gd_p C_c \rho_p}{3C_D \rho_{air}}} \quad (40)$$

where:

- g is the gravitational constant (m s^{-2});
- d_p is the drop diameter (mm);
- C_c is the Cunningham correction factor (dimensionless); and
- ρ is the drop or air density (kg m^{-3}).

Raindrop velocity can be estimated using the parameterizations of Andronache [58, 63], Loosmore and Cederwall [60] and Seinfeld and Pandis [20], as shown in Figure 14.

Figure 15 shows raindrop velocity as function of rainfall intensity. The drop diameter was calculated with the formula given by Loosmore and Cederwall [60] ($D_r = 0.97 p^{0.158}$ where p is the rainfall intensity in mm h^{-1}).

4.5.4. Sensitivity of models

Using the kinetic model developed by Golubev et al. [41], the effect of drop size distribution on the exchange coefficient was investigated. Figure 16 presents the computational dependence of the relative HTO content in precipitation for various drop size distributions.

It is seen from Figure 16 that the Best distribution and the normal distribution give similar results; the log-normal distribution, in which most drops have a radius lower than 0.5 mm, leads to higher values of the HTO concentration in precipitation. The largest discrepancy between the curves is observed at 150 m, where the plume touches the ground.

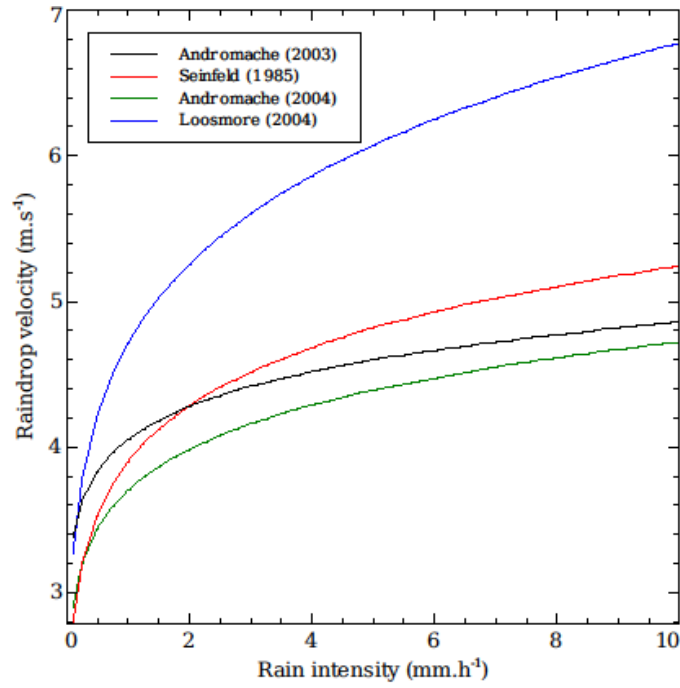


FIG. 14. Evolution of raindrop velocity as a function of diameter according to different authors [20, 58, 60, 63].

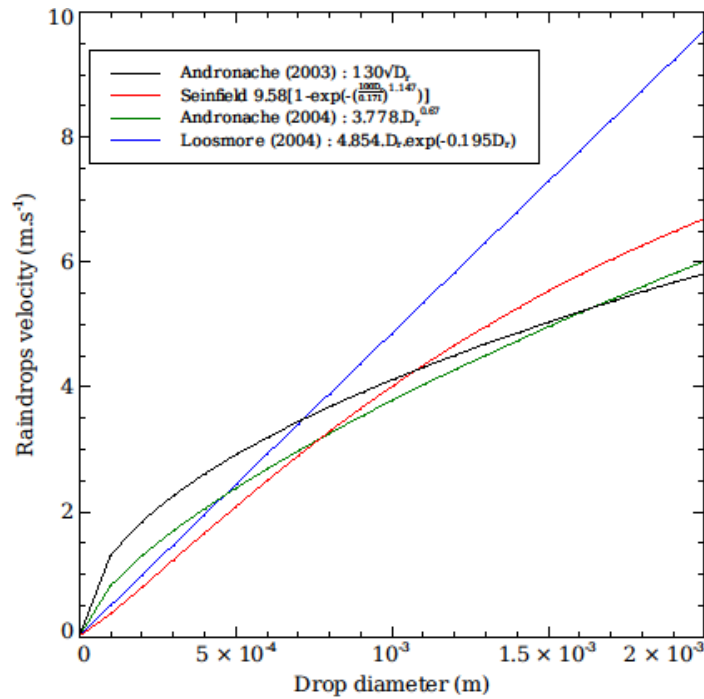


FIG. 15. Evolution of raindrop velocity as a function of raindrop diameter.

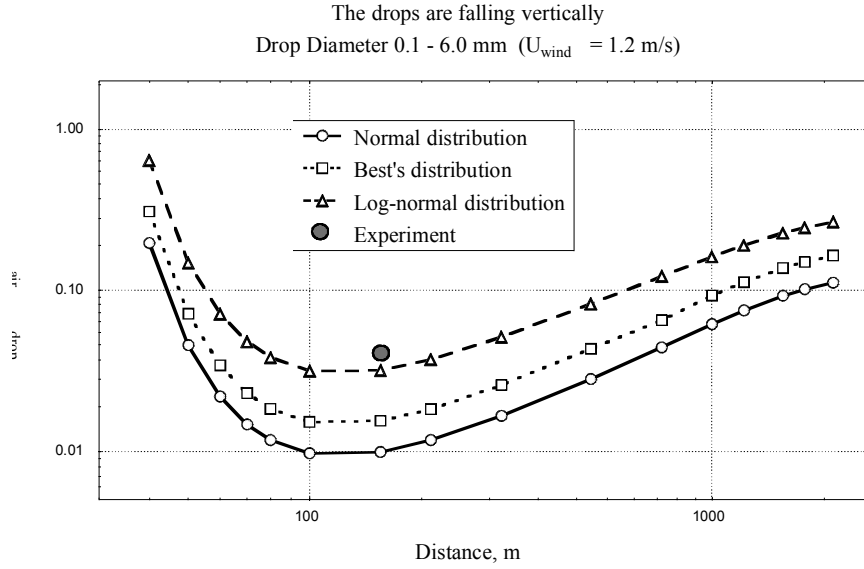


FIG. 16. The computational dependence of the relative HTO content in precipitation for various drop size distributions.

Studies with the Golubev et al. model have shown that, for a given precipitation intensity, the HTO content in rainwater depends essentially on the drop size distribution. Special attention should be given to the accuracy of the “tail” of the distribution, which correspond to the largest drops, since these make an essential contribution (20% to 50%) to the precipitation intensity.

A sensitivity analysis of HTO concentrations in drops to rain characteristics was presented elsewhere [64]. The CERES code, which is the CEA reference computational tool for impact assessment, calculates the transfer rate of HTO to the drop and the specific activity of HTO in the drop as it leaves the plume. The average diameter in cm and the velocity of the drop in cm s^{-1} are given by extrapolation of the experimental data of Chamberlain and Eggleton [22]: $\tilde{r} = 0.037 \text{LOG}(I) + 0.0661$ and $\tilde{V} = 7000 \tilde{r} - 12000 \tilde{r}^{1.97}$ where I is the rain intensity in mm h^{-1} .

$$\lambda_r = \frac{3DfC}{\beta r^2 \rho} \quad (41)$$

$$C_r = \frac{\beta}{C} X(1 - e^{-\lambda_r t}) \quad (42)$$

where:

- λ_r is the rate constant for uptake of HTO by the drop (s^{-1});
- C_r is the HTO drop activity (Bq kg^{-1});
- D is the diffusivity of HTO in air ($\text{m}^2 \text{s}^{-1}$);
- f is the ventilation factor;
- C is the concentration of H_2O in air (kg m^{-3});
- X is the specific activity of water vapour in air (Bq kg^{-1});
- r is the radius of the drop (mm);
- ρ is the density of the drop (kg m^{-3});
- β is the ratio of vapour pressure of H_2O to HTO;
- t is the time required by the raindrop to pass through the plume (s).

TABLE 13. DROP VELOCITIES (v) BASED ON DIFFERENT APPROACHES (D is drop diameter)

Reference	Formula
Belovodski [32]	$v = 130\sqrt{D}$
Belovodski et al. [31]	$v = 3.778 (1000 \cdot D)^{0.67}$
Britter and Hanna [51]	$v = 4854 \cdot D \cdot \exp(-0.195 \cdot D)$
Cerro et al. [59]	$v = 9.58 \left[1 - \exp\left(-\left(\frac{100 \cdot D}{0.171}\right)^{1.147}\right) \right]$

To investigate the dependence of rain concentration and washout rate on drop size distribution, water activities for each drop were computed for each distribution using the CERES code. Marshall-Palmer, Willis and log-normal distributions were computed for several rain intensities from 1 to 20 mm h⁻¹. Drop velocities were calculated for each diameter using several formulas (see Table 13).

The rate constant for uptake of HTO by each drop diameter was computed using the Chamberlain equation. Assuming the raindrops are spherical in shape, the concentration of rain water can be estimated by calculating the total water volume corresponding to each diameter. The HTO air concentration was assumed to be constant in time at 1000 Bq m⁻³. The vertical extent of the plume crossed by the drops was 200 m. In this study, the plume was assumed to be released near the ground, and the loss of HTO by exchange between the drops and the air below the plume was not considered.

The highest HTO concentrations in rain were calculated with the Marshall-Palmer distribution coupled to the Andronache formula for estimating drop velocity (Figure 17); the lowest concentrations arose from the log-normal drop size distribution and the Loosmore velocity formula. This can be explained by noting that the Marshall-Palmer distribution overestimates the number of fine raindrops and that the HTO rate constant, λ_r , increases as the drop size decreases. The value of λ_r calculated for an air temperature of 9°C was 3.1×10^{-1} , 1.2×10^{-2} and 3.4×10^{-3} s⁻¹, respectively, for 0.1, 1 and 3 mm drop diameters. For a rain intensity of 1 mm h⁻¹, the rain concentration ranged between 318 and 592 Bq L⁻¹, according to the drop size distribution and velocity formula used. Thus there is a factor of 2 between the minimum and maximum computed concentrations. The total surface area available for exchange between the drop and the air increases with rain intensity. High intensities remove the largest quantity of HTO from the air, but lead to lower concentrations in rain water because of higher dilution. The HTO concentrations in rain computed with the CERES code, which does not take into account drop distribution, are very close to those given by the log-normal distribution.

The sensitivity of the rain concentration to the drop velocity is shown in Figure 18 for the log-normal distribution. Rain concentrations were also computed using the CERES code to calculate drop velocities. Average concentrations and standard deviations ranged from 673±30 to 241±23 Bq L⁻¹, respectively, for rain intensities of 1 and 20 mm h⁻¹. The Loosmore formula, which leads to the highest drop velocities, gives the lowest concentrations.

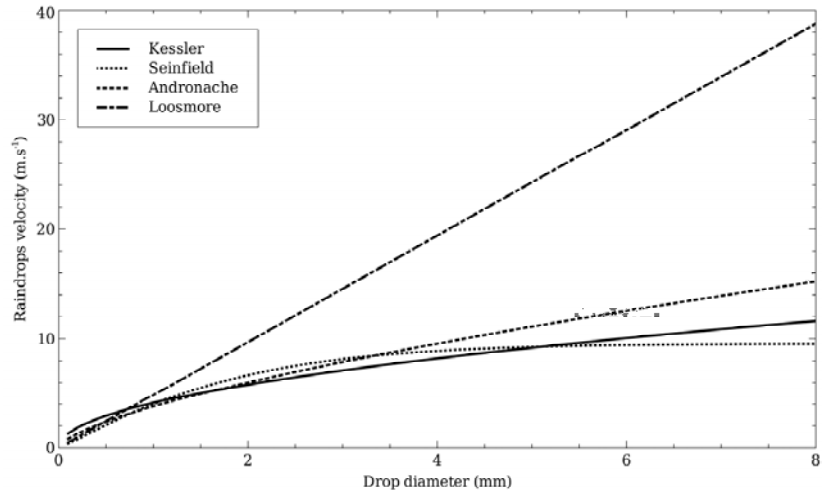


FIG. 17. Dependence of raindrop velocity on drop diameter according to different parametrization.

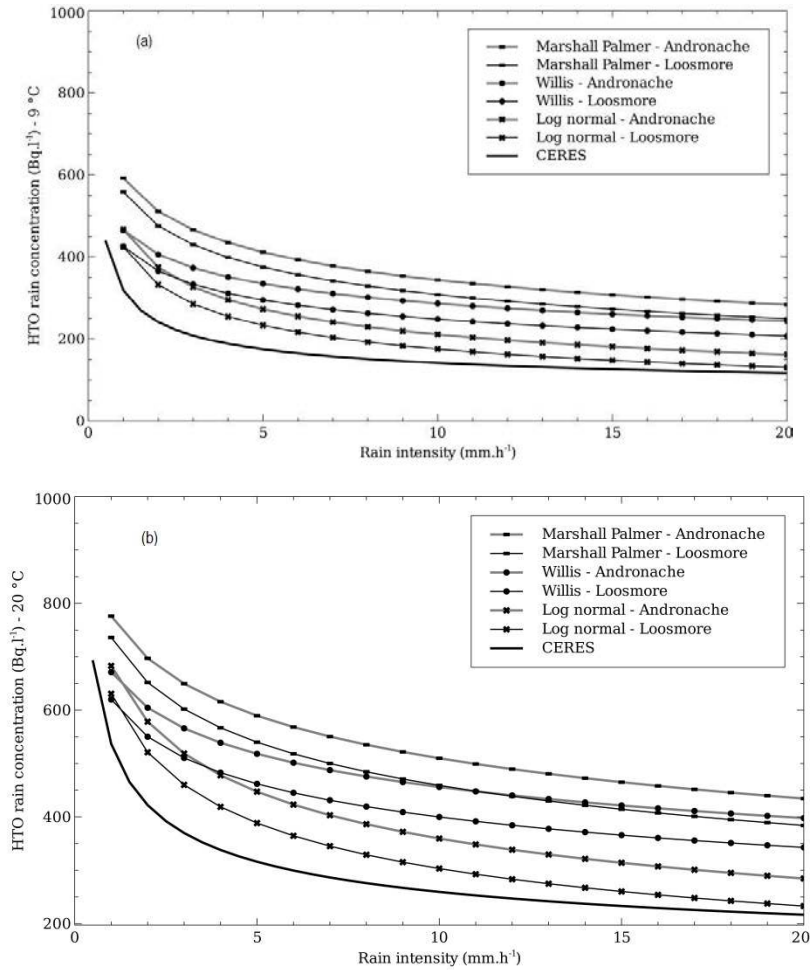


FIG. 18. HTO concentrations in rain as a function of rain intensity for the Marshall-Palmer, Willis and Log-normal drop distributions. Results are also shown for the CEA CERES code. The calculations were made for two air temperatures: (a) 9°C and (b) 20°C.

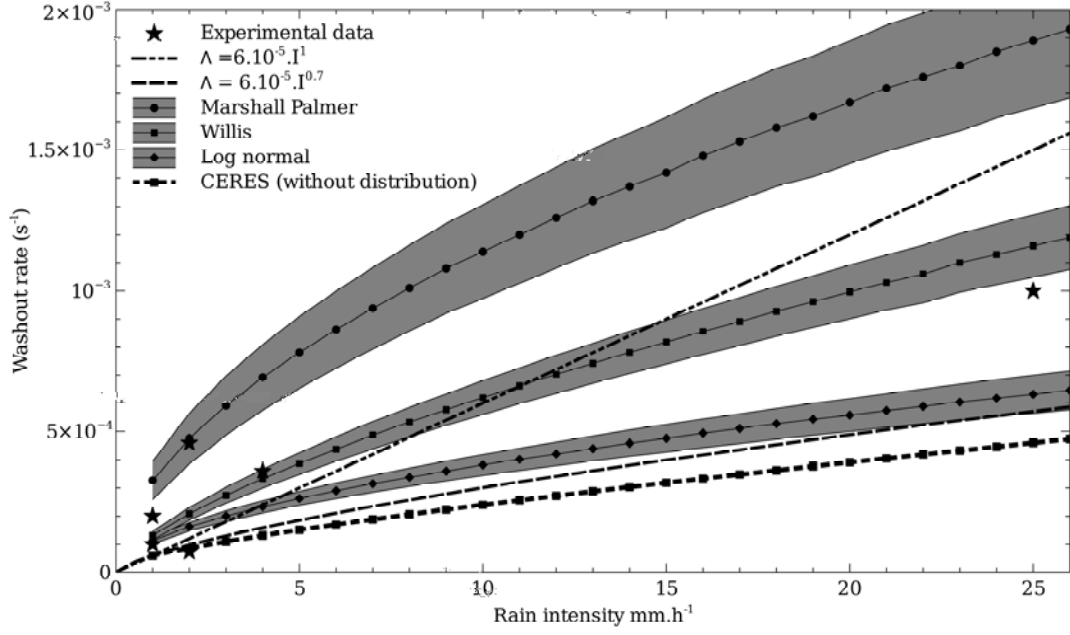


FIG. 19. Average and standard deviation washout rates for the Marshall-Palmer, Willis and log normal distributions computed using the Kessler, Seinfeld, Andronache, Loosmore and Chamberlain drop velocity equations.

The washout rate can be estimated by computing the amount of HTO removed per unit volume of air: At time t , the air concentration is:

$$C_{air}^{HTO}(t) = C_{air}^{HTO}(t=0) - C_{removed}^{HTO} \quad (43)$$

$$C_{removed}^{HTO} = \frac{\pi\beta X(t)\rho l}{6V_{tot}} \int_{r=0}^{\infty} \frac{N_r D_r^3}{\nu_r} \cdot e^{-(\lambda_r t)}$$

Here, V_{tot} is the total drop volume per unit volume of air, N_r is the number of drops of radius r and D_r is the drop diameter. Figure 19 shows the average washout computed with Eq. (43) and using the Kessler, Seinfeld, Andronache, Loosmore and Chamberlain velocity equations. The standard function with $b=0.73$ and $b=1$ and the washout rate calculated with the CERES code (which does not take into account the rain drop distribution) have been plotted. Standard deviations on each rain drop size distribution are plotted and represent the uncertainties due to drop velocity. Washout rates can be estimated within 20% error with the Marshall-Palmer distribution and within 15% error for the two others.

The washout rates calculated with the Marshall Palmer distribution are higher by a factor of about 3 than those given by the Willis and log normal distributions. For a rain intensity of 1 mm h^{-1} , the calculated washout rate is 1×10^{-4} and 3×10^{-4} , respectively, for the Willis and Marshall-Palmer distributions. Experimental data give an average washout of $2.5 \times 10^{-4} \text{ s}^{-1}$ for light rain ($<2.6 \text{ mm h}^{-1}$) [25, 26, 44], $3.6 \times 10^{-4} \text{ s}^{-1}$ for moderate rain ($2.6\text{--}7.6 \text{ mm h}^{-1}$) and $1 \times 10^{-3} \text{ s}^{-1}$ for heavy rain ($>7.6 \text{ mm h}^{-1}$) [44].

For light and moderate rain, experimentally-determined washout rates lie between those calculated with the Marshall-Palmer and Willis (or log normal) distributions. Even if the Willis distribution seems to be the best distribution for estimating washout rate, there is good agreement between experiments and calculations with all the formula used here. The evolution of the distribution during rain is not taken into account, but it certainly has an influence on the washout rate, and on the HTO rain concentration. An increase in the number of small drops of rain causes an increase in washout and thus in the rain concentration. Considering the variability in washout induced by the various rain drop distributions and the methods used to calculate it, uncertainties of about a factor 2 to 3 can be estimated on wet deposition. Empirical equations like those used in the CERES code seem to underestimate slightly the washout rate and wet deposition. Conversely, they overestimate air concentrations and thus inhalation and transcutaneous doses.

Recently, drop size distribution studies have focused on the differences between convective rain and stratiform rain. The intercept parameter N_0 of the exponential DSD underwent a sudden increase for the same rainfall rate when the precipitation type changed from uniform (widespread rain) to convective (shower or thunderstorm). For the same rainfall rate, Tokay and Short [65] found small drops were dominant in convective rainfall and large drops in stratiform rainfall. This was demonstrated for tropical condition [66]. In a Mediterranean climate (Barcelona), 2 years of rain were analyzed [59]. Thirty-second individual samples of drop size and velocity were measured with an optical disdrometer and grouped into different classes according to their rainfall rate. Using the moment method, the entire experimental dataset was fitted to three standard distribution functions: exponential, gamma, and lognormal. Relationships were found between rainfall rate R and other moments of the DSD, such as optical attenuation S , liquid water content W , and reflectivity Z . Although the gamma distribution generally reproduced the experimental measurements most accurately, the $Z(R)$ relationship, which is particularly relevant in radar meteorology, yielded the best results when calculated from a fitted exponential distribution. For washout studies it is important to note that the gamma distribution is the most suited. The gamma function is:

$$N(D) = N_0 D^\alpha \exp(-\lambda D) \quad (44)$$

where:

λ is expressed in mm^{-1} ;
 N_0 in $\text{m}^{-3} \text{mm}^{-1-\alpha}$; and
 α is dimensionless.

It was shown that all parameters depend on rain intensity.

4.6. CONCLUSION ON WASHOUT RATE

Washout of HTO by precipitation is the main process resulting in wet deposition. According to the type and intensity of precipitation, average washout rates, calculated from the experimental data, vary from $2.2 \times 10^{-5} \text{ s}^{-1}$ (snow) to $1 \times 10^{-3} \text{ s}^{-1}$ (heavy rain).

The washout rate is closely influenced by such precipitation characteristics as rain intensity, drop size distribution and drop characteristics. The Willis distribution seems to result in the best estimates of the washout rate, but there is reasonable agreement (a factor of 5) between experiments and calculations with all the formula used here. The washout rate clearly depends on release and local characteristics. At short distances, washout rate can also be influenced by building wake effects.

Simple models can be used for washout rate modeling, using parameters of the relationship between rain intensity and washout that are given by several authors from experimental data. The spread of predictions is near a factor 5-8 (Figure 8) and a conservative approach can be used.

Complex models that take into account more parameters (drop size distribution, air temperature) can also be used to calculate washout rate. Such models include those developed by VNIEF and the numerical Eulerian model from the IFIN-HH and Bulgarian collaboration. More research is needed when the concentration profile is non-Gaussian and the building influence is strong (up to few km from the building). These studies must be site specific. When only moderate conservatism is desired, the assumption that the rate-limiting step in HTO exchange is HTO transport through the boundary layer to the drop surface should be challenged. Also local rain characteristics must be considered by direct measurement of drop size distribution for the types of rain and rain intensity found at the site of concern.

Knowledge of the washout rate during fog or snow is insufficient and more experiments have to be done.

5. HT AND HTO DRY DEPOSITION AND REEMISSION

5.1. OVERVIEW

Deposition of atmospheric HTO and HT to soil is one of the key processes determining the dose consequences of releases of these radionuclides [67, 68]. Especially, the impact of the release is expected to depend critically on the efficiency of the HT deposition process [67] because HTO formed after deposition is radioecologically more toxic than HT by four orders of magnitudes.

Several models assessing the deposition and reemission of HT and HTO have been developed, and field and laboratory experiments have also been conducted to obtain the parameters necessary for modelling these processes and to assess overall tritium behaviour of the soil-atmosphere system during and after deposition. This section emphasizes the present status of the modelling efforts and introduces some field experimental studies as a helpful guide for modellers to develop and validate a model.

5.2. DRY DEPOSITION OF HTO AND REEMISSION

During passage of the primary airborne plume, atmospheric HTO vapour diffuses into the soil, and HTO condensation occurs at the soil surface (dry deposition). Soon after the passage of the primary plume, reversal of the HTO gradient across the atmosphere-soil boundary causes reemission of the deposited HTO to the atmosphere to form a secondary plume, which enhances the atmospheric HTO level over the subsequent period. The physical mechanism of the dry deposition of HTO is basically the same as that for water vapour; nevertheless the deposition and reemission of HTO and H₂O should be treated separately because each molecule follows its individual vapour-pressure deficit across the atmosphere-soil boundary and also throughout the soil profile [69–71].

Generally, the exchange process of HTO between the surface atmosphere and the underlying soil is expressed by a bulk formula [72], as:

$$F_{HTO} = v_{HTO} (\chi_{atm} - \chi_{sa}) \quad (45)$$

where:

F_{HTO} (Bq m⁻² s⁻¹) is the exchange flux;

v_{HTO} is the exchange velocity (m s⁻¹);

χ_{atm} is the HTO vapor concentration (Bq m⁻³) in the atmosphere at a given reference height; and

χ_{sa} is the HTO vapor concentration in the surface soil air.

The flux F_{HTO} defined by Eq. (45) is a deposition flux when $\chi_{atm} > \chi_{sa}$, and a reemission flux if $\chi_{atm} < \chi_{sa}$.

The exchange velocity v_{HTO} depends on both atmospheric and soil conditions, and is generally formulated as an inverse of the sum of the resistances [72–74], as:

$$v_{HTO} = (r_a + r_b + r_s)^{-1} \quad (46)$$

where:

r_a (s m⁻¹) is the aerodynamic resistance characterizing transfer of HTO vapour in the free atmosphere from the reference height to just above the soil surface;

r_b (s m^{-1}) is the boundary layer resistance describing mass transfer in the quasi-laminar-flow layer adjacent the soil surface; and
 r_s (s m^{-1}) is the soil resistance regulated by HTO evaporation (or condensation) efficiency in the soil.

The aerodynamic resistance r_a is characterized by the turbulence in the surface boundary layer. For example, the UFOTRI code [73] calculates r_a as:

$$r_a = u_r / u_*^2 \quad (47)$$

where:

u_r (m s^{-1}) is the wind speed at the reference height; and
 u_* (m s^{-1}) is the friction velocity characterizing the scale of the turbulence. The boundary layer resistance r_b is also related to the wind speed (e.g. UFOTRI [73]) and is calculated by:

$$r_b = 5 / u_* \quad (48)$$

where the factor 5 is the Stanton number.

The friction velocity u_* needed to calculate resistances r_a and r_b can be obtained from the wind profile in the near-surface atmosphere. Under conditions of neutral stability, for a bare soil surface, the vertical wind profile in the surface boundary layer is expressed by the well-known logarithm law [75, 76] as:

$$u = \frac{u_*}{\kappa} \ln \left(\frac{z}{z_0} \right) \quad (49)$$

where:

κ is von-Karman's constant ($\kappa = 0.4$); and
 z_0 (m) is the roughness length depending on the aerodynamic geometry of the ground surface [75].

When the atmosphere is stable or unstable, the wind profile in the surface layer is altered from the neutral case and is determined by the semi-empirical Monin-Obukhov similarity theory as:

$$u = \frac{u_*}{\kappa} \left\{ \ln \left(\frac{z}{z_0} \right) + \Psi \right\} \quad (50)$$

where Ψ is the integrated non-dimensional shear function calculated from the atmospheric stability using empirical formulae [77–79].

For the HTO evaporation/condensation process, the soil resistance r_s depends on the availability of HTO from the evaporation site. r_s is larger for drier soils because evaporation occurs from water that is tightly bound to soil particles through intermolecular and electrical forces. In contrast, r_s becomes smaller when the soil is wet because the evaporation occurs from free water that is weakly bound to the soil matrices [80–82]. There are several practical empirical formulations for r_s , as summarized by Mahfouf and Noilhan [81]. For example, Sun [83] proposed a formula:

$$r_s = 3.5 \left(\frac{\eta_{sat}}{\eta_w} \right)^{2.3} + 33.5 \text{ (m}^{-1} \text{ s)} \quad (51)$$

where:

η_{sat} is the soil water content at saturation (porosity); and
 η_w is the volumetric soil water content.

Kondo et al. [80] proposed a formula:

$$r_s = \frac{a(\eta_{sat} - \eta_w)^b}{D_{atm}} \quad (52)$$

where:

D_{atm} ($\text{m}^2 \text{s}^{-1}$) is the molecular diffusivity of HTO in air; and
 a (m) and b are coefficients that depend on soil texture.

After depositing on the soil, HTO migrates through the soil profile. Generally, only aqueous HTO transport is considered under the assumption that HTO in the vapour phase and in the liquid phase are in equilibrium [72, 84, 85]. The HTO vapor concentration in the surface soil air is expressed by:

$$\chi_{sa} = \frac{H_{sat}}{\rho_w} \chi_{sw} \quad (53)$$

where:

H_{sat} (kg m^{-3}) is the absolute humidity at saturation at the temperature of the soil;
 ρ_w (kg m^{-3}) is the density of liquid water; and
 χ_{sw} (Bq m^{-3}) is the aqueous HTO concentration in soil water.

Then, by considering diffusion and advection for aqueous HTO, the HTO transport in a layered soil is calculated by:

$$\eta_w \frac{\partial \chi_{sw}}{\partial t} = \frac{\partial}{\partial z} D \frac{\partial \chi_{sw}}{\partial z} - q \frac{\partial \chi_{sw}}{\partial z} \quad (54)$$

where:

t (s) is the time;
 z (m) is the vertical coordinate in the soil;
 D ($\text{m}^2 \text{s}^{-1}$) is the effective diffusivity for aqueous HTO; and
 q ($\text{m}^3 \text{m}^{-2} \text{s}^{-1}$) is the liquid water flux.

When rapid water flow exists, e.g. during and soon after rainfall, HTO dispersion in soil water can be an effective process for the downward transport of HTO in soil [85, 86]. Then, if needed, the apparent effective diffusivity is altered:

$$D = D_{dif} + \alpha q \quad (55)$$

where D_{dif} ($\text{m}^2 \text{s}^{-1}$) is the effective diffusivity for the molecular diffusion of HTO in soil water and α (m) is the dispersion coefficient [85, 86].

Several empirical formulae are available for D_{dif} as a function of soil water content [87–90]. For example, Penman's formulation [87], employed by several models such as ETMOD and UFOTRI [91, 92], calculates:

$$D_{dif} = \frac{\eta_w}{1.5} D_m \quad (56)$$

where D_m ($\text{m}^2 \text{s}^{-1}$) is the molecular diffusivity of HTO in liquid water.

Eq. (56) simply expresses that, in bulk soil, the diffusive pathway corresponds to 3/2 of the water volume. Other empirical formulations are also available, such as that given by Millington [89]:

$$D_{dif} = \frac{\eta_w^2}{\eta_{sat}^{1.5}} D_m \quad (57)$$

To calculate the above-described HTO exchange and transport, a number of variables related to soil water transport are required (e.g. η_w and q). Soil hydrology is well summarized in many textbooks [82, 93]. Generally, soil water transport is expressed by Richards' equation, as:

$$\frac{\partial \eta_w}{\partial t} = - \frac{\partial q}{\partial z} \quad (58)$$

The vertical water flux q is expressed by the Buckingham-Darcy formulation, as:

$$q = - \left(D_w \frac{\partial \eta_w}{\partial z} + K_w \right) \quad (59)$$

where D_w ($\text{m}^2 \text{s}^{-1}$) is the soil water diffusivity and K_w (m s^{-1}) is the unsaturated hydraulic conductivity. These are related to the water potential h (m) as:

$$D_w = K_w \frac{\partial h}{\partial \eta_w} \quad (60)$$

Several empirical formulae have been proposed for calculating the potential h as a function of soil water content [94–96]. For example, equations of the Clapp - Hornberger type take the form:

$$h = h_s \left(\frac{\eta_w}{\eta_{sat}} \right)^{-b} \quad (61)$$

and,

$$K_w = K_s \left(\frac{\eta_w}{\eta_{sat}} \right)^{2b+3} \quad (62)$$

where K_s (m s^{-1}) is the saturated hydraulic conductivity, and h_s and b are empirically-determined coefficients. Each of these parameters is a function of soil texture [95].

To investigate HTO deposition to soil and subsequent reemission in real environments, several field and laboratory experiments have been conducted, the results of which are valuable for model validation and improvement. HTO deposition mainly occurs within the top several millimeters of soil, decreasing steeply with depth [13, 69–71, 97], indicating that the thickness of the uppermost soil layer in deposition models should be on the order of millimeters to precisely predict HTO exchange at the soil-atmosphere interface [70]. Due to the difference in hydraulic characteristics, as theoretically expected from Eqs. (61) and (62),

the HTO deposition velocity depends on the texture of the exposed soil [69]. Throughout the reemission phase, the HTO flux from the soil to the atmosphere decreases as time passes, in concert with the decrease in the aqueous HTO concentration in the top soil layers due to HTO evaporation as well as downward HTO diffusion [13, 15, 70, 72]. The reduced HTO concentration in the top soil layers causes a re-supply of HTO through upward diffusion of from deeper zones, maintaining HTO reemission over subsequent periods [13, 15, 71, 72].

5.3. DRY DEPOSITION OF HT AND REEMISSION

Deposition of atmospheric HT to soil is caused by subsurface conversion of the HT to HTO by hydrogen-oxidizing micro-organisms ubiquitously contained in surface soils [98–100]. Emission of HTO to the atmosphere occurs even during passage of an HT plume whereas, for an HTO release, reemission of the deposited HTO occurs only after the passage of the plume.

The deposition of atmospheric HT to the soil is normally evaluated by the resistance approach [101], as:

$$F_{HT} = v_{HT} \chi_{atmHT} \quad (63)$$

where:

F_{HT} is the deposition flux for HT ($\text{Bq m}^{-2} \text{s}^{-1}$);
 v_{HT} is the deposition velocity (m s^{-1}); and
 χ_{atmHT} is the HT concentration (Bq m^{-3}) in the atmosphere at a reference height.

Similar to the exchange velocity v_{HTO} for HTO deposition, v_{HT} is expressed by the sum of resistances, as:

$$v_{HT} = (r_{aHT} + r_{bHT} + r_{sHT})^{-1} \quad (64)$$

where the aerodynamic resistance r_{aHT} (s m^{-1}) and the boundary layer resistance r_{bHT} (s m^{-1}) can be determined from Eqs. (47) and (48) respectively, because the atmospheric transport of HTO and HT is basically identical.

The soil resistance r_{sHT} (s m^{-1}) is determined by microbial HT oxidation as well as by HT diffusion in the soil, and hence models for r_{sHT} should consider these below-ground processes. Soil HT transport is expressed by a diffusion equation [84, 102], as:

$$\frac{\partial(\eta_{sat} - \eta_w)\chi_{s,HT}}{\partial t} = \frac{\partial}{\partial z} \left(D_{HT} \frac{\partial \chi_{s,HT}}{\partial z} \right) - e_{HT} \quad (65)$$

where:

η_{sat} is the soil water content at saturation (porosity);
 η_w is the soil water content;
 $\chi_{s,HT}$ is the HT concentration in soil air (Bq m^{-3});
 t is time (s);
 z is the vertical coordinate in soil (m);
 D_{HT} ($\text{m}^2 \text{s}^{-1}$) is the effective diffusivity for HT in soil;
 e_{HT} ($\text{Bq m}^{-3} \text{s}^{-1}$) is a volumetric sink for HT due to oxidation by soil.

The effective diffusivity D_{HT} can be determined from the soil water content η_w in a similar manner to the aqueous HTO diffusivity in soil (Eqs. (56) and (57)), as:

$$D_{HT} = \frac{\eta_{sat} - \eta_w}{1.5} D_{mHT}, \text{ for the Penman type approach [87] and} \quad (66)$$

$$D_{HT} = \frac{(\eta_{sat} - \eta_w)^2}{\eta_{sat}^{1.5}} D_{mHT}, \text{ for the Millington type approach [89]} \quad (67)$$

where D_{mHT} ($\text{m}^2 \text{s}^{-1}$) is the molecular diffusivity for HT in air.

HT oxidation by soils has been investigated through controlled laboratory experiments. The oxidation rate of HT (defined as the amount of HT converted to HTO per unit dry soil mass per unit time) depends on the soil temperature, the soil water content and the HT concentration in the soil air, since the biological activity of the hydrogen-oxidizing microorganisms depends on these environmental variables [103–110]. Due to the decrease in microbial activity with depth in the soil, the magnitude of the HT oxidation rate becomes smaller as the soil depth increases, with a depth scale of less than 10 cm [111]. Also, the oxidation rate of HT can depend on soil texture, with a variation over a factor of two or more [107, 110, 112].

Because of the complexity of HT oxidation by soils, few approaches have been made for modelling the resistance r_{sHT} . Early efforts assumed a first-order reaction for the oxidation process (i.e. $e_{HT} = k\chi_{s,HT}$ where the constant k (s^{-1}) is empirically-determined), so that soil resistance r_{sHT} was formulated by analytically solving Eq.(65) [70, 73, 84], as:

$$r_{sHT}^{-1} = \sqrt{(\eta_{sat} - \eta_w) D_{HT} k} \quad (68)$$

Recently, the HT oxidation process has been empirically formulated as a function of soil water content and soil temperature [108–110], leading to a sophisticated but practical formulation of r_{sHT} by Yamazawa et al. [102], as:

$$r_{sHT}^{-1} = C_{ref} F_t F_w \quad (69)$$

where $C_{ref} = 0.27 \text{ mm s}^{-1}$ is the reference soil conductance, and F_t and F_w are dimensionless functions characterizing the dependencies of r_{sHT} on the volumetric soil water content η_w and the soil temperature T ($^{\circ}\text{C}$), as:

$$F_w = a\{1 - \exp(b\eta_w)\} - c\eta_w \quad (70)$$

$$F_t = 0.0151T + 0.755 \quad (71)$$

where a , b and c are empirically determined constants ($a = 1.73$, $b = -17$ and $c = 4.2$). The moisture function, Eq.(70), reflects the regulation of the HT flux by the efficiency of HT oxidation as well as by HT diffusion in soil.

After HT deposition to soil, HTO formed at the soil surface is emitted to the atmosphere, driven by the HTO concentration gradient across the soil-atmosphere boundary. Although the soil profile of the deposited HTO differs between the HT and HTO cases [70, 104, 113–115], the dynamics of HTO emission after HT deposition is basically identical to that after HTO deposition (see Section 5.2).

To quantitatively evaluate the HT deposition velocity and to understand HT deposition and HTO emission in real environments, several field HT release experiments have been conducted. These have ranged from small-scale studies [70, 101, 116–120] to intensive, large-scale ones in France [120, 121] and in Canada [104, 113, 122–124]. These experiments demonstrated that HT deposition occurs mainly in the top few centimetres of soil and decreases with depth. The measured HT deposition velocities ranged from 10^{-5} m s^{-1} to 10^{-3} m s^{-1} [101, 104, 116, 118–120, 122–126]. These variations, over two orders of magnitude, seem to be mainly driven by soil conditions (water content and temperature), which regulate HT diffusion in soil and microbial HT oxidation, as theoretically described above [101, 104, 116, 118, 119, 121].

5.4. CONCLUSIONS

The status of modelling of deposition of atmospheric HTO and HT to surface soil and the reemission of HTO from the soil to the atmosphere have been briefly reviewed, and basic formulations for these processes have been presented. Because the resistances for the elemental processes comprising the deposition/reemission process critically depend on the gaseous and aqueous transport phenomena in the surface atmosphere and in the soil, basic theories for boundary layer diffusion and soil hydrology were also presented. Overall, many formulations are available for HTO deposition, which are generally based upon the water evaporation process from soil to the atmosphere. However, formulations of the HT deposition process are still limited, and further development is necessary, including models that treat the HT oxidation process in soil as a function of soil texture.

6. HTO UPTAKE IN PLANTS AND OBT FORMATION DURING DAY LIGHT

6.1. OVERVIEW

Tritium is a radioactive isotope of hydrogen that can be released to the environment in small amounts during routine operation of nuclear facilities, and in higher amounts during some types of accidents.

Tritium emitted into the atmosphere is subject to meteorological conditions, such as:

- Diffusion, which causes the tritium concentration decreases due to local mixing conditions;
- Advection, when the wind transports the tritium downwind.

The atmospheric transport of all forms of tritium, including tritium vapours (i.e. HTO and T₂O) and molecular tritium (i.e. HT and T₂) is similar to the transport of other radionuclides in that atmospheric tritium plumes are depleted via wet and dry deposition mechanisms. While dry deposition occurs for most non-noble gas radioactive species and results in diminished plume concentrations downwind, the mechanisms governing dry deposition of tritium are unique.

The major biophysical processes that characterise tritium dry deposition are:

- Initial deposition to ground and vegetation;
- HT conversion to HTO in soil, due to bacterial action;
- HTO uptake by plants, with some HTO being converted to OBT;
- HTO re-emission to atmosphere from soil and plant;
- HTO uptake by roots;
- HTO transport downward in the soil.

The above processes can be generalized as the deposition velocity, V_{dep} , or exchange velocity, V_{ex} , (because tritium transfer is a reversible process), which is the quotient of the net tritium flux to the ground and vegetation, and the tritium air concentration at the same location. For HT and T₂, V_{dep} is largely a function of soil oxidation, ambient wind speed, and stability conditions. For HTO and T₂O, V_{dep} is controlled by vegetation uptake (subject to diurnal fluctuations), deposition to soil, and, as for molecular tritium, existing meteorological conditions.

6.2. DYNAMICS OF HTO UPTAKE IN LEAVES

The dynamics of tritium in SVAT (soil-vegetation-atmosphere transport) may be described in three phases. The first phase is the period of the deposition, when the cloud of HTO passes over the area of interest and atmospheric concentration is the driving force for tritium uptake. The second stage is when HTO is re-emitted from vegetation and soil surfaces into the atmosphere. This process occurs rapidly immediately after the passage of the tritium cloud but later slows. The first and second phases are sensitive to existing meteorological parameters (sunshine, humidity, temperature, and rainfall), as well as on plant physiology and the growth stage of the plants. The third phase starts a few days after the tritium cloud has passed, when soil water tritium is the driving force. In the third stage, the processes that must be considered are the movement of HTO in the root soil, the depth distribution of roots,

evapotranspiration and plant photosynthesis. These can be modelled as slowly-varying processes, using climatic data and approximate dynamics for some plant parameters.

After a brief period of dry deposition, the HTO concentration in the plant decreases rapidly, while the OBT concentration in the whole plant decreases very slowly; but part of the OBT will be translocated to storage parts of the plant. For crops harvested once a year, most of the tritium is in form of OBT. In contrast, for continuously harvested plants, such as forage grass and leafy vegetables, the concentration of HTO will be high in the first few days after an accident. An operational model must include both situations under various agrometeorological conditions. More details are given elsewhere [127].

The driving equation for the transfer of HTO from atmosphere to leaves, ignoring the fraction of tritium input from OBT respiration and tritium output for OBT formation is [12]:

$$\frac{dC}{dt} = \frac{\gamma V_{exc}}{M_w} \left(C_{air} - \frac{\rho_s C_s}{\beta} \right) + \frac{V_{exc}}{M_w} (\rho_s - \rho) C_s \quad (72)$$

where:

- C is the HTO concentration in plant water (mainly leaf water) (Bq kg⁻¹);
- C_{air} is the HTO concentration in air (Bq m⁻³);
- C_s is the HTO concentration in the sap water (transpiration water), resulting from water extraction by roots at different depths (Bq kg⁻¹);
- ρ_s is the saturated air humidity at the vegetation temperature (kg m⁻³);
- ρ is the air humidity at the reference height (kg m⁻³);
- M_w is the mobile water mass in the leaves per unit soil surface (kg m⁻²);
- V_{exc} is the exchange velocity between the atmosphere and plant canopy (m s⁻¹);
- γ is the ratio between HTO exchange velocity and water exchange velocity (typically 0.95); and
- β is the isotopic fractionation between tritium and hydrogen (typically 1.1).

Eq. (72) is used for the whole canopy, ignoring the transfer of air HTO to stems, because the exchange velocity to stems is smaller than that to the canopy by one order of magnitude. The initial diffusion of leaf water to stems is also ignored, because of its slow exchange velocity and the flushing of the stems by a sap flux with definitely lower HTO concentrations initially. In the transition period, the stem water and leaf water gradually equilibrate with the soil water but, generally, the details of this period are ignored for stems, because of their minor contribution to plant water concentration. The second term in Eq. (72) includes in fact the transpiration flux.

Eq. (72) can be simplified, if it is assumed that the HTO concentration in air, C_{air}, is constant, that the exchange velocity between atmosphere and plant canopy, V_{exc}, is constant and that the tritium transfer to soil can be ignored:

$$C_{TFWT} = C_{\infty} (1 - e^{-kt}) \quad (73)$$

where:

- C_{TFWT} is the HTO concentration in plant at time *t* (Bq L⁻¹);
- C_∞ is the steady-state tissue free water tritium (TFWT) concentration (Bq L⁻¹);
- k is the constant rate for HTO uptake (h⁻¹); and
- t is the time after the beginning of the exposure (h).

In Eq. (73), the steady-state TFWT concentration, C_∞ , and the constant rate for HTO uptake, k , are given by the following equations:

$$C_\infty = \frac{\rho_a}{\beta\rho_s} C_{ah} \quad (74)$$

$$k = \frac{\gamma W_{exc} \rho_s}{\beta M_w} \quad (75)$$

where:

ρ_s is the water vapour density in the stomata (g m^{-3});
 ρ_a is the water vapour density in the atmosphere (g m^{-3}); and
 C_{ah} is the HTP concentration in atmospheric moisture (Bq L^{-1}).

The Eqs. (73)–(75) were used in different studies [128–131] in order to explain the experimental data for various plants and environmental conditions. In all these studies [128–131], the large variability between plants and the different environmental conditions emphasized the need to account for the variability of the exchange velocity.

6.3. EXCHANGE VELOCITY APPROACH

It is well known that there is a similarity between water vapour transport in nature and electrical circuits, because, in both cases, the transport is due to specific gradients: the specific humidity in the case of water transport and the electric potential in the case of electricity. Consequently, all environmental resistances have analogies with electrical resistances, because, in both cases, the resistance represents the ratio between a potential difference and a flux of a certain scalar.

It is well established that HTO transfer from air to leaves depends on leaf resistance [12]. At the canopy level, the transfer from the reference height to the canopy (atmospheric resistance, R_a (s m^{-1})) must be considered together with the transfer from the canopy air to the leaves (boundary layer resistance, R_b (s m^{-1})) and the transfer from leaf surface to leaf interior (canopy resistance, R_c (s m^{-1})) (see Figure 20). The canopy resistance, R_c , is an integral over the all stomatal resistances of the plant leaves. The exchange velocity, V_{exc} (m s^{-1}) is defined as:

$$V_{exc} = \frac{1}{R_a + R_b + R_c} \quad (76)$$

In Eq. (76), the canopy resistance, R_c , is the predominant factor.

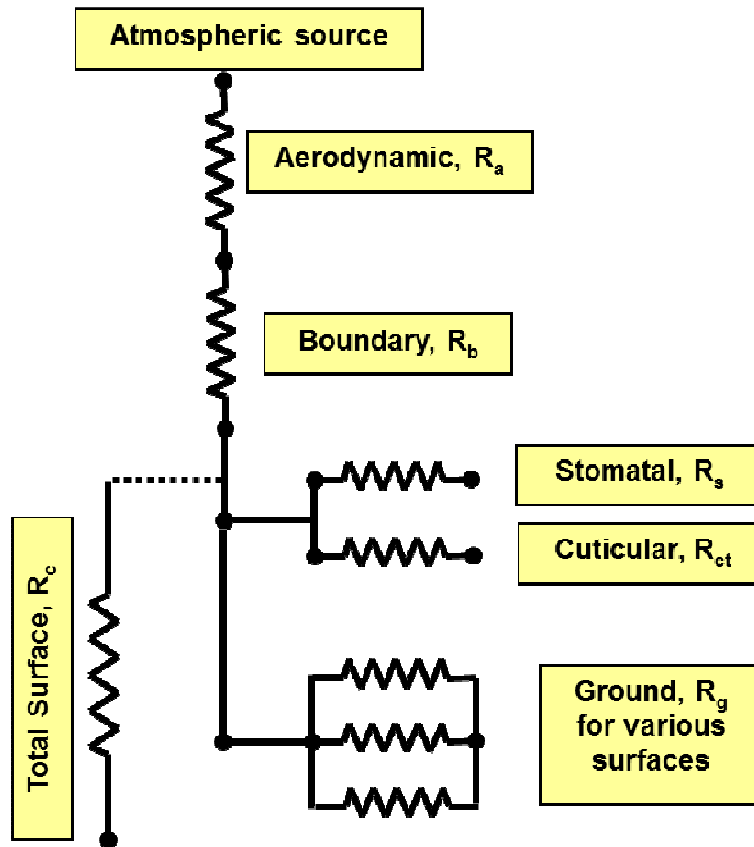


FIG. 20. The analogy between environmental resistances and electrical resistances.

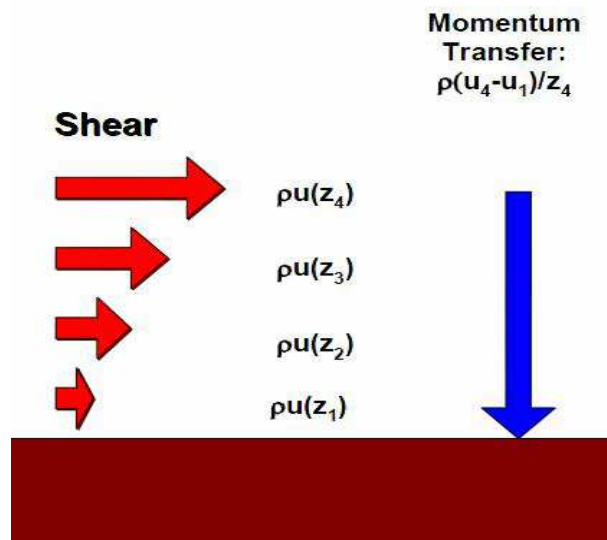


FIG. 21. Visualization of momentum transfer (taken from [132]).

The layer of air adjacent to leaves or soil surface is called the boundary layer. This boundary layer is extremely important for life, as it is a critical path for the transfer of trace gases, momentum and energy between the atmosphere and biosphere [133].

Turbulent eddies are responsible for transporting tritium through the surface boundary layer. The transport processes associated with the transfer of heat, mass and momentum modify the properties of the atmosphere. The momentum must be transferred downward (see Figure 21). A force is needed to change the momentum transfer from one level to another. This drag force or shear stress is equivalent to the momentum flux density.

The classical view of the evolution of flow over a leaf starts with a uniform and laminar stream of air upwind from the leaf. As the air encounters the leaf, there is drag at the surface and shear starts. A wind velocity profile and a boundary layer evolve. Initially the flow remains laminar throughout the boundary layer, but, a short distance from the edge, flow becomes perturbed and turbulence is generated. A logarithmic wind profile develops in the turbulent zone. However, there is always a laminar boundary layer in close contact with the leaf. In the turbulent zone, there is a turbulent and laminar boundary layer. The logarithmic wind profile is given by:

$$u(z) = \frac{u_*}{k} \ln\left(\frac{z}{z_0}\right) \quad (77)$$

where:

- u_* is the friction velocity (m s^{-1});
- k is von Karmann's constant (typically 0.40)
- z is the height above the ground (m); and
- z_0 is the roughness parameter.

It defines the effectiveness of a canopy to absorb momentum and is valid only for very short vegetation and for a neutrally stratified atmosphere.

Aerodynamic resistance determines the rate that momentum and other scalars are transported between a given level in the atmosphere and the vegetation's effective surface sink and is given by:

$$R_a = \frac{1}{ku_*} \ln \frac{z-d}{z_0} - \Psi_c \quad (78)$$

where:

- d is the Zero-Plane Displacement Height which represents the level at which surface drag acts on the roughness elements or the level which would be obtained by flattening out all the roughness elements into a smooth surface; and
- Ψ_c is the adiabatic correction function.

In the boundary layer, heat and water vapour are transferred through molecular diffusion (conduction). The long timescale involved can be represented by a large resistance, the boundary layer resistance, given by the following relationship:

$$R_b = \frac{1}{ku_*} \ln \frac{z_0}{z_c} = \frac{const}{ku_*} \left(\frac{Sc}{Pr} \right)^{\frac{2}{3}} \quad (79)$$

where:

z_c is the scalar roughness length (m);

Sc is the Schmidt number;

Pr is the Prandtl number; and

const is a constant often assumed to be 2 uniform canopies, but which can be much larger over rough, incomplete canopies.

The magnitude of boundary layer resistance, R_b , depends mainly on the depth of the boundary layer and is proportional to the ratio between leaf size and wind speed.

Both R_a and R_b are affected by meteorological conditions like wind speed and atmospheric stability, as well as crop height and leaf size and both of them decrease with increasing wind speed and crop height. Typically, these resistances are smaller over tall forests than over short grass; in addition, they are smaller under unstable atmospheric thermal stratification than under neutral and stable stratification. Some typical values for boundary layer resistance are given in Table 14 for a wind speed of 4 m s^{-1} [134].

A study [134] indicates a typical value less than 20 m s^{-1} for both atmospheric resistance and boundary layer resistance over a temperate deciduous forest during the daytime; the same study [134] gives a value greater than 150 m s^{-1} for atmospheric resistance during the night, when the turbulent mixing height is reduced. In most cases, canopy resistance prevails.

6.4. MODELLING APPROACHES FOR CANOPY CONDUCTANCE

Canopy resistance, R_c , is a function of canopy stomatal resistance, R_{stom} (s m^{-1}), canopy cuticle resistance, $R_{cuticle}$ (s m^{-1}), and soil resistance, R_{soil} (s m^{-1}), all of them acting in parallel, according to the following simple relationship:

$$\frac{1}{R_c} = \frac{1}{R_{stom}} + \frac{1}{R_{cuticle}} + \frac{1}{R_{soil}} \quad (80)$$

All resistances in Eq. (80) are affected by leaf area, stomatal physiology, soil pH, and the presence and chemistry of the liquid drops and films.

The simplest approach to describe canopy resistance is the so-called ‘Big-Leaf’ resistance approach that assumes that the whole canopy is a single big leaf. This approach is based on an electric analogy, because the current flow (i.e. mass or energy flux density) in such a transfer scheme is given by the ratio between a potential and the sum of the resistances to the flow, according to the relationship:

$$F_C = \frac{C_a - C_0}{R_a + R_b + R_c} \quad (81)$$

where:

F_C is the flux of a scalar ($\text{Bq m}^{-2} \text{ s}^{-1}$);

C_a is the concentration of a scalar in the atmosphere over vegetation (Bq m^{-3});

C_0 is the internal concentration of the scalar (Bq m^{-3}).

The scalar in the case of Eq. (81) is tritium.

TABLE 14. TYPICAL VALUES FOR BOUNDARY LAYER RESISTANCE OVER DIFFERENT TYPES OF VEGETATION FOR A WIND SPEED OF 4 m s⁻¹ [134]

Vegetation type	Crop height (m)	R _b (s m ⁻¹)
Grass	0.1	60
Crop	1	20
Coniferous forest	10	10

More elaborate and complex approaches for canopy resistance use a multilayered canopy and consider the partial flux for each layer. The key point for both simple and complex approaches is the scaling from stomatal resistance to canopy resistance, because water and carbon dioxide diffuse across the stomatal cavity, while the leaf is a sum of all the stomata.

Water and carbon dioxide, CO₂, move by diffusion in opposite directions between stomata and air. Water evaporates from cell walls, and moves from the stomata to the air, whereas CO₂ moves from the air, via the stomata into the mesophyll, where it is reduced to sugars by chemical reactions in the Calvin cycle. If the resistance for CO₂ transport from the stomata to the mesophyll is neglected, then the diffusion equations can be written as:

$$E = 1.6 * g * \frac{\rho_a}{M_a} * \frac{e_i - e_a}{p} = 1.6 * g * D \quad (82)$$

$$A_n = A_g - R_d = g_{sc} * (C_s - C_i) \quad (83)$$

where:

- E is the rate of water evaporation (mol m⁻²s⁻¹);
- g is the effective aerodynamic and stomatal conductance (m s⁻¹);
- ρ_a is the specific mass of air (kg m⁻³);
- M_a is the molar mass of air (kg mol⁻¹);
- e_i and e_a are the vapour pressures in the intercellular spaces and in the ambient air, respectively (Pa);
- p is the atmospheric pressure (Pa);
- D is the molar vapour concentration gradient between the intercellular space and the air (mol m⁻³);
- A_n and A_g are the net and gross CO₂ assimilation rates, respectively (mol m⁻²s⁻¹);
- R_d is the respiration rate (mol m⁻²s⁻¹);
- g_{sc} is the stomatal conductance (m s⁻¹);
- C_s and C_i are the molar CO₂ concentrations at the leaf surface and in the leaf interior, respectively (mol m⁻³).

Many descriptions of stomatal resistance have been reviewed [135]. In the Jarvis approach [136], environmental factors such as: light, temperature, vapour pressure deficit (abbreviated as VPD), and soil water deficit are uncorrelated and behave as modifying factors (between 0 and 1) for a minimal canopy resistance. These several variables make the calculation somewhat inconvenient. The basic equation of the Jarvis approach is:

$$R_c = \frac{R_{c_min}}{LAI \times F1 \times F2 \times F3 \times F4} \quad (84)$$

where:

- R_{c_min} is the minimum leaf resistance, which is plant specific ($s\ m^{-1}$);
- F1 is a factor dependent on photosynthetic active radiation (PAR);
- F2 is a factor dependent on air temperature (heat stress);
- F3 is a factor dependent on air humidity (dry air stress);
- F4 is a factor dependent on soil moisture (dry soil stress).

In the Ball-Woodrow-Berry model [137] (abbreviated as BWB), the stomatal conductance for CO_2 , g_{sc} , is dependent: (i) directly on the CO_2 concentration at the leaf surface, C_s ; (ii) directly on the relative humidity at the leaf surface, h_s ; and (iii) indirectly on temperature and radiation, via photosynthesis. The stomatal conductance is:

$$g_{sc} = g_0 + \frac{a * A_n * h_s}{C_s} \quad (85)$$

where:

- g_0 is the minimal stomatal conductance ($m\ s^{-1}$); and
- a is an empirical coefficient.

The main limitation of the BWB model is that “a” in Eq. (85) is an empirical factor.

An improved version of the BWB model [138] (referred to here as the Leuning model) includes the compensation point for CO_2 , Γ (i.e. the CO_2 concentration for which CO_2 uptake equals the CO_2 production) and replaces the relative humidity at leaf surface, h_s , with a function dependent on VPD.

A different approach [139] suggested that the stomata operate to minimize the evaporative cost of plant carbon gain. This condition is met if the marginal water cost of assimilation is constant in time. However, this is not the general case.

In the laboratory experiments, C_i is often found to be a fraction of C_s . For sufficiently high levels of solar radiation, it appears that the ratio between C_i and C_s is only a function of VPD [140, 141]. This formulation [141] has some difficulties for low light conditions. Recently, a better approach [142] has been proposed for stomatal conductance:

$$g_{sc} = g_0 + \frac{a_1 A_g}{(C_s - \Gamma)(1 + \frac{D_s}{D_*})} \quad (86)$$

where:

- D_s is VPD at plant level (Pa);
- a_1 and D_* (Pa) are parameters derived from the closure relationship of C_i ;

$$\frac{(C_i - \Gamma)}{(C_s - \Gamma)} = f_0 - a_d D_s \quad (87)$$

where f_0 and a_d are empirical parameters found as regression coefficients of experimental data based on complex studies [143] (see Table 15).

In Eq. (86), the key parameter, D_* also depends on the mesophyll conductance, g_m .

TABLE 15. EXPERIMENTAL VALUES OF THE EMPIRICAL PARAMETERS f_0 AND a_d FOR DIFFERENT TYPES OF VEGETATION [143]

Vegetation type	f_0	a_d (kPa ⁻¹)
Low vegetation C3	0.89	0.07
Low vegetation C4	0.85	0.015
Scots pine	0.093	0.12
Rice and Phalaris grass	0.89	0.18
Temperate forest	0.875	0.06
Boreal forest	0.4	0.12

In a recent paper [144], the dependence of D^* on g_m was tested and found to be weak. Melintescu and Galeriu [144] found for D^* an average value of 1.2 kPa (range 1.09–1.3) for C3 plants and 8 kPa (range 7.8–8.33) for C4 plants. Details about C3 and C4 plants are given elsewhere [140, 143]. The assimilation rate of CO_2 can be seriously affected by soil water stress, especially during the summer time when the water supply is low. Using a correction for water stress [142], gross CO_2 assimilation rate is given by:

$$A_g = A_g^*[2\beta(\bar{\theta}) - \beta^2(\bar{\theta})] \quad (88)$$

$$\beta(\bar{\theta}) = \max[0, \min(1, \frac{\bar{\theta} - WP}{FC - WP})] \quad (89)$$

where:

A_g^* is the unstressed assimilation (mol m⁻²s⁻¹);

$\bar{\theta}$ is the average soil water content in the root zone;

WP is the wilting point; and

FC is the field capacity.

For physiological approaches, the scaling from leaf to canopy involves the integral of the photosynthetic rate for the entire canopy at the canopy height (i.e. LAI). For example, starting with the Eq. (86), the canopy conductance is given by:

$$g_{c,w} = \int_0^{LAI} \left[g_0 + \frac{a_l A_g}{(C_s - \Gamma)(1 + \frac{D_s}{D_*})} \right] dL = g_0 LAI + \frac{a_l \int_0^{LAI} A_g dL}{(C_s - \Gamma)(\Gamma + \frac{D_s}{D_*})} \quad (90)$$

Physiological approaches are based on rates of photosynthesis. Many models from the simplest to the most complex describe photosynthesis. Some of them are reported below.

The assimilation rate depends on environmental conditions (e.g. temperature, CO_2 concentration, light intensity, humidity, and oxygen concentration). Many approaches are used to estimate the assimilation rate. The most comprehensive approach [145], a biochemical model (referred to here as the Farquhar model), treats CO_2 assimilation as a process limited by a number of factors, each of them controlling different sub-processes, such as rubisco-limited carboxylation, light-limited electron transport, and carboxylase–oxygenase production. Each limiting factor results in a maximum allowable assimilation rate, and the

minimum of these allowable rates is considered the actual assimilation. On the scale of a leaf, the model needs eleven parameters, six of which are plant dependent. In nature, assimilation of CO₂ depends on nutrients and plant age.

Another approach [146] ignores the limitation resulting from carboxylase–oxygenase production in C3 plants and only considers a combination of both rubisco-limited carboxylation and light-limited electron transport limiting processes (co-limitation). A simplified biokinetic model for C4 plants was reported [147] with parameters fitted to a maize cultivar from the Southern United States. A simplified biochemical model [148] was carefully fitted with experimental data from three C4 grass species.

The biochemical models [145, 149] were intensively used with the stomatal conductance defined in the BWB model [137] for land-atmosphere interaction modelling purposes, despite a limitation during the drought conditions.

The leaf-level photosynthesis model [150] (herein abbreviated as TJ (Thornley-Johnson)) featuring simplified gas exchange, but emphasizing stomatal control of assimilation, has received less attention in the literature. Recently, field data [151], obtained for eleven plant species, helped to refine the model parameters for the Farquhar and TJ models. When the results of both models were compared, the Farquhar model explained on average 66% and 82% of the observed variation in the net net photosynthesis rates of C3 and C4 plants, respectively, while the TJ model explained 72% and 76% of the variation, respectively. The more mechanistic, detailed approach to biochemical processes in the biochemical photosynthesis model (i.e. the Farquhar model) was not significantly better than the simpler leaf photosynthesis model (i.e. the TJ model) at predicting the field data.

Although parameter values are known or agreed upon for large scale environments (biomes), realistic model parameter values are difficult and expensive to obtain for specific cultivars of many agricultural crops (e.g. around a nuclear facility).

For practical reasons, another approach [144] uses the canopy photosynthesis model from the WOFOST crop growth model [152]. The leaf gross photosynthesis rate, A_{Lg} , is:

$$A_{Lg} = A_{\max} (1 - \exp(-\frac{\epsilon \times I_{aL}}{A_{\max}})) \quad (91)$$

where:

- A_{Lg} is the gross assimilation rate (kg m⁻²d⁻¹)
- A_{\max} is the maximum photosynthesis rate at light saturation (kg m⁻² d⁻¹);
- ϵ is the initial slope or light use efficiency (kg J⁻¹); and
- I_{aL} is the absorbed photosynthetically active radiation (PAR) (μmol m⁻²s⁻¹).

TABLE 16. MAXIMUM PHOTOSYNTHESIS RATE (A_{\max}) AND LIGHT USE EFFICIENCY (ϵ) AT DIFFERENT TEMPERATURES (T) FOR MAIZE USING WOFOST PARAMETERS

T (°C)	A_{\max} (kg CO ₂ m ⁻² h ⁻¹)	ϵ (kg CO ₂ J ⁻¹)
15	19.0	0.33
20	36.5	0.33
25	55.5	0.32
30	74.0	0.32
35	70.7	0.32

A_{max} depends on the crop type and age, as well as on ambient temperature, while ϵ depends on the crop type, but the weak temperature dependency is ignored in Eq. (91). A_{max} depends also on C_i (determined by ambient concentration, boundary and stomatal conductance). A parameter database for many cultivars of the main agricultural crops in Europe has been established and adapted for Romanian conditions [127, 153]. Many plant specific results given by the biochemical models can be reproduced using the simplified WOFOST model. For example, experimental data for maize [147] (Table 16) and grass [148] (Figure 22) are well reproduced, using the WOFOST model.

The Romanian approach [144] was tested against experimental data for the stomatal resistance of different plant types and the comparisons between model and data are good (see Table 17).

To scale from leaf to canopy, it is necessary to distinguish between sunlit and shaded leaves and to take into account the difference between the air temperature (above the crop) and the canopy temperature. To explain experimental data, the effect of the stage of crop development on photosynthesis and canopy resistance (aging effect) must be considered. All these effects are taken into account in using the WOFOST model and the bulk canopy energy budget, although Melintescu and Galeriu [144] ignored the difference between temperature and stomata resistance for shaded and sunlit leaves in field conditions.

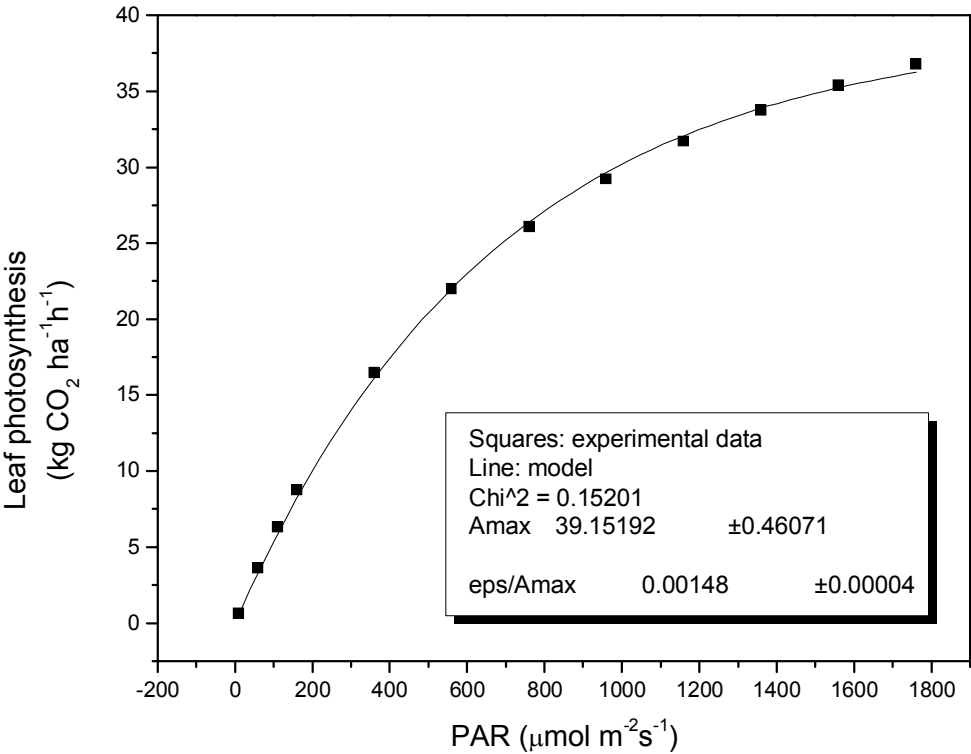


FIG. 22. Comparison between the WOFOST model and experimental data for Kansas grass at an ambient temperature of 40°C.

TABLE 17. COMPARISON BETWEEN THE EXPERIMENTAL AND THEORETICAL DATA FOR THE MAXIMUM STOMATAL RESISTANCE

Plant type	Exp. val. (s m ⁻¹)	Model val. (s m ⁻¹)	References
Wheat (vegetative stage)	41–52	56	Baldocchi [154]
Wheat (anthesis)	62–100	60	Baldocchi [154]
Maize (vegetative stage)	121–131	111	Baldocchi [154]
Wheat	17–20	18	Choudhury and Idso [155]
Potato	100–130	130	Vos and Groenwold [156]
Alphalpha	100–120	110–130 (depends on VPD)	Saugier and Katerji [157]
Soya	66	70	Oliosia et al. [158]
Grass C3	74	74–120 (depends on VPD)	Knapp [159]
Grass C4	151	156–178 (depends on VPD)	Knapp [159]

6.5. OBT FORMATION DURING DAYTIME

Based on the photosynthetic reaction and stoichiometric relationships, OBT production during daytime is linked to the HTO concentration in leaves and the rate of photosynthesis. The dynamics of OBT concentrations in plant parts (ignoring OBT production during the night) [144] are given by the following equation:

$$\frac{dC_{OBT}}{dt} = \frac{P_D}{Y} * (0.6 * FD * C_{HTO} - C_{OBT}) \quad (92)$$

where:

C_{OBT} is the OBT concentration in the whole plant (Bq kg⁻¹ dry matter (dm));

C_{HTO} is the HTO concentration in leaf water (Bq L⁻¹);

P_D is the dry matter net production rate (kg dm m⁻²s⁻¹) and is time dependent, with

$$P_D = \frac{30}{44} P_C ;$$

P_C is the CO₂ assimilation rate (net respiration) (kg m⁻²s⁻¹);

Y is the total plant yield and is time dependent (kg dm m⁻²);

0.6 is a stoichiometric factor which links water assimilation by organic molecules with dry matter production;

FD is the discrimination ratio (the ratio between OBT formation and organically bound hydrogen (OBH) formation), with an average of 0.5, but with a range between 0.45 and 0.55.

In Eq. (92), the net dry matter production (gross assimilation minus respiration and the subsequent conversion to dry matter) is a first approximation that cannot accurately reproduce the dynamics the week after the passage of the plume. An improved approach is being developed.

The results of the Romanian model [144] and experimental data for wheat [160] are compared in Table 18. Model results [144] for potato are given in Table 19.

TABLE 18. COMPARISON BETWEEN THE EXPERIMENTAL DATA [160] AND MODEL PREDICTIONS [144] FOR RELATIVE OBT CONCENTRATION IN WHEAT AT HARVEST

Time	Rel. OBT conc. at harvest (%)		Exposure conditions	
	Exp.	Model	Solar radiat. (W m^{-2})	Temperature ($^{\circ}\text{C}$)
Dawn	0.18	0.29	90–170	11–26
Day	0.25	0.34	400–800	26–36
Dusk	0.20	0.34	26–38	15–24
Night	0.15	0.31	0	12–17

TABLE 19. MODEL PREDICTIONS [144] FOR RELATIVE HTO UPTAKE, HTO HALF-TIME AND RELATIVE OBT CONCENTRATION IN POTATOES AT HARVEST

Day of year	DVS *	LAI	Canopy resistance (s m^{-1})	Rel. HTO uptake # (%)	HTO half-time (min)	Rel. OBT & (%)
162	1.02	2	75	43	44	3.6×10^{-3} ; 0.03
177	1.16	3.5	60	51	32	0.026; 0.21
193	1.31	4	60	49	52	0.051; 0.42
202	1.4	4	45	50	68	0.075; 0.6
219	1.55	3.4	95	44	62	0.03; 0.25
236	1.71	1.9	125	37	90	0.039; 0.33
177 (night)	1.16	3.5	690	14	600	0.022; 0.23

* DVS represents the development stage of the plant and is 0 at emergence, 1 at anthesis and 2 at harvest;

Relative HTO uptake is the concentration of HTO in leaf water at the end of exposure relative to HTO concentration in air moisture;

& Relative OBT is the OBT concentration at harvest (per kg fw or per L of combustion water, assuming 0.2 g dm in tuber) relative to the HTO conc. in leaf water at the end of exposure.

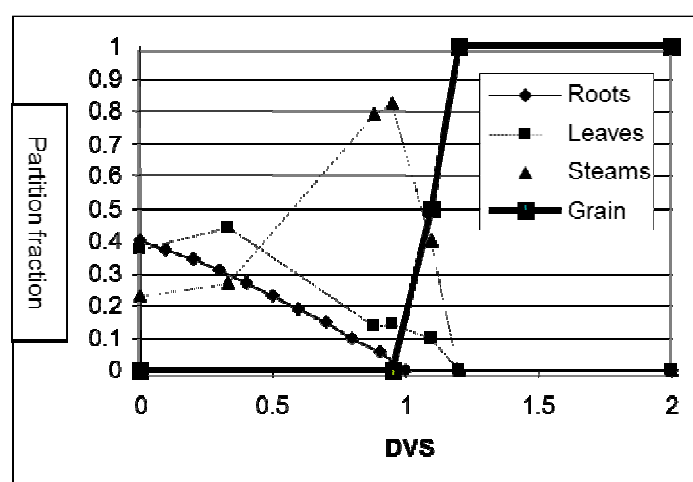


FIG. 23. Partition fractions of newly produced dry matter of roots, leaves, stems and edible grains as functions of DVS (0 - emergence; 1 - flowering; 2 - full maturity) for a maize cultivar F320 (Southern Romania).

6.6. OBT PARTITION IN PLANT PARTS

The dynamics of OBT concentration in a plant part also include the partition factor (fraction of newly produced dry matter translocated to different plant parts). Gross photosynthesis and respiration must be modeled for crops that are continuously harvested because the dynamics of OBT concentration are complex. Partition factors depend on the plant cultivar (genotype), not just on the plant type. The net assimilation rate depends on crop type, development stage (DVS), leaf area index (LAI), temperature, light and water stress (air vapour deficit and soil water deficit). At each stage of plant development, the newly formed net dry matter is differently distributed between the various plant parts, which means that the initial uptake and change over time depends on plant part. Consequently, we must know the partition factors in order to assess OBT production in edible plant parts. Even for leafy vegetables and pastures, the partition to roots must be known.

Examples of partition fractions of newly produced dry matter for different plant parts of a Romanian maize cultivar are given in Figure 23 [127].

6.7. CONCLUSIONS AND RECOMMENDATIONS

This section is a preliminary attempt to analyze the present status of a robust, relatively simple, model of plant uptake of HTO and OBT production during the day. Models for accidental tritium releases that participated in EMRAS I and EMRAS II vary greatly in their complexity. The simplest models use constant exchange velocities for both daytime and nighttime differing from the average value for the day and night; for OBT production at harvest, the integrated HTO concentration in leaves is multiplied by a coefficient. The most complex models use a layered canopy, extensive dynamics of HTO in leaves, and a combination of the BWB model and a generic Farquhar model for photosynthesis; OBT formation and dynamics are based on carbohydrate formation and translocation in a single plant, *Beta Vulgaris*.

Up to the present, there was no attempt to analyze the available models from the point of view of their transparency, user friendliness and robustness of the predictions. An overly complex model is difficult to apply in practice, because it requires too many input parameters values that either do not exist or would be very expensive to obtain from experiments. A very simple model cannot cover environmental variability and crop specific properties. A quality assurance procedure does not yet exist for accidental tritium models. More research, along with open collaboration and interaction between nuclear regulators and utilities, is needed to produce an operational model that will be able to satisfy the requirements of transparency, ease-of-use and moderate conservatism. The work done in WG7 must continue until a model is developed that satisfies such demands.

7. OVERVIEW OF EXPERIMENTS ON TRITIUM TRANSFER FROM AIR TO PLANTS AND SUBSEQUENT CONVERSION TO OBТ

7.1. OVERVIEW

Tritium, as an isotope of hydrogen, enters into many organic forms, but the interest for nuclear safety resides in its bio-available forms [2]. Organically Bound Tritium (OBТ) is defined as “the activity in the combustion water of dry bio-matter that has been washed repeatedly with tritium free water. It represents carbon-bound tritium and buried tritium that was originally formed in living systems through natural environmental or biological processes from HTO (or HT via HTO)” [4] and is primarily formed through photosynthesis in plants, in the presence of tritiated water in leaves. During the night, specific metabolic processes are involved. Knowledge of OBТ concentration in crops is essential for assessing ingestion doses. The “non-exchangeable” form of OBТ is of primary interest, because its dose coefficient is about 3 times higher than for tritiated water.

Moses and Calvin [161] initially observed OBТ formation in the dark by exposing *Chlorella* algae to HTO in nutrient solution under conditions of light and dark for 3 minutes. Tritium incorporation into the non-exchangeable positions of the organic matter in the dark was one-third of that in the light. Thompson and Nelson [162] exposed primary leaves of soybeans to HTO under conditions of light and dark for 1 or 30 minutes. For the same exposure time, the assimilation of tritium in the dark was only 10% of that in the light.

Formed in leaves, OBТ is translocated to the edible plant parts, most of which are reproductive organs. The extent to which OBТ is incorporated in edible plant parts depends on the growth stage of the plant at the time of exposure. OBТ concentration in the edible plant part is highest in the generative period when the fruits develop [163, 164].

The contribution of OBТ to ingestion dose was first recognized in 1994 [165], but only recently was included in the Canadian Standard for routine releases [166].

For routine releases, the contribution of OBТ to ingestion dose is less than 30% and greatly depends on local consumption. For accidental releases, there is still debate as to its importance; in some situations, it can contribute as much as 80% to the tritium dose [68]. Even now, it is not possible to harmonize different views and to agree on the best model for risk assessment after an accidental tritium release. The requirements for a robust, transparent and relatively simple model that is moderately conservative have been formulated, but the development of such a model is difficult, because tritium transfer to crops is subject to changing environmental conditions (meteorology) and depends on many plant physiological processes with site specific parameters (adaptation). Models must be based on physical reality and must be subjected to quality assurance procedures including uncertainty and sensitivity studies; they must also be tested with experimental data [167]. Only a few blind tests of models against experimental data have been done in the past [4, 168] and this limits our ability to demonstrate model reliability.

The debate over the impact of night production of OBТ is ongoing. Experimental results show that the formation of OBТ at night is usually less than during the day for similar air concentrations. However, for the same source term, the air concentration of tritiated water at night is up to 40 times higher than during the day. Uptake of HTO by leaves at night is higher than expected, up to a third that of the day. In a few cases, conversion of OBТ at night has been observed to be higher than during the day (see later in this section).

A recent review of tritium in plants [5] mentioned the impact on ingestion dose of OBT resulting from short term releases ; normally French and Canadian nuclear safety authorities [169, 170] concentrate on the dose impact of routine releases. No detailed review of experimental findings for short term exposures exists, and the present report hopes to remedy this shortcoming. In this section, published, but obscure results, that include nighttime data from the open literature are presented. A brief review of processes involved in the production and transport of assimilates in crops is included, but modelling approaches will be a subject of a further report.

The experimental data presented are organized according to the country of origin. Key aspects are reviewed. Existing difficulties and the need for further international collaboration will be emphasized.

7.2. EXPERIMENTS IN GERMANY: WHEAT, BEAN, POTATO

7.2.1. Wheat

In the first systematic experimental approach [160], a dedicated climatic chamber was used in the laboratory for the dark experiments. A diminished leaf uptake rate was observed, because of a significant, but not complete, closure of the stomata. The plant/air concentration ratios in dark conditions were reduced to 23% in leaves, to 25% in stems and to 59% in ears, compared with those observed in high light conditions. No significant difference in the HTO uptake between spring wheat and winter wheat leaves was observed. In leaves, initial OBT concentrations in the dark were typically half those in high light conditions. It was clearly demonstrated that a small, but not insignificant, amount of OBT is incorporated under night conditions in leaves, stems and ears. This indicates that tritium can be incorporated into organic matter not only by photosynthesis, but also by metabolic pathways independent of light (e.g. by reactions of the tricarboxylic acid cycle or other metabolic conversions). In an extended night experiment, the OBT concentrations in the ears increased by a factor of 3 during the extended dark period. This indicates high rates of metabolic turnover in the ears, which does not result in *de-novo* synthesis of organic material.

The total OBT in the plant increased until day 1 after exposure, because the HTO concentrations in the exposure chamber decreased slowly, as did the TFWT concentrations in the plants. OBT had been transported into the grains by the end of day 1. While the fractions of OBT to total tritium in leaves, stems and husks decreased with time, OBT in grain increased considerably until harvest. Apparently, little loss of OBT occurs from grain once translocation has taken place.

To quantify the translocation of OBT to grain, a so-called translocation index (TLI) was defined. The TLI is the fraction of the OBT concentration in grain at harvest (Bq mL^{-1} water of combustion) relative to the TFWT concentration in leaves (Bq mL^{-1}) at the end of exposure to HTO. This definition will be used in this section.

The TLI, observed in a series of exposure experiments with potted spring wheat in different growth stages between anthesis and maturity, shows that the final OBT concentration in the grain was highly dependent on the time of exposure (Table 20 and Figure 24). Under night time conditions (experiments Wn2b WN2a in Table 20) the uptake into TFWT of leaves was about four times lower than that under daylight conditions. Relative to the same TFWT concentration, the initial OBT concentration in leaves in the dark is about half that in daylight conditions. The values of TLI in Figure 24 are not relevant, because the OBT concentrations

at harvest are being compared with HTO concentrations in leaves at the end of the 2 hour experiment when HTO concentrations in leaves are still high. Note that night and day values are similar.

The general processes of wheat growth explain the shape of the time dependence of the translocation index in Figure 24. Results for growth of grain (dry matter – dm) and the growth rates of grain and above ground plant (Table 21) were obtained using the WOFOST crop growth model [152] for a generic winter wheat and average weather in Central Germany. Partition reflects the share of new dry matter translocated to the grain (after respiration). When the grain starts to fill, the partition to grain is small and the growth dilution effect is high (compare ear at day 1 and harvest in Table 20), thus resulting in a low TLI. Once the grain has matured, much of the OBT formed in the leaves is being used for maintenance respiration and little remains to be translocated to grain.

A series of experiments were done in the field to observe daily variations in the OBT accumulation in grain at harvest [171, 172]. A plastic box was mounted in a field and tritium was released into the box for 1 hour (with ventilation). Subsequently, the box was opened and the plants were left to grow naturally. Conditions in the box (relative humidity, temperature) were recorded, as was the photosynthetically active radiation above the box (PPFD). Experimental data (hour of the start of the experiment, average temperature and relative humidity, PAR outside the box, and day after flowering) for the hour-long exposure in the box are given in Table 22. Note that the experiments in 1996 (shown in bold and shaded in Table 22) are of better quality, because the levels of CO₂ in the box were maintained at natural values.

The initial (1 h) concentration of HTO in the leaves relative to the average concentration of HTO in air moisture in the box is given in Figure 25.

The atmospheric HTO concentrations in the box during the 1 hour exposures were difficult to maintain at constant levels, and their mean values (as applied in Figure 25) are not the same as those for the last quarter hour (see Figure 26 for the dynamics of HTO in air moisture). Using the experimental results of air concentrations, light and temperature, the leaf HTO at the end of exposure can be successfully modelled [173–175].

Maximum relative Tissue Free Water Tritium (TFWT) concentrations were reached in the leaves under strong sunlight when the stomata were open (mean = $73 \pm 19\%$). Uptake was only slightly reduced in senescing leaves. In the night experiments, a diminished uptake into the TFWT of leaves, stems and ears was observed because of the closure of the stomata (mean = $18 \pm 1\%$). The day vs night difference can also be observed in stems and ears, although the relative TFWT concentrations are much lower than for leaves because the surface area relative to mass is smaller. The HTO uptake into leaves under laboratory conditions was $86 \pm 2\%$ in high light conditions and $20 \pm 7\%$ during the night after 2 hours [172].

The half-lives of HTO concentrations in the first hour after the end of exposure are given in Table 23; their values demonstrate the diurnal pattern of canopy conductance.

TABLE 20. EXPERIMENTAL DATA FOR HTO AND OBT CONCENTRATIONS (Bq mL⁻¹) IN WHEAT [172]

Exp.	W6b	W7b	W6a	W7a	WN2b	W8b	WN2a	W8a	W9b	W9a
DAF*	1	6	7	12	13	15	19	21	27	33
OBT										
ear (1 day)	831	478.6	568	787		822	427	384		
ear (harvest)	81.2	113.7	151	381	222	523	357	481	394	296
grain (harvest)	51	229	179	483	474	657	447	610	543	362
HTO										
leaf (2 hours)	81899	89379	94254	86642	72911	106130	67441	93513	98587	96886
leaf (>1 hours)		64347		66938	59431		71115		91702	80361
leaf (> 2 hours)	49727		50433	52124		45824	56562	50115	73764	74301
leaf (1 day)	2934	4720	3903	4677		6329	6051	6383	4675	

* Day after flowering.

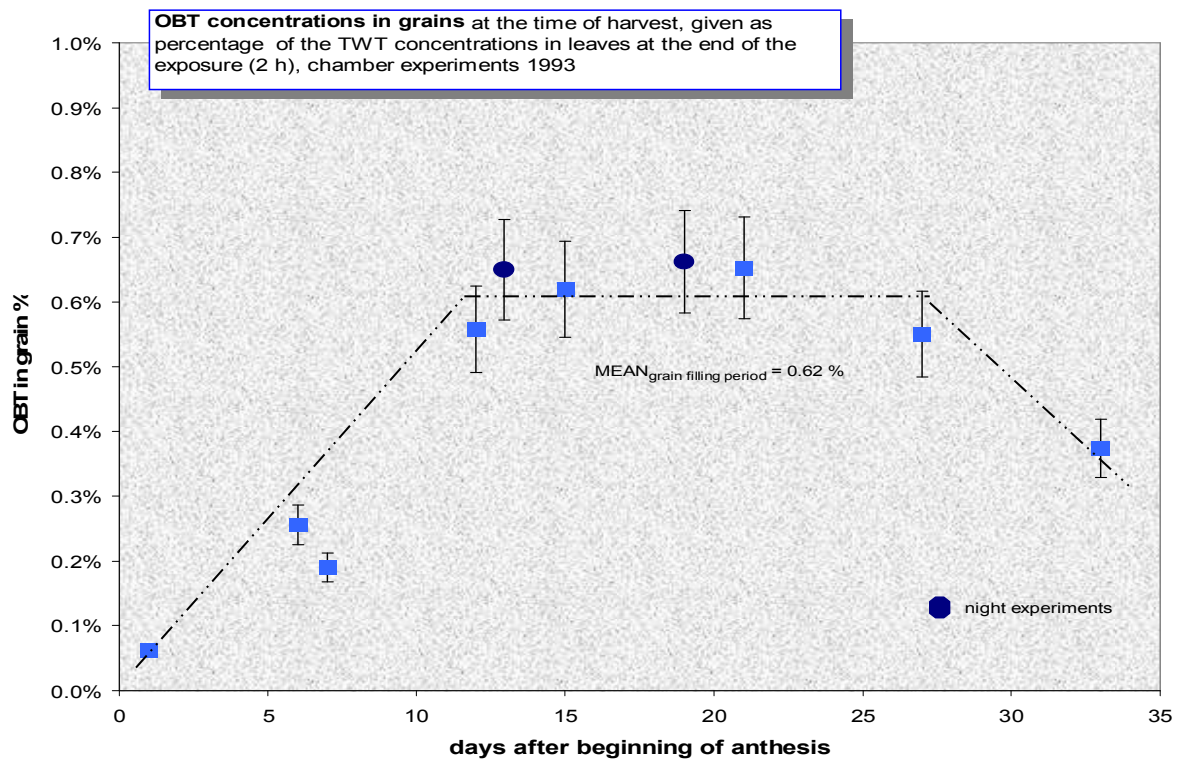


FIG. 24. Translocation index for OBT in grain (taken from [171]).

TABLE 21. RESULTS FOR WINTER WHEAT GIVEN BY THE WOFOST MODEL

Daa *	grain (kg ha ⁻¹)	Grain rate (kg ha ⁻¹ d ⁻¹)	Plant rate (kg ha ⁻¹ d ⁻¹)	Partition	LAI	WLV ^{&} (kg m ⁻²)	M/G [§]
-2	28	28	254.2	0.1	6.91	0.326	0.28
0	309	178	261.2	0.7	6.79	0.3203	0.29
2	820	255	258	1.0	6.68	0.3152	0.29
6	1828	250	251.4	1.0	6.49	0.3063	0.31
11	3061	244	242.5	1.0	6.3	0.2971	0.33
19	4933	222	216.3	1.0	6.06	0.2858	0.36
21	5360	211	205.8	1.0	6.01	0.2836	0.37
26	6335	183	177.5	1.0	5.37	0.2534	0.41
33	7407	124	113.9	1.1	3.09	0.1456	0.45
34	7521	114	103.4	1.1	2.86	0.135	0.47
37	7799	82	70.2	1.2	2.25	0.1059	0.52
44	8012	0	0		1	0.047	0.92
56	8012	0	0		0.06	0.003	1.00

* Day after anthesis (flowering); [&] weight of green leaves; [§] the ratio between maintenance respiration and gross assimilate production.

TABLE 22. EXPERIMENTAL DATA FOR THE HOUR-LONG EXPOSURE IN THE BOX [171]

Exp.	f3	f14	f7	f2	f4	f10	f15	f1	f9	f13	f5	f11	f6	f12
Start (h)	7	7	8	9	10	11	11	14	15	15	20	20	23	23
T (°C)	18	11	26	28	29	26	32	33	36	29	24	15	17	12
RH [*] (%)	76	93	76	76	63	75	63	70	70	72	84	89	89	93
PPFD ^{&} ($\mu\text{mol m}^{-2}\text{s}^{-1}$)	160	179	370	644	1230	1160	1830	1180	1375	1170	54	86	0	0
DAA [§]	18	22	24	17	18	14	28	15	12	21	22	20	22	20

* Relative humidity; [&] photosynthetically active radiation; [§] day after anthesis.

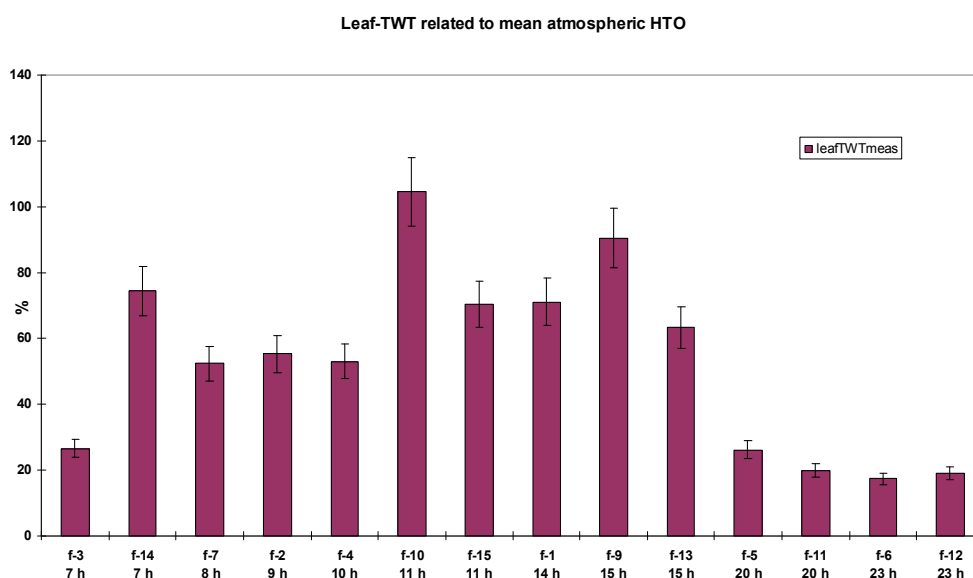


FIG. 25. Concentration of HTO in leaves relative to the average concentration of atmospheric HTO during the 1 hour exposure) (taken from [171]).

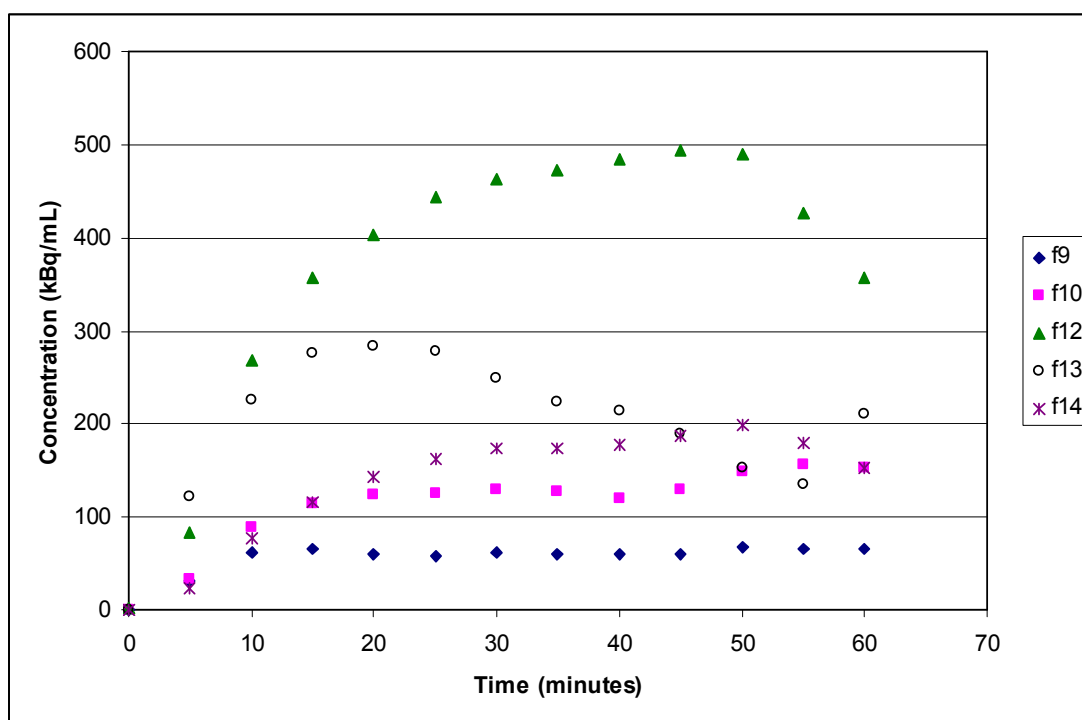


FIG. 26. Time-dependence of HTO concentrations in air moisture in the box.

TABLE 23. HALF-LIVES OF TISSUE WATER TRITIUM (TFWT) CONCENTRATIONS IN WHEAT WITHIN THE HOUR AFTER THE END OF EXPOSURE TO HTO

Plant parts	TFWT half-lives (min)			
	Exposure at dawn (3 exp.)	Exposure at day time (6 exp.)	Exposure at dusk (2 exp.)	Exposure at night (2 exp.)
Leaves	40–60	25–49	230–660	110–170
Stems	45–49	20–26	130–320	60–190
Ears	79–91	50–126	210–330	150–920
Total plant	50–72	27–60	220–340	100–250

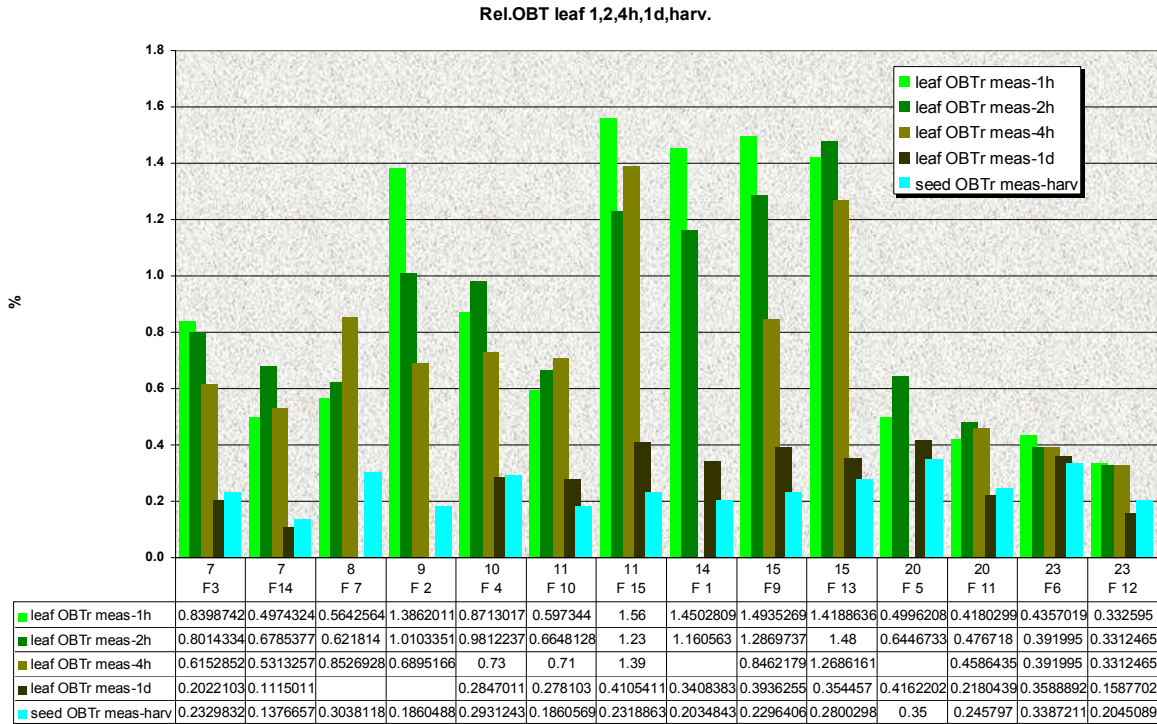


FIG. 27. The dynamics of OBT in leaves after a 1 hour exposure to HTO (taken from [171]).

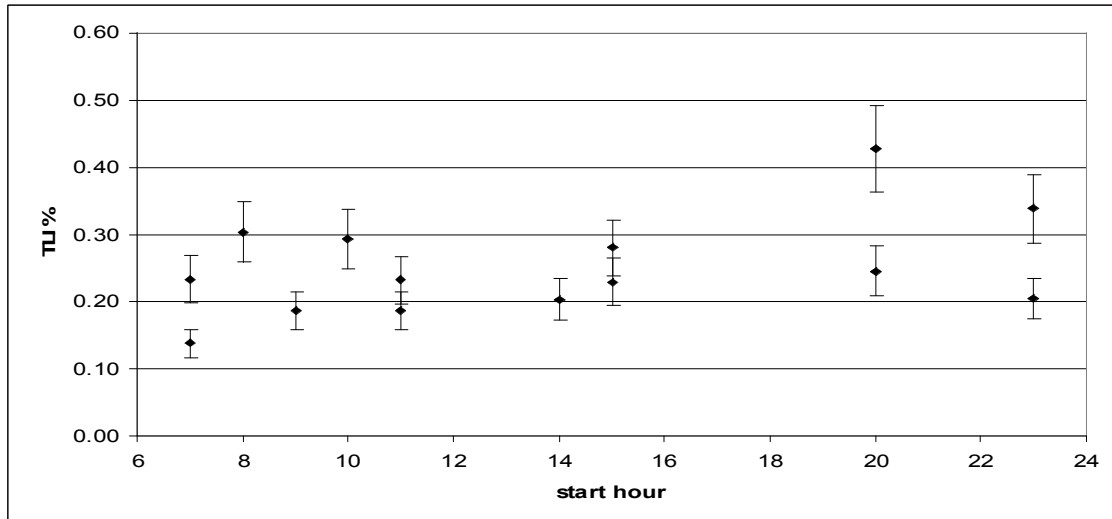


FIG. 28. Translocation index for wheat at different starting hours of exposure.

If we normalize OBT concentrations (combustion water) to the HTO concentrations in leaves at the end of a 1 hour exposure, the dynamics reveal some interesting differences between OBT in leaves under day or night conditions (see Figure 27). Immediately after the end of exposure, the highest relative OBT concentrations were observed in leaves under daylight conditions ($1.25 \pm 0.34\%$); these daylight results were about 3 times higher than those under night conditions ($0.38 \pm 0.05\%$). For daylight exposures, at the end of the first day post-exposure, leaf OBT is clearly reduced due to assimilate export, which seems to start immediately after the end of exposure. For night conditions, assimilate export is slower and perhaps more active after 24 hours. Despite the large differences in leaf OBT at the end of the exposures at various times of day and night, the OBT in grain at harvest shows similar relative values (mean = $0.25 \pm 0.07\%$) in all cases. This can be partly explained by HTO being resident longer in leaves during night time experiments (F6, F12) allowing a larger contribution of metabolic processes to OBT formation. The translocation index for each experiment is given in Figure 28.

The average dynamics of OBT in leaves and grain are shown in Figure 29 for day and night experiments. Translocation in the night experiments appears to be delayed until the next morning and lasts longer compared with experiments in daylight.

Total OBT per plant increases during the first 2 days post-exposure and can decrease to 80% of maximum value at harvest (Figure 30). The large decrease of OBT in leaves is due to translocation to grain and growth dilution. Although maintenance respiration is low in grains, it explains the decrease in total plant OBT.

The correlation between OBT in grain and the integrated HTO concentration in leaves and ears was investigated [172]. The best fit was obtained by adding half the ear concentration to the leaf concentration for day time and using a general factor of 0.2 for the integrated night concentrations (see Figure 31). The total HTO integrated concentration is the sum over the day and night.

Using the slope (0.48) of the line in Figure 31 combined with the average value (0.6) of water released from the combustion of dry matter, a relationship between the harvest value of OBT in grain (Bq kg^{-1}) and the integrated and weighted HTO activity in leaf and ear (distinguishing between day and night) can be deduced. Assuming an average time for grain maturation of 40 days, and a proportionality constant of 0.27,

the following relationship can be deduced:

$$\begin{aligned} \text{OBT (Bq kg}^{-1}\text{)} &= 0.6 * 0.48 * \text{INT (kBq hour L}^{-1}\text{)} = 0.6 * 0.48 * \\ &\text{INT (Bq d L}^{-1}\text{)} * 24/1000 = \text{INT (Bq d L}^{-1}\text{)} * 0.27/40 \end{aligned} \quad (93)$$

This result shows a simple relationship between OBT concentration in grains and the integrated HTO concentration in leaves and ears. Previously, it was unknown whether or not the correlation was real.

Insights first gained from chamber experiments about the relatively high OBT concentration in grain following exposures at dawn (i.e. partial darkness) and during the night (i.e. complete darkness) were confirmed. Gas exchange measurements showed that assimilation in chloroplasts starts early in the morning when the TFWT concentration in leaves is still high [176].

For wheat, the experimental data obtained from field and chamber studies show that the translocation factor at night is similar to that in the day. For a 1 hour exposure the average value is 0.23%.

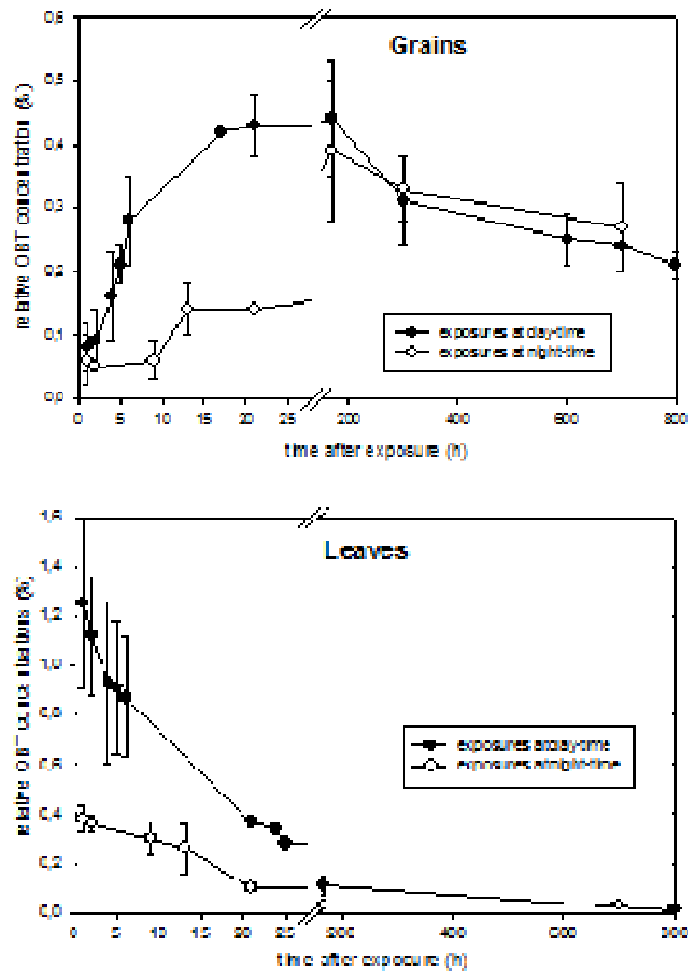


FIG. 29. Patterns of relative OBT concentrations in leaves and grains after exposure to HTO and harvest. The data represent means \pm 1SD of 7 exposures under day time conditions and of 2 exposures under night-time conditions (taken from [172]).

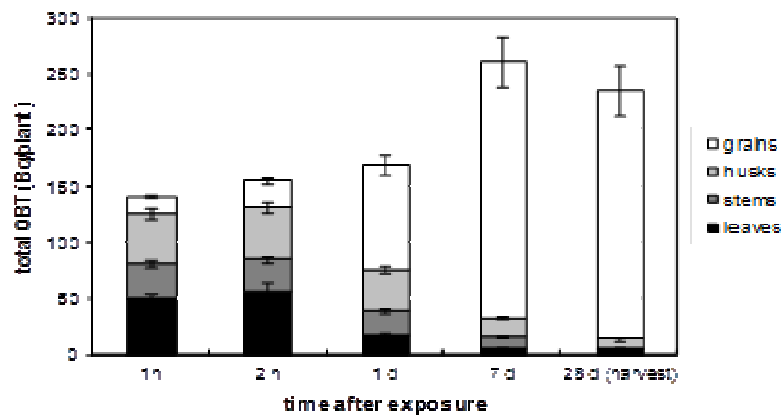


FIG. 30. The distribution of OBT within wheat plants exposed to atmospheric HTO during the dusk on the 20th day after anthesis (error bars represent counting plus analytical errors) (taken from [172]).

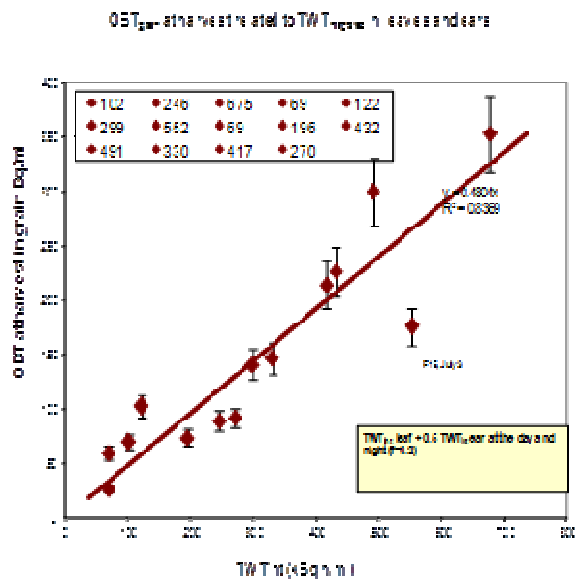


FIG. 31. Correlation between OBT in grain and integrated HTO concentration in leaves and ears (taken from [171]).

TABLE 24. EXPERIMENTAL DATA FOR BEAN AND POTATO [177]

Plant part	Exposure at 900 $\mu\text{mol m}^{-2} \text{s}^{-1}$	Exposure at 120 $\mu\text{mol m}^{-2} \text{s}^{-1}$	Exposure at night
Beans			
Time after flowering (days)	4	1	12
Leaves	0.7	0.3	0.5
Stems	0.4	0.2	0.3
Pods	0.1	0.03	0.4
Potato			
Time after flowering	20	13-25	15-23
Leaves	0.2	0.2	0.2
Stems	0.2	0.1	0.2
Tubers	0.3	0.2	0.2

7.2.2. Beans and potatoes

A limited number of data from chamber experiments were obtained for beans and potatoes [177]. Cultivars of bean (*Phaseolus vulgaris* L., cv. Hilds Maja) and potato (*Solanum tuberosum* L. cv. Erstling and Sieglinde) were grown in pots; the experimental protocol was the same as for the wheat in the first experiment described [160]. The experiments were carried out at 0–24 days after flowering for the bean and 13–45 days for the potato. After 2 hours of exposure at night, the relative leaf/air concentration was 15% in bean and 14% in potato; in the light (900 $\mu\text{mol m}^{-2} \text{s}^{-1}$) the relative concentrations were 77% and 83%, respectively. These data are similar to those for wheat and demonstrate a relatively high leaf conductance at night.

The relative OBT concentration at harvest (in terms of leaf HTO at end of 2 hours exposure) is given in Table 24. Based on these data, night translocation in beans appears to be similar to that of wheat, but lower than that of potato. More experimental data are needed.

During the night exposures, the rate of OBT formation was 4–5 times lower than under daylight conditions because the plants were not photosynthesizing. OBT formed at night was created by metabolic processes, independent of light, which are responsible for energy supply, growth and maintenance of plant structures.

As already shown in the above studies with spring wheat, green beans and potatoes, the storage organs represent a sink for organically bound tritium within agricultural ecosystems, which should be considered in models predicting the dynamics of tritium transfer in these systems.

7.3. EXPERIMENTS IN JAPAN: RICE, SOYBEAN AND TANGERINE

Due to restrictions on the use of tritium in experiments, Japan has used deuterium instead. Deuterated water (D_2O) release experiments were conducted in a greenhouse using many types of vegetation at the Mito site of Ibaraki University and in a climate controlled chamber at the Japan Atomic Energy Agency using rice.

7.3.1. Rice

Rice is an important food in Japan and in many Asian countries and contributes up to 36% of the ingestion intake from background tritium. Potted rice plants were exposed to D_2O vapour in two identical greenhouses [7.2 m(L) \times 1.8 m(W) \times 1.8 m(H)]. One was used for daytime experiments, while the other was used for night time experiments [178]. The ripening period of rice, 40–60 days depending on cultivar and climatic conditions, is the stage between flowering (anthesis) and . A rice cultivar (Yumehitachi) harvested after 25 days was used in the experiment. Rice plants were grown in both flooded and non-flooded pots. D_2O vapour, with a concentration of 20%, was released using an ultrasonic humidifier in a small box connected to the greenhouse and supplied with a flow of dried air. The inside temperature was 29.6–34.1°C during the day and 19.6–23.6°C during the night. The air relative humidity was 44–57% in the daytime and 71–94% at night. Light intensity, as photosynthetic photon flux density, was $158 \mu\text{mol s}^{-1} \text{m}^{-2}$ on average (range 23–370 $\mu\text{mol s}^{-1} \text{m}^{-2}$) during 8 hours of daylight. The release duration was 8 hours and the deuterium concentration in the greenhouse increased gradually. Deuterium concentration in air moisture in the daytime did not increase as expected, so a larger amount of deuterated water was released during the night time experiment. Therefore, deuterium concentrations in air moisture at night were much higher than that in the daytime.

The concentration of the tissue free water deuterium (TFWD) in leaves followed the air D_2O concentrations, and the ratio reached 0.53 at the end of exposure. The rate constants of D_2O uptake in leaves in the daytime were 4–5 times higher than that in night time. At the end of release the organically bound deuterium (OBD) in leaves normalized to the same air concentration was 3–4 times less in night time than in the daytime; in grain, the difference was larger. Total OBD formation during the daytime D_2O release was about 10 times higher than that during night time exposure. After the exposure stopped, the OBD concentration in grain continued to increase for about 4 days. Then, due to growth dilution, the OBD concentration in grain decreased until harvest. The translocation indexes for deuterium concentration in air moisture at the end of the exposure (TLIa) were about 0.2% for unhulled rice and 0.3% for hulled rice for both the daytime and night time experiments, but the TLIa

for daytime was slightly higher than that for night for both flooded and non-flooded cases. The translocation indexes for leaf TFWD at the end of the exposure (TLI) were 0.42% for day unhulled, 0.73% for day hulled, 0.36% for night unhulled and 0.54% for night hulled. Although the exposure lasted 8 hours, these results are lower than in wheat (0.23% for a 1 hour exposure).

At the same time and in the same greenhouse, a different rice cultivar (Koshihikari) was exposed to D₂O vapour 1 week after flowering [179]; this is the period of grain maturation or filling. The background deuterium concentration in Mito air was 150 ppm (D/H), while the background OBD in grain was 144 ppm. After 8 hours of exposure, the OBD concentration in the rice grain had increased by 25 ppm, after both day and night exposure. The day/night ratios of OBD concentrations normalized to the same air concentrations immediately after exposure were 2.5 for the grain and 2.9 for the leaf. The OBD concentration in grain was measured after the harvest on the 45th day of the experiment, and the OBT concentration in grain after the night time exposure had decreased faster than that after the daytime exposure. The TLI (normalized to TFWD at the end of exposure) was 0.36% for the grain exposed during the daytime and only 0.03% for grain exposed at night. For this case, when the rice was exposed just when the grain was starting to mature, the night translocation index was 10 times less than that for the day. The time dynamics of the TLI from exposure until harvest show a clear distinction between day and night (see Figure 32).

Potted rice plants were exposed to D₂O vapour, as a substitute for tritium, in a climate controlled chamber (temperature, humidity and light intensity) for 4 hours at five different times during the grain-ripening period to estimate the influence of the growth stage on the formation and retention of OBD in rice [180]. The plants were grown outside before and after the exposure experiments. Concentrations of TFWD and OBD in rice leaves, stems and grains were measured up to harvest.

At the end of the 4 hour-exposure, TFWD in leaves reached 55–74% of the D₂O concentration in air moisture. After 1 day the TFWD in leaves was close to background concentrations. The TFWD in the grain remained for a longer time after the end of exposure than it did in the leaves and stems. The mass of OBD in grain at harvest showed the highest value when the exposure took place in the early stage of the ripening period. When the exposure occurred after 26 days after the flowering, the increase of OBD in the grain was small. Most OBD in the rice plant was formed within 24 hours after the initial exposure and was transferred immediately to the grain. The amount of OBD in grain did not decrease until harvest. The translocation indexes for grains and stems are given in Table 25 for each experiment performed at days after flowering (DAF).

7.3.2. Soybeans

The TLI (for TFWD) for soybeans [128] at an early stage of pod development had a low value (0.14% for day and 0.17% for night) in a preliminary experiment.

For more D₂O exposure experiments [129], soybeans were grown on the ground in the greenhouse or in pots. Soybean plants were exposed at various stages of development for 8 hours; both relatively young (consumption of green soybeans is common in Japan) and fully ripened beans were harvested. Details of the growth conditions in the experiments are given in Table 26. The uptake rate of TFWD depended on the age of the plant. The rate constants of D₂O uptake in leaf were several times higher during the day than during the night. The D₂O uptake in bean and hull was very low in both daytime and night time exposure.

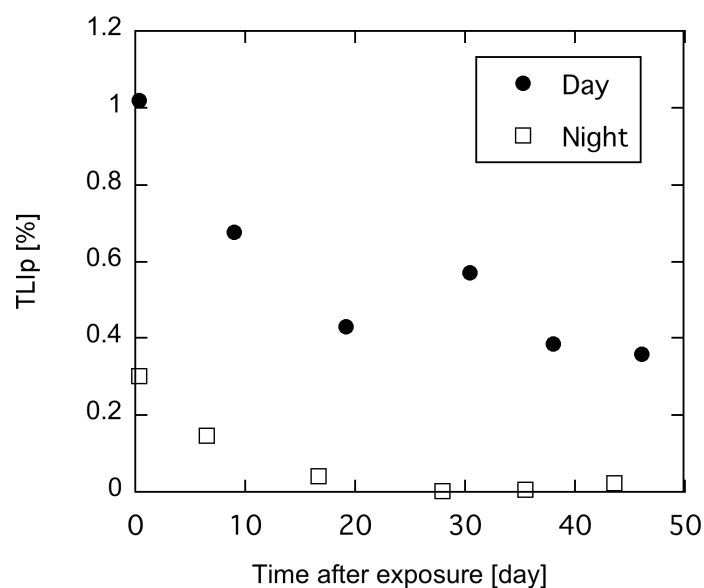


FIG. 32. Dynamics of the translocation index for Koshihikari rice as a function of time after exposure.

TABLE 25. TRANSLOCATION INDEX (TLI) FOR RICE (4 HOURS EXPOSURE)

TLI (%)	Days after flowering				
	6	14	21	26	35
Grain	0.39	0.55	0.43	0.15	0.045
Stem	0.05	0.03	0.04	0.03	0.03
Leaf	0.19	0.14	0.17	0.18	0.12

TABLE 26. GROWTH CONDITIONS AND SAMPLING TIMES FOR SOYBEANS DURING DIFFERENT EXPERIMENTS

Exp. No.	Year	Non-harvest			Harvest		
		Exp. date	Condition	Seeding	Flowering	Young bean	Ripened bean
I	1999	21, 22 Aug	ground	6 Jun			23 Oct (63, 62)**
II	2000	10 Aug (25)*	pot	6 or 21 Jun	16 Jul	4 Sep (26)**	10 Oct (61)**
III		12 Sept (58)*	pot	6 or 21 Jun	16 Jul	19 Sep (7)**	10 Oct (28)**
IV		30 Apr (-)*	pot				22 Jun (53)**
V	2002	27 Aug (13)*	pot		14 or 18 Aug	3 Sep (7)**	4 Oct (38)**
VI		12 Sep (29)*	pot		14 Aug	16 Sep (4)**	11 Oct (29)**
VII		12 Sep (25)*	pot		18 Aug	16 Sep (4)**	11 Oct (29)**

* Numbers in parentheses indicate the elapsed days after flowering.

** Numbers in parentheses indicate the elapsed days after the experiment.

In 2000, the beans exposed were in the early middle stage of growth on August 10 and in the late stage on September 12. In the early stages, the TLI was about 0.2% from a daylight exposure and lower at night. In 2002, the soybeans on were in the early stage of growth on August 27 and were in the early retardation phase on September 12. The highest TLI of 4.3% (for daytime exposure) was observed a few days after exposure, but at harvest the TLI had decreased to 0.8% (see Figure 33). The TLI for green soybeans after a night time exposure was 1/5th that from a daytime exposure, while for ripened beans the ratio was 1/2. Table 27 summarizes the soybean results and demonstrates that the TLI during the night is lower than that during the day. Soon after exposure, the TLI is high and decreases until the final harvest (28 days later). At final harvest, the TLI is about 0.7% for the daytime experiment and 0.5% for the night time experiment.

Note that these results are for an exposure of 8 hours, during which time the deuterium concentration gradually increased in the greenhouse. A rough approximation for a 1 hour exposure would be to divide the TLI by 4–6.

7.3.3. Tangerine

Tangerine (*Citrus unshiu* Marc.) was exposed to D₂O vapour in greenhouses 6 times during the D₂O release experiments of 2000–2002 [130]. Exposures were before and after flowering, as well as in the middle or end of the ripening period. The duration of exposure was 8 hours for both the daytime and night time experiments. Depending on growth stage, temperature, light and humidity, the uptake rate constants from air to tangerine leaf in the daytime varied between 0.2 and 1.1 h⁻¹. At night, the rate constants were several times lower (0.03–0.12 h⁻¹). These values were lower than for rice and soybean used in the greenhouse experiments because cuticle structure for tangerine leaves differs from rice or soybean. After the exposure the loss rate constants for leaf TFWD were 0.8–1.2 h⁻¹ in the daytime and 0.03–0.2 h⁻¹ at night. Lower values were observed in winter than in summer. The translocation index (as defined in this report) varied from 0.08–0.28% in the daytime and from 0.21–0.71% in at night, with the maximum in the middle of the ripening period. Note that for this experiment, the night OBT formation rate is higher than the daytime rate.

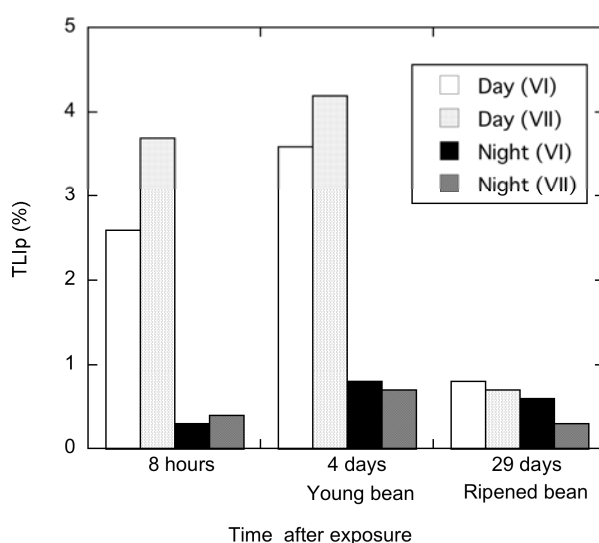


FIG. 33. The TLI after the start of the exposure at 8 hours, at 4 days for young soybeans, and at 29 days for ripened soybeans for experiments VI and VII on 12 September 2002.

TABLE 27. THE TLI INDEX AFTER THE START OF EXPOSURE AT 8 HOURS AND FOR YOUNG AND RIPENED SOYBEANS [129]

Exp. No.	Year	Exp. Date	TLI (%)					
			Daytime release			Night time release		
			8hr after the exp. start	Young bean harvest	Ripened bean harvest	8hr after the exp. start	Young bean harvest	Ripened bean harvest
I	1999	21, 22 Aug			0.14			0.17
II	2000	10 Aug		0.19	0.23		0.05	0.16
III		12 Sept		0.63	0.43		0.23	
IV	2002	30 Apr		0.0	0.0		0.0	0.0
V		27 Aug		0.28	0.2			
VI		12 Sep	2.6	3.6	0.8	0.3	0.8	0.6
VII		12 Sep	3.7	4.2	0.7	0.4	0.7	0.3

TABLE 28. RESULTS FOR THE KOREAN EXPERIMENT WITH RICE (ADAPTED FROM [181])

Exp.	Date	Stage	DAA*	Stage rel.	OBT grain per shoot	OBT grain (Bq g ⁻¹)	OBT grain (Bq ml ⁻¹)	TLI (%)
E1	11-Aug	booting	-7	-0.130	0.480	0.291	0.485	0.005
E2	18-Aug	heading	0	0.000	0.930	0.564	0.939	0.009
E3	21-Aug	milky ripe	4	0.074	4.190	2.539	4.232	0.042
E4	25-Aug	milky ripe	8	0.148	8.530	5.170	8.616	0.086
E5	28-Aug	milky ripe	11	0.204	32.100	19.455	32.424	0.324
E6	1-Sep	dough ripe	14	0.259	36.300	22.000	36.667	0.367
E7	5-Sep	dough ripe	19	0.352	22.700	13.758	22.929	0.229
E8	10-Sep	dough ripe	24	0.444	18.300	11.091	18.485	0.185
E9	19-Sep	yellow ripe	33	0.611	3.170	1.921	3.202	0.032
Harvest	10-Oct		54					

Note that the experiments E1, E2, and E7 are less accurate than the rest of experiments, due to the experimental problems. *Days after anthesis

7.4. EXPERIMENTS IN KOREA: RICE, SOYBEAN, CABBAGE, RADISH

7.4.1. Rice

The experimental techniques developed in Germany for wheat were applied in South Korea for rice, the main grain in Asia [181]. A rice cultivar (*Oryza Sativa L.* var., called Jangan-byeo) was grown in plastic pots and exposed for 1 hour to HTO in a Plexiglas box at various times during development. Exposures occurred about 10 a.m. under normal meteorological conditions. Rice was exposed at nine different stages of grain development from before heading until yellow ripe (20 days before the final harvest). All conditions during exposure were recorded (e.g. changes to air HTO concentrations, light, temperature, and humidity). At the end of the exposures, the concentration of HTO in leaf water ranged from 60% that of air moisture to nearly 100% when light and temperature conditions were optimal. Grain HTO concentrations were 35–100% those of air moisture. In the first 5–6 hours after exposure, the TFWT concentration was reduced by a factor of about 1000 in leaves and about 100 in stems. This decrease is much more rapid than that observed for grape, potato and cabbage. The reduction factor (TFWT at the end of exposure/TFWT at harvest) is higher for rice than for tomato, potato, sunflower and maize. The OBT in different rice plant parts at the end of exposure is influenced by exposure conditions and by developmental stage of the plant. At the

end of the hour-long exposure, the OBT content (water of combustion) in leaves was 1.0–1.2% that of TFWT, which is comparable to data for wheat. The decrease in leaf OBT is slower than for leaf TFWT. At 4–5 hours post exposure, OBT predominates in leaves. Because rice is ingested by humans only as grain, the harvest concentration of OBT is of most interest. Table 28 summarizes the results for exposures at various days after anthesis (DAA) (booting). Intermediate stages refer to time between booting and harvest. Initial data were normalized to 10^4 Bq mL⁻¹ of the initial leaf TFWT concentration. Yields of grain per shoot were 1.65 g.

Night experiments were described in a different paper [182]. One experiment was conducted during the milky ripe stage and the other in the early dough ripe stage at 45 and 40 days before harvest (August 25 and September 1). Temperature and relative humidity were in the normal range (21°C and 93%, respectively). After 1 hour of exposure, the concentration of HTO in the leaf HTO reached 30–40% that of the mean air moisture concentration. This result is twice that for wheat and about 3 times lower than rice during the day. HTO concentrations in the grain reached 15–30% that of air moisture, which is again higher than that observed for wheat. The OBT concentrations in combustion water of leaves at the end of exposure were 0.1–0.2% those of the concentrations of HTO in leaf water. At harvest the translocation index for grain was 0.1–0.14% at night, which is equal or slightly less than for exposure during the day. The authors concluded that OBT at night was produced at about a third the daytime rate (mostly due to the lower uptake of HTO at night).

7.4.2. Soybean

In the EMRAS I programme, unpublished data on HTO exposure of a Korean cultivar of soybean [7] were used in a blind test of participating models. The soybean scenario [7] addressed the tritium absorption by soybean foliage and the subsequent tritium behaviour in the plant. To provide data for model testing, soybean plants were exposed to elevated levels of atmospheric HTO in a glove box. The exposure was carried out for 1 hour at various stages of growth. The tritium behaviour in the plant body and pods was observed by sampling the various plant parts and measuring their tritium concentrations.

Six pots of plants (SB1 to SB6) were exposed, each for an hour. Seeds were sowed on 22 May. The plants flowered on July 7 and were harvested on October 5. The pots (SB1 to SB6) were exposed on July 2, July 13, July 30, August 9, August 24 and September 17, respectively. SB1 and SB4 were sampled several times between exposure and harvest to measure the tritium concentrations of each plant part as a function of time. The other plants were sampled and analyzed twice, once at the end of the exposure and once at harvest. The surface soil of the pots was covered by vinyl paper during the exposure to prevent tritium from depositing to the soil. Following exposure, the plants were removed from the glove box and grown outdoors.

Information about growth rates, tritium concentrations in air in the glove boxes during the exposure, background tritium concentrations outdoors and meteorological conditions were included in the scenario for the blind test. The observed tritium concentrations are shown in Tables 29, 30 and 31. The free water tritium and organically bound tritium concentrations were normalized to the mean concentrations of tritium in the air moisture in the glove boxes during the exposures. The normalized quantities make it easier to compare predictions and observations between experiments, particularly for OBT, because the mean tritium concentrations in air moisture in the glove boxes differed from experiment to experiment.

The TFWT concentrations in the plant body dropped off much more quickly in experiment SB1 than in SB4, with values of an order of magnitude or more lower between 24 and 120 hours post-exposure. This result suggests that the tritium dynamics in the plants depend on the timing of the exposure relative to the growth stage of the plant. The difference in results may also be caused by differences in the growth rates of the plants and differences in the meteorological conditions that they experienced after the exposure.

For experiments SB3–SB6 (Table 31), the OBT concentrations in stems were quite different than in leaves, so the average must be viewed with caution. A similar result (and caution) is seen for shells and seeds.

The observations clearly show that the OBT concentrations in the pods relate to the stage of growth at which the exposure occurred. OBT concentrations increased across experiments SB1–SB4, which covered the period of active plant growth. The normalized OBT concentrations in the pods for SB3, SB4 and SB5 were much higher than in the leaves. The exposures for these experiments were made when the fruits were developing rapidly and much of the tritium absorbed through the leaves may have been transferred directly to the pods rather than being stored in the leaves. The relatively low concentration in the pods for SB6 may be due to the fact that development of the pods was close to complete when the exposure occurred. This might have caused a reduction in the tritium transfer to the pods and in the OBT concentration in pods.

Concentrations of HTO in leaves were only measured at the end of exposure in plants from pots SB1 and SB4. These concentrations, relative to the mean air moisture concentrations, were low, about 0.13, showing an uptake rate that is lower than for the Japanese experiments. Assuming the same low relative uptake for all experiments, a translocation factor (as it was defined in this section) can be obtained (see Table 32).

These experimental data exhibit a higher maximum TLI compared with the Japanese experiments. This might be due to an incomplete extraction of exchangeable OBT.

TABLE 29. OBSERVED AND NORMALIZED TISSUE FREE WATER TRITIUM (TFWT) CONCENTRATIONS FOR THE SB1 EXPERIMENT [7]

Time and date	Elapsed time after exposure (hr)	TFWT (Bq mL ⁻¹)	Normalized TFWT*
In the plant body (stem and leaves)			
10:40 July 2	0.2	9580	1.23×10^{-1}
11:30 July 2	1	1050	1.35×10^{-2}
July 3	24	3.92	5.05×10^{-5}
July 7	120	1.32	1.70×10^{-5}
July 16	336	0.33	4.25×10^{-6}
Aug. 10	936	0.11	1.42×10^{-6}
Sept. 7	1608	0.06	7.73×10^{-7}
Oct. 5	2280	0.06	7.73×10^{-7}
In the pods (shell and seeds)			
Aug. 10	936	0.21	2.70×10^{-6}
Sept. 7	1608	0.06	7.73×10^{-7}
Oct. 5	2280	0.06	7.73×10^{-7}

* Tissue free water tritium concentration in the plant divided by the average tritium concentration in air moisture during the exposure (7.77×10^4 Bq/mL for SB1).

TABLE 30. OBSERVED AND NORMALIZED TFWT CONCENTRATIONS FOR THE SB4 EXPERIMENT [7]

Time and date	Elapsed time after exposure (hr)	TFWT (Bq mL ⁻¹)	Normalized TFWT*
In the plant body (stem and leaves)			
10:40 Aug. 9	0.2	7000	1.33×10^{-1}
11:30 Aug. 9	1	3200	6.08×10^{-2}
Aug. 10	24	25.9	4.92×10^{-4}
Aug. 14	120	2.1	3.99×10^{-5}
Aug. 23	336	0.8	1.52×10^{-5}
Sept. 10	768	0.27	5.13×10^{-6}
Oct. 5	1368	0.14	2.66×10^{-6}
In the pods (shell and seeds)			
10:40 Aug. 9	0.2	10500	1.99×10^{-1}
11:30 Aug. 9	1	8000	1.52×10^{-1}
Aug. 10	24	2700	5.13×10^{-2}
Aug. 14	120	63.5	1.21×10^{-3}
Aug. 23	336	1.49	2.83×10^{-5}
Sept. 10	768	0.84	1.59×10^{-5}
Oct. 5	1368	0.26	4.94×10^{-6}

* Tissue free water tritium concentration in the plant divided by the average tritium concentration in air moisture during the exposure (5.27×10^4 Bq/mL for SB4).

TABLE 31. OBSERVED NON-EXCHANGEABLE ORGANICALLY BOUND TRITIUM (OBT) CONCENTRATIONS IN PLANT PARTS AT HARVEST FOR EXPERIMENTS SB1 TO SB6 [7]

Case	Mean activity of air moisture during exposure (Bq mL ⁻¹)	OBT concentration at harvest (Bq mL ⁻¹) *							
		body				pods			
		Stem	Leaves	Avg.	Nor.avg.&	Shell	Seeds	Avg.	Nor.avg.&
SB1	7.77×10^4	18.0	14.0	16.0	2.06×10^{-4}	0.83	0.5	0.67	8.63×10^{-6}
SB2	1.47×10^5	59.8	50.8	55.3	3.75×10^{-4}	3.5	3.7	3.6	2.44×10^{-5}
SB3	1.14×10^5	37.8	17.7	27.8	2.44×10^{-4}	101.3	19.3	60.3	5.28×10^{-4}
SB4	5.27×10^4	19.8	8.8	14.3	2.71×10^{-4}	74.7	200.0	137.4	2.61×10^{-3}
SB5	9.19×10^4	44.3	13.5	28.9	3.14×10^{-4}	73.3	214.2	143.8	1.56×10^{-3}
SB6	1.37×10^5	180	19.5	99.8	7.28×10^{-4}	33.5	77.0	55.2	4.03×10^{-4}

* 1 g of dry matter yields about 0.6 mL of combustion water; & Normalized OBT: average OBT concentration divided by the mean activity of air moisture.

TABLE 32. APPROXIMATE TRANSLOCATION INDEX FOR KOREAN SOYBEAN

Case	DAA	TLI (%)
SB1	-5	0.002
SB2	6	0.008
SB3	23	0.053
SB4	33	1.18
SB5	48	0.73
Sb6	60	0.176
Harvest	78	NA

7.4.3. Radish

Radish (*Raphanus sativus L.*) has been used as a typical root vegetable in many experiments, including the chronic HT release of in Canada (1994). A Korean cultivar was used for short exposures (1 hour) at various stages of plant development [183]. Radish plants have a high water content in leaves (92%) and roots (94%). The high moisture content of the root, which is the edible part of the radish plant, contrasts with the low moisture content of mature grain. At the end of exposure, the TFWT (tissue free water tritium) in the above-ground portion (the top) was 1–2 orders of magnitude higher than for roots, but later, at harvest, concentrations were comparable. When the plants were exposed to tritium just before harvest, the concentrations in tops and roots at harvest increased, as expected. Driven by atmospheric forces, most of the HTO is translocated from leaves to root as photosynthate in the phloem in the opposite direction to the main movement of water (root to leaves) in the xylem. Relative to the mean concentration of tritium in air moisture during exposure, the root TFWT at harvest was minimal and exceeded 0.001 (relative units) only 2 weeks before harvest.

Some important results are found in different tables and figures in reference [183]. At the end of exposure, the HTO concentration in leaves was 20–40% that of the mean concentration in air moisture, a smaller value than for cereals. The concentration of OBT in the radish root at harvest ($\text{Bq g}^{-1} \text{ dm}$) was less than 0.3% of the concentration of HTO in the leaf water at the end of exposure. At harvest, the ratio of the OBT concentration to that of TFWT strongly depended on the number of days before harvest that the exposure took place; the ratio decreased when the exposure takes place close to harvest. OBT contributed more to ingestion dose than did TFWT unless the exposure was less than 7 days before harvest. The translocation index was less than 0.4%. Table 33 summarizes the experimental results.

7.4.4. Cabbage

In the same paper [183], results are reported for a leafy vegetable. A Korean cultivar of Chinese cabbage (*Brassica pekinensis Rupr.*) was exposed at various times for 1 hour in a box with known concentration of HTO in air moisture, temperature, humidity and light. The above-ground portion of cabbage contained 95% water, and the number of leaves and the fresh-weight mass increased significantly between the first exposure (51 days before harvest) and harvest. The first leaves produced become the outer leaves as the cabbage grows. About half-way through the growing period, the leaves begin to form a tight leaf arrangement. Towards the end of growth, several old leaves become senescent and fall off the plant. When this happens, the outmost leaf of the inner part replaces the deciduous leaf. Outer leaves are more exposed to contamination than inner ones, and the outer leaves change over the course of plant growth. A summary of exposure conditions, concentrations of HTO in the edible portion of the cabbage at the end of exposures, concentrations of OBT at harvest, and translocation indexes is given in Table 34.

7.5. EXPERIMENTS IN CANADA: CHERRY TOMATO

The ETMOD model used in Canada by Atomic Energy of Canada Limited (AECL) does not account for OBT formation in plants during the night. Relevant processes were identified [184], and a conceptual model was proposed [185]. To clarify the processes that result in OBT formation, an experiment was designed to determine transfer rates of tritium from air to leaves and fruits of tomato plants following acute HTO exposures [186, 187]. A series of 1 hour experiments were carried out during both night and day, and a dataset was collected on the build-up of OBT concentrations in the plant leaves and fruit. The experiments were carried out in an exposure chamber; cherry tomato plants (*Lycopersicon esculentum var. cerasiforme*) at three different growth stages (early [i.e. flowering], intermediate [i.e. young fruit], and late

[i.e. red, maturing fruit) were studied. Separate experiments were conducted to determine the short-term and long-term dynamics of HTO and OBT concentrations in leaves and fruits from the end of exposure to harvest. Both HTO and OBT concentrations in leaves at the end of the day-time exposure were greater than those exposed at night. This supports the understanding that OBT is produced mainly by photosynthesis in the presence of sunlight. OBT can be produced in leaves in the dark, but these processes operate at slower rates. At harvest, the HTO and OBT concentrations in the fruit depend on the length of time between exposure and harvest and on the time of day at which the exposure was carried out. HTO persisted much longer in the fruit than in the leaves, but OBT showed a similar persistence in both plant parts.

Transplanting was done on June 3, 2002, when the plants were about 3 weeks old and the final harvest was in late September. Experiments 1 to 6 occurred in the dark and experiments 7 to 8 were done in daylight. Daytime experiments exposed only maturing tomatoes. Leaf area per plant, leaf water content, fruit growth and starch dynamics in the leaves were measured.

The translocation indexes (harvest OBT/leaf HTO at the end of exposure) calculated for cherry tomatoes reveal some interesting results (Table 35). In experiment 2, at 4.3 days after flowering, there was an abnormally high translocation index (2%). In experiment 4, the fruit was measured 14 hours post-exposure and, taking growth dilution into account, the translocation factor is about 0.007%, a value only two times lower than in experiment 3. Experiments 5 and 6, carried out during the night with ripe fruit, showed consistent values of about twice the night-time values observed in German experiments. Unexpectedly, the daytime experiments (7 and 8) showed lower values than those observed at night (experiments 5 and 6, respectively). The fact that the value for a cloudy day was higher than for a sunny day was also unexpected. The degree of ripening of the fruit may not influence the OBT produced in leaves. After analyzing the details of the experimental protocols, the causes for these unexpected results have not been identified.

The OBT dynamics in leaves exposed during day and night when fruit was ripe are shown in Figure 34. Data were normalized to the HTO concentration at the end of exposure. The period of the increased OBT concentration in leaves was shorter (2 to 6 hours) in the daytime experiments than in the night-time experiments (>6 hours). Decrease in the concentration of OBT in the leaves was faster during the day than at night. The values at the end of exposure are comparable and slightly lower than those for wheat (Figure 29).

When fruits were ripe (experiments 5–8), the initial uptake of HTO in the leaves was about 6% during the day and 2.5% during the night. When fruit was immature, the night-time uptake of HTO by leaves was higher, about 5%. All of these values are lower than those for wheat. Canopy resistance in the dark is a plant-specific trait. The large resistance in leaves during the night will maintain the HTO concentration until the next morning, and the leaf OBT produced during the night will consequently be a large fraction of OBT produced during the day.

HTO and OBT trends for daytime and night-time experiments were clearly different, but estimated ingestion dose, which depends primarily on the OBT concentration in fruit at harvest, was quite similar for daytime and night time exposures.

To understand OBT production, more experiments were done. The daily starch production was measured in tomato (Figure 35), as well as the concentration of starch in tomato leaves at dusk and dawn (Figure 36). Starch concentrations in tomato leaves, radish leaves, and lettuce over the course of the night were also measured (Figure 37). Modelling has not succeeded in explaining these experimental data.

TABLE 33. BEHAVIOUR OF TRITIUM IN KOREAN RADISH AFTER A 1 HOUR EXPOSURE TO HTO IN AIR MOISTURE (ADAPTED FROM [183])

Experiment	R1	R2	R3	R4	R5
DTH (days to harvest)	45	35	27	15	7
HTO in leaves at end of exposure					
C_{end} (kBq mL ⁻¹)	21	25	40	37	42
C_{end} relative to mean air moisture during exposure					
rel C_{end} (%)	46	40	22	33	44
$C_{\text{OBT_root}}$ (Bq mL ⁻¹ OBT water of combustion) at harvest	23	75	113	93	140
TLI (translocation index) (%)	0.11	0.30	0.28	0.25	0.33

TABLE 34. DATA FOR FOR 4 HOUR-LONG EXPOSURES OF A KOREAN CULTIVAR OF CHINESE CABBAGE TO HTO IN AIR MOISTURE (ADAPTED FROM [183])

Experiment	C1	C2	C3	C4
DTH (days to harvest)	51	42	29	17
number of leaves	18	22	30	40
fresh mass (in grams)	170	500	850	1000
hour of the start of exposure	10	10	10	10
T (°C)	26.8	29.1	30.4	19.4
RH (%)	86	83	78	89
light (klux)	42	52	61	23
mean HTO concentration in air moisture (kBq mL ⁻¹)	71	30	43	147
HTO in leaves at the end of exposure C_{end} (kBq mL ⁻¹)	34	18.8	12.3	14
C_{end} relative to mean air moisture during exposure	48.2	62.2	28.4	9.5
rel. C_{end} (%)				
$C_{\text{OBT_top}}$ (Bq mL ⁻¹ , OBT water of combustion) at harvest	17	32	56	105
TLI (translocation index) (%)	0.05	0.17	0.45	0.75

TABLE 35. TRANSLOCATION INDEXES FOR CHERRY TOMATOES EXPOSED AT DIFFERENT TIMES DURING GROWTH

Experiment	Day after exposure	TLI (%)	Remarks
Exp 1	90	0.00356	Night exposure, no fruit
Exp 2	4.3	2.12	Night exposure, no fruit
Exp 3	74	0.016	Night exposure, green fruit
Exp 4	0.58	0.149	Night exposure, green fruit
Exp 5	42	0.51	Night exposure, ripe fruit
Exp 6	1.7	0.346	Night exposure, ripe fruit
Exp 7	49	0.44	Day exposure, ripe fruit
Exp 8	48	0.12	Day exposure, ripe fruit

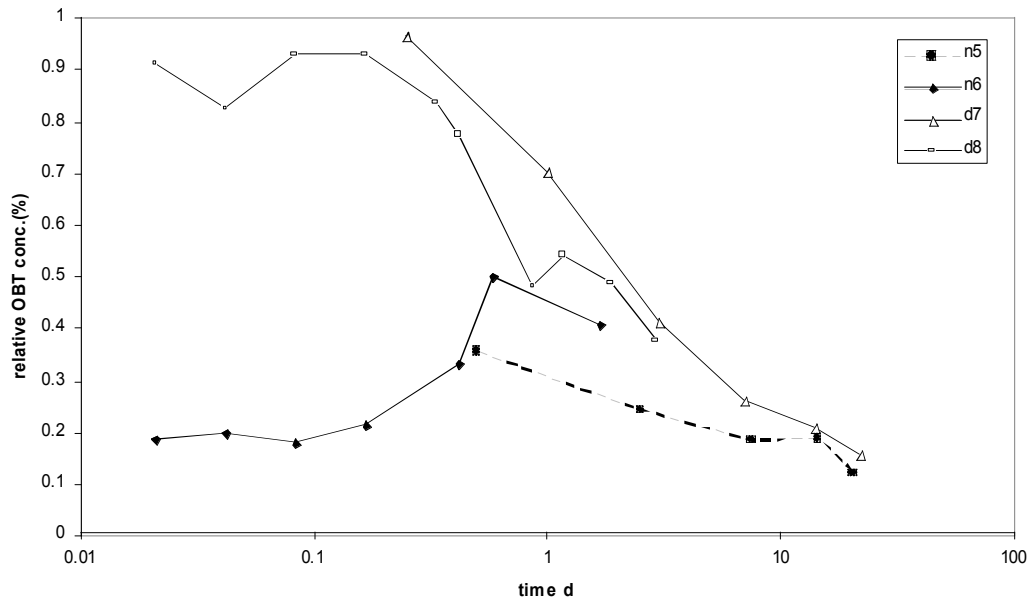


FIG. 34. Dynamics of relative OBT concentration in leaves of cherry tomatoes for experiments 5 and 6 at night and 7 and 8 during the day.

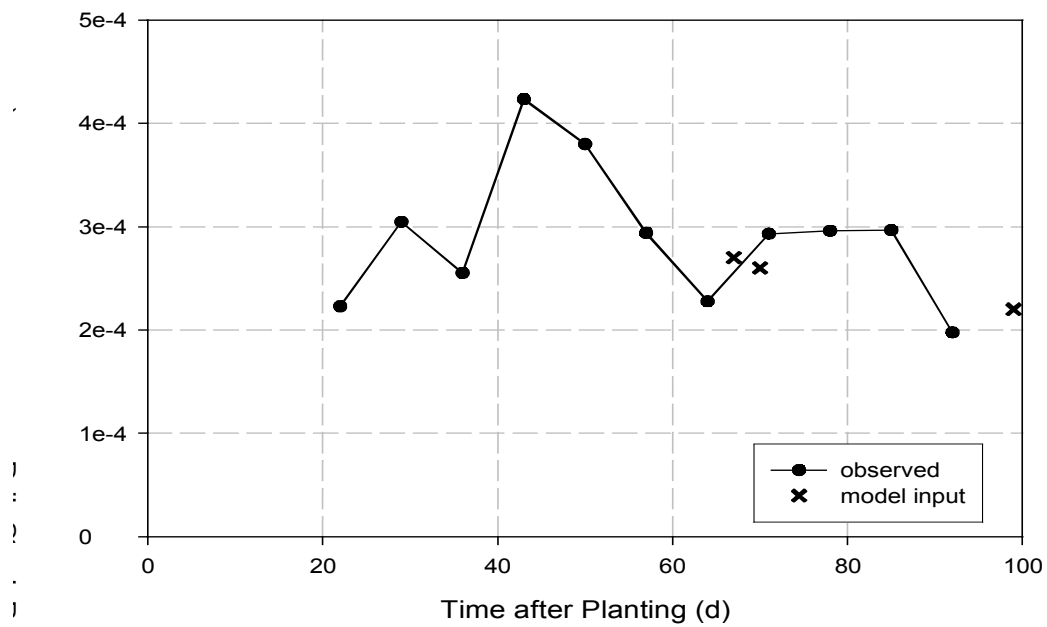


FIG. 35. Daily starch production per unit area of the tomato leaf.

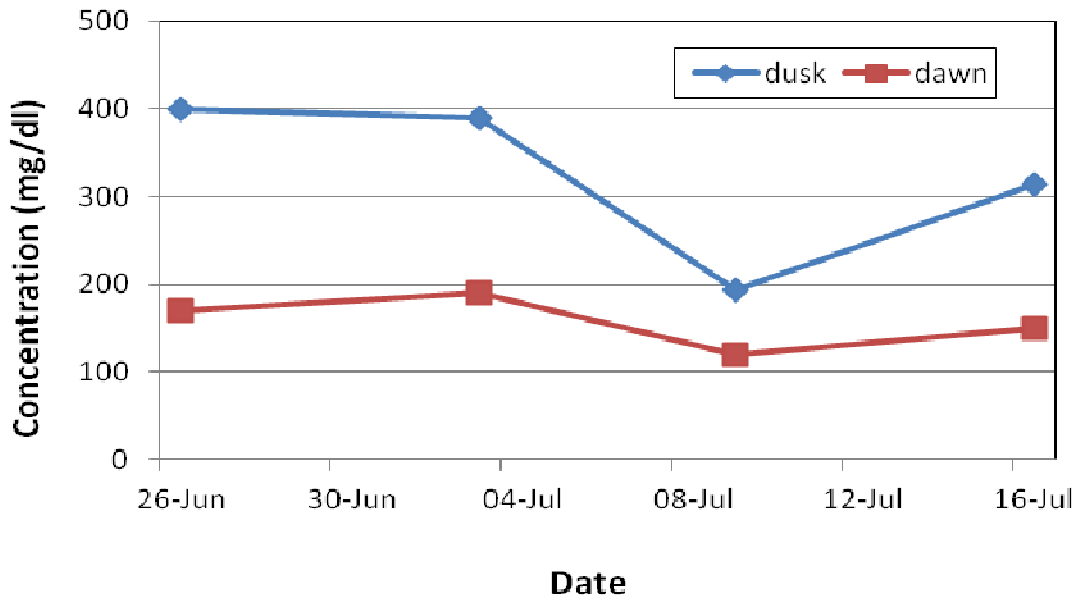


FIG. 36. Starch concentration at dusk and dawn in tomato leaves.

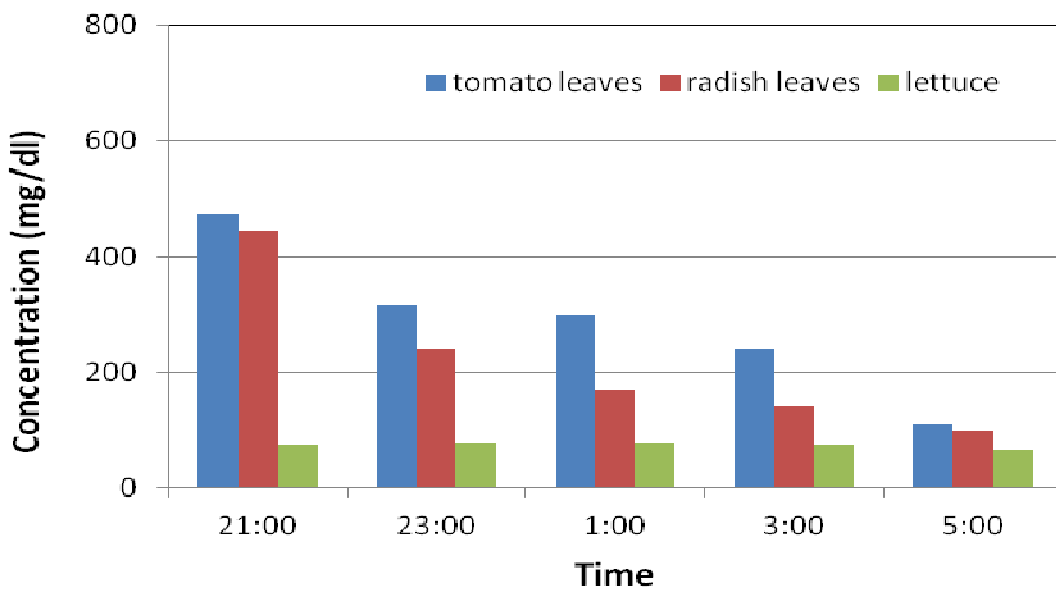


FIG. 37. Pattern of starch concentration at night for tomato, radish and lettuce.

7.6. EXPERIMENTS IN FRANCE: LETTUCE

Recently, experiments with lettuce (variety “feuille de chene blonde”, or *kitare*) were done in France [188] either in a controlled-climate chamber or in the field. In the chamber experiments, the light to which the plants were exposed was much lower than normal ambient. For tritium extraction of the exchangeable form of OBT from the plant, two methods were used: (1) the well-known cold isotopic exchange, and (2) a new hot technique used in analytical chemistry. The two approaches have not been compared, but both estimate total organically bound tritium. The method used for extraction of non-exchangeable organically bound tritium was combustion and catalytic oxidation. Experimental errors were higher for samples with a mass less than 1 g. Light or dark conditions were maintained for 24 hours, and the dynamics of HTO incorporation were followed for young, mature and relatively old plants (respectively 40, 60 and 70 days after germination). Temperature, humidity and light conditions were about the same for all ages of plants. The transfer of tritium from air to leaf is regulated by stomatal resistance, and a slower transfer is expected in the dark. A direct link between stomatal resistance and photosynthetic rate was observed for leaves of varying age. From the measured photosynthetic rates of leaves, older plants (before flowering but with larger leaf area indexes) might be expected to have higher rates of HTO uptake. However, from the data presented, it is quite difficult to assess the photosynthetic rate of the whole plant. Data for the young plant showed no difference between uptake during the day and at night [188], an observation that is not understood.

From all the results presented in this section, the transfer rate at night is expected to be 3–5 times slower than in the day. More research needs to be done to confirm this because of its potentially important radiological impact.

In these controlled experiments, the OBT/TFWT ratio was about 5 and never smaller than 1. A review of all the potential experimental errors that could have been the cause of these unexpected results suggests that light levels in the chamber were too low compared with what plants are exposed to in nature. Furthermore, the experiments took place in a waste treatment area that quite possibly was contaminated with many impurities. These impurities could have concentrated in the lettuce and appeared later in the combustion water as volatile organic compounds. Even with purification of “normal” combustion water some significant errors may occur. In contrast, when the source of tritium is a stack, there can be few, if any impurities.

Due to this potential cross contamination of OBT in these experiments, the extent of OBT production is misleading. However, for model testing, controlled experiments are extremely useful for understanding plant growth and uptake of HTO from air and soil into the water of leaves.

For long-term exposure under natural conditions, the following can be noted about OBT incorporation. First, under equilibrium conditions (as the ratio of total OBT to integrated HTO concentration in the air moisture or plant water), the data are similar to other experimental values with a mean transfer rate between 0.13–0.16% h⁻¹. Second, under acute conditions, the variability of the rate of OBT production and its clear link between plant growth processes and environmental conditions is demonstrated. The first experiment took place between the end of April and the beginning of July under optimal conditions of temperature and light, while the second experiment took place in late autumn when plant growth was slower. When plant growth dynamics and OBT incorporation are considered in terms of available energy, both cases are seen to behave similarly given the same total available energy. In addition, the

OBT incorporation rate depends on the stage of plant development and various environmental factors. The experimental results and the above conclusions can be used to test recent dynamic tritium models.

7.7. DEPENDENCE OF TLI OF RICE ON DURATION OF EXPOSURE

Daylight experiments on rice have been carried out with exposures of 1 hour [181], 4 hours [180], and 8 hours [128, 179]. Values for TLI are shown for different exposure times and different times of sampling after flowering (Table 36).

When these data are compared visually (Figure 38), it is clear that cultivar characteristics, meteorological factors and HTO concentrations during exposure, in addition to exposure time, influence the TLI at the same stage.

7.8. UPTAKE OF HTO AT NIGHT AND LEAF RESISTANCE

If stomata are completely closed, only cuticular resistance remains. Many models consider a default value of about 4000 s m^{-1} for cuticular resistance. Cuticular permeability to water is usually characterized by the variable permeance (P), which is the ratio of water flow rate density to the driving force, the latter being expressed as a concentration difference [189]. At 25°C and standard pressure, the density of liquid water is 43 384 times greater than the saturation water vapour concentration in air and, correspondingly, the values of P referenced to the gas phase are larger by the same factor than values referenced to the liquid.

Increased cuticular permeability to water is frequently observed with increasing air humidity and temperature. Cuticular transpiration cannot automatically be assumed to be negligible. Aqueous pores enhance cuticular conductance [190]. Data on water permeance in leaves [191] suggest a large variability in the uptake rate of water at night. In different tritium experiments, low uptake has been seen for tomato leaves and lettuce [188] and high uptake for sunflower. Rice also has a high uptake rate at night, while wheat, bean and potato exhibit intermediate values. Having direct experimental data for each major crop of interest would be valuable. When stomatal resistance was measured at night with a porometer [97] the value for komatsuma and radish was 300 s m^{-1} , but, for cherry tomato, it was $700\text{--}1500 \text{ s m}^{-1}$. Stomatal resistance decreases by a factor of 2 when relative humidity increases from 40% to 90%. In another experiment [192] values of 500 s m^{-1} for komatsuma, but only 250 s m^{-1} for cabbage, were reported.

When data on deuterated water uptake [97] were compared with the porometer measurements, results for komatsuma were variable, the value for cherry tomatoes was about 2000 s m^{-1} and orange leaves had very high values (Table 37). In the 1995 experiment [97], komatsuna samples were at their early growth stage and soils in the experimental pots were not covered with vinyl. Therefore, it is likely that the D_2O concentrations in komatsuna leaves were higher than expected because they included uptake via the root.

Exchange rates (h^{-1}) for lettuce [188] are very low (perhaps due to low light) and, for young plants, the day and night uptake rates are similar. Mature plants (before flowering) have high resistances (Table 38).

Experimental data gathered thus far demonstrate that, even under nearly identical conditions, plants exhibit different stomatal conductances.

TABLE 36. VALUES OF TLI OBTAINED FROM DAYLIGHT EXPERIMENTS OF DIFFERENT DURATION

Exposure (h)	Stage*	TLI (%)	Reference
8	0.1	0.36	Atarashi-Andoh et al. [179]
8	0.45	0.63	Ichimasa et al. [128]
4	0.14286	0.4	Atarashi-Andoh et al. [180]
4	0.33333	0.55	Atarashi-Andoh et al. [180]
4	0.5	0.42	Atarashi-Andoh et al. [180]
4	0.61905	0.15	Atarashi-Andoh et al. [180]
4	0.83333	0.045	Atarashi-Andoh et al. [180]
1	-0.0526	0.005	Choi et al. [181]
1	0.07018	0.0093	Choi et al. [181]
1	0.12281	0.04	Choi et al. [181]
1	0.19298	0.085	Choi et al. [181]
1	0.24561	0.32	Choi et al. [181]
1	0.31579	0.363	Choi et al. [181]
1	0.38596	0.227	Choi et al. [181]
1	0.47368	0.186	Choi et al. [181]
1	0.66667	0.032	Choi et al. [181]

* The stage is the exposure time (days after flowering) divided by the number of days between flowering and final harvest.

TABLE 37. NIGHT UPTAKE RATE AND RESISTANCE (ADAPTED FROM [97])

Exp.	Plant	Rate (h^{-1})	Resistance using porometer (s cm^{-1})	Rate using porometer (h^{-1})
Night 1995	Komatsuna	0.65 ± 0.19	5.7–40	0.06–0.44
	Orange	0.06 ± 0.29	49–55	0.04–0.05
Night 1996	Komatsuna	0.20 ± 0.04	2.7–3.2	0.82–0.97
	Radish	0.31 ± 0.05	2.6–3.4	0.72–0.95
	Tomato	0.12 ± 0.02	6.9–15	0.16–0.36

TABLE 38. LETTUCE UPTAKE RATES (h^{-1})(AFTER [188])

Plant	Day	Night
Young	0.023	0.027
Mature	0.04	0.005
Before flowering	0.11	0.035

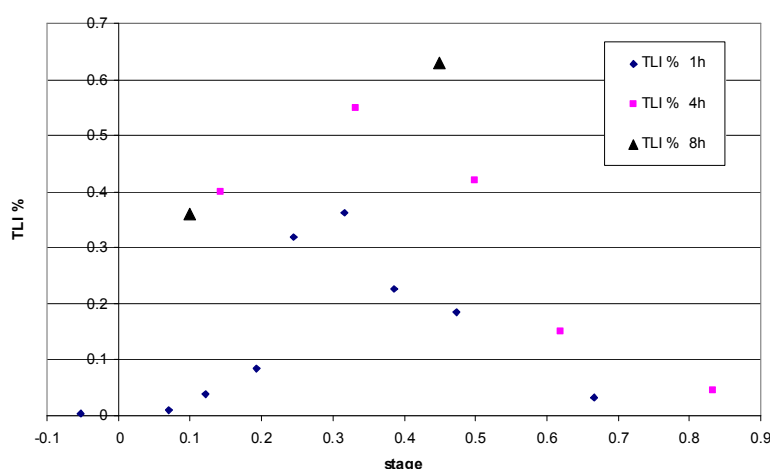


FIG. 38. Comparison between different experimental data (see Table 36).

7.9. PRELIMINARY CONCLUSIONS FOLLOWING REVIEW OF THE EXPERIMENTAL DATA

Experimental data have been collected for wheat, rice, soybean, tomato, cabbage, radish, and tangerine; preliminary results for lettuce and potato are also available. Uptake and loss rates of HTO in plant water (of leaves, primarily) depend mostly on environmental conditions (e.g. light, temperature and relative humidity), but crop characteristics such as stomatal density and age of leaves are important factors as well. Leaves require about 10-20 minutes to adapt to the new parameters if environmental conditions change abruptly. Stomatal resistance decreases by a factor of 2 as relative humidity increases, and it decreases by a factor of 2-4 with the leaf age [97]. Measured stomatal resistance exhibits a diurnal cycle and is apparently different for each leaf of the same age on the same plant [97]. Sunflower, grape, rice and wheat show higher uptake rates than komatsuma and cabbage, while tomato and orange have the lowest uptake rate. Water in veins and stems is less contaminated than in leaves. The ears of rice and wheat have uptake rates of 30% for wheat [171, 172] and 70-100% for rice [181]. Immediately after exposure to HTO, there is a rapid loss of HTO from leaves with a half-time of 0.5 hours at noon, but the half-time if the exposure ends in the night. After a night-time exposure, the concentration of HTO in leaves is still 10-20% the next morning. There is a diurnal pattern to the loss rate. Under night conditions, even if the stomata are completely closed, cuticular conductance occurs, and it varies among plant species. Uptake of HTO at night can be relatively high. The orange and tomato have very low loss rates at night, while rice and wheat have high loss rates. For young lettuce, the day and night uptake rates are practically the same, but for other crops night rates of uptake are 3-5 times lower than those during the day.

There are difficulties in the laboratory with the extraction of the exchangeable fraction of OBT, and presently there is no standardized method. Some experimental data show unexpectedly high amounts of non-exchangeable OBT, which may be due to laboratory methods that allow for the contribution of exchangeable OBT. In daytime, the direct conversion of HTO to OBT through photosynthesis contaminates the assimilate and subsequent processes of assimilate export to plant parts are less relevant. For OBT produced at night, the situation is more complex: there are 2 cases (tomato and tangerine) for which production of OBT at night is higher than during the day.

OBT is produced in leaves. After a 1 hour exposure during the day, the OBT concentration in the water of combustion can be up to 1.5% that of the HTO concentration at the end of exposure; for exposures at night, the percentage is between 0.1% and 0.4% (wheat and rice). For plants with edible roots (potato, radish) or fruit (wheat, rice, tomato), OBT is exported from the leaves with a loss rate that is much lower than for HTO. After 6-20 hours the OBT concentration in the combustion water of the leaf is equal to the HTO concentration; later on, it is much higher. At harvest, OBT predominates. For leafy vegetables (and grass perhaps), the OBT in leaves slowly decreases through respiration loss. OBT predominates just a few hours after an exposure during the day and by the next morning for the night exposures. Experimental data are still needed for leafy vegetables and grass.

For longer exposure times, the OBT/HTO ratio increases if environmental conditions are constant.

These experimental data were collected in environmental chambers or relatively small boxes. As a result, the environmental factors affecting tritium transfer and conversion to OBT differ from field experiments. In these experiments, artificial ventilation was used to minimize

boundary and atmospheric resistance. Thus both uptake and loss rate were increased. Under field conditions, the exchange velocity and transfer rate between air and plants are lower. In the box experiments, the temperature increased by about 10°C during the exposures, and, in some cases, the plants experienced temperature stress and consequently lower uptake and loss rates. Only as a first approximation can these experimental data be considered valid for field conditions. Due to the diurnal pattern of uptake and conversion to OBT, a diurnal pattern in the ingestion dose can be seen. Qualitative results are given in Figure 39.

The transfer of OBT into an edible plant part (translocation index, or TLI) depends largely on the stage of plant development. Under field conditions, plants have different developmental stages each day of the year. Consequently, a seasonal pattern of ingestion dose arises, as shown quantitatively in Figure 40.

Local tastes, consumption of local products, and climatic conditions influence both diurnal and seasonal patterns of ingestion dose. Figures 39 and 40 were created assuming a constant HTO air concentration for a 1 hour release from a Romanian CANDU reactor that exposed plants and animals that make up part of the Romanian diet. The important crops are wheat, maize, sunflower, grapes, vegetable and fruits (apple, peach). Not all of them are included in this overview.

For estimating doses from releases from ITER, the important crops are hay, corn, wheat, Mediterranean vegetables, grapes, olives, tomatoes, salad greens, root vegetables (carrots), and fruit (apples). Experimental data are lacking for these crops. However, it is clear that the local consumption of cereals around ITER is less than in Romania, and more experimental data are needed for grass, salad greens, olives and grapes. Other data are needed to estimate ingestion dose around fuel reprocessing plants in Japan or France.

Natural variability has a large impact on the conclusions that can be drawn from experimental data. There is a large variability in stomatal conductance for leaves of the same age on a single plant. When experimental data are compared with the best model results we have, variability is at least a factor 2. To define a “reference plant”, a large number of samples must be analyzed, which is not cost effective. Normally, about 3 plants are combined into a composite sample, and this is inadequate to describe a true average. Consequently, the experimental results are affected not only by counting statistics and sample preparation errors, but also by a systematic error due to so few plants being analyzed. When model predictions are compared with experimental data, these systematic errors must be taken into account. Experimental data errors can be at least 50%, while analytical and statistical errors are often less than 20%.

For modelling needs, formation of OBT in day-time seems adequately understood, but much more needs to be done to understand the processes at night. Production of OBT at night cannot be ignored because HTO dispersion in night is weak and concentrations at a receptor can be as high as 40 times the value during the day. The experimental evidence noted above revealed that leaf HTO will be only 3–5 times less at night than during the day given the same air concentration. Experimental data show that the TLI at night is similar to that during the day. Consequently, formation of OBT at night cannot be ignored in a safety assessment. Understanding of processes that occur in the dark must be increased to develop robust models. This topic will be addressed in the next IAEA programme.

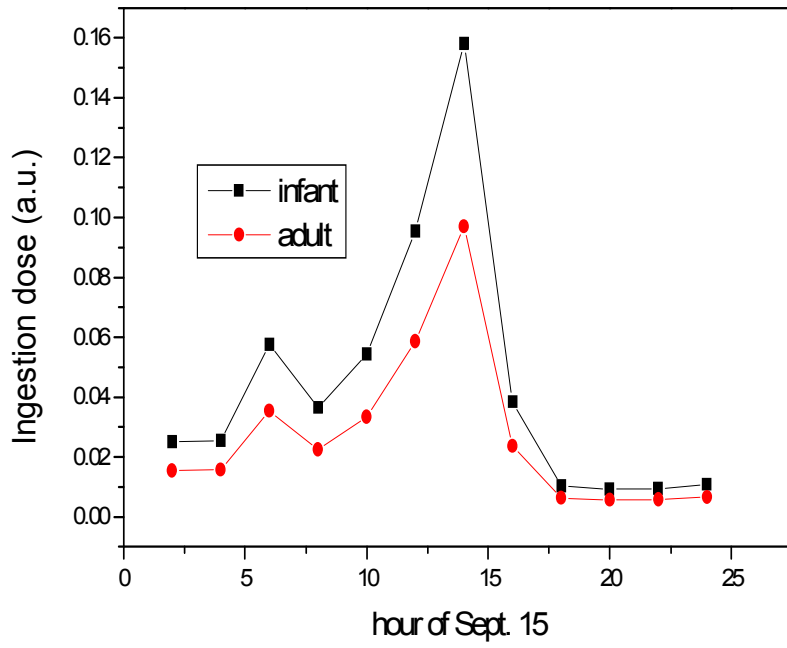


FIG. 39. Diurnal pattern of ingestion dose (assuming Romanian diet exposed to 1 hour of constant air concentration).

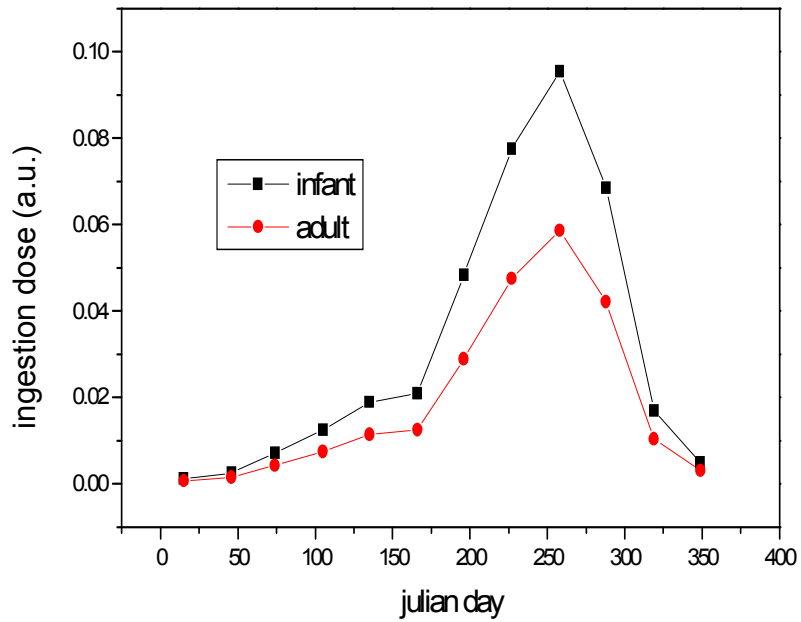


FIG. 40. Seasonal pattern of ingestion dose (constant air concentration).

8. REVIEW OF SOIL-PLANT TRITIUM TRANSFER

8.1. OVERVIEW

Tritium transfer can be viewed as a combination of diffusion and transport in water. Water includes atmospheric water vapour, soil moisture, groundwater and tissue-free water within the plant biomass of a terrestrial ecosystem. Processes of diffusion are addressed in detail in other sections of this report, while those water transport processes that are critical for the quantification of tritium retention in soil and plants and re-emission back to atmosphere are addressed in this chapter.

The relationship between soil moisture and evapotranspiration is of particular importance, because evapotranspiration is responsible for tritium re-emission. Vegetation interacts with soil and is critical in the transfer of tritium after an accident. Soil in the root zone (rhizosphere) contains the large repository of water into which tritium enters via direct deposition during the accident and via root respiration shortly afterwards. Tritium (HTO) re-emitted into secondary plumes provides a key route of recycling, because certain fractions of this HTO are deposited back to the soil and intercepted by foliage. The rest of soil HTO is removed by infiltrating water and by aquifer recharge, but some fraction of it is returned back to the rhizosphere due to water table fluctuations and a subsequent rise of the capillary fringe. All these processes, and particularly evapotranspiration, are significantly constrained by the availability of soil moisture and the depth of the water table. Spatial distribution of these depends on soil texture and topography [193–198]; a mixture of water-stressed locations and wetter valleys can result in significant differences in evapotranspiration across the landscape [199–203]. It is important to note, that this significant heterogeneity (a combination of dry and wet locations) occurs due to lithological and pedological complexity [204, 205] rather than to terrain complexity (steep slopes). Hydrological complexity of a gently rolling terrain is commonplace (e.g. in Canada).

8.2. APPROACH TO THE ROLE OF SOIL MOISTURE IN THE SPATIAL VARIABILITY OF EVAPOTRANSPIRATION

The dynamics of soil water are an integral part of the hydrological cycle and control interrelationships between precipitation, infiltration, drainage, groundwater recharge and evapotranspiration. Spatial variability in soil moisture affects a significant part of the spatial variability of evapotranspiration. Traditional empirical formulae used for assessment of evapotranspiration do not account for this variability except through uncertainties associated with evapotranspiration measurements [206]. With increased computational power and the development of numerical weather prediction systems in the last 2 decades, crude empiricism in estimating actual evapotranspiration has been replaced by more accurate parameterization of underlying processes. New parameterization has mainly targeted coupling between evapotranspiration and its major source – soil moisture. Quantification of the strength of the coupling remains the subject of intense research. This research has culminated in the development of a lysimeter situated in the wind tunnel at the Colorado School of Mines. Theorists have approached the same subject with a fully coupled groundwater-atmosphere system, “PF.WRF”. “PF” stands for the popular hydrological module, ParFlow, and “WRF” stands for the Weather Research Forecast system, which is used worldwide, particularly in emergency response systems for real-time atmospheric dispersion assessments. PF.WRF was jointly developed by the Colorado School of Mines and Lawrence Livermore National Laboratory (LLNL) [207]. This elaborate approach should help clarify the otherwise vague limits of applicability of traditional empirical formulations. One of the key objectives of

tritium modelling is seen in the assimilation of breakthrough knowledge gained in the fields of hydrology, hydrometeorology and weather prediction.

8.3. HANDLING THE SPATIAL VARIABILITY OF EVAPOTRANSPIRATION IN HYDROLOGICAL MODELS

The assessment of the spatial variability of evapotranspiration in watershed hydrology models requires a 3D model to account for vertical soil structure. Simplification to a 2D model can be achieved when the primary horizontal coordinate is aligned with the local water route. However, because most of the model complexity is inherent in the vertical coordinate, it is preferable to start with the one-dimensional (1D) approach, which is currently commonplace in tritium modelling.

One of key hypotheses underlying a simpler 1D tritium transfer model is that long-term water balance is determined only by locally fluctuating water supply (precipitation) and demand (potential evapotranspiration) moderated by water storage in the soil. This hypothesis was proved by Milly [208] and holds for a uniform climate and simple terrain. The definition of “simple” terrain compared with “complex” terrain is a topic of considerable debate, however, because different models are differently sensitive to sub-grid orography. Further support of this hypothesis was offered by Kim, et al. [209], who demonstrated that lateral flow is relatively unimportant compared with groundwater flow. As a result, processes in the vadose zone actually appear 1D, with all lateral flow information reflected in a single parameter – fluctuating water table depth.

The partitioning of precipitation into evapotranspiration and runoff is essential for the assessment of HTO re-emission. According to Milly [208] partitioning depends on the following dimensionless numbers:

- The ratio of average annual potential evapotranspiration to average annual precipitation (index of dryness);
- The ratio of the spatially averaged plant-available water to the annual average amount of precipitation;
- The ratio of the spatially averaged water-holding capacity of the soil to the annual average amount of precipitation;
- The mean number of precipitation events per year;
- The shape parameter of the gamma distribution describing the spatial variability of the storage capacity;
- Seasonality in:
 - Precipitation intensity,
 - Storm arrival rate, and potential evapotranspiration.

Apart from being 1-dimensional (and thus supportive of the 1D tritium transfer in the soil-plant system), Milly’s model provides a convenient and simple framework for tritium transfer at the level of complexity suitable for regulatory algorithms. Milly’s model, however, has not yet been implemented in a tritium model.

It is also important to note that the supply-demand-storage hypothesis of Milly neglects soil moisture dynamics to a certain degree. For example, infiltration causes dynamical effects that are not included in Milly [208], although such effects still permit a 1D description. Other finite-permeability effects further complicate the issue [210]. If water table dynamics are

taken into account, a very important enhancement to the model [211], quantification of recharge due to lateral flow, and thus a 2D model, is required.

A minimal 2D model (which will be sufficient, if the x-coordinate is aligned with the water route) requires an adequate balance between robustness and accuracy. Effective 2D approaches to handling spatial variability in evapotranspiration (and thus HTO transfer) across the landscape can be illustrated by the field-scale model, Root Zone Water Quality Model (RZWQM) [212, 213] and by two watershed hydrology models: APEX [214–216] and WEPP [217]. All three models are designed for PC, are sufficiently robust and user friendly, and are applicable to the micro- and landscape scales needed to predict secondary HTO plume evolution. Models like RZWQM, APEX and WEPP provide appropriate and convenient frameworks for modelling soil water and HTO movement within the soil-plant system. Another approach to handling certain 2D effects is to improve existing algorithms of HTO translocation in the rhizosphere using some of key modelling features of RZWQM, APEX WEPP, or other hydrological models. Key features for each model include:

- WEPP handles digital elevation data, enhanced subsurface lateral flow and cropland, rangeland and forest hydrology. Its plant growth model uses data for available N and P. WEPP removes root zone water, has a kinematic storage sub-model for lateral subsurface flow, uses measurements for groundwater flow, and includes a return flow from an unconfined aquifer. Effective hydraulic conductivity is calculated by WEPP.
- APEX accounts for the soil temperature profile, the N cycle, N and P uptake, and associated phenology, particularly root growth. Vertical and horizontal subsurface flow is calculated using storage routing and pipe flow equations; groundwater flow is calculated as per percolation rate and return flow rate. APEX calculates evaporation and transpiration by Ritchie method. Spatial heterogeneity of the watershed is based on a combination of homogeneous sub-areas, which are linked via water routes down to the watershed outlet.
- In RZWQM, water, organic matter and nitrogen cycles are modelled within fast and slow residue compartments, three humus compartments (fast, transition and stable), and the aerobic and anaerobic compartments of the heterotroph and autotroph compartments. Movement of water C and N is calculated within, above and below the root zone. C and N uptake are modelled along with transformations of C and N throughout the soil profile, CO₂ assimilation, C allocation, dark respiration periodic tissue loss, plant mortality and root growth. RZWQM utilizes sensible and latent heat flows, soil water dynamics using Richard's equation, Poiseuille's law for macropore flow subject to gravity, Green-Ampt formulation for lateral flow, pseudo-2D drainage flow and water table fluctuations.

8.4. COMPLEXITY OF THE SOIL-PLANT-ATMOSPHERE SYSTEM IN THE CONTEXT OF TRITIUM TRANSFER

Certain features of existing models of tritium transfer in the soil-plant-atmosphere system are more complex than in distributed hydrological models. Tritium models are similar to the land surface schemes of global circulation models (GCM, or weather prediction systems) because of the need for both types of models to handle the details of water, energy and carbon cycles at the vegetated surface [218–224]. Herein follows a review of soil-plant modules using four typical tritium models of significantly different complexity as examples. Models considered are GAZAXI (CEA, France), ETMOD (AECL, Canada), UFOTRI (KIT, Germany) and SOLVEG-II (JAEA, Japan). The soil modules of these models are analyzed in the context of

the generic structure of typical operational land surface schemes (LSS) dealing with soil-plant-atmosphere exchange and components of surface water and energy balance. The latter are also grouped with respect to processes modelled.

In the soil-plant system, tritium can be re-emitted, lost to deeper soil layers (thus making a tritium sink) or stored, thus causing a lag in both re-emission and loss. Tritiated water vapour (HTO) from an atmospheric release moves with water and follows the water cycle in the soil-plant-atmosphere system. HTO can also diffuse against the flow of water vapour along a concentration gradient. Tritium gas (HT) diffuses the same way as HTO in the atmosphere. It is assumed that HT undergoes a very fast transformation into HTO once in contact with the soil due to microbial activity. By means of diffusion and transport with water, HTO is supplied to green vegetation, mostly leaves, where it is photosynthesized into carbohydrates as OBT.

In the one-dimensional model the rainwater can leave the soil-plant system through leaves (via stomata and or through the cuticle), through pores in the soil and through the bottom layer of soil (deep aquifer recharge via drainage). Water also leaves the system via surface runoff, which can be specified in one dimension as a point sink. Sub-surface lateral flow correspondingly becomes a line sink. Diffusion of tritium is also assumed one-dimensional.

8.5. GENERAL OVERVIEW OF THE SOIL-PLANT SYSTEM

8.5.1. Compartments of the soil-plant system

It is advisable to make a distinction between compartments responsible for holding and transferring tritium, both above- and below-ground. Most models separate the live matter (roots) and dead matter (soil organic matter and litter) from the soil. Advection of HTO occurs due to the movement of water in roots and soil pores; HTO also diffuses in soil. OBT is transported to the root via photosynthate allocation and is decomposed (back to HTO) in the processes of autotrophic root respiration and heterotrophic respiration due to microbial decomposition of dead matter (soil carbon and litter). The use of a single root compartment is considered appropriate.

8.5.2. Processes in the soil-plant system

Processes in sub-surface compartments can depend on such variables as soil temperature, gaseous, liquid and frozen soil moisture content, root distribution and phenomenological status. The empiricism of the previous generation of tritium transfer models is being replaced with a process-based description of maintenance, autotrophic respiration and heterotrophic respiration governed by a series of parameters. New parameter values could be either obtained from direct measurements in dedicated experiments, or derived from known parameters of exchange processes in soil and plants; for example, decomposition of litter and soil organic matter could be expressed in terms of soil temperature and soil moisture. In addition to the enhanced description of in-soil processes associated with HTO transfer and OBT decomposition, advantage could be gained from the revision of such soil surface properties as roughness length and albedo) [225–227]. These turn out to depend on soil moisture and so become new dynamical feedbacks to surface fluxes and HTO re-emission. The root mortality process also enhances the dynamics of the soil organic matter compartment.

8.6. INTERACTION OF THE SOIL-PLANT SYSTEM WITH THE ATMOSPHERE: COUPLING OF ATMOSPHERE TO SOIL AND THREE GENERATIONS OF LAND SURFACE SCHEMES

Modelling systems devoted to soil-plant-atmosphere interactions play the role of extended dynamical lower boundary conditions for larger weather prediction models. For this reason the soil-plant-atmosphere systems are called land surface schemes (LSS). These schemes are required to be robust and universally applicable; third generation LSS schemes are in development today.

Traditionally tritium models either follow LSS or are directly imbedded into these schemes. Spatial variability in soil HTO subsequently could be treated from the standpoint of energy budget analysis, the traditional approach in weather prediction modelling.

The partitioning of tritium between re-emission and losses to sinks, and the size (and role) of the soil-plant system repository, are presently the subject of ongoing research [203, 228, 229], primarily to clarify land surface classification with respect to partitioning of surface fluxes between sensible and latent heat. The latent heat flux is also known as evapotranspiration (ET) and provides a route of tritium re-emission. In some situations partitioning can be simply defined (and parameterized) at the surface; one approach, known as the bucket model, uses a virtual bucket to represent the soil as a single slab. Precipitation exceeding the size of the bucket simply causes the bucket to overflow, thus simulating surface runoff; no feedback to partitioning is expected. Modifications such as the use of leaking buckets to reflect known drainage rates are also often encountered. In certain other situations however, apparent feedback occurs in the soil-atmosphere system; this feedback is known as coupling. If the concept of the bucket is retained, large uncertainties arise in the case of strong coupling. The bucket approach makes up the first generation of land surface schemes, as coupling in the soil-plant-atmosphere system is included in very little detail. The minimum amount of detail typically requires three soil layers and a one or two layer canopy (the big-leaf approach). Models of this complexity are called second generation models, and were used for climate change analysis as they much better represent the partitioning of the surface energy budget components. The latter purpose lead to the inclusion of the carbon cycle, and photosynthesis in particular, and models of this sort became immensely useful for tritium studies. Many tritium models fall into the category of second generation schemes.

Notwithstanding the progress made, the second generation models were not universally applicable, as the coupling associated with transition to limited soil water supply required elaborate parameterization of soil water feedback on ET and on other processes such as photosynthesis. Third generation model development was subsequently started about 2 decades ago; this development is on-going because progress has been incremental. This has caused a renewal of interest in simple modelling concepts [202, 230–236].

Third generation models are characterised by inclusion of processes such as soil and leaf thermodynamics, plant phenomenology (quite helpful for handling tritium translocation), phase transitions between water vapour and liquid water in soil pores and multiple layers in the soil and the canopy. Third generation tritium models, built into the framework of third generation land surface schemes, subsequently have inherited very large uncertainties associated with model predictions.

8.7. SPATIAL VARIABILITY OF COUPLING AS A BASIS FOR ROBUST TRITIUM MODELING

Coupling is known to be weak in the vicinity of valleys and on flatlands with adequate precipitation [234, 237, 238]. Coupling also vanishes on highlands with deep water tables and in semi-arid climates. The development of tritium models subsequently can follow two routes. The first is in the revision of simple robust models of tritium transfer, which are appropriate where coupling is weak. The second route is to use sophisticated research-grade models to carry out sensitivity analyses to identify narrow critical zones responsible for strong coupling of the atmosphere to the land [201]. Such analysis is already being carried out by the weather and climate research community, where interest in this subject is strong. Meanwhile it seems logical to apply robust but different soil-plant tritium algorithms in wet and dry regions divided by narrow critical zones. This will address spatial variability and diminish associated uncertainties. Experimental evidence in Canada at AECL CRL suggests smaller inter-species (cultivar) variability compared to variability in space; on these grounds cultivar analysis of HTO transfer could be assigned a low priority.

8.8. OVERVIEW OF SOIL-PLANT TRITIUM MODULES

The tritium models considered below are GAZAXI [239], ETMOD [91], UFOTRI [92] and SOLVEG-II [240]. The capabilities of these models are listed in Table 39.

8.8.1. Processes in the soil-plant system

Water infiltration, which is responsible for HTO advection, can be modeled via the Green-Ampt solution, or via the numerical solution to Richards' equation with free Darcian flow. Root uptake is quantified by plant transpiration. Soil thermodynamics is taken into account and independent diffusion of HTO is modelled.

8.8.2. Boundary conditions for HTO

- Gaseous deposition on the surface;
- Rainfall, irrigation and dew-fall (amplifying tritium transport to the soil);
- Re-emission (loss to the atmosphere according to the concentration gradient);
- Evaporation-assisted transport to the atmosphere; and
- Drainage to the aquifer (advection via recharge/discharge).

8.9. LAND-ATMOSPHERE COUPLING AND REMARKS ON APPLICABILITY OF ANALYSED MODELS

The third-generation models (e.g. SOLVEG-II) are directly applicable to critical zones with strong coupling. Due to this fact, these complex models could help resolve the question of the sensitivity of tritium transfer to the degree of coupling, which is expected to be high. Comparison to second generation models (e.g. UFOTRI or ETMOD) is recommended. In the case of ETMOD the canopy conductance depends on soil water availability (see Section 8.11).

Two basic cases of weak coupling, shown in Table 40, demonstrate the applicability of first and second-generation models (e.g. GAZAXI, ETMOD, or UFOTRI).

TABLE 39. MODEL CAPABILITIES

Model	Type	Specification
GAZAXI	Boundary conditions	Wet deposition (Chamberlain’s approach), dry deposition (gradient exchange based on exchange velocity V_{ex} , which depends on LAI)
	Processes	Root uptake
ETMOD	Boundary conditions	Dry deposition only (V_{ex} given by the resistance approach)
	Processes	Root uptake via ET (resistance approach); diffusion and infiltration (semi-analytical approach with bottom – no flow boundary condition)
UFOTRI	Boundary conditions	Wet deposition (scavenging coefficient approach), dry deposition (V_{ex} given by the resistance approach), re-emission (based on ET following Monteith’s approach)
	Processes	Root uptake via ET (Monteith’s approach); infiltration (matrix force (suction tension, hydraulic conductivity with bottom – no flow boundary condition))
SOLVEG II	Boundary conditions	Wet deposition (scavenging coefficient approach); mixed boundary conditions (V_{ex} , carbon-modelled stomatal resistance); re-emission independently via V_{ex} and carbon-based ET
	Processes	Soil thermodynamics, CO ₂ diffusion; 2-phase HTO diffusion and advection (1-phase Richards’ equation for soil water movement)

TABLE 40. OCCURRENCE OF WEAK COUPLING OF LAND WITH ATMOSPHERE

Case	Description
1	Zones with deep water table and generally low soil moisture contents; water-limited conductance g_c and ET. Leaking bucket or free drainage are assumed as the bottom boundary conditions.
2	Zones of discharge, zones with shallow water table and high levels of soil moisture; partitioning of latent and sensible heat fluxes favours latent heat (ET). Actual ET approaches energy-limited potential ET and as such only depends on meteorology – spatial variability becomes secondary and corresponding adjustments to ET formulation can be performed. No-flow bottom boundary conditions and the bucket model approach could be implemented.

Some investigation into the role of soil thermodynamics and related model sensitivity could be useful in both cases.

A complete tritium model could contain a mapping of soil texture to elevation and further parameterization of HTO re-emission in each grid-cell using a combination of Case 1 and Case 2 HTO re-emission algorithms based on differently defined ET.

Coupling of soil-atmosphere surface fluxes occurs via correlation of surface fluxes and water table depths. Certain narrow zones on terrain slopes (termed critical zones) are known to be responsible for high correlations of this kind. Critical zones separate dryer highlands (where the latent heat flux is capped by a limited surface moisture supply) and valleys (where the soil moisture allows vegetation to operate much closer to potential ET). The variability of surface fluxes within critical zones appreciably exceeds the variability away from critical zones and so spatial variability could be seen as a contribution from two uncoupled zones with a constant effective ET in each. The influence of the third (critical) zone merits examination.

8.10. OVERVIEW OF FEEDBACKS IN THE SOIL-PLANT SYSTEM

Soil thermodynamics, soil moisture and plant physiology exert important feedbacks on each other. The role of these feedbacks has been assessed in a range of studies under the umbrella of the Intergovernmental Panel on Climate Change (IPCC). Subsequent coupling of these processes with the atmosphere caused the emergence of third generation land surface schemes targeted at clarification of land-atmosphere coupling. The parameterization of soil processes [241] offered in the Canadian submission to the IPCC are particularly useful and readily available for tritium transfer modelling; root growth parameterization follows recent work [241].

The important feedback from soil moisture to photosynthesis is only briefly outlined in Section 8.11.3, as it is addressed in other sections of this report.

The dynamical consideration of leaf and stem mortality results in a dynamical description of the size of the litter compartment, which is responsible for HTO respiratory re-emission and water (and HTO) interception. Subsequent enhancements to the modelling of respiration could be suggested. This subject is however omitted in this section and some relevant studies are mentioned in Section 8.12.

The process of root growth is presently not implemented in tritium transfer models. This process is however known to play an important role in the dynamical interaction of the atmosphere with soil moisture in general and with the fluctuating water table in particular. Parameterization of this process is considered an important step in enhancing the capability to model water transport [241–244]. This parameterization is relatively simple and could be implemented in tritium models, and is therefore addressed in the next section.

8.11. PARAMETERIZATION OF DYNAMICAL FEEDBACK FROM ROOTS: ROOT GROWTH

8.11.1. Biomass Growth

The partition of carbon (C) between leaf (L), stem (S) and root (R) compartments over long time periods could be considered allometric [245]. The equation is:

$$(C_R + C_S) = \varepsilon C_L^k \quad (94)$$

where $k = 1.6$ as defined by the Frankfurt Biosphere Model – FBM [245] and ε is a constant related to the plant functional type (PFT) (e.g. $\varepsilon=0.5$).

Detailed dynamics of C_R , C_S and C_L are given in [241]:

$$\begin{aligned} dC_L/dt &= A - R_{gL} - R_{mL} - A_{\text{roots}} - A_{\text{stem}} - D_L \\ dC_S/dt &= A_{\text{stem}} - R_{gS} - R_{mS} - D_S \\ dC_R/dt &= A_{\text{roots}} - R_{gR} - R_{mR} - D_R \end{aligned} \quad (95)$$

where:

- C_i is carbon concentration in the leaf ($i=L$), stem ($i=S$) and root ($i=R$) compartments;
- A is gross photosynthetic uptake;
- A_{roots} is carbon allocated to roots from leaf;
- A_{stem} is carbon allocated to stem from leaf;

R_{gi} is growth respiration for leaf ($i=L$), stem ($i=S$) and root ($i=R$) compartments;
 R_{mi} is maintenance respiration for leaf ($i=L$), stem ($i=S$) and root ($i=R$) compartments;
 D_i dead matter (litter) in the leaf ($i=L$), stem ($i=S$) and root ($i=R$) compartments.

The amount of photosynthate formed in the leaf and transferred to the roots can be calculated on the basis of a dynamically changing allocation fraction a_r of gross photosynthetic uptake:

$$A_{\text{roots}} = a_r A \quad (96)$$

The dynamics of a_r are known to be governed by soil moisture content and light availability. One simple parameterization is offered in Eqs. (97) and (110) below. The degree of soil saturation required for calculations can be parameterized the following way:

$$\beta = \max\{0, \min[1, (\theta - \theta_{\text{wilt}})/(\theta_{\text{field}} - \theta_{\text{wilt}})]\} \quad (97)$$

where, θ , θ_{wilt} and θ_{field} are the soil moisture content, wilting point soil moisture, and field capacity respectively, and β is the depth dependent degree of soil saturation.

The functional dependence of β on depth can be reflected in a set of β_i values in different layers. This requires different θ_{wilt} and θ_{field} in the soil layers weighted by the fraction of roots in these layers. a_r thus appears sensitive to the latter, and the commonly used constant rooting depth (and root distribution) may not be adequate when it comes to accurately accounting for HTO re-emission.

The other variable needed for calculation of a_r is the light availability. We can introduce the scalar pertaining to the availability of light (L) using the Leaf Area Index (LAI):

(1) for trees and crops with stems:

$$L = \exp(-k_n LAI) \quad (98)$$

where:

k_n is the light extinction coefficient; and

(2) for grasses:

$$L = \max(0, 1 - LAI/4.0) \quad (99)$$

The fraction of photosynthate moved to the roots can then be parameterized in the following way:

(1) for trees and crops with stem:

$$a_r = (\varepsilon_r + k_l(1 - \beta))/(1 + k_l(2 - L - \beta)) \quad (100)$$

where:

ε_r is a plant physiological parameter for photosynthate allocation to roots; and

(2) for grasses:

$$a_r = (\varepsilon_r + k_l(1 - \beta))/(1 - k_l(1 + L - \beta)) \quad (101)$$

An increase in water stress is known to increase allocation to the roots. Thus a large value of k_l provides high sensitivity of these process to L and β . A default value of $k_l = 0.8$ is recommended.

8.11.2. Root density profile

Root biomass arising from photosynthate allocation can be converted to rooting depth and a root distribution profile. Seedlings access water from shallow soil layers whereas mature plants draw water from deeper layers [246]. Dynamical handling of root distribution [247] results in different concentrations of HTO transported with the transpiration flux compared to a constant (i.e. static) rooting depth and vertical root distribution.

Following the study of Arora and Boer [247], an exponential root density profile, ρ (kg C m^{-2}), can be parameterized as:

$$\rho = A(t) \exp(-a z) \quad (102)$$

where A is the surface root density and a is a constant independent of root biomass, B . The total root biomass above depth z is obtained by integrating Eq. (102) in the vertical:

$$B = A(t)(1 - \exp(-a z))/a \quad (103)$$

The whole root system has a total biomass of $B = A(t)/a$. Conversely, we can define the fraction f_r of total root mass as:

$$d = -\ln(1 - f_r)/a \quad (104)$$

which permits definition of the “rooting depth” d , the depth containing 95% of roots ($f_r = 0.95$):

$$d \approx 3/a. \quad (105)$$

Jackson et al. [248] estimate that the mean root biomass is about 4.4 kg m^{-2} for trees, with the maximum reaching 8.7 kg m^{-2} ; for other species the mean root biomass can be as small as 0.1 kg m^{-2} .

The constant a provides a poor fit to the field root biomass data analyzed in Arora and Boer [247]. Major deviations were caused by the rooting depth, which was observed to change appreciably with time. In particular, the relation $d \sim B \sim a^{-1}$ was established. This is an important implication for HTO uptake and re-emission by transpiration. A revised formulation of Eqs. (102)–(105) can be obtained by replacing a with two cultivar-dependent constants α and b :

$$a = b B^{-\alpha}(t) \quad (106)$$

Eqs. (102)–(105) then become:

$$\rho = b B^{(1-\alpha)}(t) \exp(-b B^{-\alpha}(t) z) \quad (107)$$

$$f_r = 1 - \exp(-b B^{-\alpha}(t) z) \quad (108)$$

$$d = 3 B^{\alpha}(t) b^{-1} \quad (109)$$

The two new constants α and b are cultivar-dependent. Values can be found in Arora and Boer [247] or inferred from Jackson et al. [248], where various plants and their a and B values are discussed. α is responsible for partitioning between horizontal and vertical root growth; $\alpha \in [0; 1]$. For example, simple horizontal root growth occurs with a constant root depth if $\alpha=0$ ($b=a$ is also implied in this case). Growth is mostly vertical if $\alpha=1$. A default value of $\alpha=0.8$ is recommended by Arora and Boer [247].

Some minor modification to α is required when root growth is limited, e.g. by bedrock, which is a frequent case in Canada.

8.11.3. Constraint on transpiration

Constraints on the transpiration flux are typically modelled at the plant/air interface, implying that they are controlled by the stoma and not the roots. Closure of the stomata in response to soil moisture stress can be modelled by decreasing the rates of photosynthesis and canopy conductance [249, 250]. In particular the following formulation can be used:

$$A_{\text{stressed}} = A(1-(1-\beta)^\alpha), \quad (110)$$

The implications of soil water stress on transpiration are addressed in detail in other sections of this report.

8.12. RESPIRATION

Direct re-emission of HTO from soil and plant tissue is complemented by the decomposition of the maintenance fraction of intermediate carbohydrates (and OBT) via autotrophic respiration shortly after OBT formation, and by the microbial decomposition of below-ground organic matter and litterfall (and OBT) via heterotrophic respiration [251–254]. Inputs to these processes are the distribution of root biomass and the litter density. Respiration processes essentially depend on soil temperature and soil moisture [255–264], require extensive parameterization [265, 266] and merit separate examination within the next generation of soil-plant models.

9. TRITIUM TRANSFER IN WHEAT EXPERIMENTS AND MODEL TESTS

9.1. OVERVIEW

Successful testing of models against experimental data is key to accepting the models for use in real situations [167]. For tritium models, the first international testing exercise occurred in the 1990s [267]; in addition, other tests have been carried out on the UFOTRI [173] and ETMOD [91] models. Because of the Fukushima reactor accident in March 2011, requirements for nuclear safety have increased, including the robustness of (radiological) risk assessment models. In the EMRAS I programme, the working group dedicated to ^{14}C and ^3H modelling tested several models against experimental data for simulated hypothetical accidental releases to the atmosphere (^{14}C in potato plants and ^3H in soybean). The conclusions were not promising.

In the EMRAS II programme, having access to all the data for tritium experiments in winter wheat that were conducted in Germany in 1995–1996, a scenario for model testing was developed to add to the understanding of the processes involved. The results of the original experiment had been used to calibrate the ‘plant-OBT’ model [175], and were only partially published [174, 176]. The scientific impact of the experiment was high, and some of the experimental conditions and results were shared between scientists. The main results were incorporated into the present study (Section 7) but all the experimental conditions and results were not fully accessed by the scientific community. The scenario for EMRAS II was defined using all of the original experimental conditions. The test was not really a blind one, however, because some of the participants already knew the results (i.e. the Romanian and German participants).

9.2. EXPERIMENTS AND SCENARIO DEFINITION

In 1995 at KfK (now Karlsruhe Institute of Technology, KIT), winter wheat plants were grown in a small experimental field and short-term HTO exposure experiments were conducted during the grain-filling stage of the wheat. For the HTO exposure, a transparent plexi-glass box (30 × 30 cm, 100 cm high) was used as the field-exposure chamber. An HTO-evaporation unit was installed inside the box. The amount of HTO maintained in the box was adjusted using the power supply for the heating system of the evaporation unit, so that a constant evaporation rate of HTO during an HTO-exposure period of 1 hour was achieved. The mixing of air by a fan inside the box resulted in an almost homogeneous tritiated-air humidity inside the box.

Air-moisture was withdrawn from the box by a calibrated bubbler system and trapped in vials with a scintillation cocktail. Vials were changed every 5 minutes.

The following parameters were also measured in the box during the exposure:

- Air temperature ($^{\circ}\text{C}$);
- Relative air humidity (%);
- Light intensity (PPFD) ($\mu\text{E}/\text{m}^2\text{s}$).

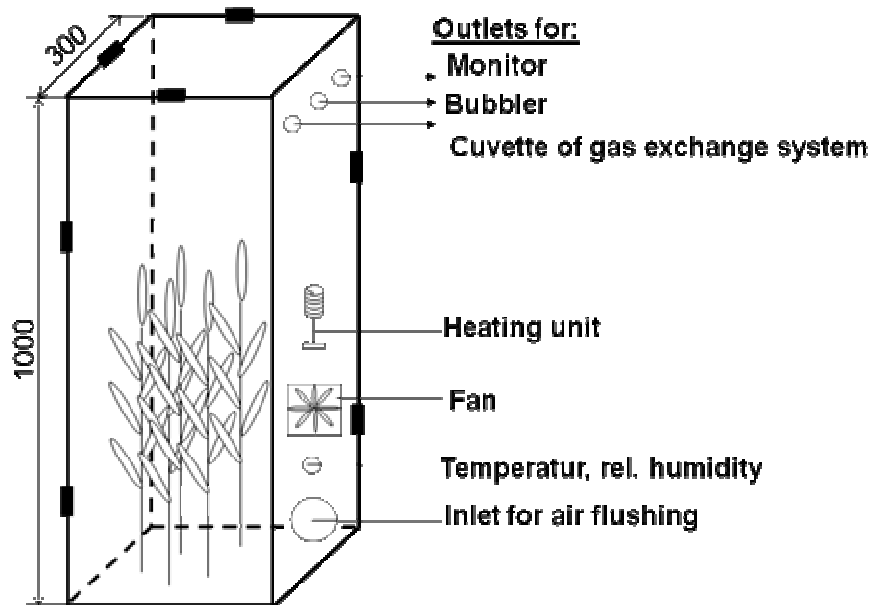


FIG. 41. Experimental design for studying wheat uptake of HTO (taken from [172]).

TABLE 41. INPUT DATA FOR WHEAT SCENARIO

Set 1							
Experiment	f3	f14	f7	f2	f4	f10	f15
Year	1995	1996	1995	1995	1995	1996	1996
Month	6	6	6	6	6	6	7
Day	22	27	28	21	22	19	3
Days after flowering	18	22	24	17	18	14	28
Days from flowering to harvest	47	48	47	47	47	48	48
Start hour	7	7	8	9	10	11	11
HOURLY average exposure time							
Average Temperature °C	18	11	26	28	29	26	32
Average RH %	76	93	76	76	63	75	63
Average PPFD	160	179	370	644	1230	1160	1830
HTO mean-air moisture	114	147	222	59	66	121	180
Set 2							
Experiment	f1	f9	f13	f5	f11	f6	f12
Year	1995	1996	1996	1995	1996	1995	1996
Month	6	6	6	6	6	6	6
Day	19	17	26	25	25	26	25
Days after flowering	15	12	21	21	20	22	20
Days from flowering to harvest	46	48	48	45	48	46	48
Start hour	14	15	15	20	20	23	23
HOURLY average exposure time							
Average Temperature °C	33	36	29	24	15	17	12
Average RH %	70	70	72	84	89	89	93
Average PPFD	1180	1375	1170	54	86	0	0
HTO mean-air moisture	19	60	213	268	504	365	395

Immediately after exposure, the box was removed from the field, and TFWT concentrations (measured after lyophilisation) and OBT concentrations (measured after combustion with a Packard Oxidiser) were obtained from samples of leaves and ears. Before combustion, the samples were kept in a tritium-free humid atmosphere to remove all the exchangeable tritium from the samples. After exposure, the remaining wheat plants were grown under ambient field conditions until harvest. At certain intervals during that time, leaf and ear samples were taken to follow the changes of tritium concentrations in the plants.

A series of seven exposures at different times of day and night in 1995 was performed (Table 41) to upgrade and improve the existing model. In 1996 another series of seven experiments was carried out (Table 41). These data were used to validate the plant-OBT model developed from the 1995 data.

For each experiment, the hourly averages of air temperature, relative humidity, light intensity and HTO concentration in the air moisture inside the box were collected during the 1 hour exposure. These data became the input data for the modellers in the scenario (see Table 41). For each experiment, these input data were supplemented with 10 minutes averages of the same parameters and with hourly meteorological data from 1995 and 1996 (e.g. solar radiation, relative humidity and temperature). The growth in biomass of the wheat plant (leaves, stems, ears or grains in kg per plant) at anthesis and harvest each year was also included in the scenario.

The modellers were asked to submit their predictions concerning:

- HTO in leaf water at the end of exposure and its dynamics for the next 24 hours (Bq L^{-1});
- OBT in leaves at the end of exposure and its dynamics for the next 24 hours and at harvest (Bq kg^{-1});
- OBT in grain (ear) at the end of exposure and its dynamics for the next 24 hours and at the harvest (Bq kg^{-1}).

Four models participated in this scenario:

- JAEA model (SOLVEG H3), a complex research-grade model, recently published [240] and briefly presented in this report (see Section 11);
- CEA model (CERES), a simple approach with a constant exchange velocity for day or night and with OBT production depending on the integrated leaf HTO concentration [268];
- IFIN model [269], with an upgraded version presented in this report (see Section 6)
- Plant-OBT model [175] as it was in 1997.

These models differed in how the uptake of HTO in leaves and the formation of OBT were treated. The most complex model (SOLVEG H3) calculated the HTO uptake and the re-emission from leaves based on the Ball-Berry formalism [137] for canopy resistance together with the advanced photosynthesis model of Farquhar [145]. A carbohydrate allocation model based on the experimental data from a single plant was used to calculate carbohydrate exchange in leaves. OBT production at night was treated no differently than that during the day. The simplest model, CERES, used a single value for the exchange velocity during the day or night that was independent of plant type, temperature or light intensity. The OBT concentration at harvest was simply calculated from the integral of the HTO

concentration in leaves using an average incorporation rate of tritium into the organic matter. The Plant-OBT model made a distinction between leaves, stems and grain and treated photosynthesis using a simple model that included the contribution of the ear. Its exchange velocity incorporated the classic Jarvis approach [136] for stomatal resistance without the link to photosynthetic rate. Night OBT production accounted for the basic metabolic processes with calibrated coefficients. The Plant-OBT and IFIN models used similar approaches to OBT production during the day along with night calibration constants, but the IFIN model used photosynthesis to define the exchange velocity.

9.3. MODEL RESULTS

While the OBT concentration in grain at harvest is the most important endpoint, modellers were asked to submit predictions for more observations and time steps to detect potential compensatory errors and to help improve the models.

The predicted to observed ratios of the leaf HTO concentrations at the end of exposure, given in Figure 42, indicate that the largest mispredictions seem to occur at the transition between day and night (starting hour of 20 in Figure 42). Generally, however, the predictions are good.

For the OBT concentrations in leaves at the end of exposure, the predicted to observed ratios (P/O) are more spread (Figure 43) with a tendency towards over-prediction by the Plant-OBT model [175] and under-prediction by the CERES model. For the night exposure (starting hour of 23), the JAEA model essentially predicted no OBT, while the other models under-predicted the observations.

At harvest, the JAEA model exhibited a large spread in its predicted to observed ratios for grain OBT concentrations with practically no OBT in grain predicted at night. The Plant-OBT model over-estimated most observation, while the other models (Figure 44) mostly under-predicted.

The translocation index is defined in the literature as the ratio between the harvest concentrations of OBT in grain (combustion water) to the leaf HTO concentrations at the end of exposure. The P/O ratios for the translocation indexes are given in Figure 45. The Plant-OBT and CEA CERES models over-predict the TLI at night.

The complete database of observations contains many intermediate time steps and can be used by each modeller for a deeper analysis. In general, under-prediction of OBT at harvest can have many possible causes that will not be reviewed here.

9.4. STATISTICAL ANALYSIS OF RESULTS FOR MODELS ACCEPTANCE

There are no international guidelines to assess model robustness in operational cases, but there are recommendations at the country level. The Environmental Protection Agency (EPA) in the USA published a series of recommendations [167, 270] including classical works [271, 272]. Based on EPA recommendations [167, 270], any model can be evaluated from at least three perspectives: statistical, scientific and operational.

Statistical evaluation primarily compares model predictions with observations. It provides concise information on model performance. The potential user must be alert, however, for the presence of the compensatory errors, which cause the model's predictions to agree with observations for the wrong reasons.

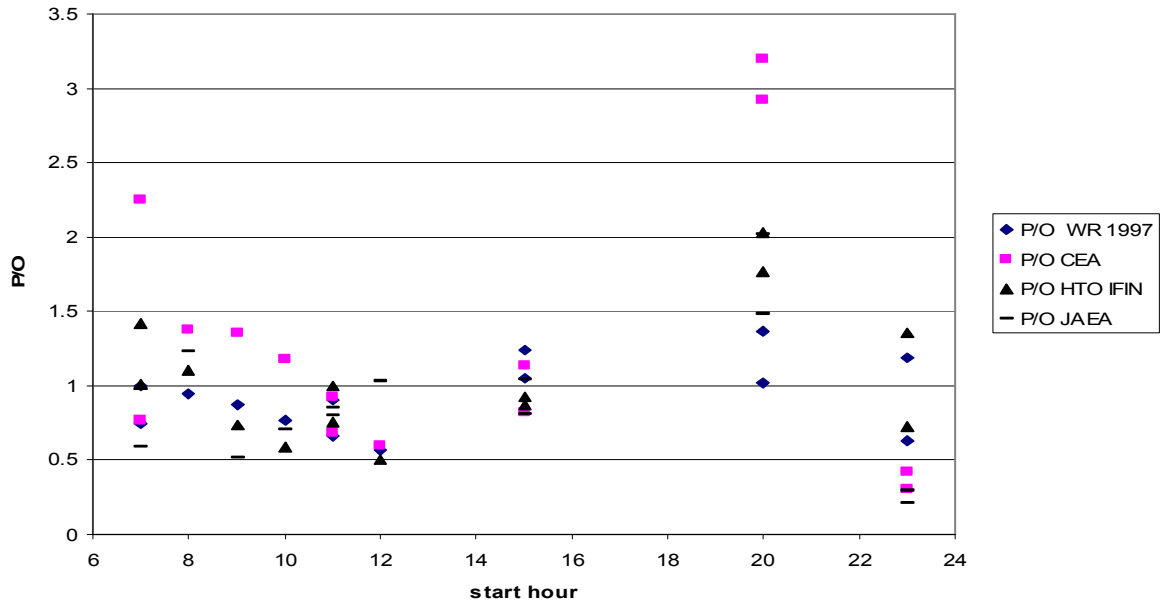


FIG. 42. Predicted to observed ratios for leaf HTO concentrations at the end of a 1 hour exposure.

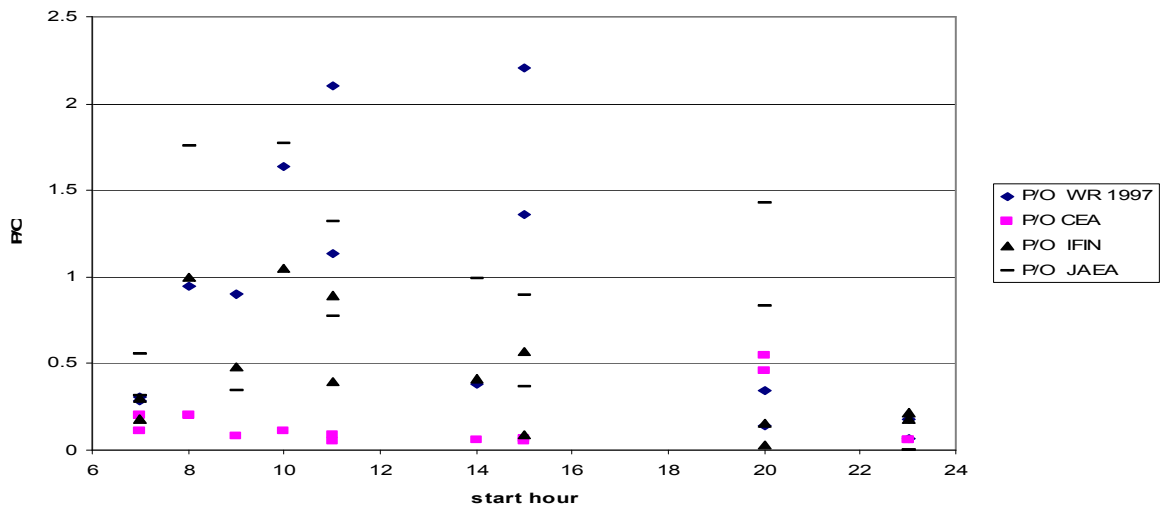


FIG. 43. Predicted to observed ratios for leaf OBT concentrations at the end of a 1 hour exposure.

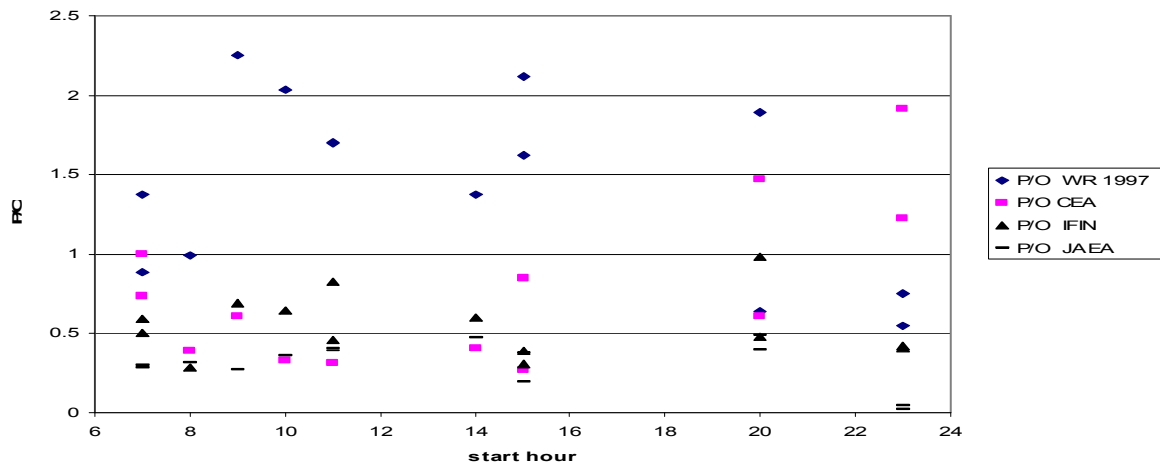


FIG. 44. Predicted to observed ratios for concentrations of OBtin grain at harvest.

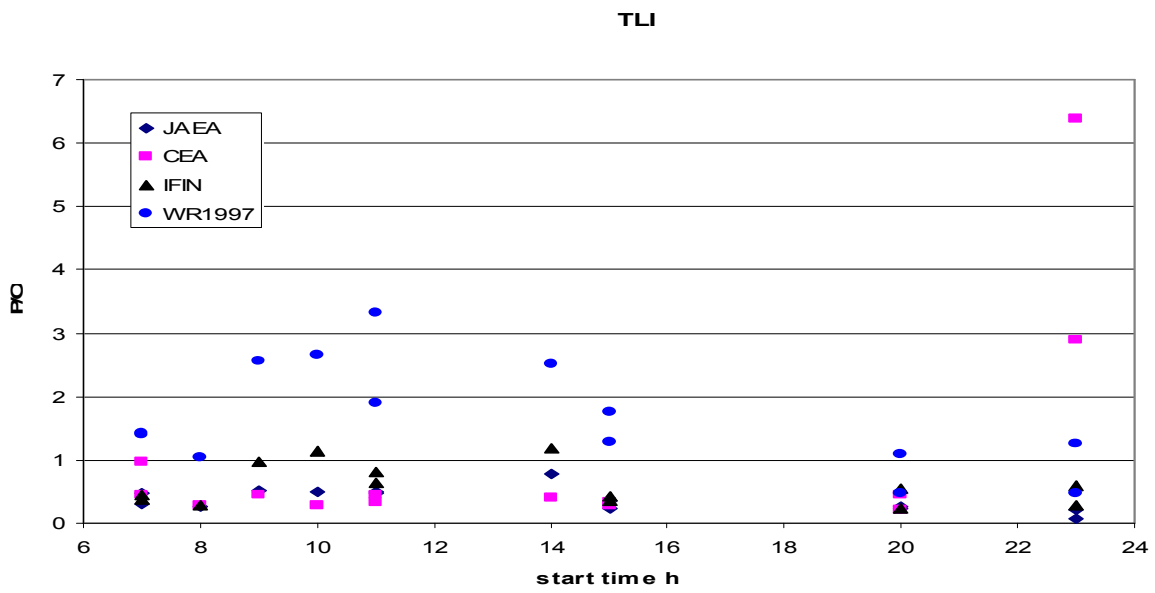


FIG. 45. Predicted to observed ratios for the translocation index.

The EPA references will be used here for a statistical evaluation of the CEA, JAEA and IFIN models that participated in the test.

Systematic bias refers to the ratio of the prediction (C_p) to the observation (C_o). Fractional bias (FB) and geometric mean bias (MG) are measures of mean bias and the systematic errors that always lead to under- or over-estimating the measured values. FB is based on a linear scale, and the systematic bias refers to the arithmetic difference between C_p and C_o . MG is based on a logarithmic scale:

$$FB = \frac{\sum_i (C_{oi} - C_{pi})}{0.5 \sum_i (C_{oi} + C_{pi})} = FB_{FN} - FB_{FP} \quad (111)$$

$$MG = e^{\left(\overline{\ln C_o - \ln C_p} \right)} \quad (112)$$

where i is the number of data employed for the comparison.

Non-systematic errors, called random error, are due to unpredictable fluctuations. Values are scattered around the true value and tend to have null arithmetic mean when the measurement is repeated. Normalized mean square errors ($NMSE$) and geometric variance (VG) are measures of the scatter, and reflect both systematic and non-systematic (random) errors.

$$NMSE = \frac{\overline{(C_o - C_p)^2}}{\overline{(C_o C_p)}} \quad (113)$$

$$VG = e^{\left(\overline{\ln C_o - \ln C_p} \right)} \quad (114)$$

The fraction of the predictions within a factor of two of the observations (FAC2) is the most robust measure, because it is not influenced by high or low outliers.

$$FAC2 = \text{fraction of data that satisfy } 0.5 \leq \frac{C_p}{C_o} \leq 2.0 \quad (115)$$

In order to assess accuracy in the model performance, multiple performance-measures have to be considered. Advantages of each performance measure are partly determined by the distribution of the variable. For example, with a log-normal distribution, MG and VG provide a more balanced treatment of extremely high and low values. However, MG and VG are strongly influenced by extremely low values and are undefined for zero values. Therefore, it is necessary to impose a minimum threshold for data that have extremely low values or zero, which can be the limit of detection (LOD). In this case, if C_p or C_o are lower than the threshold, they are set to the LOD. MG and VG would be more appropriate for a dataset in which both the predicted and the observed values vary by many orders of magnitude. FB and $NMSE$ are strongly influenced by infrequent high observed and predicted values.

The fractional bias (FB) is symmetrical and bounded; values for the fractional bias range between -2.0 (extreme underprediction) to +2.0 (extreme overprediction). FB is a dimensionless number, which makes it convenient for comparing results from studies with different concentration levels. The value of FB equal to -0.67 is equivalent to underprediction

by a factor of two; the value of FB equal to +0.67 is equivalent to overprediction by a factor of two. Model predictions with a fractional bias of zero are relatively free from bias.

When the geometric mean bias (MG) is +0.5, the observations are underpredicted by a factor of two; when MG is +2, the observations are overpredicted by a factor of two.

When the value of the normalized mean square error ($NMSE$) is 0.5, it is equivalent to a factor of two mean bias, but it does not indicate whether the factor of two mean bias is an under- or over-prediction.

The geometric variance (VG) at 1.6 is equivalent to a factor of two mean bias, but it also does not indicate whether the factor of two mean bias is an under- or over-prediction .

The ratio C_p to C_o can be assessed with the following equations using FB , MG , $NMSE$ and VG .

$$\frac{\overline{C_p}}{\overline{C_o}} = \frac{1 - 0.5FB}{1 + 0.5FB} \quad (116)$$

$$\frac{\langle C_p \rangle}{\langle C_o \rangle} = \frac{1}{MG} \quad (117)$$

$$\frac{\overline{C_p}}{\overline{C_o}} = \frac{2 + NMSE \pm \sqrt{(2 + NMSE)^2 - 4}}{2} \quad (118)$$

$$\frac{\langle C_p \rangle}{\langle C_o \rangle} = \exp[\pm \sqrt{\ln VG}] \quad (119)$$

A set of perfect predictions would produce MG , VG , and $FAC2$ equal to 1.0 and FB and $NMSE$ equal to 0. Chang and Hanna [271] proposed the following criteria of statistical acceptance for a model:

- More than 50% of the predictions fall within a factor of two ($FAC2 > 0.5$);
- The mean bias is within $\pm 30\%$ of the mean ($|FB| < 0.3$ or $0.7 < MG < 1.3$);
- Random scatter falls within about a factor of two to three of the mean ($NMSE < 1.5$ or $VG < 4$).

These statistical performance measures have been used to compare the results of the CEA, JAEA and IFIN models for the wheat scenario. 61 experiments were modelled and predicted time-dependent calculations of HTO concentrations in leaf water and OBT concentrations in leaves and grain at harvest (14 results) were compared with the observations.

Statistical results for the activity of tritium in leaf water are shown in Table 42. Because some of the values were zero or smaller than the detection limits, only arithmetic scales (FB , $NMSE$) are illustrated. Statistical results for OBT concentrations in grain at harvest obtained using arithmetic and logarithmic scales are shown in Tables 43 and 44, respectively. $NMSE$ and FB with 95% confidence limits for tritium concentrations in leaf water of wheat plants for the 61 experiments are plotted against each other in Figure 46. In Figure 47, the geometric variance and the geometric mean bias are plotted against each other for OBT concentrations in the wheat grain at harvest.

TABLE 42. STATISTICAL RESULTS FOR TRITIUM IN LEAF WATER OF WHEAT

Model/Performance (factor 2)	NMSE (0.5)	FB ($\pm 2/3$)	FAC2
CEA	0.7	0.16	0.31
JAEA	1.13	0.26	0.30
IFIN	0.42	0.15	0.36

TABLE 43. STATISTICAL RESULTS FOR OBT IN GRAIN AT HARVEST (ARITHMETIC SCALE)

Model/Performance (factor 2)	NMSE (0.5)	FB ($\pm 2/3$)	FAC2
CEA	0.7	0.4	0.5
JAEA	1.8	1.0	0.07
IFIN	0.8	0.7	0.5

TABLE 44. STATISTICAL RESULTS FOR OBT IN GRAIN AT HARVEST (LOGARITHMIC SCALE)

Model/Performance (factor 2)	VG (1.6)	MG (2.0 or 0.5)	FAC2
CEA	2.1	1.8	0.5
JAEA	15.2	4.0	0.07
IFIN	1.8	1.9	0.5

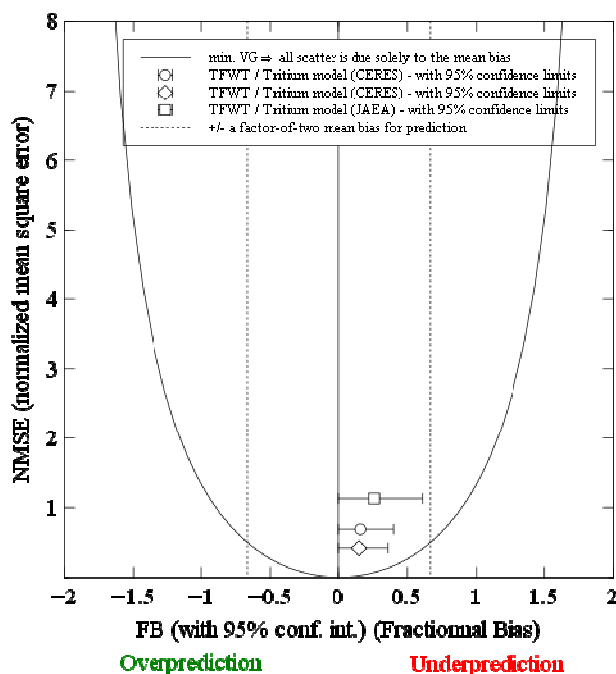


FIG. 46. NMSE plotted against FB with 95% confidence limits (indicated by thin horizontal bars) for HTO concentrations in the leaf water of winter wheat. The parabola represents the minimum NMSE for a given value of FB, assuming all scatter is due solely to the mean bias. Dotted lines represent a plus and minus factor-of-two mean bias for the predictions.

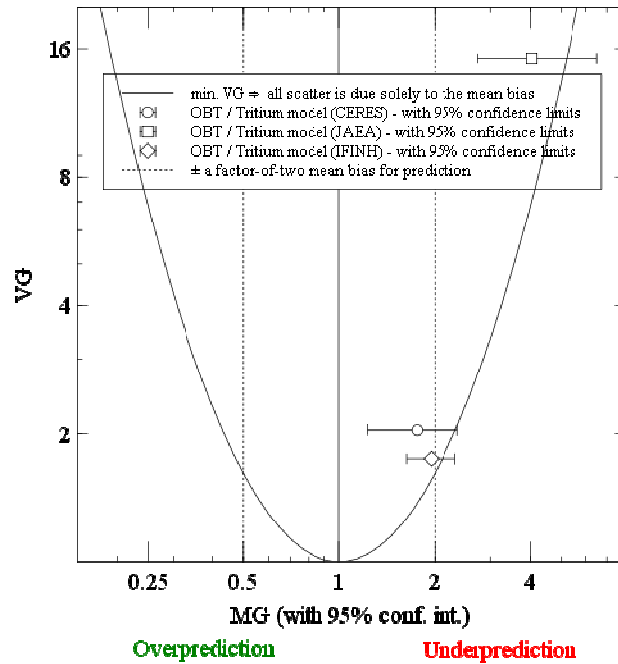


FIG. 47. VG plotted against MG with 95% confidence limits (indicated by thin horizontal bars) for concentrations of OBT at harvest. The parabola represents the minimum VG for a given value of MG , assuming all scatter is due solely to the mean bias. Dotted lines represent a plus and minus factor-of-two mean bias for the predictions.

TABLE 45. COMPARISON BETWEEN STATISTICAL PERFORMANCE MEASURES AND ACCEPTANCE CRITERIA FOR HTO AND OBT IN WHEAT

HTO Leaf				
Test/models	CEA	IFIN	JAEA	
FAC2 > 0.5	no	no	no	
Mean bias within $\pm 30\%$ of the mean ($ FB < 0.3$ or $0.7 < MG < 1.3$)	ok	ok	ok	
Random scatter ($NMSE < 1.5$ or $VG < 4$)	Ok	ok	ok	
Acceptance	ok?	ok?	ok?	
OBT Grain				
Test/models	CEA	IFIN	JAEA	
FAC2 > 0.5	ok	ok	no	
Mean bias within $\pm 30\%$ of the mean ($ FB < 0.3$ or $0.7 < MG < 1.3$)	no	no	no	
Random scatter ($NMSE < 1.5$ or $VG < 4$)	ok	ok	no	
Acceptance	ok?	ok?	no	

The predictions of the CEA and JAEA models for HTO in leaf water are greater than a factor of 2 for *NMSE* (random and systematic errors), and only about 30% of the predictions for all models are within a factor of 2 of the observations (Table 42 and Figure 46). All models tend to underestimate the activity in the leaf by less than a factor of 2.

The results for predictions of OBT in grain at harvest (Tables 43, 44, Figure 47) are about the same whether the arithmetic or logarithmic scale is used for the comparison. All models exhibit underpredictions; the underpredictions for the JAEA model are a factor of 3 to 4 depending on which scale (arithmetic or logarithmic) is used. OBT activity is underestimated by about a factor of 2 for the IFIN model and less than a factor of 2 for the CEA model. Systematic and non-systematic scatter is less than a factor of 3 for the CEA and IFIN models and a factor of 5 for the JAEA model.

9.5. DISCUSSION OF STATISTICAL ANALYSIS

Performance measures must be used to compare predictions to observations, and statistical analysis can definitely help model intercomparisons. Although systematic errors were found in the predictions of the models participating in the wheat scenario, the modelling of HTO in the wheat leaf seems acceptable for the three models. Studies of systematic errors lead to a ratio (prediction to observation) of 0.76 for the JAEA model and 0.86 for the CEA and IFIN models. Underpredictions are common for OBT in wheat grain at harvest, with ratios of prediction to observation of 0.3 for the JAEA model, 0.48 for the IFIN model and 0.7 for the CEA model. If statistical results are compared with acceptance criteria (Table 45), no model meets all criteria for both HTO and OBT concentrations in the wheat scenario. For HTO in wheat leaf, only FAC2 is not met by the three models. For OBT, the JAEA model does not meet any of the criteria, while the CEA and IFIN models only do not meet the mean bias acceptance, which is greater than 30%.

The statistical tests (Table 45) scientifically analyze model predictions compared with observations to detect sources of misprediction. The lack of information about wind parameters and atmospheric stability after the exposure period can partially explain model under-estimates of leaf HTO after exposure. The experimental field was situated near the laboratory, and local conditions can increase atmospheric and boundary resistances. The processes modelled for the production of OBT must be analyzed for each model and compared between models. The assumptions and approaches of each model must be explained and justified: the JAEA model ignores the formation of OBT at night, the IFIN model uses a calibration constant for OBT at night, and the CEA model treats day and night OBT production similarly.

9.6. CONCLUSIONS

Experimental data acquired in the experiments of 1995 and 1996, mostly unpublished, have been used to test models developed in IFIN-HH, CEA, and JAEA in recent years. Predictions of the older PLANT_OBT model were included for comparison.

Statistical analysis was used to detect systematic errors that led to overestimating or underestimating the measured values.

10. TRITIUM TRANSFER IN FARM ANIMALS

10.1. OVERVIEW

As part of the IAEA's EMRAS (Phase I) Programme, which ran 2003–2007, Working Group 2 the “Modelling of tritium and carbon-14 transfer to biota and man working group” (EMRAS WG2) was set up to address ^3H and ^{14}C . The aim of the EMRAS WG2 was to decrease the uncertainty about the models assessments, focusing on the formation of organically bound tritium (OBT) and its transfer through the environment to humans. The final report in EMRAS WG2 [4] includes only a single test case for farm animals [273]. It was concluded that more tests and model inter-comparisons are needed before the best operational model can be selected. Practitioners must also be aware of the user's influence on model performance. This report is intended to be a step towards developing a simple operational model, based on parameters values for animal metabolism, that satisfies the requirements of robustness necessary in radiological assessments.

The tritium contribution to ingestion dose is highly dependent on dietary habits and can have a large range (from 5–95% of ingestion dose). For current European diets, the tritium contribution to ingestion dose is estimated at about 20%, but it can be up to 50% of an infant's ingestion dose. For routine releases, transfer coefficients and concentration ratios can be used with reasonable confidence to predict ingestion doses, [274], but, for accidental releases, the experimental data base is very limited (Table 46) and, in many cases, there are no dynamic data. The products of interest are milk (cow, sheep), meat (beef, sheep, pork, and broiler), and eggs. Tritium can be ingested by animals as either (or typically both) HTO (food and drinking water) and organic matter, including OBT. Inhalation and skin absorption are also possible routes of HTO intake. Exchangeable organic tritium and HTO rapidly equilibrate with body water. Organically bound tritium found in food is metabolised by animals and partially converted to HTO. Body HTO is also partially metabolised to OBT. If only tritiated water is given to an animal, only a small fraction is metabolized to OBT while the rest (99%) stays in the water cycle of the animal. Half-time for water turnover is well known for domestic animals: about 3.5 days for a cow, 4 days for a pig and, 2.5 days for a sheep. When a cow ingests HTO, a second component with a half-time of about 60 days is observed in both the body water and milk water. This is due to the catabolism of OBT and contributes less than 2% to the integrated activity of the body water [275]. In the milk constituents, after a cow is fed HTO, half-times of 33 and more than 200 days are observed in casein and fat, respectively. After a cow is fed with OBT, the milk constituents additionally show a very fast component with a half-time of 1.5 days [276].

To understand the experimental data for OBT transfer in milk or meat, it is useful to briefly discuss the fate of the organic food components. The relatively long molecules of carbohydrates, proteins and fats will undergo digestion, which is essentially a process of hydrolytic cleavage that involves the uptake of water. After absorption of water, the resulting smaller molecules (amino acids, monosaccharides and fatty acids) will enter the general pool of metabolic precursors where they can be used for any of the following processes [277]:

- *Formation of energy.* This is a metabolic oxidation involving the conversion of OBT to HTO. After feeding with OBT, about half of the tritium is transferred to milk water (HTO);
- *Synthesis of functional body constituents* (enzymes, hormones, structural elements, secretions [e.g. milk]). This involves conversion from one form of OBT to another form;
- *Synthesis of body reserves, particularly fats.* This again converts one form of OBT to another.

TABLE 46. QUALITY AND AVAILABILITY OF EXPERIMENTAL DATA

Food item	Experiments
Cow milk after HTO intake	good exp.
Cow milk after OBT intake	1 exp.
Goat milk after OBT intake	good exp.
Goat milk after HTO intake	no exp
Sheep milk after HTO intake	no exp
Sheep milk after OBT intake	no exp
Broiler meat after HTO intake	no exp
Broiler meat after OBT intake	no exp
Eggs after HTO intake	Russian exp.
Eggs after OBT intake	no exp
Beef meat after HTO intake	2 exp.
Beef meat after OBT intake	no exp.
Veal after OBT intake	poor exp.
Pig after OBT intake	poor exp.
Piglets after OBT or HTO intake	medium exp.
Sheep after OBT intake	partial exp.

Daily animal feed intake is highly variable due to breed, diet quality, production level, and environment. Average values and ranges are given elsewhere [274], but no guidance exists to help choose a specific value. At best, a distinction must be made between intakes for highly efficient industrial farming and intakes for subsistence farming in an unfavourable environment. As an example of the variability of intake, sheep with similar mass and growth rate can consume two times more food in mountain rangeland than in a stable [278]. As another example, a small cow with a milk production of 5 L d⁻¹ consumes about 8 kg dry matter (dm) of grass per day, while a large cow with a milk production of 40 L d⁻¹ needs up to 25 kg dm per day. A highly concentrated diet reduces feed intake compared with a diet high in roughage. Consequently, a variability of up to a factor of 3 arises only from feed intake.

10.2. CLASSIC APPROACH

Animal intake of tritium as OBT includes both exchangeable and non-exchangeable forms, and the fractions of each before digestion can be assessed from the composition of feed (see Appendix I). Digestion processes can change these fractions, with the effect being larger for ruminants. The bound hydrogen in the organic matter of plants that is digested to carbohydrates, proteins, and lipids by the animal is more likely to be synthesized into the organic matter of the animal than is the tritium atom that enters the body as water [279]. The likelihood that one form of hydrogen in the diet will transfer to the same or another form in animal products in decreasing order of occurrence is (names of transfer factors are given in parentheses):

- Hydrogen in water to hydrogen in water (F_{HH});
- Bound hydrogen in organic matter to bound hydrogen in organic matter (F_{OO});
- Bound hydrogen in organic matter to unbound hydrogen in water (F_{OH});
- Unbound hydrogen in water to bound hydrogen in organic matter (F_{HO}).

The classical approach for other radionuclides considers the convolution integral for the concentration in animal product at time T [280]:

$$C_{m,k} = \sum_{i=H,O} TF_{m,i,k} \sum_{J=1}^J \left\{ a_{m,i,k,J} \int_0^{\sigma} I_{m,i}(t) \lambda_{b,m,i,k,j} \bullet \exp[-(\lambda_{b,m,i,k,j} + \lambda_r)(T-t)] dt \right\} \quad (120)$$

where:

- $C_{m,k}(T)$ is the activity concentration (Bq kg⁻¹) in animal product m at time T;
- $TF_{m,i,k}$ is the transfer factor (d kg⁻¹) for animal product, m;
- J is the number of biological transfer rates;
- $a_{m,i,k,j}$ is the fraction of biological transfer rate, j; and
- $\lambda_{b,m,i,k,j}$ is the biological transfer rate j (d⁻¹) for animal product, m;
- $I_{m,i}$ is the feeding rate (kg d⁻¹) ; and
- λ_r is the radionuclide decay rate (d⁻¹).

Given the four transfer pathways discussed above for tritium, it is necessary to have four transfer factors and, for the dynamic case, at least four biological loss rates. However, not enough experimental data exist to accomplish this, with the exception of tritium in cow milk after an intake of HTO. In this case, there are six data sets from which to infer both the transfer coefficients and biological transfer rates [275, 281, 282]. The data can be analyzed as a contribution of two terms, and the partition factors were normalized to 1. As shown in Table 47, the slow turnover of total tritium in cow milk (after intake of HTO) is only a small part of the total transfer because it mostly accounts for the conversion of the OBT in the body to the HTO in body-water and to OBT in milk. The fast transfer rate (λ_1) corresponds to the body water half-time, but the range for HTO is lower than the range given in the literature for water [283]. In a metabolic model [284] the transfer coefficient is correlated with the water turnover rate and the body water content. Using recommended values, an average biological transfer rate of 0.22 d⁻¹ can be used. For other animal products, the values of the fast transfer rates given by water turnover rates, were recently revised [283] and can be used as defaults. Seasonal variation in quantities of water drunk and changes in diet and production must be taken into account.

For cow milk after an intake of OBT, a single report [276] emphasizes the importance of milk production and diet on the transfer, but not on biological half-times. The transfer coefficient of total tritium varies by 30%, with a higher value for a cow with lower milk production and without concentrate in its diet (as was demonstrated in the metabolic model [284]). Using the data in Eq. (120), the biological transfer rates, λ_i , and coefficients, a_i , were obtained (Table 48).

The values in Table 48 must be used with caution because there is an inherent variability among lactating animals, as is demonstrated by data on 2 minigoats [276]. On average, the transfer rates for minigoats are similar to those for cows, but variability is up to 40% for the fastest transfer rate and 20% for the intermediate one. The values in Table 48 show the importance of various processes in milk contamination: more than 85% of the OBT in milk is produced by *de novo synthesis* (the fastest transfer in Table 48), a moderate fraction is linked with the intermediate transfer and a very small fraction can be produced by recycling body reserves (in muscle and adipose tissue). The specific activity of milk fat seems to be lower in the minigoat than in the cow [276], and the partition coefficients for cows in Table 48 are not recommended for minigoats.

Transfer factors and bio-kinetic half-times can be deduced from complex but robust models, and the differences can be compared with past assessments. An example is given in Table 49 for pig meat [285] where the old values used in the FDMH (Food Dose Module Tritium) model in RODOS [269] were compared with the results using MAGENTC (MAMmal GENeric model for transfer of Tritium and Carbon) model [285].

TABLE 47. TRANSFER COEFFICIENTS AND BIOLOGICAL TRANSFER RATES FOR TRITIUM IN COW MILK AFTER AN INTAKE OF HTO

Exp.	F[#]	$\lambda_1^{\\$}$	$\lambda_2^{\&}$	a_{2n}^*
Mullen et al. [281]	0.0128	0.217	0.005	0.007
Mullen et al. [281]	0.0167	0.207	0.0046	0.007
Mullen et al. [281]	0.0221	0.218	0.004	0.003
Mullen et al. [281]	0.02242	0.244	0.006	0.006
Potter et al. [282]	0.01	0.239	0.008	0.001
Van den Hoek and Tenhave [275]	0.016	0.206	0.024	0.009
Mean	0.0167	0.2212	0.0086	0.0055
sd ⁺	0.005	0.016	0.0077	0.0029

[#] transfer factor; ^{\$} fast transfer rate; [&] slow transfer rate; ^{*} long term contribution to milk production; ⁺ standard deviation.

TABLE 48. BIOLOGICAL TRANSFER RATES AND ASSOCIATED COEFFICIENTS MILK FOR OBT AND HTO AFTER OBT INTAKE

OBT	fast rate	medium rate	slow rate
λ_i	6.67×10^{-1}	1.25×10^{-1}	1.14×10^{-2}
a_i	1.10×10^{-1}	2.65×10^{-1}	6.24×10^{-1}
HTO	fast rate	medium rate	slow rate
λ_i	2.00×10^{-1}	1.49×10^{-2}	NA [*]
a_i	9.48×10^{-1}	5.23×10^{-2}	NA [*]

* Not available.

TABLE 49. TRANSFER FACTORS AND BIO-KINETIC HALFTIMES FOR PIG MEAT FOR OBT GIVEN BY FDMH AND MAGENTC MODELS

Parameters	FDMH	MAGENTC
TF [*] (d kg ⁻¹)	0.2	0.346
A ₁ [#]	1	0.314
A ₂ ^{\$}	0	0.686
T _{1/2 1} ^{&} (d)	10	23.6
T _{1/2 2} ⁺ (d)	NA [^]	219.7

* transfer factor; [#] short bio-kinetic half time contribution; ^{\$} long bio-kinetic half time contribution; [&] short bio-kinetic half time; ⁺ long bio-kinetic half time; [^] not available.

10.3. OBT BIOKINETIC RATES AND BASIC MODELS

In the absence of a complete experimental data set for biokinetic transfer rates and transfer factors for all farm animals, available models and partial data sets must be used. Hybrid models, in which some compartments are linked by the specific activity approach and others are linked by transfer factors, are also used. Process oriented models, used for accidental releases are more complex, but they can be run until equilibrium conditions are reached (although this is not cost effective). Dynamic models of tritium and carbon in farm animals have different levels of complexity. Some have a single organic compartment [92, 286–292] while others have five or six compartments (see below) and an additional compartment for tritium, the whole body water compartment. Some models are based on a specific experimental data set [293, 294] and therefore apply only to the conditions of that experiment; others consider a wider range of data and have more general use [288, 295, 296].

This review starts with simple models and continues with complex models. The simplest models use a single organic compartment for the whole body or animal product.

There are many pools of organic carbon or OBT in any developed organism, but, using flux conservation, a single half time for the whole body or a specific tissue (organ) can be defined. Biological half-times have been assessed in the past by a simple relationship between the body content of stable carbon and carbon intake [297]; these have also been applied to organic tritium [92]. The use of common halftimes for ^{14}C and ^3H in organic forms is supported by basic science and modelling results [284, 294]. Using simple carbon balance to deduce biological half-times is only an approximation, however. Traditionally, the whole body Carbon Loss Rate (CLR) was assessed based on intake of digestible carbon and the carbon content of the body [297]:

$$CRL = f_d * I_f * \frac{C_{C,f}}{M * C_{C,b}} \quad (121)$$

where:

- CLR is the whole body carbon loss rate;
- f_d is the digestible fraction in food intake;
- I_f is the daily food intake (kg dm d^{-1});
- $C_{C,f}$ is the carbon fraction in food ($\text{kg C kg}^{-1} \text{ dm}$);
- $C_{C,b}$ is the carbon fraction in body ($\text{kg C kg}^{-1} \text{ fm}$); and
- M is the fresh body mass (kg).

This estimate of CLR has been used in the past [297] (see the last column in Table 50), but in this report actual, specific data are examined (for a list of references see Galeriu et al. [284]) and the growth of animals is taken into account. In Table 50, the carbon loss rate due to maintenance needs (T_{Cmaint}) and to total growth dilution and maintenance (T_{C}) are also given. When updated values [298] are compared with the older ones [297], some differences are observed. The updated values [299] are higher for pigs, sheep and cows, lower for hens, and similar for rats. These results show the influence of choice of inputs in Eq. (121). For growing animals (veal calves, lambs, broilers), the updated approach [298] accounts for changes in food intake with growth according to the energy needs of the animal, but disregarding different energy efficiencies [300].

TABLE 50. UPDATED CARBON HALF TIMES

Animal	m^1 (kg)	G^2 (kg d ⁻¹)	I^3 (kg dm d ⁻¹)	MI^4 (%)	C_b^5 (kg C kg ⁻¹ fw)	f_d^6	C_f^7 (kg C kg ⁻¹ dm)	T_c^8 (d)	$T_{C_{maint}}^9$ (d)	T_c^{10} (d)
Veal	160	0.8	4.85	52	0.173	0.7	0.42	13.45	25.86	
Beef	400	0.8	8.6	55	0.230	0.7	0.42	25.26	45.93	
Cow (no milk)	550	0.1	6.7	92	0.254	0.7	0.42	49.15	53.42	36
Lamb	20	0.2	1	40	0.164	0.7	0.415	7.84	19.61	
Sheep	50	0.08	1.22	75	0.273	0.7	0.415	26.71	35.61	27
Pig	100	0.8	2.8	30	0.339	0.9	0.47	19.82	66.08	45
Pig (fast growth)	100	1.25	3.8	35	0.200	0.9	0.47	8.61	24.59	
Hen	2.5	0.007	0.12	78	0.251	0.83	0.47	9.28	11.90	18
Broiler	1.7	0.03	0.11	56	0.241	0.83	0.47	6.61	11.81	
Rat	0.45	0.0008	0.025	94	0.220	0.9	0.45	6.78	7.22	7

¹ mass; ² growth rate; ³ intake rate; ⁴ maintenance intake; ⁵ carbon fraction in body; ⁶ digestible fraction in food intake; ⁷ carbon fraction in food; ⁸ half time for total carbon; ⁹ half time of carbon due only to maintenance; ¹⁰ half time for carbon given by Jones and Jackson [297].

TABLE 51. MASSES AND LOSS RATES FOR SOME ANIMALS [301]

Animal	a	m_0 (kg)	M (kg)	loss rate (d ⁻¹)	Halftime (d)
cow	0.28	33.3	442	0.010858	63.8262
pig	0.31	0.9	320	0.013032	53.17742
hen	0.47	0.043	2.1	0.069418	9.98294

There is also a metabolic approach that defines the whole body loss rate of organic matter, starting with the Metabolic Theory in Ecology [301]. West et al. [301] developed a metabolic model for ontogenetic growth with the central assumption that the basal metabolic rate depends on the body mass at power 0.75. Much criticism is directed at this single and universal exponent, but, nonetheless, some results of West et al. [301] can be used for this present study. The mass equation proposed by West et al. [301] depends on mass at birth, m_0 , the mass at full maturity, M , and a species-dependent parameter, a . The actual mass, m , in the equation of West et al. [301] can be re-written to emphasize the rate of gain, λ_{gain} , and the loss rate, λ_{loss} :

$$\frac{dm}{dt} = \left(a * m^{-1/4} - \frac{a}{M^{1/4}} \right) * m \quad (122)$$

The loss rate can be defined now as:

$$\lambda_{loss} = 0.1778 * a * M^{-0.25} \quad (123)$$

$$\lambda_{gain} = \lambda_{loss} * \left(\frac{m}{M} \right)^{-0.25}$$

with masses in kg.

Then, it follows:

$$\frac{dm}{dt} = (\lambda_{gain} - \lambda_{loss}) * m \quad (124)$$

$$\frac{d\mu}{dt} = (\lambda_{gain} - \lambda_{loss}) * \mu$$

where μ is degree of maturation, ($\mu = m/M$).

The Relative Growth Rate (RGR) is simply:

$$RGR = \left(\frac{1}{m}\right) \frac{dm}{dt} = \lambda_{gain} - \lambda_{loss} \quad (125)$$

From Eqs. (122)–(125) it is seen that the rate of gain, λ_{gain} , depends on the degree of maturation, μ and that the loss rate, λ_{loss} , depends on the species, a , and mature mass, M .

An estimate of the loss rates of some animals is given in Table 51.

10.4. DERIVATION OF THE DYNAMIC EQUATION FOR A SINGLE ORGANIC COMPARTMENT

A dynamic model is obtained by combining a generic equation for animal growth [300] with the balance of radioactivity in the body.

The energy balance for an animal of mass M is well known:

$$RE = k_g * (MEI - MEm) \quad (126)$$

where:

RE is the retained energy in the body (MJ d^{-1});
 k_g is the growth efficiency;
 MEI is metabolisable energy intake (MJ d^{-1}); and
 MEm is the maintenance energy need (MJ d^{-1}).

The retained energy, RE , is deposited in protein or lipids and increases with an increase in empty body weight, EBW . EBW is the live body weight, LBW , minus the gastrointestinal content. Based on animal growth models or empirical data, a formal relationship is found:

$$LBW = g(M) * EBW \quad (127)$$

where $g(M)$ is a non-dimensional function with a weak mass dependence.

The empty body gain, EBG , is given by an increase of body protein, ash, lipid and water:

$$EBG = \frac{dEBW}{dt} = RE * f(EBW) \quad (128)$$

The relation between EBG and RE needs a function, f , depending on EBW . The function transforms the gain in energy into the gain in mass and has as units $\text{kg d}^{-1} / (\text{MJ d}^{-1}) = \text{kg MJ}^{-1}$.

So, it follows:

$$\frac{dM}{dt} = EBW * \frac{dg}{dt} + \frac{dEBW}{dt} \quad (129)$$

Because g is quite constant, the first term in Eq. (129), is ignored and Eq. (129) becomes:

$$\frac{dM}{dt} = g * EBG = (g * f) * RE = (g * f) * k_g * (MEI - MEm) \quad (130)$$

Considering the level of nutrition, $L = MEI/MEm$, and the parameterization, $MEm = aM^b$, the following equation is obtained:

$$\frac{1}{M} \frac{dM}{dt} = k_g * f * g * aM^{b-1} * (L - 1) = \lambda_{gain} - \lambda_{loss} \quad (131)$$

For a particular species, parameter “ b ” is constant, but parameter “ a ” depends on genotype and nutrition, which influences visceral mass and maintenance energy).

The following equations are now defined:

$$\lambda_{loss} = (k_g * f * g) * a * M^{b-1} = (k_g * f * g) * \frac{MEm}{M} \quad (132)$$

$$\lambda_{gain} = L * \lambda_{loss}$$

$$RGR = \lambda_{loss} * (L - 1) \quad (133)$$

Knowing the metabolisable energy density, MD , in animal food and the dry matter ingestion rate, I_d , it follows that $MEm = MD * I_{d,m}$ and $MEI = MD * I_d = L * MEm$

At maturity, M_{mat} , there is no growth and the intake rate $I_{d,m}$ balances the loss rate, $I_{d,m} = \lambda_{loss} * M_{mat}$.

Generally, the loss rate can be assessed by knowing the composition of the animal and its metabolic needs for maintenance. For a lactating animal (constant mass) the metabolisable energy for milk production must be used to assess the rate of gain.

To determine the balance of radioactivity (^{14}C or OBT) in the whole body, three methods are use: (1) the derivation for ^{14}C [291], (2) the approach for biota [302] and (3) the fact that the loss rate for radioactive organic matter is the same as for matter [303], while the rate of gain is:

$$\lambda_{gain} = \left(\frac{I_d}{M}\right) * D * \left(\frac{C_f}{C_o}\right) \quad (134)$$

where C_f and C_o are the radionuclide concentrations in food and animal, respectively ($Bq \text{ kg}^{-1} \text{ dm}$) and D is the feed digestibility factor.

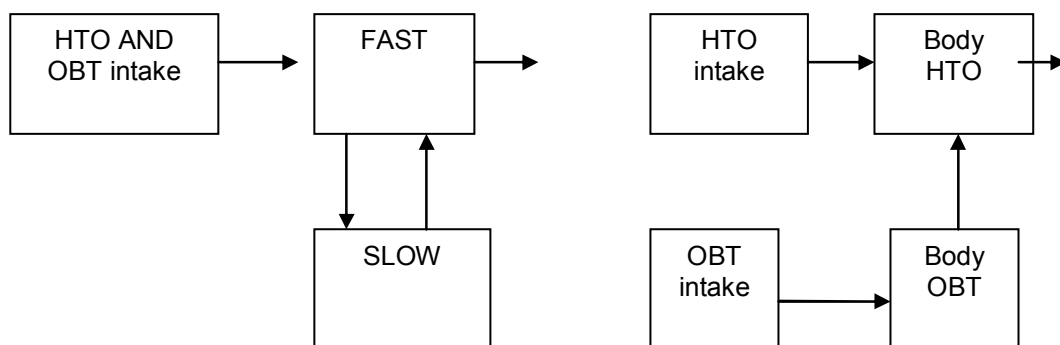


FIG. 48. Flowcharts for STAR (left) and OURSON (right) simple models.

Then, the radionuclide concentration in animal is:

$$\frac{dC_o}{dt} = (I_d * \frac{D}{M}) - (\lambda_{loss} + RGR) * C_o \quad (135)$$

The loss rate is driven by the maintenance metabolism (intake rate for maintenance only), while the rate of gain depends on the current intake (level of nutrition). The digestibility factor D is derived from the ratio between metabolisable and gross energy in animal food and is a measure of how well food is metabolized.

For tritium, a whole body water compartment is added in all models. For the simplest model, there are two compartments (organic and water) and for the complex models, the organic body compartment is split in many components.

10.5. ANALYSIS OF SIMPLE MODELS

There are two simple models: STAR-H3 [287, 288] and OURSON [304, 305], the last one being used in the pig scenario [273]. Their flowcharts are shown in Figure 48. The models differ in their intake routes and transfers between HTO and OBT and OBT and HTO, respectively. In the STAR model, the input of OBT is only in the fast (body water) compartment, while in OURSON model it is only in the slow (Body OBT) compartment. STAR considers the metabolism of OBT from body HTO, but this is ignored in OURSON.

The simplest model STAR-H3 [287, 288] was developed in 1995-1998 and has a single organic compartment (slow turnover). The model is implemented in a software platform (AMBER) which restricts intake to pasture alone. Fast and slow turnover compartments are considered in the STAR model for both ¹⁴C and ³H. In the case of tritium, the fast compartment can be identified with body water and the slow with organically bound tritium in the animal body. In the case of ¹⁴C, the fast compartment can be linked with the fast component of animal respiration. The model considers 1 kg of animal meat and the intake of water or feed is normalized to this. Because pasture is the only intake, a pasture equivalent feeding rate is assessed for non-ruminant animals. All intake enters the fast compartment, and all excretion leaves the fast compartment. STAR is intended to be simple and conservative for animal products in British radiological assessments, but the degree of conservatism is not documented. A weak point when applying STAR in the case of tritium is its inability to

distinguish between separate intakes of HTO or OBT, as well as its inability to distinguish between milk and egg. The dynamics in these products cannot be predicted because STAR only considers slow turnover, while OBT in milk and egg is mostly produced in *de novo* synthesis. Using only pasture equivalent as animal feed, STAR cannot be applied in cases of dried diets (winter hay, concentrates and grains) fed in many countries. Furthermore, for all animals, the slow turnover rate is 0.03 d^{-1} (half-time of 23 d). A complete description and list of parameters and values were reported in the pig scenario [273].

The OURSON model [273, 304, 305] considers that all OBT in the diet enters the organic compartment, and a dynamic equation is derived for the specific activity (SA) including the growth dilution. Input OBT is corrected for the difference in SA between food and whole body. The transfer rate to Body HTO is given by digestible intake per body dry weight. HTO concentration in urine is considered to be the same as Body HTO, while OBT concentration in urine urea is taken to be equal with the OBT concentration of the body. OBT in faeces corresponds to OBT in the non digestible fraction of food. It was assumed that OBT specific activity was identical in digestible and non digestible fractions and that whole body OBT was representative of muscles. Concentrations in other organs were derived from the concentration in muscle using a correction factor based on the fat and protein content of each organ, fat and protein turn-over rates, and hydrogen content of fats, proteins and carbohydrates. Both in the original model and subsequently, values for OBT halftime were unclear (a range only). The equations in OURSON for a growing animal (no lactation) are given below:

$$\frac{dC_{urine}^{HTO}(t)}{dt} = -\lambda_w C_{urine}^{HTO}(t) + \frac{1}{H_2O_{pig}} (HTO_{diet} + k_{ing} \cdot OBT_{pig}(t)) \quad (136)$$

$$\frac{dA_{meat}^{OBT}(t)}{dt} = -k_{ing} A_{meat}^{OBT}(t) + k_{ing} \cdot \frac{H_{food}}{H_{meat}} \cdot A_{food}^{OBT}(t) \quad (137)$$

where:

C_{urine}^{HTO} is the HTO concentration in urine (and animal body water H_2O) (Bq L^{-1});

$$\lambda_w = \frac{\text{waterconsumption}(L)}{\text{bodywater}(L)};$$

HTO_{diet} is the HTO activity in diet (drinking water + food) (Bq d^{-1});

k_{ing} is the OBT turn-over rate (day^{-1}), given by $k_{ing} = \frac{I \cdot D}{W}$;

$OBT_{pig}(t)$ is the total OBT in pig (Bq);

I is the food intake (kg dm day^{-1});

D is the digestibility (unitless);

W is the animal dry weight (kg);

A_{meat}^{OBT} is the OBT specific activity in meat ($\text{Bq g}^{-1} \text{H}$);

A_{food}^{OBT} is the OBT specific activity in food ($\text{Bq g}^{-1} \text{H}$);

H_{food} is the average food OBH ($\text{g kg}^{-1} \text{dm}$); and

H_{meat} is the average meat OBH ($\text{g kg}^{-1} \text{dm}$).

In the OURSON model there is no metabolic transfer from Body HTO to Body OBT. The transfer from Body HTO to Body OBT is ignored and all OBT intakes enter the OBT body compartment only. This contradicts experimental evidence, at least at equilibrium.

Consequently the intake of organic tritium must be distributed between Body OBT and Body HTO and not as in STAR or OURSON. This explains why STAR over-predicts the OBT in urine and OURSON under-predicts it. Because STAR assumes that all organic intakes enter the fast compartment, under-prediction of the OBT in animal organs is expected. The under-prediction of HTO in meat observed for OURSON is explained by the intake route of OBT, only into Body OBT, with a subsequent slow transfer to Body HTO.

The TOCCATA model [306] is also simple [290] and maintenance loss is defined, but the quantitative relationships are not given and the OBT half-time is described improperly and unpractically.

For tritium in cow (milk and meat) a commonly used model is included in UFOTRI [92], a standard code for fusion reactor design and licensing. This model is discussed in more detail, because it has particular accomplishments. Despite its simplicity, it can be generalized to apply to other animals. A single animal organic compartment is used in UFOTRI, but milk HTO and milk OBT compartments are treated explicitly. All HTO intake enters the animal body water (HTO) compartment, but OBT intake is distributed between body HTO, body OBT and milk OBT. This last transfer is not a physical transfer, but it helps to model the *de novo* synthesis. The cow in UFOTRI has a mass of 500 kg and produces 15 L d⁻¹ of milk. The model transfer rates are obtained using the mass balance of free and bound hydrogen and a few assumptions (e.g. OBT loss rate). The model was tested with published [275, 307] and unpublished experimental data [308] as below:

- (1) A cow of 461 kg giving 12 L d⁻¹ of milk was fed for 30 days with HTO. Milk was monitored for total T and OBT. At the end of the feeding the cow was sacrificed and the organs were measured for OBT. At day 30, the time integrated ratios (the ratios between predicted and observed [P/O] results) for total tritium, T, were 0.85, for milk OBT 0.64., and for muscle OBT 0.78.
- (2) A cow of 550 kg giving 22 L d⁻¹ of milk was fed for 25 days with HTO. Total T and OBT in milk were measured for 70 days. UFOTRI's P/O ratio for total T was 0.6 and for OBT was 0.68.
- (3) Single HTO intake: Total T in milk integral at day 70 was very close to the observed data; for OBT in milk, the P/O was 0.8.
- (4) A cow of 566 kg giving 9.2 L d⁻¹ of milk received OBT in hay for 28 days, followed by milk monitoring. At day 28, UFOTRI under-predicted OBT in milk by a factor of 2 (P/O=0.5); predictions of total T were 70% those of the observed data (P/O=0.7). The integral between day 28 and day 100 was also under-predicted by the same factor (a factor of 2 for OBT).

Predictions of OBT in meat and milk of the UFOTRI model seem to be slightly underestimated by a factor of less than 2, which is remarkable for a simple model. The approach taken in UFOTRI can be expanded for sheep and goat.

10.6. COMPLEX MODELS

Complex models with many organic compartments have also been published; for sheep [294] ¹⁴C and ³H cases are treated using similar transfer rates, but the parameters are derived from sheep experiments [294] and cannot be generalized to other animals. The occurrence of fast and slow turnovers of OBT can be included using two organic compartments as in MCT [273] and PRISM [289, 295]. The flowcharts of MCT and PRISM models are given in Figure 49.

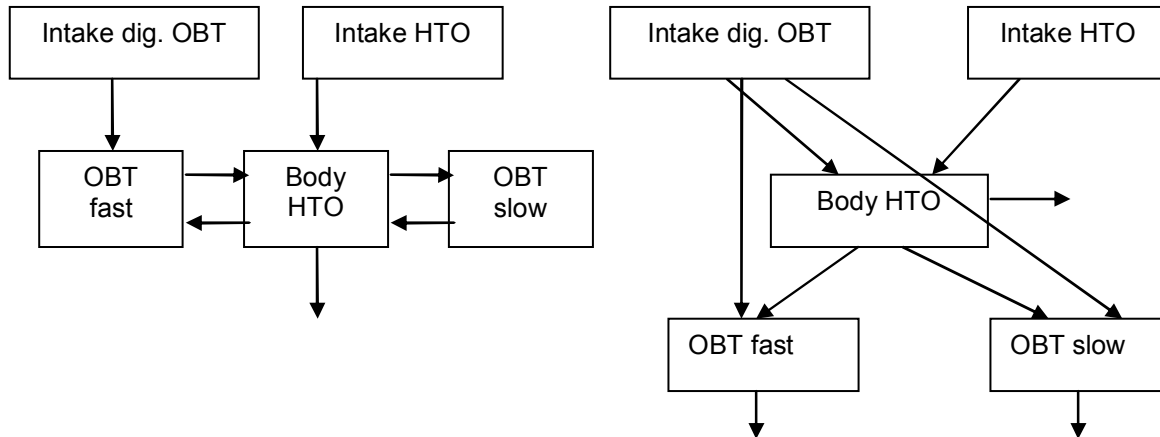


FIG. 49. Flowcharts of MCT (left) and PRISM (right) models.

In these models, two OBT compartments and one FWT compartment are assumed. Both models have a fast and slow OBT compartment, but MCT transfers the catabolic OBT to the body water, while PRISM transfers it out of the body, which simplifies the model. The MCT model was initially developed specifically for Japanese humans [309]. Because the hydrogen metabolism in the pig is expected to be similar to that of humans, the MCT model was used with minimal changes for pigs in the Pig scenario [273]. PRISM, in its initial version [295] did not model urine and faeces, but the model was expanded [310]. PRISM uses a simplified gastro-intestinal (GI) tract, and OBT intake is partitioned between body water and two organic compartments. A fraction of 0.79 (range 0.61-0.94) is converted to HTO and distributed to body water. The rest enters both organic compartments with two times more entering the fast organic compartment (fast OBT). The fast organic compartment contains two times more hydrogen than does the slow one (similar to MCT for humans) on average, but the range is very large (between 1/9 and 9). As in STAR, milk *de novo* synthesis cannot be modelled. Transfer routes are very different, as are many transfer rates, but both models give predictions relatively close to the observations for the pig scenario [273]. MCT does not account for the fraction of input organic tritium that is directly absorbed into the body OBT, which explains an under-prediction in urine. MCT was only used to model the pig, and PRISM parameters are given as ranges, with little information on selected animals. PRISM was not tested with experimental data (except for tsheep). PRISM is commercially available.

MAGENTC (Mammals GENERIC model for the transfer of Tritium and Carbon) was developed as a research model and is more complex. The model is well documented in the literature and default parameters are given [298, 311, 312]. The model considers six organic compartments and a single body water compartment. Its flowchart is given in Figure 50.

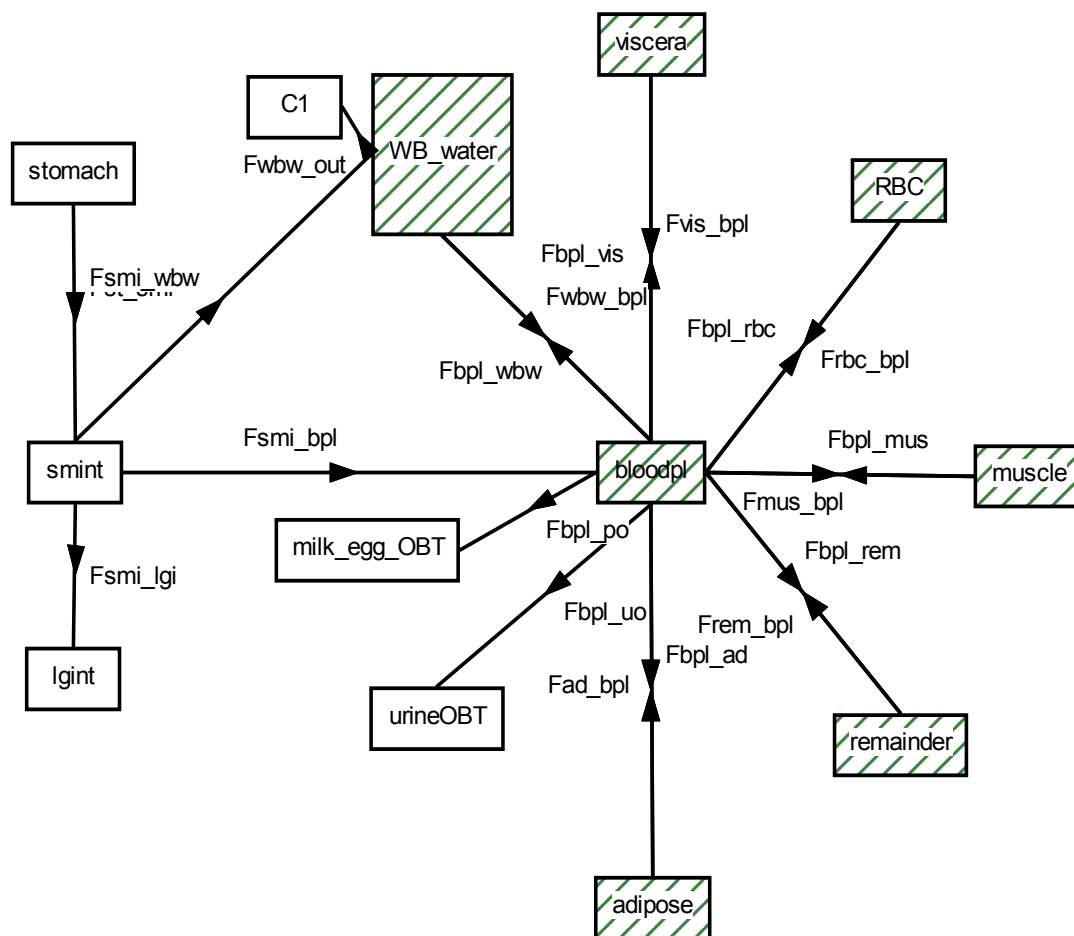


FIG. 50. Flowchart of MAGENTC model.

For adult mammals, the model for T&C transfer in body compartment is based on the following assumptions:

- The most important body organic compartments are viscera (including the heart), muscle, adipose tissue, blood (plasma and red blood cells [RBC]) and remainder (including the brain). Their masses and compositions are known.
- Tritium in body water equilibrates fast with water and a single body water compartment is enough, when only tritium is being modeled.
- Loss rate from the organic compartments is similar for intakes of HTO, OBT or OBC and can be assessed directly from energy turnover rate (net maintenance).
- Net maintenance is considered the sum of the basal metabolic needs and activities; thermal stress is not considered. The basal metabolic rate is the sum over organs of the product of the organ-specific basal metabolic rate and organ mass.
- The specific metabolic rate (SMR) for organs in adult mammals varies slightly, except for muscle and compared with the basal state. Basal SMR shows a dependence on mass at maturity. SMRs are obtained experimentally for a few mammals, and a zero order approximation is generally used depending on mass at maturity.

- There is a metabolic conversion of HTO to OBT, and the equilibrium value for the ratio of OBT derived from HTO or OBT intake does not vary among mammals.
- The energy (heat) and the additional matter lost in the transformation of the metabolisable input into the net requirements are assumed to be a single, fast process.

The net daily energy expenditure of animals is referred to as the net ‘field’ (for active animals) metabolic rate (FMR; MJ d⁻¹), whilst the daily energy expenditure per unit fresh body mass is termed the specific metabolic rate (SMR; MJ kg⁻¹ d⁻¹). The energy turnover rate or relative metabolic rate (ReMR; d⁻¹), can be defined as the ratio of SMR and the energy content of the body (determined by the body composition (protein, lipids, and carbohydrates)):

$$\text{ReMR} = \frac{\text{FMR}}{\text{EBW} * \text{BED}} = \frac{\text{SMR}}{\text{BED}} \quad (138)$$

where EBW is the empty body weight (kg) defined as the live-weight less the mass of the gastro-intestinal contents and BED is the body energy density (MJ kg⁻¹ fresh weight (fw)). The BED is estimated from the body tissue composition of lipids and protein and the combustion energy of lipids and protein

Under these hypotheses the model gives reliable predictions without calibration.

Prior to the development of the model, a re-examination of animal growth and nutrition was done [313], as well as a re-examination of the experimental data base [314]. The model was also applied to wild animals and birds [296, 298, , 315].

For growing farm animals, the model has an additional growth model, which gives both the growth rates of the organic compartments in the model and changes in body composition with age and management practices [298]. The growth model depends on the animal and can be adapted to each country based on research results. For ruminants, a generic model was used [316], for pigs a French model was implemented [317], while for the hen and broiler, different reports from the literature [318, 319] were used.

Results are given in the Figure 51 for a constant OBT concentration in the diet (1 Bq kg⁻¹ dm) administered to 3 pig genotypes. It is seen that genotype has little effect on concentrations after continuous intake and that whole body concentrations (that include adipose fat) will be a certain factor higher than concentrations in muscle.

10.7. QUALITY ASSURANCE OF MODELS

For any operational application, an environmental model must be subject to the quality assurance process [167] that includes sensitivity and uncertainty analysis and tests (validation) with experimental data. The same analyses and tests are recommended for research models to assess the robustness of predictions. In the present section, the only dynamic models subjected to intensive tests are the MAGENTC model based on energy metabolism and the UFOTRI tritium cow-milk model. Some examples of these tests are given below.

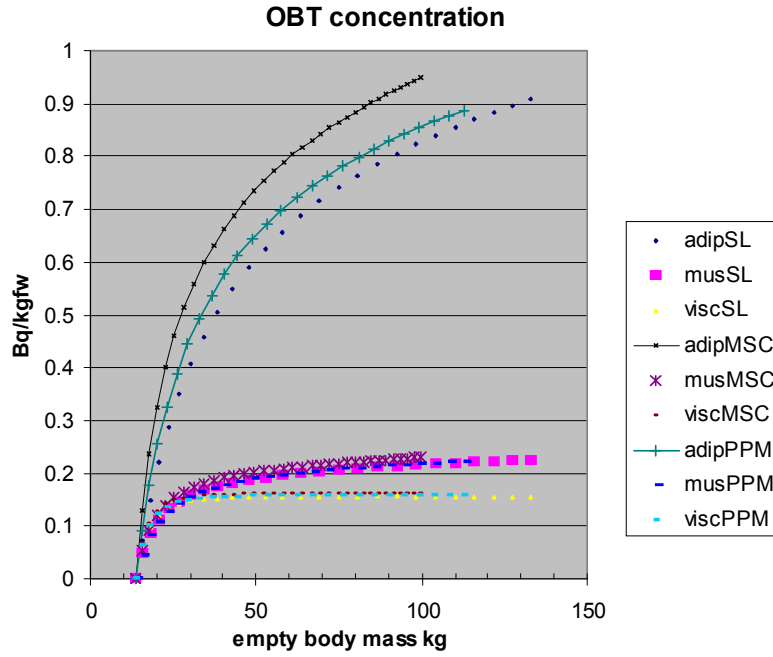


FIG. 51. OBT concentration in pig organs ($Bq\ kg^{-1}\ fw$) for 3 pig genotypes (SL#, MSC\$, PPM*) for viscera, muscle and adipose tissue. (# – conventional genotype; \$ – fat genotype; * – lean genotype)

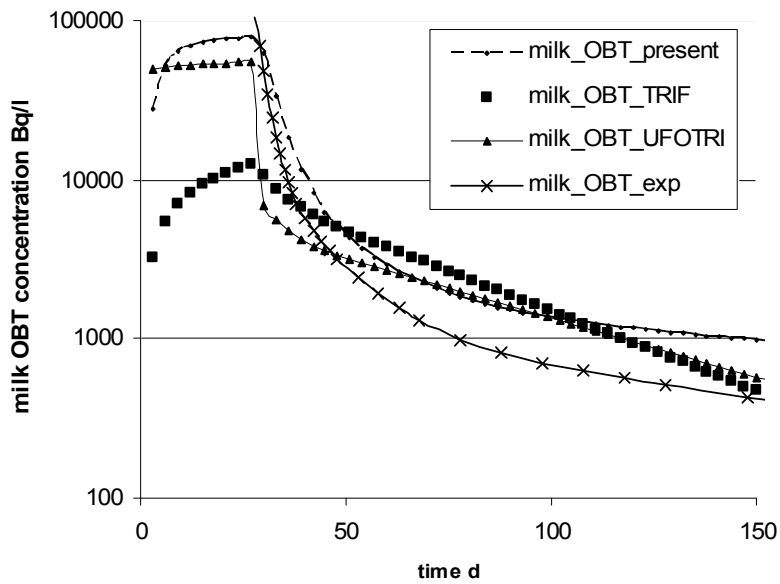


FIG. 52. Test of TRIF, UFOTRI and MAGENTC models with experimental data for OBT in cow's milk.

TABLE 52. PERFORMANCE OF MAGENTC FOR TRITIUM CONCENTRATIONS IN COW'S MILK AND URINE

Experiment	R ²	Milk total ³ H		Milk OBT	Urine HTO
		P/O	Mean ± standard deviation (range presented in parenthesis)		
Cow_P	0.97		2.60 ± 1.7 (0.8–1.9)	1.68 ± 0.8 (0.5–2)	2.90 ± 2.34
Cow_C	0.89		0.97 ± 0.08 (0.9–1.4)	0.73 ± 0.17 (0.65–1.7)	0.97 ± 0.06
Cow_H3	0.67		1.02 ± 0.15 (0.9–1.5)	0.49 ± 0.12 (0.4–0.9)	1.36 ± 0.42
Cow_H	0.88		1.45 ± 0.59 (0.6–2.3)	1.86 ± 0.38 (0.55–2.12)	NA

NA: not calculated/available.

TABLE 53. PREDICTED TO OBSERVED RATIOS (P/O) FOR ORGANS (DAY 84 AFTER THE START OF EXPOSURE)

Organs	MCT	FSA	P/O (OBT)			
			IFIN_HH (2005)	PRISM (DG)	STAR	EDF
Heart	2.05	9.89	1.40	1.51	1.29	1.29
Lungs	2.79	4.11	1.90	2.06	0.13	1.30
Liver	1.92	1.04	1.11	1.20	0.08	0.84
Jejunum	3.00	3.23	1.73	1.88	0.12	1.09
Ileum	2.24	13.00	1.53	1.65	0.10	0.96
Colon	3.28	2.23	2.24	2.42	0.15	1.40
Kidney	2.17	8.46	1.48	1.60	0.10	1.17
Muscle	4.44	0.23	1.90	3.65	0.23	3.11
Brain	3.91	4.69	na	3.17	0.20	1.65
Blood	3.04	969.56	1.27	1.92	0.12	1.22

The MAGENTC model includes a parameter for the non-exchangeable fraction of organic intake which remains after digestion. Prior to digestion, this value is known from the composition of the diet, but digestion can change this value by half (for ruminants). The predicted concentration in meat can be sensitive to this parameter, the model considers the homeostatic control of tritium and the sensitivity of OBT concentration in meat is proven to be low. A change of a factor of 2 in the non-exchangeable fraction results in a change of 10% in the concentration of meat.

An inter-comparison with experimental data for OBT in milk after being fed OBT included the TRIF [286], UFOTRI [92] and MAGENTC [312] models (Figure 52). It is clear that the TRIF model underestimates results by more than a factor of 5 in the uptake phase and overestimates later. The predictions of the UFOTRI and MAGENTC models are reasonably close to the values of the experimental data.

The MAGENTC model was intensively tested with all available experimental data for cow's milk. The predicted to observed ratios are given in Table 52 as averages and standard deviations. There is an under-prediction of OBT in milk after an intake of HTO and an over-prediction after an intake of OBT. This is due to features of ruminant digestion not considered in the model. Most of the intake is in form of carbohydrates which are transformed in the rumen by digestion of exchangeable forms; the equilibration with hydrogen (tritium) in water

is almost complete. The precursors of milk glucogenesis in ruminants have more tritium after an intake of HTO and less tritium after an intake of OBT than do the precursors in monogastric animals. This shortcoming of the model is of no of major practical concern because the misprediction is less than a factor of 2, which is of the same order as the variability of cow productivity and diet in assessments.

In the past, the pig scenario in EMRAS I [273, 311] was the only test of models internationally. A blind test asked for predicted OBT in organs after 84 days of feeding a pregnant sow (Table 53). Predictions for HTO and OBT concentrations in various organs were supplied by the Food Standard Agency (FSA), UK (PRISM model), Japan (MCT model), Electricite de France (EDF), France (OURSON model) and National Institute for Physics and Nuclear Engineering (IFIN-HH), Romania (MAGENTC model, but also STAR and PRISM). The predicted to observed ratios for HTO show that, except for the FSA model, predictions of all models were good, although the EDF model underestimated by a factor of 5. The STAR model, as expected, underestimated by a factor of 10 due to assumptions about the intake of OBT in the fast compartment (body water). The EDF model, with all OBT intakes in the organic compartment, was similar to the observations, although the OBT in muscle was overestimated. These results must be analysed and understood. The MCT model overestimated by a factor of between 2 and 4, while the IFIN-HH model (in the initial version) overestimated by a factor of 2. The reconstructed PRISM model overestimated by only 50%. The large range of overestimation in the FSA model results demonstrates the user's influence.

10.8. FINAL DISCUSSION

An operational radiological model must satisfy some of the following requirements:

- Use available input information (model parameters, etc);
- NOT be calibrated to specific experiments;
- Give predictions with an uncertainty better than a factor of 5 and, preferably, within a factor of 2;
- Be applicable to both dose assessment in human food chains and radioprotection of biota;
- Over-predict, rather than under-predict;
- Be as simple as possible (but no simpler);
- Be internationally agreed upon.

For routine emissions, transfer coefficients are mostly used, but concentration ratios seem to provide a robust basis for model predictions. The ^{14}C and tritium parts of the IAEA report [274] are robust and internationally accepted. Many experimental results are still not published in the open literature, and it is important that all relevant information be disclosed. The countries represented by EMRAS participants have different practices, regulatory requirements, and transparency. Thus, agreement on a common way to model an accidental case may be hard to reach.

Progress has been made on recommendations of biokinetic transfer rates. Not enough experimental data are available, and new experiments are improbable due to financial and ethical constraints. For mature mammals the situation is fairly good and recent advances in animal sciences can be of great help. However, for growing animals there are still

uncertainties in handling maintenance and growth. This can partially explain, the divergence in model assumptions and predictions described in the present study.

To further progress, more experiments and expert judgment are needed. In addition, complete communication between modellers is essential to guarantee an understanding of how the models work. To be accepted by the international community, the models must be subjected to benchmarks and validation tests. Although MAGENTC is relatively complex, it needs only available input data and shows reasonable agreement with available experimental data.

Because regulatory bodies prefer quite simple equations with a minimum number of parameters, it is proposed to use Eq. (135) for a simple dynamic approach to predicting concentrations in non-lactating farm animals. Lacking a complete experimental data base, both experimental data and modeling approaches must be combined. Furthermore, the results must be sufficiently conservative to satisfy the regulatory agencies of various countries. When a special radionuclide is released accidentally, a screening model must be run first to establish the mandatory countermeasures or, at least, the necessary special monitoring programs. Screening model predictions include the first year ingestion dose and feed contamination levels for the first few days post-accident. Later the first measurements of feed contamination can be input to the model to improve the radiological assessment. To agree on a simple operational model, there must be much collaboration between EMRAS members and each country's regulatory body. The aim of this study was to encourage a relaxed communication between members and not to promote a certain view.

A simple but robust model for tritium transfer must:

- Use an appropriate definition of rates of loss and gain;
- Make a distinction between gain in mass and gain in radioactivity;
- Account for the partitioning of the organic tritium intake between body water and body organic bound tritium;
- Include the formation of OBT from body HTO;
- Include the approach taken in UFOTRI for lactating animals;
- Test the model with experimental data and compare with the complex MAGENTC model.

This activity can be included in the next programme coordinated by IAEA.

11. DESCRIPTION OF A COMPLEX MODEL

11.1. OVERVIEW

The complex model SOLVEG-II has been developed by the Japan Atomic Energy Agency. The model considers transport and exchange processes for heat, water and CO₂ in a multi-layered atmosphere-vegetation-soil system [86, 320]. With the outputs from these meteorological components, HTO transfers and organically bound tritium (OBT) formation are computed [86, 240]. The processes considered are schematically drawn in Figure 53. The performance of SOLVEG-II in calculating the uptake of tritium by vegetation has been validated through a simulation of a short term exposure of grape plants to HTO vapor [240].

In this section, only the model components calculating HTO transfers and OBT formation are described, although these processes are closely related to the components for heat, water and CO₂.

11.2. ATMOSPHERIC MODEL

Air HTO concentration χ_a (Bq m⁻³) in the surface atmosphere is calculated by a diffusion equation [240], as:

$$\frac{\partial \chi_a}{\partial t} = \frac{\partial}{\partial z} K \frac{\partial \chi_a}{\partial z} + \varphi \quad (139)$$

where t (s) is the time, z (m) is the vertical coordinate, and K (m² s⁻¹) is the turbulent diffusivity controlling the heat and water transport process. The source term φ (Bq m⁻³ s⁻¹) expresses HTO exchange between canopy air and leaf cellular water through the stomata. Furthermore, if wet deposition of HTO exists, φ also covers HTO exchange between canopy air and rain drops, and between canopy air and leaf surface water formed by the interception of rain by the leaves.

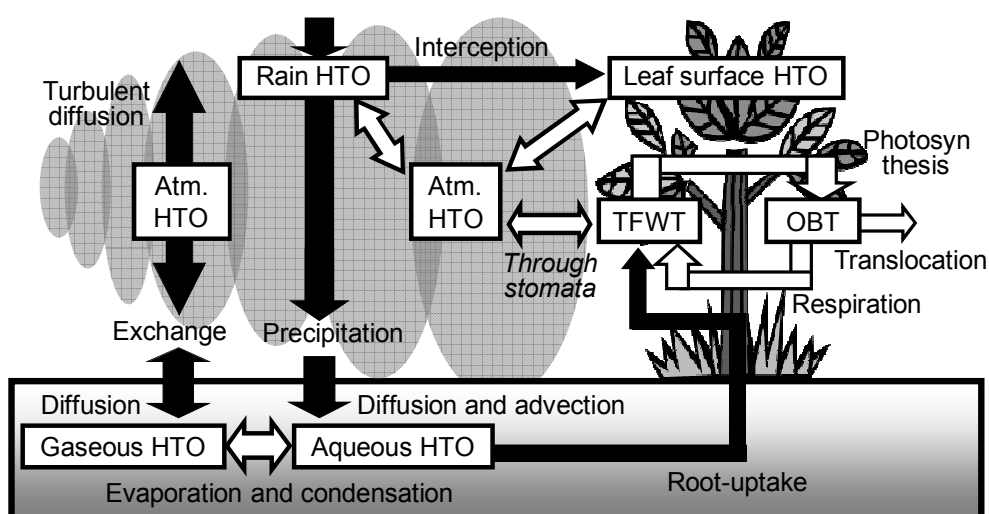


FIG. 53. Land surface tritium transfer (black arrows) and exchanges (white arrows) considered in SOLVEG-II.

11.3. SOIL MODEL

The soil sub-model of SOLVEG-II treats the advection and diffusion of aqueous and gaseous HTO transport separately [86]:

$$\frac{\partial \eta_s \chi_{sw}}{\partial t} = -\frac{\partial E_w \chi_{sw}}{\partial z} + \frac{\partial}{\partial z} D_w \frac{\partial \chi_{sw}}{\partial z} - e_b - e_r \quad \text{for aqueous HTO} \quad (140)$$

$$\frac{\partial \{(\eta_{sat} - \eta_s) \chi_{sa}\}}{\partial t} = \frac{\partial}{\partial z} D_a \frac{\partial \chi_{sa}}{\partial z} + e_b \quad \text{for HTO vapour} \quad (141)$$

where χ_{sw} and χ_{sa} are the aqueous and gaseous HTO concentrations (Bq m^{-3}), η_s and η_{sat} are the soil water content and the porosity, E_w ($\text{m}^3 \text{m}^{-2} \text{s}^{-1}$) is the liquid water flux, and D_w and D_a ($\text{m}^2 \text{s}^{-1}$) are the effective diffusivities for gaseous and aqueous HTO. The variables related to soil water transport (η_s , E_w , D_w and D_a) are calculated by the soil-water sub-model [86]. Assuming that root uptake of soil water is fully driven by transpiration, the root-uptake term e_r ($\text{Bq m}^{-3} \text{s}^{-1}$) is calculated from χ_{sw} and the aboveground transpiration flux [240]. Eqs. (140) and (141) are linked by the HTO evaporation e_b ($\text{Bq m}^{-3} \text{s}^{-1}$) in the soil (or condensation if negative) formulated by a resistance approach [86], as:

$$e_b = \frac{1}{r_b} \left\{ \chi_{sw} q_{sat}(T_s) \frac{\rho}{\rho_w} - \chi_{sa} \right\} \quad (142)$$

where $q_{sat}(T_s)$ is the specific humidity at saturation (kg kg^{-1}) at soil temperature T_s , ρ (kg m^{-3}) is the air density and ρ_w (kg m^{-3}) is the liquid water density. The evaporation resistance r_b (s^{-1}) is calculated from the soil water content using an empirically-determined formula parameterized by soil texture [86, 321].

The soil model is connected to the atmospheric model through the HTO vapour exchange and through the gain of aqueous HTO by rain at the ground surface.

11.4. VEGETATION MODEL

The vegetation model [240] computes the tissue free water tritium (TFWT) budget per unit leaf area by considering HTO exchanges and OBT formation, as:

$$\frac{\partial \eta_v \chi_v}{\partial t} = E_{stom} + E_{root} - E_{phot} + E_{res} \quad (143)$$

where η_v ($\text{m}^3 \text{m}^{-2}$) is the volume of the leaf cellular water per unit leaf area and χ_v (Bq m^{-3}) is the TFWT concentration in the leaf cellular water. The terms E_{stom} , E_{root} , E_{phot} and E_{res} ($\text{Bq m}^{-2} \text{s}^{-1}$) respectively express the HTO fluxes through HTO exchange between canopy air and leaf cellular water, through HTO loading by root uptake, through TFWT assimilation by photosynthesis and through TFWT production by respiration.

HTO exchange between canopy air and leaf cellular water is expressed by a resistance approach, as:

$$E_{stom} = \frac{1}{r_a + r_s} \left\{ \chi_a - \frac{\rho}{\rho_w} q_{sat}(T_c) \chi_v \right\} \quad (144)$$

where r_a ($\text{m}^{-1} \text{s}$) is the leaf boundary-layer resistance, r_s ($\text{m}^{-1} \text{s}$) is the stomata resistance, and $q_{sat}(T_c)$ is the specific humidity (kg kg^{-1}) at saturation at the leaf temperature T_c . The leaf boundary layer resistance r_a is assumed to depend on the aerodynamic characteristics of the leaves and the wind velocity in the canopy. The stomata resistance r_s is calculated using a relationship between r_s and net CO_2 assimilation [322], the latter calculated by Farquhar's photosynthetic CO_2 assimilation model [320].

The flux E_{root} for the root uptake is calculated from the root uptake term e_r in Eq. (139) by relating the below-ground root distribution to the above-ground leaf transpiration.

Given that 1 mole of CO_2 reacts with 1 mole of H_2O through photosynthesis, the photosynthetic TFWT assimilation E_{phot} is calculated by:

$$E_{phot} = \chi_v \frac{m}{\rho} fP \quad (145)$$

where $m = 0.018 \text{ kg mol}^{-1}$ is the molar weight of water, $f = 0.78$ is the isotopic discrimination factor between HTO and H_2O in photosynthesis reactions [323], and P ($\text{mol-CO}_2 \text{ m}^{-2} \text{ s}^{-1}$) is the net CO_2 assimilation flux per unit leaf area calculated by the vegetation sub-model of SOLVEG-II [320].

In respiration reactions, the decomposition of $1/6$ -mole of glucose ($\text{C}_6\text{H}_{12}\text{O}_6$) yields 1 mol of H_2O . Hence TFWT production E_{res} through respiration is modeled as:

$$E_{res} = S_{int} \frac{1}{6} MR \quad (146)$$

where S_{int} (Bq kg^{-1}) is the OBT contained in a unit mass of dry matter in an intermediate carbohydrate pool, $M = 0.18 \text{ kg mol}^{-1}$ is the molar weight of glucose and R ($\text{mol CO}_2 \text{ m}^{-2} \text{ s}^{-1}$) is the respiration rate per unit leaf area calculated by the vegetation sub-model [320].

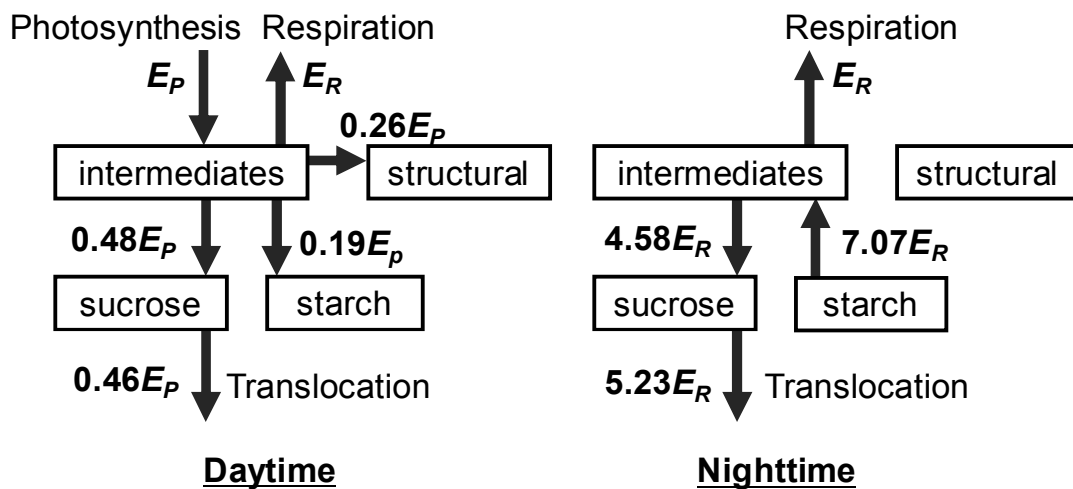


FIG. 54. Carbohydrate compartment model in SOLVEG-II (taken from [240]).

In order to calculate translocation of the assimilated tritium, leaf OBT dynamics are predicted by a carbohydrate compartment model, shown in Figure 54, which is based on observations of carbohydrate fluxes in a source leaf [324, 325]. The model has four pools. Carbohydrate fluxes ($\text{kg m}^{-2} \text{s}^{-1}$) into and out of the intermediate pool, where photosynthates first enter, are calculated from the photosynthesis rate P and the respiration rate R as:

$$E_P = \frac{1}{6}MP \quad \text{for input} \quad (147)$$

$$E_R = \frac{1}{6}MR \quad \text{for output} \quad (148)$$

Here the factor $1/6$ is the stochastic ratio of CO_2 to $\text{C}_6\text{H}_{12}\text{O}_6$ molecules in photosynthesis and respiration reactions. Daytime carbohydrate flows between the pools are determined by E_P and nighttime flows by E_R as shown in Figure 54. The amount of carbohydrate w_i (kg m^{-2}) in each pool is calculated by integrating the net carbohydrate flux in the pool. With the carbohydrate flows shown in Figure 54 and the OBT inputs (E_{phot}) and outputs (E_{res}) (Eqs. (145) and (146)) at the intermediate pool, the OBT content S_i (Bq kg^{-1}) in each pool is calculated. Then the total OBT amount Q (Bq kg^{-1}) contained in the unit mass of dry matter in the leaf is determined by summing S_i (Bq kg^{-1}) and w_i (kg m^{-2}) in the four pools, as:

$$Q = \frac{\sum S_i w_i}{\sum w_i} = \frac{S_{int} w_{int} + S_{suc} w_{suc} + S_{sta} w_{sta} + S_{str} w_{str}}{w_{int} + w_{suc} + w_{sta} + w_{str}} \quad (149)$$

where S_{int} , S_{sta} , S_{suc} , S_{str} is the OBT weight in intermediate, starch, sucrose, and structural pool, respectively (Bq kg^{-1}); and w_{int} , w_{sta} , w_{suc} , w_{str} is the carbohydrate weight in intermediate, starch, sucrose, and structural pool, respectively (kg m^{-2}).

11.5. CONCLUSIONS

A brief description is presented on a sophisticated model SOLVEG-II, which covers physical HTO transport in the surface atmosphere and in the soil, and physiological HTO uptake and OBT formation in vegetative leaves. Although such a complex model is not intended as an operational or regulatory tool, it can be an effective research tool for understanding overall tritium behaviour in a real environment. It can also be used to clarify the role of each process and parameter to define a strategy of model simplification without significant loss of predictive power.

12. TRITIUM IN THE AQUATIC FOOD CHAIN

12.1. OVERVIEW

Tritium (^3H) is released from some nuclear facilities in relatively large quantities. It is a ubiquitous isotope because it behaves essentially identically to its stable analogue (hydrogen) and rapidly enters organisms. Tritium is a key radionuclide in the aquatic environment, in some cases contributing significantly to the doses received by aquatic, non-human biota and by humans.

Models commonly used in dose assessments of exposure to tritium in aquatic systems are steady-state specific-activity models based on the assumption of complete isotopic mixing with the stable element and isotopic equilibrium between all environmental compartments [274]. These models may not be able to predict doses from fluctuating tritium levels in water bodies that result from discontinuous radioactive discharges or accidental releases. To take into account variations in radioactive discharges, dynamic river, lake and coastal water models have been developed ([326], SisBAHIA⁶, TELEMAC⁷, Mascaret⁸ [327], RIVTOX [328], POSEIDON [329]) that associated with time-dependent food chain models [304, 330, 331]. A description of tritium dynamics in coastal waters for tropical environments is given in Appendix II.

Tritium movement in water bodies is governed by two important processes: (i) the advection of the pollutant by flow that defines the position of the pollution peak in time and space (advection is defined by flow velocities), and (ii) the eddy diffusion of the pollutant due to turbulence, that influences the magnitude of the pollution peak and its spatial spreading [326].

Tritium interaction with bottom sediments and suspended matter is generally ignored in the models, but some instances of tritiated water [332] or organically bound complexes of tritium [333] have been studied. A minor pathway in terms of dose impact to the population is the tritium transfer between surface water and atmosphere [334]. For liquid releases, an important pathway is irrigation [305]; however, because irrigation can be treated like precipitation in the terrestrial food chain, it is not included in this report. A review of organic tritium in fresh water sediment, animals and plants has been conducted in France [335]. It shows that organic tritium from soils (formed over several decades from exposure of vegetation and soil to atmospheric tritium) is the main OBT contributor to sediments and suspended matter. Recently, dissolved organic tritium (DOT) from radiopharmaceutical production has been treated as a separate pathway of concern [331].

The importance of tritium transfer in aquatic ecosystems was emphasized in recent studies in Canada and France [169, 170]. Thus, based on the results of a questionnaire addressed to participants in advance of WG7 decided to address transfer in the aquatic tritium food chain.

Some models of tritium transfer in aquatic organisms have been developed over the years. The first model of tritium transfer in aquatic organisms was developed for crayfish [336] but did not include OBT intake from foodstuff. A later effort planned to update the BURN (Biological Uptake model of RadioNuclides) model [337] with a robust tritium sub-model developed within the framework of a contract with KEMA NRG (The Netherlands) [338].

⁶ See <http://www.sisbahia.coppe.ufrj.br/>.

⁷ See <http://www.opentelemac.org/>.

⁸ See <http://innovation.edf.com/recherche-et-communauté-scientifique/logiciels/code-mascaret-41197.html>.

Further developments of an aquatic food chain model have been reported taking seasonality into account and adding a metabolic model for the OBT biological loss rate in fish, as well as a first attempt to consider the Cardiff case of DOT [333]. Tritium modelling has been considered in the OURSON (French acronym for “Tool for Environmental and Health Risk Assessment”) model applied to the Loire River [305]. For the EMRAS programme, an updated version of OURSON was developed, but it has not yet been published in the open literature. This updated version considers a carbon-14 metabolic model [291, 292] and adapts it for tritium based on the ratio between carbon and hydrogen. The updated version was tested in the EMRAS programme for the mussel contamination and depuration scenarios and exhibited good performance compared with experimental data [339, 340]. Recently, an updated model (AQUATRIT) of dynamic tritium transfer in the aquatic food chain has been released. It incorporates more information about the aquatic food chain than previous models. It includes benthic flora and fauna, can apply explicitly to the Danube ecosystem, and addresses the special case of dissolved organic tritium (DOT) [331].

In this report, the calculations of the models are reviewed for each step in the food chain from bottom to top, and screening and more complex models, if available, are examined with emphasis on how well model predictions compare with experimental data. Tritiated water in an aquatic organism equilibrates quickly (minutes to hours) with the surrounding water; generally, an instant equilibrium is assumed:

$$C_{HTO} = C_w * (1 - Dryf) * 0.001 \quad (150)$$

where:

C_{HTO} is the HTO concentration in an aquatic organism (Bq kg⁻¹ fresh mass (fm));
 C_w is the HTO concentration in water (Bq m⁻³);
0.001 is the conversion m³L⁻¹; and
Dryf is the dry mass (dm) fraction of an aquatic organism.

To describe OBT dynamics, the primary producers (i.e. the autotrophs, such as phytoplankton and algae) and the consumers (i.e. the heterotrophs) are treated separately, because the producers convert light and nutrients into organic matter, while the consumers metabolize organic matter from food and a fraction of organic matter from water.

12.2. DYNAMICS OF ORGANIC TRITIUM TRANSFER IN PRODUCERS

12.2.1. OBT dynamics in phytoplankton

In the OURSON model [305, 341], the basic equation for specific activity of OBT in phytoplankton is:

$$\frac{dA_{phyto}^{OBT}(t)}{dt} = k_{photo} [DF \cdot A_{water}^{HTO}(t) - A_{phyto}^{OBT}(t)] \quad (151)$$

where:

A_{phyto}^{OBT} is the specific activity of OBT in phytoplankton (Bq g⁻¹ H dm);
 k_{photo} is the relative gross photosynthetic rate (day⁻¹);
 DF is the isotopic discrimination factor; and
 A_{water}^{HTO} is the HTO activity in river or sea water (Bq g⁻¹ H) ($A_{water}^{HTO} = 9 * 10^{-6} HTO_{water}$ (Bq m⁻³)).

Photosynthetic rates k_{photo} vary according to temperature, nutrient availability, solar radiation, etc. Either average parameter values can be chosen for each season or more complex models of phytoplankton growth can be used. A default average daily value of 0.5 day^{-1} (averaged over daytime and nighttime periods in spring and summer) and a maximum value of 0.1 h^{-1} (i.e. the maximum hourly photosynthetic rate) can be used for both marine and freshwater phytoplankton. For phytobenthos, an average value of 0.015 day^{-1} [342] and a maximum value of 0.005 h^{-1} are recommended based on measurements of O_2 production by different species of marine benthic algae [343]. The value of the discrimination factor, DF, observed in various experiments and reported by Kirchmann et al [344], is 0.6 with no difference between freshwater and marine environments.

In the AQUATRIT model [331], the authors derived the following expression from experimental data [330, 338]:

$$\frac{dC_{o,phpl}}{dt} = 0.4 \cdot \mu \cdot Dryf \cdot 0.001 \cdot C_w - \mu \cdot C_{o,phpl} \quad (152)$$

where:

$C_{o,phpl}$ is the OBT concentration in phytoplankton ($\text{Bq kg}^{-1} \text{ fm}$); and
 μ is the phytoplankton growth rate (day^{-1}).

The phytoplankton growth rate depends on the nutrients in water, on light, and on water temperature. Details are given elsewhere [331].

12.2.2. OBT dynamics in macrophytes

In the OURSON model, the same equation as for phytoplankton (Eq. 151) is used for macrophytes:

$$\frac{dA_{plant}^{OBT}(t)}{dt} = k_{photo} \cdot [DF \cdot A_{tissue-water}^{HTO}(t) - A_{plant}^{OBT}(t)] \quad (153)$$

If part of the plant body is at or above the water surface, HTO in the plant will equilibrate between the water and the atmosphere. For these semi-aquatic macrophytes, the specific activity of HTO in the plant tissue water can be considered to be equal to the average between the HTO in water and the HTO in air moisture. In the case of completely submerged macrophytes, the specific activity of HTO in the plant tissue water is equal to that in water.

To assess the OBT concentration in macrophytes following an accidental release, the AQUATRIT model uses the same equation as for phytoplankton (Eq. 152) but with a specific growth rate. Growth processes of macrophytes are described in the literature [345, 346]. Growth rate depends on the species, temperature, water turbulence, water depth where the plants grow, and water surface irradiance; it can vary widely, depending on local conditions. To apply the model in a specific case, known local values for growth processes [345, 346] are used. In the AQUATRIT model, when applied to the Danube ecosystem, a maximum growth rate of 0.01 day^{-1} is assumed for benthic algae, depending on water temperature, and daily average irradiance:

$$\mu_{ba} = 0.01 * 1.07^{(T-8)} * \text{mod light}^{0.31} \quad (154)$$

where:

μ_{ba} is the growth rate of benthic algae (day^{-1});
 T is the average water temperature ($^{\circ}\text{C}$); and
 modlight is the moderator of seasonal irradiance variability, which is the same as for phytoplankton.

The approach considered in the AQUATRIT model is conservative and ignores the recently recommended [274] discrimination factor (i.e. the ratio between tritium and hydrogen, T/H) of about 0.6.

The mass fraction of dry matter in benthic algae has a mean value of 0.08, and other default values for the water content of various aquatic organisms are given in Table 87 in TRS 472 [274]. Note that the growth rate used for the Danube ecosystem is site-specific, and variations of a factor of 3 in this parameter are expected for other locations.

12.3. DYNAMICS OF ORGANIC TRITIUM TRANSFER IN CONSUMERS

In the OURSON model, the following description refers to fish, but it can be applied to molluscs and crustaceans as well. The model assumes that the animal organic biomass can be represented by a single compartment and that OBT turnover in biotic compartments has the same characteristics as carbon turnover. The model also takes into account the mass balance of OBT and the change in fish biomass which is equal to the difference between the gain through ingestion and the loss through respiration. After preliminary calculations given elsewhere [291], the basic equation for the specific activity of OBT in fish is given as:

$$\frac{dA_{fish}^{OBT}(t)}{dt} = k_{ing} \left[\frac{H_{diet}}{H_{fish}} A_{diet}^{OBT}(t) - A_{fish}^{OBT}(t) \right] \quad (155)$$

with:

$$k_{ing} = I.D$$

where:

A_{fish}^{OBT} is the OBT specific activity in fish ($\text{Bq g}^{-1} \text{ H dm}$);
 k_{ing} is the relative ingestion rate (day^{-1});
 H_{diet} is the mass ratio between hydrogen and carbon in diet ($\text{g H g}^{-1} \text{ C}$);
 H_{fish} is the mass ratio between hydrogen and carbon in fish dry matter ($\text{g H g}^{-1} \text{ C}$);
 A_{diet}^{OBT} is the specific activity of OBT in diet ($\text{Bq g}^{-1} \text{ H dm}$);
 I is the relative food intake rate (day^{-1}); and
 D is the feed digestibility.

The turnover rate of OBT ultimately depends on two metabolic parameters, the relative food intake rate of fish I (kg of ingested C per kg of C in fish biomass) and the feed digestibility. The average values of the relative ingestion rate, k_{ing} , are given in Table 54 and the ratio between hydrogen and carbon in diet, H/C, ($\text{g H g}^{-1} \text{ C}$) is given in Table 55.

In the OURSON model, equations are based on the specific activity approach and tissue HTO and OBT activities are thus expressed in $\text{Bq g}^{-1} \text{ H}$. but in concentrations in fresh mass are needed for the dose assessment model. The following equations for HTO and OBT, respectively, convert specific activity to concentrations:

$$C_{fw}^{HTO} = WC \cdot C^{HTO} \quad (156)$$

$$C_{fw}^{OBT} = (1 - WC) \cdot WEQ \cdot C^{OBT}$$

where:

C_{fw}^{HTO} is the HTO concentration in biota (Bq kg⁻¹ fw);

C_{fw}^{OBT} is the OBT concentration in biota (Bq kg⁻¹ fw);

WC is the fractional water content of the organism (kg water kg⁻¹ fw);

WEQ is the water equivalent factor of the organism (i.e. volume of water obtained by combustion of dry tissue) (L kg⁻¹ dm);

$C^{HTO} = 111 * A^{HTO}$ is the tritium concentration in tissue free water (Bq L⁻¹);

$C^{OBT} = 111 * A^{OBT}$ is the tritium concentration in combustion water (Bq L⁻¹); and

A^{HTO} , A^{OBT} are the tissue HTO and OBT specific activities, respectively (Bq g⁻¹ H).

Values of WC for various aquatic organisms are available in Table 87 of TRS 472 [274]. Values of WEQ are given in Table 56.

In the AQUATRIT model, the dynamics of OBT concentrations, including the specific hydrogen (tritium) metabolism, are described in a previous paper [330] for all aquatic organisms except phytoplankton, benthic algae, and macrophytes. The general equation for dynamics of OBT in consumers is:

$$\frac{dC_{org,x}}{dt} = a_x C_{f,x}(t) + b_x C_w(t) - K_{0.5,x} C_{org,x} \quad (157)$$

where:

$C_{org,x}$ is the OBT concentration in the animal, x (Bq kg⁻¹ fm);

$C_{f,x}$ is the OBT concentration in the food of animal, x (Bq kg⁻¹ fm);

a_x is the transfer coefficient from OBT in the food to OBT in the animal, x (day⁻¹);

b_x is the transfer coefficient from HTO in the water to OBT in the animal, x (day⁻¹); and

$K_{0.5,x}$ is the biological loss rate of OBT from animal, x (day⁻¹).

For a proper mass balance, it is necessary to introduce the following relationship [330]:

$$C_f = \sum_{i=1}^n C_{prey,i} P_{prey,i} \frac{OBH_{pred}}{OBH_{prey,i}} \quad (158)$$

where:

C_f is the OBT concentration in animal's food (Bq kg⁻¹ fm);

$C_{prey,i}$ is the OBT concentration in prey, i (Bq kg⁻¹ fm);

$P_{prey,i}$ is the preference for prey, i; and

OBH_x is the organically bound hydrogen (OBH) content in organism, x (prey or predator) (g OBH kg⁻¹ fm).

TABLE 54. AVERAGE VALUES OF RELATIVE INGESTION RATES FOR AQUATIC FAUNA

Animal type	k_{ing} (day ⁻¹)	Reference
Fish	0.001	Sheppard et al. [292]
Mussel	0.02	IAEA [339]
Shrimp (aquaculture Madagascar)	0.1	Franco et al. [347]

TABLE 55. EMPIRICAL HYDROGEN TO CARBON RATIOS IN VARIOUS BIOTA FROM ENVIRONMENTAL MONITORING AT A FRENCH NPP

Type of biota	H/C
Phytoplankton	0.16 ¹
Macrophytes	0.14
Fish	0.15
Mussel	0.17
Shrimp	0.15

¹ Theoretical ratio from photosynthesis.

TABLE 56. WATER EQUIVALENT FACTORS (WEQ) FOR VARIOUS AQUATIC ORGANISMS

Organism	Water equivalent factor (g water g ⁻¹ DW)	Reference
Marine algae	0.50	EDF*
Marine fish	0.65	EDF*
Molluscs (soft part)	0.60	EDF*
Crustaceans (soft part)	0.60	EDF*
Freshwater fish	0.65	IAEA [274]

* Empirical values from radioecological monitoring at a French NPP.

TABLE 57. SPECIFIC ACTIVITY RATIO (SAR) AND STANDARD DEVIATIONS (sd) FOR AQUATIC ORGANISMS WHEN THE SOURCE IS HTO

Aquatic organisms	SAR (HTO source) ± sd
Zooplankton	0.4±0.1
Molluscs	0.3±0.05
Crustaceans	0.25±0.05
Planktivorous fish	0.25±0.05
Piscivorous fish	0.25±0.05

In the absence of relevant data, the ratio of OBH in predator and prey can be assessed from the dry matter ratio, with some loss of accuracy.

Eqs. (157) and (158) are those of a model with a single OBT compartment with sources of OBT production from HTO in water or OBT in food. When HTO is the primary source, the specific activity approach can be used. The specific activity (SA) of tritium is defined as the ratio between the tritium activity and the mass of hydrogen in a specific form. The specific activity ratio (SAR) is the ratio between the SA of OBT in the animal and the SA of HTO in water. Based on a literature review [330, 338], the values for SAR in different aquatic organisms when the source is HTO are given in Table 57.

Using the specific activity approach and equilibrium conditions, the transfer coefficients in Eq. (157) are now defined as:

$$a_x = (1 - SAR_x) * K_{0.5,x} \quad (159)$$

$$b_x = SAR_x * K_{0.5,x} * \frac{SA_{pred}}{111}$$

where:

SAR_x is the specific activity ratio in animal, x;
 SA_{pred} is the specific activity of bound hydrogen (BH) in the predator (kg BH kg⁻¹ fm); and
 111 is the mass of free hydrogen (kg) in 1 m³ of water.

With the exception of fish fat, SA_{pred} is dependent on the dry matter fraction of the predator at about 0.06*Dryf_{pred}. For fish fat, a value of 0.08*Dryf_{pred} is recommended for SA_{pred} .

12.3.1. OBT dynamics in zooplankton

In the AQUATRIT model, the OBT biological loss rate, $K_{0.5}$, for zooplankton depends on growth rate and temperature [348]. At a reference temperature of 20°C and accounting for the zooplankton volume, the OBT biological loss rate is given by:

$$K_{0.5_o} = (0.715 - 0.13 * \log(V)) + (0.033 - 0.008 * \log(V)) \quad (160)$$

where:

$K_{0.5_o}$ is the OBT biological loss rate at the optimal reference temperature of 20°C (d⁻¹); and
 V is the zooplankton volume (μm³).

The dry matter fraction of zooplankton varies between 0.07 and 0.2; in the AQUATRIT model, a value of 0.12 is used as a default value. All details are given elsewhere [331].

12.3.2. OBT dynamics in zoobenthos

In the AQUATRIT model, the benthic fish consume macroinvertebrates, especially, aquatic insect larvae of the Order Diptera. The most common ones are from the Chironomidae (or chironomid) Family, which have 2–6 life cycles per year. Generally, chironomid larvae are assumed to have a growth rate of 0.05 day⁻¹ and a respiration rate of 0.01 day⁻¹ [349]. Consequently, the OBT biological loss rate for chironomid larvae, $K_{0.5}$, is 0.06 day⁻¹ [349]. A higher value ($K_{0.5} = 0.2$ day⁻¹) is used in the CASTEAUR (acronym for “Simplified Calculation of radioactive nuclides Transfer in Receiving WATERways” in French) model [350]. In the AQUATRIT model, an average value, $K_{0.5} = 0.1$ day⁻¹ is used. These values for

$K_{0.5}$ correspond to an average water temperature of 12°C. In the absence of relevant data, for other water temperatures, the temperature correction functions are assumed to be the same as those for molluscs and crustaceans.

Small molluscs and crustaceans are highly variable, and OBT biological loss rates must be calculated for each case. For molluscs, a literature review [338] gives a $K_{0.5}$ of 0.02 day⁻¹ for a body mass of 1 g fm, but a $K_{0.5}$ of 0.005 day⁻¹ is listed for 30 g of soft tissue. For crustaceans, the same review [338] cites an average value of 0.007 day⁻¹ for $K_{0.5}$. By comparison, for molluscs, a value of 0.017 day⁻¹ for $K_{0.5}$ is given in another paper [349]. Based on experimental data for the growth rate and the energy content (2,386 J per g wet tissue) of *Mytilus edulis* soft tissue, the following relationship can be derived [351]:

$$K_{0.5_o} = 0.024 * W^{-0.246} \quad (161)$$

where W is the wet mass of mussel soft tissue (g fm).

Recent experiments on the OBT dynamics of *Elliptio complanata*, with a total mass of 90 g (40 g wet mass), determined a value of 0.02 day⁻¹ for $K_{0.5}$ [339, 340], a value which is a few times higher than that for *Mytilus edulis* [351].

Molluscs and crustaceans are important to food chain modelling because they are consumed by humans, and various species of zoobenthos are consumed by fish. The model has two separate compartments. For human consumption, mussels and crabs of large body mass (about 20 g fm for both mussels and crabs) are modelled, and the parameter values are selected for this assumption. By default, a biological loss rate of 0.007 day⁻¹ is assumed for OBT, but model users must adjust this value to their specific cases.

The temperature dependence of the OBT biological loss rate for molluscs and crustaceans is modelled based on experimental data for a *Tridacna* species [352], but there is no guarantee the assumptions are correct for specific applications (i.e. the cases addressed by the AQUATRIT model).

The influence of body mass and temperature on aquatic invertebrate respiration [353] is highly variable, and in specific cases, the literature must be consulted for appropriate parameter values.

12.3.3. OBT dynamics in fish

There are very few experimental data for OBT biological loss rates in fish. Thus, because it has been experimentally demonstrated that the mass dependence of the basal metabolic rate of fish is a combination of the tissue-specific respiration rate and the relative size of different tissues [354], models based on bioenergetics have been developed. In addition, the energy metabolism approach [330], used to model mammals, can also be used to model tritium transfer in aquatic fauna.

Bioenergetics involves the investigation of energy expenditure, losses, gains and efficiencies of transformations in the body. The basic equation in models based on the bioenergetics (BEMs) of fish growth is [355]:

$$\frac{1}{W} \frac{dW}{dt} = [C - (R + S + F + E + P)] \frac{cal_p}{cal_f} \quad (162)$$

where:

W is fish mass (g fm);
 t is time (day);
 C is consumption (g prey g⁻¹ fish day⁻¹);
 R is respiration or losses through metabolism (g prey g⁻¹ fish day⁻¹);
 S is specific dynamic action or losses due to the energy costs of digesting food (g prey g⁻¹ fish day⁻¹);
 F is egestion or losses through faeces (g prey g⁻¹ fish day⁻¹);
 E is excretion or losses of nitrogenous wastes (g prey g⁻¹ fish day⁻¹);
 P is egg production or losses through reproduction (g prey g⁻¹ fish day⁻¹); and
 cal_p, cal_f are caloric equivalents of prey (J g⁻¹) and fish (J g⁻¹), respectively.

The equation for consumption is:

$$C = C_{max} * p * f_c(T) \quad (163)$$

where:

C is consumption (g prey g⁻¹ fish day⁻¹); and
 C_{max} is the allometric equation for maximum specific consumption rate (g prey g⁻¹ fish day⁻¹).

with:

$C_{max} = aW^b$ with a, b being allometric coefficients for fish;
 p is the proportion of maximum consumption; and
 $f_c(T)$ is a temperature-dependent function.

Respiration is measured as oxygen consumption and is converted to consumed prey by knowing the energy equivalent of oxygen (13 560 J g⁻¹ O₂) and the prey energy density. Respiration depends on temperature, fish mass (allometric function) and activity:

$$R = a_r W^{b_r} f_r(T) ACT * conv \quad (164)$$

where:

R is respiration (g prey g⁻¹ fish day⁻¹);
 a_r, b_r are allometric coefficients (a_r is usually given in units of O₂ consumption per g fish and unit time);
 $f_r(T)$ is the temperature function of respiration;
 ACT is an activity multiplier that depends on the average swimming speed of the fish; and
 $conv$ is oxygen consumption converted to consumed prey (13 560 J g⁻¹ O₂ cal_p⁻¹).

Note that all the units in Eqs. (162)–(164), are reported on an fm basis.

In many applications, the specific dynamic action (S), the egestion (F), and the excretion (E) depend on consumption as an overall fraction (ε), and the relative growth rate (RGR) is given as:

$$RGR = \frac{1}{W} \frac{dW}{dt} = [(1 - \varepsilon)C - R] \frac{cal_p}{cal_f} \quad (165)$$

The OBT biological loss rate, $K_{0.5}$, can be given as:

$$K_{0.5} = RGR + R \frac{cal_p}{cal_f} \quad (166)$$

In Eq. (165), the effect of growth dilution (RGR) and metabolic (respiration) rate must be noted.

At maintenance (RGR=0), the OBT biological loss rate is given only by respiration. The development and application of BEMs increased substantially in the last decade. BEMs are appealing because they are based on balanced energy-fate equations that are thought to result in reasonable predictions. However, most BEMs have not been well evaluated over the ranges of conditions to which they have been applied. Results indicate that many BEMs are substantially inaccurate when predicting fish growth with higher feeding rates or estimating consumption with higher growth rates, even when the higher consumption levels or growth episodes are of short duration [356]. Further work is needed to evaluate temperature, sub-maintenance-feeding, and prey-type effects on the performance of BEMs, as well as possible influences of swimming activity level (i.e. ACT in Eq. (163)). In a recent review [357], BEMs were compared with field and laboratory experimental data. Field tests of bioenergetics models have generally revealed poor fits between model predictions and field measurements. although a reasonable agreement (15%) was obtained between model and field values for lake trout (*Salvelinus namaycush*), largemouth bass (*Micropterus salmoides*), and sockeye salmon (*Oncorhynchus nerka*) [357]. Laboratory tests also demonstrate the poor performance of BEMs [356]. Disagreement between BEMs and laboratory data are largest when the BEMs attempt to account for a range of temperatures and variable ration levels. Subtle physiological adaptations of fish species to local environments can also have an important influence on the accuracy of BEMs predictions.

12.4. DISSOLVED ORGANIC TRITIUM (DOT)

The models previously described (OURSON and AQUATRIT) are based on the assumption that the OBT specific activity in fish is directly linked with the HTO in water or the OBT in fish food. This is completely valid if the water contamination is due only to an HTO source. Assuming this, the concentration factor (CF) in fish must be less than or equal to 1. Classically, the concentration factor has been defined as the ratio between the concentration per unit mass of biota at equilibrium and the dissolved concentration per unit volume in ambient water.

Concentration factors for tritium in aquatic marine biota have been measured at Cardiff, UK [358, 359]. For flounder (*Platichthys flesus*) and mussels (*Mytilus edulis*), CFs of up to 4×10^3 (fresh mass equivalent) were reported. This significant increase in CF compared with unity has been attributed to the uptake of tritium in organic forms from a mixture of compounds legally released as waste to the Bristol Channel from the Nycomed-Amersham (now GE Healthcare) radiopharmaceutical plant at Whitchurch, Cardiff, UK. A review of past monitoring results was recently published [333], and problems with the methods used to analyze OBT were noted. However, the extremely large CFs cannot be explained by analytical errors alone, and many hypotheses have been advanced. These include (1) concentration of organic tritium by bacteria and subsequent transfer up the food chain; (2) ingestion of contaminated sediment; (3) ingestion of contaminated prey; and (4) direct uptake of DOT from the sea water. The first suggestion is that bioaccumulation occurs via a pathway in which tritium-labelled organic compounds are converted into particulate matter (via bacterial uptake / physico-chemical sorption) with subsequent transfer to the food chain [358]. The second suggestion has been discounted based on the observation that OBT concentrations

in benthic fauna are much higher than OBT concentration in both sediments and suspended particulate matter.

Assuming that molecules of DOT are highly bioavailable, a conservative approach considers that dissolved organic compounds are the only carbon source for aquatic plants and animals. Then, the OURSON equation (155) for the transfer of organic tritium to consumers can be used by replacing the specific activity in the diet with the specific activity in DOT. Similarly, OURSON Eqs. (151) and (153) for OBT dynamics in phytoplankton and macrophytes, respectively can be used by replacing $DF.A^{HTO}$ with the specific activity of DOT. The turnover rate depends on the relative rate of carbon intake. Thus, the kinetic parameters previously described, k_{photo} and k_{ing} can also be applied to plant and animal uptake of dissolved organic molecules. The specific activity of organic tritium in dissolved organic matter A_{DOM}^{OBT} (in $Bq\ g^{-1}\ H$) is expressed as:

$$A_{DOM}^{OBT} = \frac{C_{water}^{OBT}}{DOC.H_{DOM}} \quad (167)$$

where:

- C_{water}^{OBT} is the organic tritium activity in filtered river or sea water ($Bq\ L^{-1}$);
- DOC is the dissolved organic carbon concentration in river or sea water ($g\ L^{-1}$); and
- H_{DOM} is the hydrogen to carbon mass ratio in dissolved organic matter (theoretical ratio of 0.166 corresponding to 2 atoms of hydrogen for 1 atom of carbon) ($g\ H\ g^{-1}\ C$).

Concentrations of dissolved organic carbon, DOC, in various aquatic ecosystems is given in Table 58.

Then, activity in plants and animals can be calculated with the following equations, assuming DOM is the only carbon source for the plant or animal (a conservative assumption):

$$\frac{dA_{plant}^{OBT}(t)}{dt} = k_{photo} \cdot \left[\frac{H_{DOM}}{H_{plant}} \cdot A_{DOM}^{OBT}(t) - A_{plant}^{OBT}(t) \right] \quad (168)$$

$$\frac{dA_{animal}^{OBT}(t)}{dt} = k_{ing} \cdot \left[\frac{H_{DOM}}{H_{animal}} \cdot A_{DOM}^{OBT}(t) - A_{animal}^{OBT}(t) \right] \quad (169)$$

where:

- H_{DOM} is the mass ratio between hydrogen and carbon in DOM (theoretical ratio of 0.166 corresponding to 2 atoms of hydrogen for 1 atom of carbon) ($g\ H\ g^{-1}\ C$);
- H_{plant} is the mass ratio between H and C in the aquatic plant ($g\ H\ g^{-1}\ C$);
- H_{animal} is the mass ratio between H and C in the aquatic animal ($g\ H\ g^{-1}\ C$);
- A_{DOM}^{OBT} is the specific activity of organic tritium in dissolved organic matter ($Bq\ g^{-1}\ H$);
- A_{plant}^{OBT} is the specific activity of organic tritium in the aquatic plant ($Bq\ g^{-1}\ H$); and
- A_{animal}^{OBT} is the specific activity of organic tritium in the aquatic animal ($Bq\ g^{-1}\ H$).

TABLE 58. CONCENTRATION OF DISSOLVED ORGANIC CARBON IN VARIOUS WATER BODIES

Water body	DOC (mg C L ⁻¹)	Reference
Loire River	3	Abril et al. [360]
Loire Estuary	9	Abril et al. [361]
English Channel	2	Abril et al. [361]
North Pacific	0.9	Peltzer and Hayward [362]

In the AQUATRIT model, the direct uptake of DOT can be introduced in the dynamic equation for phytoplankton (Eq. 152) and consumers (Eq. 157), respectively:

$$\frac{dC_{o,phpl}}{dt} = 0.4 \cdot \mu \cdot Dryf \cdot 0.001 \cdot C_W + V_{DOT} \cdot C_{DOT} - \mu \cdot C_{o,phpl} \quad (170)$$

$$\frac{dC_{org,x}}{dt} = a_x C_{f,x}(t) + b_x C_w(t) + V_{DOT} \cdot C_{DOT} - K_{0.5,x} C_{org,x} \quad (171)$$

where:

C_W is the HTO concentration in water (Bq m⁻³);

C_{DOT} the DOT concentration (Bq L⁻¹); and

V_{DOT} the uptake rate of DOT (L kg⁻¹fm day⁻¹) and obtained from a simplified form of Michaelis-Menten equation (complete details are given elsewhere [331, 363]).

12.5. EXAMPLES OF MODELLING A TYPICAL FISH USING THE AQUATRIT MODEL

In this example, we choose the rainbow trout (*Oncorhynchus mykiss*), because it is a fish found in many countries and is also considered a representative fish by the ICRP [364].

OBT dynamics were studied in juvenile [365], and adult rainbow trout (*Oncorhynchus mykiss*) [366]. Juvenile rainbow trout were kept in tritiated water at a constant temperature of 15°C and/or received a diet labelled with tritiated amino acids. The average mass of fish increased from 7.0 ± 0.2 g fm up to 15.7 ± 0.6 g fm during the course of the 10 week experiment (with 56 days for tritium uptake). Based on the experimental data during exposure to a tritiated diet, the OBT rate constant was 0.0218 ± 0.002 day⁻¹, while in the two weeks after exposure, the estimated value was 0.0308 ± 0.003 day⁻¹. For the juvenile rainbow trout model in AQUATOX [367], the OBT rate constant for the experimental conditions (e.g. mass range and water temperature) was about 0.03 day⁻¹. More recently, an updated model for rainbow trout was developed [368]; its rate constant for OBT dynamics was 0.037 day⁻¹. These results must be viewed with caution, however, because under laboratory conditions, the physical activity of fish is lower than under field conditions and the models use a mixture of parameters that are not completely understood.

The bound hydrogen (BH) content and energy density (ED) in fish and its prey can be assessed by knowing the composition of carbohydrates, proteins and lipids in the fish and its prey. The values of BH and ED per kg of carbohydrates, proteins and lipids are found in the literature [323, 369]. The model needs the OBT biological loss rate (defined by Eq. 164) which is obtained from fish bioenergetics models that have been tested with laboratory and field data on fish growth. The application of fish bioenergetics is well established, and

software and a default data base are available [355]. The most appropriate parameters for the fish of interest must be found in recent literature, and end users must be aware that data for juvenile and adult fish are very different. In the case of rainbow trout, the parameters are given in reference [368] for the youngest fish (mass less than 50 g). For adult fish, different parameters are recommended [370, 371]. The models in the referenced papers [370, 371] use experimental data on fish respiration in normal and active state, as well as data on fish growth for fish fed a controlled diet. These parameters are essential input for tritium models. AQUATRIT was blind tested using the results of laboratory experiments done at Chalk River Laboratories (AECL, Canada). Predicted to observed ratios were less than a factor of 2 (Figure 55), and the discrepancies between predictions and the data can be partially explained by details of fish mass dynamics in the experiment being unknown [372].

To apply the model to realistic field conditions, other important information about prey composition, energy density, and availability of prey [373] is needed. The seasonal variability of prey (composition and density) influences fish growth, and the variability of seasonal water temperature may greatly affect the OBT concentration in fish.

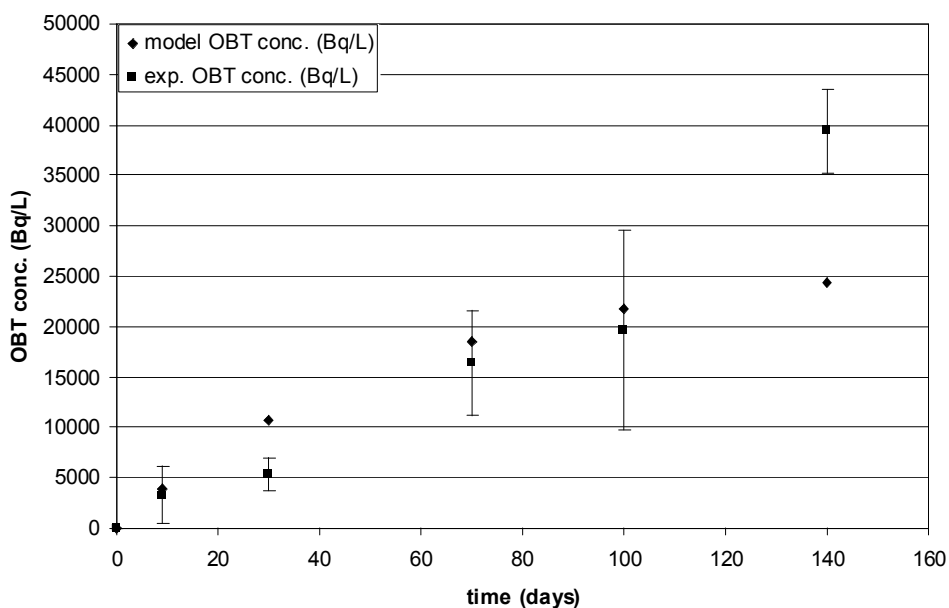


FIG. 55. Comparison between model results and experimental data for OBT concentrations in fish for uptake of OBT.

13. QUALITY ASSURANCE OF DATA

13.1. OVERVIEW

Tritium can be bound to organic compounds either by exchange reactions or by enzymatically-catalyzed reactions [5, 323]. In exchange reactions, tritium binds to oxygen, sulphur, phosphorous or nitrogen atoms as hydroxides, thiols, phosphides or amines, respectively. Conventionally, this is referred to as exchangeable or labile organically bound tritium (OBT). Exchangeable OBT is considered to be in equilibrium with tritiated water (HTO) in the plant or animal in question. In enzymatically-catalyzed reactions, tritium binds to the carbon chain of an organic molecule as fixed or non-exchangeable OBT. Such bonds are strong and can be dissolved only during catabolic reactions, meaning that non-exchangeable OBT has a longer retention time in the body than does HTO or exchangeable OBT.

Differing views on whether the definition of OBT should include exchangeable OBT are found in the literature. Diabate and Strack [323] state that OBT should include only non-exchangeable OBT. On the other hand, the Environmental Agency [374] has argued for a wider definition that includes any organic matter containing tritium, either exchangeable or fixed. This definition ensures that both forms of OBT are taken into account in dose assessments, thus ensuring a conservative approach that compensates for the large uncertainty surrounding OBT. More recently, Baumgärtner and Donhärsl [375] and Baumgärtner [376] have identified another form of OBT, called buried tritium, which is defined as the tritium in exchangeable positions in large biomolecules in dry matter that is not removed by rinsing with tritium-free water. Such tritium is not carbon bound but is simply folded into large molecules that are not accessible for exchange by tritium-free water. Buried tritium contributes to the concentration in the traditional experimental determination of OBT, but it quickly exchanges with hydrogen atoms in the body and acts as HTO rather than OBT following ingestion. The rapid increase in plant OBT concentrations observed in the first few hours following acute HTO exposure in some experiments may be evidence of buried tritium that forms by exchange through non-metabolic processes [176, 377].

The nature of OBT was debated by the Tritium and C-14 Working Group of the IAEA's Environmental Modelling for Radiation Safety (EMRAS) program, which settled on the following definition: "OBT is carbon-bound and buried tritium formed in living systems through natural environmental or biological processes from HTO. Other types of organic tritium (e.g. tritiated methane, pump oil, radiochemicals and so on) should be called tritiated organics, which can exist in any chemical or physical form" [4]. This definition was clarified over time; the full EMRAS definition is given in Appendix III.

The EMRAS definition is consistent with the quantity measured in the traditional experimental determination of OBT, namely, the tritium in the combustion water produced by the oxidation of dry matter that has been washed with tritium-free water. The definition was deliberately chosen to maintain this connection to preserve the meaning of past analyses and current analytical techniques. The definition does not include exchangeable OBT but does include buried tritium. It also distinguishes between organically bound tritium that is formed in the environment and tritiated organics, which are produced through industrial processes.

The concept of buried tritium was accepted by the EMRAS Working Group [4], but its significance is still under debate. Baumgärtner and Donhärsl [375] and Baumgärtner [376] suggest that buried tritium makes up 50% or more of what is traditionally measured as OBT. On the other hand, a study by Kim et al., [377] indicates that the fraction is typically 5% and

at most 20%. In the face of this discrepancy, the question remains open pending new experimental data. Because buried tritium is included, current OBT dose calculations lead to a conservative estimate of OBT dose.

13.2. ANALYTICAL ISSUES

There are many different methods for analyzing the tritium (HTO and OBT) in environmental samples [378, 379]. However, there is no standard method.

OBT is an important tritium species that can be measured in most environmental samples, such as plants, animals and soils [380]. Currently, OBT is not routinely measured by environmental monitoring laboratories around the world. Also, there have been differences between many analytical laboratories in the analysis of OBT samples. One possible reason for the discrepancies may be differences in analytical methods [381]. Therefore, inter-laboratory OBT comparisons within the OBT community are important and would provide a good opportunity to choose and adopt a reference OBT procedure.

13.2.1. Issues with the OBT analysis process

There are no certified reference materials (CRMs) for environmental OBT samples, and, thus, quality assurance (QA) of OBT measurement is not available. Alternatively, quality control (QC) will be available. Figure 56 and Table 59 show conventional procedures for OBT analysis in environmental samples. The measurement of OBT concentrations in environmental samples takes longer and is more complex than the measurement of HTO; it also has a higher associated uncertainty. The uncertainty can be introduced in three ways: (1) the water residue is not extracted completely from the fresh sample; (2) the exchangeable OBT is not removed from the dry matter; and (3) for a Parr instrument, the combustion water has to be distilled to neutralize and purify it, which may affect counting efficiency.

13.2.2. HTO measurement

The measurement of the HTO concentration in an environmental sample is achieved by first extracting the free water from the fresh sample (Figure 56). This is usually done either by freeze-drying (Figure 57) or by azeotropic distillation with toluene. Freeze drying is preferred if the OBT concentration is to be determined from the dry matter of the same sample, because the organic residue left after azeotropic distillation can affect the OBT measurement. The extracted water is mixed with scintillation fluid and placed in a liquid scintillation counter (LSC), which measures the HTO beta activity in the sample.

13.2.3. OBT measurement

The measurement of OBT concentrations in environmental samples is more difficult and complicated than the measurement of HTO. The sample dry matter remaining after freeze drying is washed repeatedly with tritium-free water to remove exchangeable OBT and then freeze-dried again (Figure 56). The dried material is combusted in a combustion bomb or furnace [382]. The combustion water is distilled to neutralize and purify it and then counted in a LSC. In addition, over the last few decades, an alternative method of counting based on the detection of tritium's radioactive daughter, ^3He , by mass spectrometry (MS) has been used for routine measurements of very low levels of tritium [383].

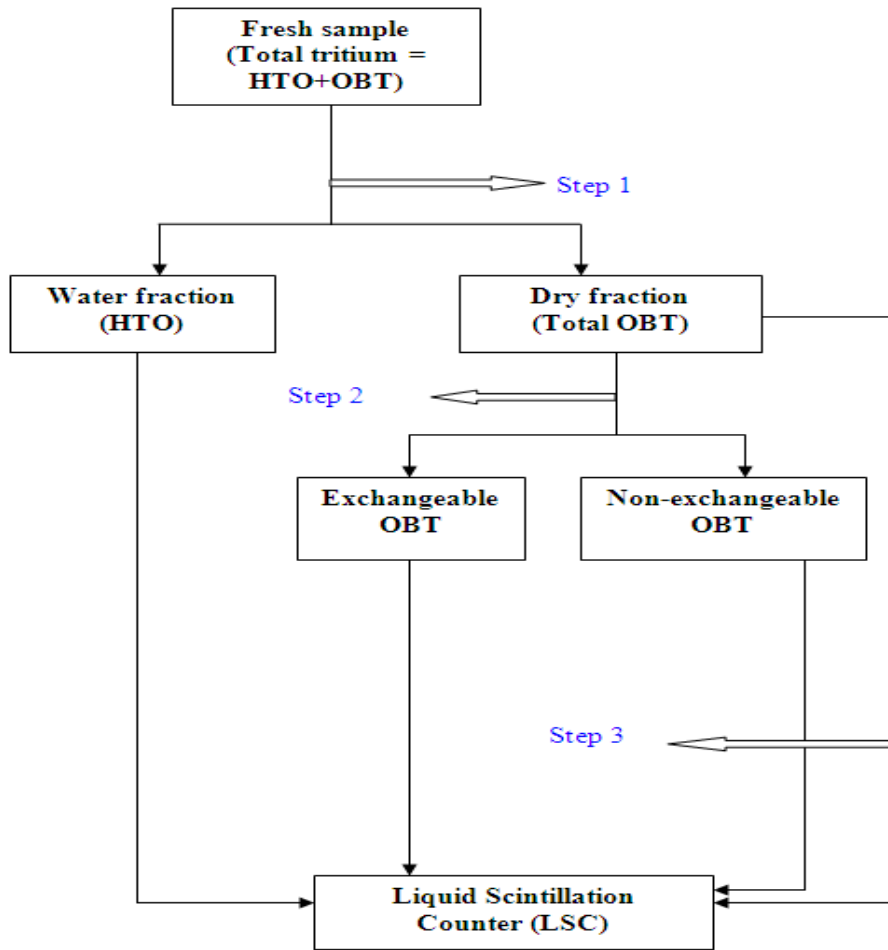


FIG. 56. Conventional steps of OBT analysis. The steps are described in Table 59.

TABLE 59. PROCESSES FOR MEASURING OBT IN ENVIRONMENTAL SAMPLES

Step	Process
Step 1	Freeze-dry (water residue) Oven-dry (temperature, duration) Azo-distillation (old fashioned)
Step 2	Rinse (volume, duration) or no rinse Combustion (Parr bomb, tube furnace) Distillation (remove impurity)
Step 3	Liquid scintillation counter (Quantulus, Packard) Cocktail (Ultima Gold series) Counting condition (background, time)

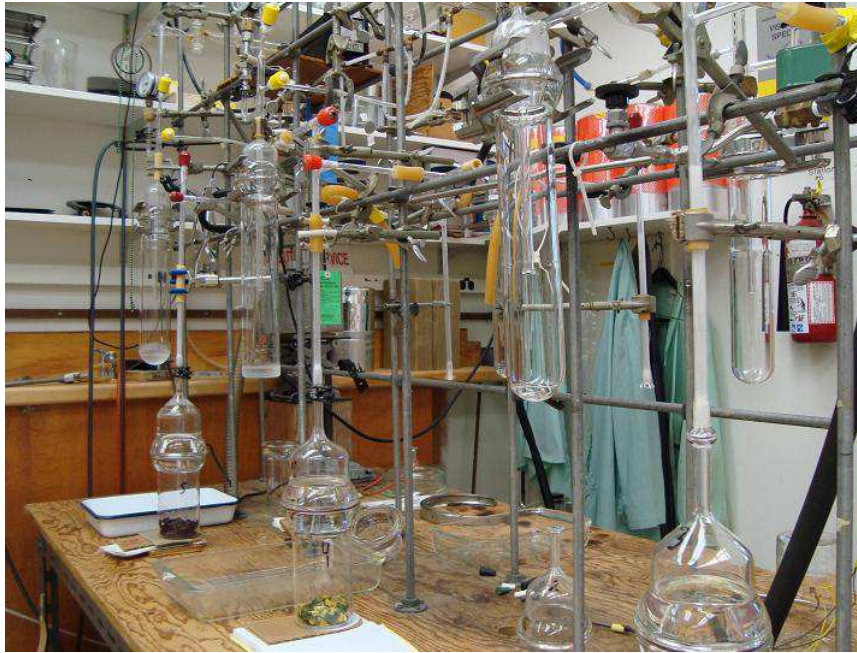


FIG. 57. Tissue free water tritium extraction apparatus (freeze-drying system) in a laboratory.

Uncertainties can arise at all steps in this procedure. If the free water is not completely extracted from the fresh sample, some HTO may be included in the OBТ measurement. Similarly, exchangeable OBТ must be completely removed from the dried sample. Because of the small amount of dried material that can be held in the cup of the Parr bomb, the volume of combustion water may be too low or too scattered within the bomb to yield a sufficient quantity for reliable analysis by LSC. Also, it is not clear how well the methods work with mixed inorganic and organic samples, such as soil and sediments.

Wassenaar and Hobson [384] report that exchangeable OBТ accounts for about 20% of the total tritium in dehydrated organic materials. Exchangeable OBТ is not usually considered explicitly in calculating ingestion OBТ doses but it is accounted for implicitly since, in the models, all of the contaminated dry matter in ingested food is assumed to be non-exchangeable OBТ. The exchangeable OBТ is therefore replaced by non-exchangeable OBТ in the calculations, which results in a slight overestimate of dose. When HTO and OBТ activities are measured for more accurate dose calculations, the fraction of exchangeable OBТ that is removed from the dried sample by rinsing should be included in the HTO fraction rather than the OBТ fraction when HTO and OBТ doses are calculated.

13.2.4. Uncertainties

The measurement of tritium in all environmental samples consists of two basic steps: extraction of the water (combustion water in the case of OBТ) from the sample and counting by LSC. Counting errors in the second step can be kept low by ensuring that: (i) the sample volume is adequate; (ii) the sample is not exposed to ambient air, which could result in cross-contamination; (iii) background tritium levels in the laboratory are well below the sample concentration; and (iv) the sample is counted for a sufficiently long time. The tritium concentration in the sample is determined as the difference between the gross count rate and the count rate of a tritium-free water sample, or blank. In practice, it is difficult to obtain

water that is truly free of tritium. At environmental levels, the counts from the sample and the blank may be similar and lead to large errors.

The detection limit associated with the analytical procedure must be significantly lower than the tritium concentrations being measured. The detection limit depends on the sample size, the counting time and the efficiency of the counter [385]. It also varies from laboratory to laboratory and analysis to analysis. A detection limit of about 5 Bq L^{-1} is readily achievable and suitable for environmental samples.

HTO is relatively easy to extract from plant and animal samples via freeze-drying or azeotropic distillation with toluene. Procedures for measuring HTO are well established in most laboratories around the world [386–388]. If these procedures are carefully followed, the uncertainty in the measured HTO concentration in plants and animal products can be kept to around 10–20% [389, 390].

The measurement of OBT concentrations in environmental samples is a longer and more complex procedure than the measurement of HTO and has a higher associated uncertainty. Errors can be introduced if all the HTO is not extracted completely from the fresh sample, or if all the exchangeable OBT is not removed from the dry matter. If all of the combustion water is not collected, the water volume may be too small to be counted reliably. In addition, the combustion water may have to be distilled to neutralize and purify it, and this may affect counting efficiency and the detection level. Overall, the uncertainty in measured OBT concentrations in plants and animal products is about 70% [390, 391]. This estimate is supported by the results of inter-laboratory comparisons using environmental OBT materials [379].

13.3. PREVIOUS OBT INTER-COMPARISON PROGRAMS

OBT is considered one of the new species of tritium in environmental samples. Only limited information is available on its measurement. Past international OBT inter-laboratory methods [378, 379, 392, 393] were reviewed and are outlined in this section.

13.3.1. Canada (Chalk River Laboratories, CRL)

Inter-comparisons of OBT are rare due to the lack of a suitably calibrated standard reference material and to the relatively low number of measurement laboratories worldwide. In 1998, a study to develop a vegetation standard reference material and carry out an inter-comparison of OBT was initiated at CRL [379]. This was a good opportunity to compare analytical methodologies with other laboratories, to discover the sources of errors and statistical deviations, and to promote confidence in the measurement of OBT concentrations in environmental samples. Figures 58 and 59 show the concentrations of OBT in lettuce and crabapple, the two vegetation samples used for the inter-comparison. This inter-laboratory comparison has suggested a better agreement at higher OBT than at lower OBT concentrations.

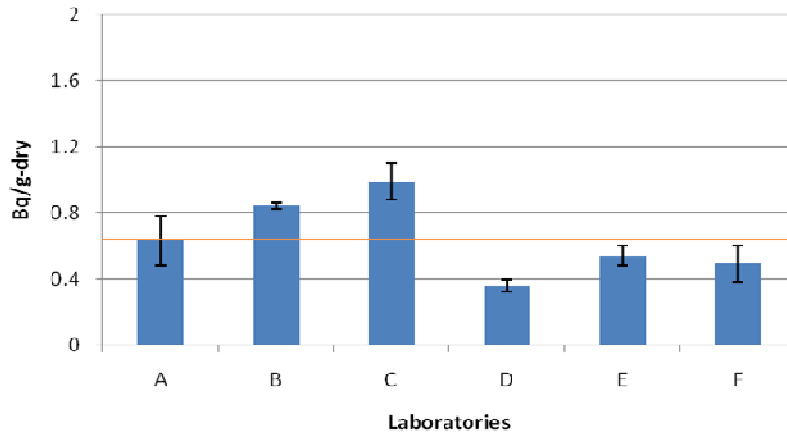


FIG. 58. Inter-laboratory comparison of OBt (1998) in lettuce conducted by CRL (Highest OBt concentration).

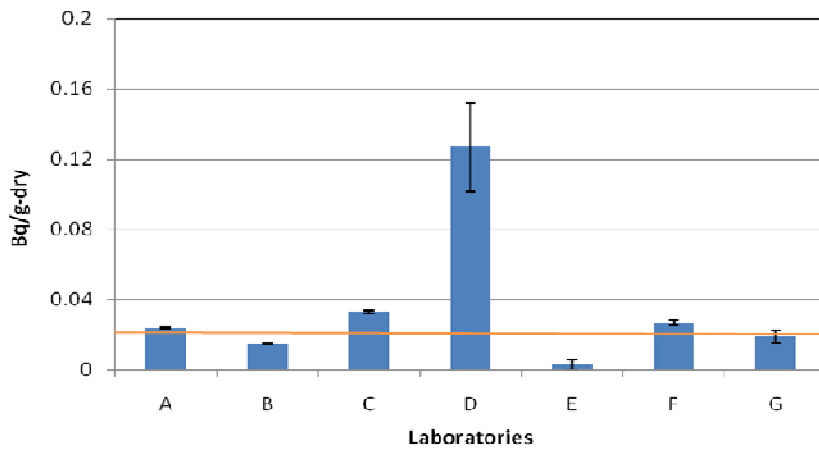


FIG. 59. Inter-laboratory comparison of OBt (1998) in crabapple conducted by CRL (Lowest OBt concentration).

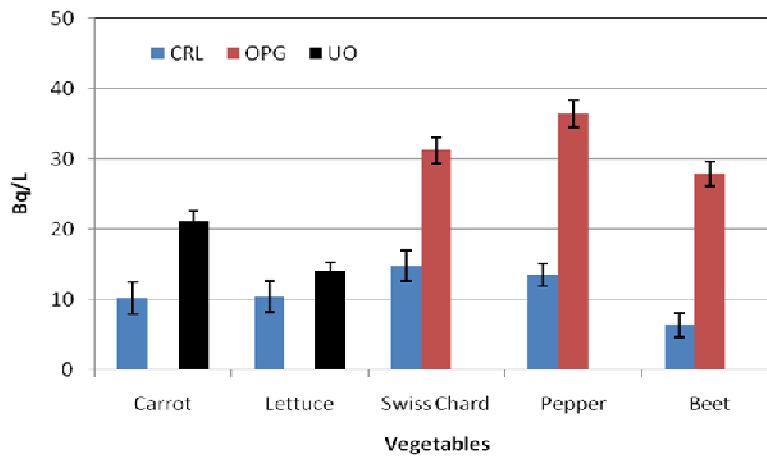


FIG. 60. Inter-laboratory comparisons of OBt in vegetables conducted by CRL with OPG and UO in 2008.

In 2008, two inter-comparisons within Canada were conducted; one with Ontario Power Generation (OPG) and one with the University of Ottawa (UO). Figure 60 shows the comparison between the CRL and OPG measurements of OBT concentrations in three vegetables. While the HTO concentrations determined by the two laboratories were in agreement when uncertainties were taken into account (not shown), OBT results differed considerably. The OBT concentrations measured by OPG were 2.1 times higher in leafy vegetables, 2.7 times higher in fruit and 4.3 times higher in root crops compared with CRL's measurements. There were some differences in analytical procedures between the two laboratories. For example, the drying temperature differed. In addition, OPG did not rinse the sample to remove the exchangeable OBT while CRL did. There were differences in counting parameters too, with CRL having lower counting background and counting efficiency. However, these factors alone cannot explain the difference in the OBT results. Potential causes for the observed differences are discussed in Section 13.3.1.1.

Figure 60 also presents OBT concentrations from the inter-laboratory comparison between CRL and UO. Again, the HTO results (not shown) were similar for both labs. In contrast, the OBT concentrations of the two samples were not similar between labs, differing by approximately a factor of 2 for carrot and about 35% for lettuce. Ottawa University used the same approach as CRL (i.e. rinsing was used to remove exchangeable OBT), but CRL used a combustion technique to measure the OBT activity concentration, while UO used mass spectrometry.

13.3.1.1. OPG compared to CRL

The measurement of OBT in vegetables presents many challenges [381, 394]. There are two significant differences between the analytical procedures at CRL and OPG. First, CRL uses an oven temperature of about 55°C to dry fresh plant samples, whereas OPG uses a temperature of about 80°C. Generally, drying samples at higher temperatures increases the risk that the components within the sample will break down. It is assumed that the drying processes of the two laboratories completely remove the water from the fresh samples. This means that, for all practical purposes, no residual water is left in the samples that will be used to determine OBT concentrations. As pointed out by OPG, neither lab has a metric for determining or verifying sample moisture content. Furthermore, residual free water or the recently proposed “buried” water can be present in the “dried” samples. This can have an impact on measured OBT concentrations, although it is not enough to explain the different results obtained by the two labs. If it is not possible to remove all residual water from a sample, quantifying and correcting for its presence may be the only practical solution.

The second major difference between the CRL and OPG procedures for determining OBT lies with the treatment of exchangeable OBT. CRL uses a rinsing process to remove exchangeable OBT while OPG does not. Because it is difficult to remove all labile OBT from vegetables, residual amounts will result in an overestimate of the concentration of non-exchangeable OBT. Exchangeable OBT behaves much the same as HTO in the plant, increasing or decreasing rapidly in response to changes in air concentration. Thus, rinsing could have a significant effect on measured OBT concentrations at locations close to a tritium source. This may be the main reason for the differences observed between the measurements of CRL and OPG. Differences in these measurements will persist until the two approaches to the treatment of exchangeable OBT are quantified and understood.

Even though both CRL and OPG have appropriate procedures in place for OBT analysis and tritium counting, being located in different areas, they experience different levels of background tritium. To determine the OBT background activity concentration at CRL,

commercial polyethylene beads [379] were combusted. The beads are petroleum products that contain no tritium, and so provide a realistic OBT background for CRL's analytical system. The OBT concentration in the combusted beads was about 1.5 Bq L^{-1} . The determination of OBT background activity concentration using this method was not carried out at OPG.

13.3.1.2. *UO compared with CRL*

There was a meaningful difference (up to a factor of 2) in the OBT activity concentrations measured by CRL and by UO. Theoretically, the ^3He MS technique applied by UO is more accurate compared with the LSC method used by CRL. To confirm this, however, a certified reference environmental material for OBT measurement is needed.

13.3.2. **France (CETAMA)**

Because OBT is of increasing importance, improved analytical methods are necessary. The CETAMA (Comité d'Établissement des Méthodes d'Analyse) plays an important role in the field of analytical science in France. One of its main tasks is to support French analytical laboratories by providing analytical OBT procedures and organizing user groups and round-robin exercises. In 2009 and 2010, CETAMA organized an inter-comparison program for the measurement of environmental levels of OBT in grass samples. This program was conducted to determine needed improvements in analytical procedures at the participating laboratories.

To validate CRL's measurement of OBT activity concentrations in vegetables, CRL participated in this program along with several participants from France (Figures 61 and 62).

The results of the inter-comparison demonstrated that several steps of the procedure, such as combustion and tritium measurement, are well understood. Moreover, exposing samples to the laboratory atmosphere during the drying stage or when moving samples from the drying system to the combustion system were confirmed as potential sources of contamination. The average OBT value among French participants varied from 251 Bq L^{-1} to 304 Bq L^{-1} (Figure 61). CRL's result was 270 Bq L^{-1} , which is very close to the average value. The results were very encouraging, as all participants obtained OBT concentrations in good agreement with each other when uncertainties were taken into account. However, in the 2010 inter-comparison (Figure 62), the OBT concentration in the sample was slightly higher than that measured by CRL, and no firm conclusions can be drawn about CRL's ability to obtain accurate results at near background levels.

13.3.3. **Japan (Akita University School of Medicine)**

Because the fraction of OBT to total tritium intake is important for estimating dose to people from tritium released to the environment [392], Japan wanted to check the reliability of OBT measurements. In 1988, 6 laboratories in Japan participated in an inter-laboratory comparison of measurements of OBT in environmental samples. Figures 63 and 64 show the results for swine liver and polished rice.

All laboratories used a specific liquid scintillation counter (the Aloka LSC-LB) using either a Teflon 100 mL vial or a quartz vial, and all used the same methodology. The results suggested that coefficients of variation were 68% for the polished rice and 35% for the swine liver.

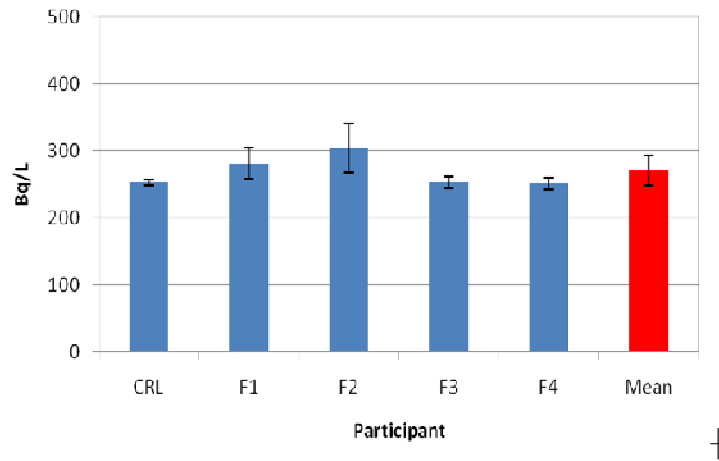


FIG. 61. OBT concentrations in grass measured by various laboratories as part of a inter-comparison exercise organized by CETAMA in 2009.

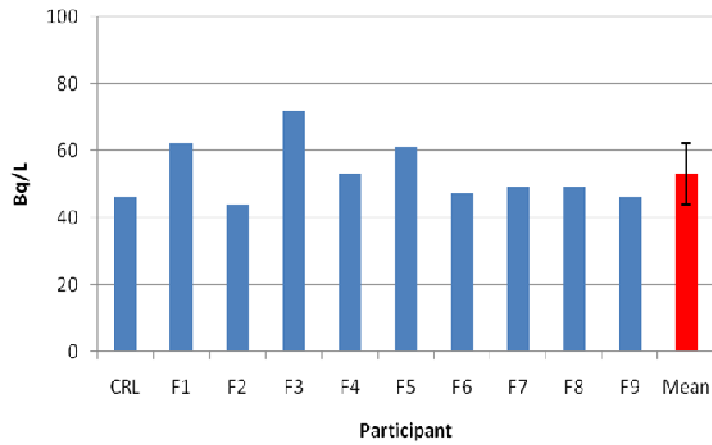


FIG. 62. OBT concentrations in grass measured by various laboratories as part of a inter-comparison exercise organized by CETAMA in 2010.

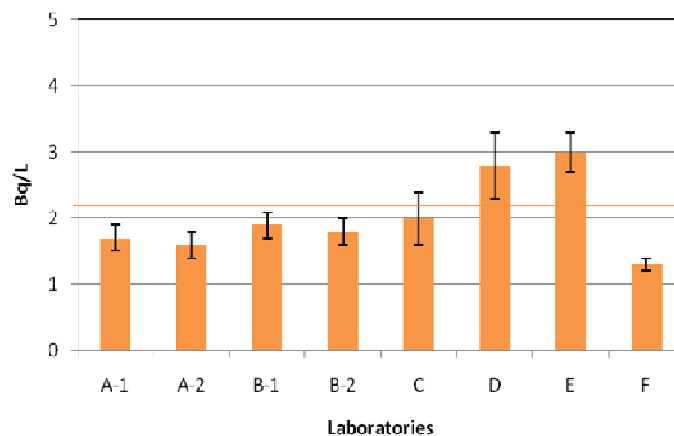


FIG. 63. OBT concentrations in swine liver measured by various laboratories as part of a Japanese inter-comparison exercise in 1988.

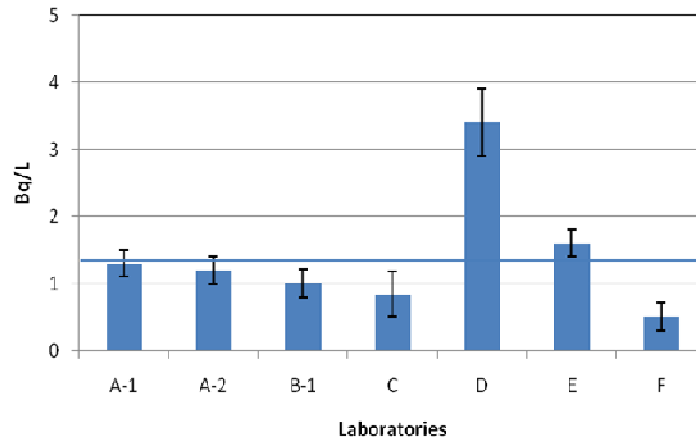


FIG. 64. OBT concentrations in polished rice measured by various laboratories as part of a Japanese inter-comparison exercise in 1988.

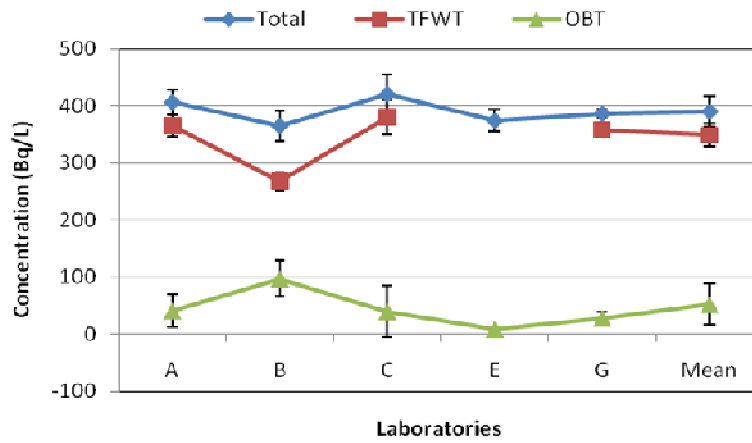


FIG. 65. Tritium concentrations in a tritiated sucrose solution measured for an inter-laboratory exercise organized by NCAS in 1999.

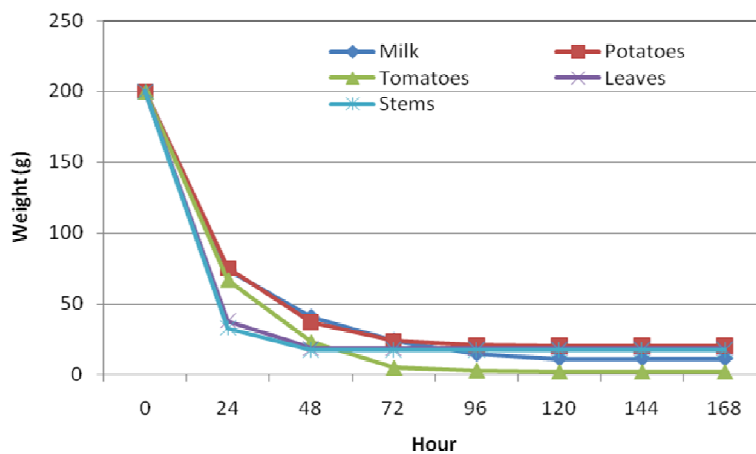


FIG. 66. Validation of the freeze-drying time using a conventional freeze-dryer (Labconco, USA) with various environmental samples.

TABLE 60. WATER RESIDUE REMAINING AFTER FREEZE-DRYING AND OVEN-DRYING

Sample	Fresh weight (g)	% water removed after Freeze-drying (3 days)	% water removed after Oven-drying after freeze-drying (1 day)
Tomato	212	98.3	99.8
	198	98.8	100
Lettuce	205	99.8	99.9
	210	100	100
Beet	209	98.2	99.9
	203	95.6	99.9
Average	206 ± 5.2	98.5 ± 1.6	99.9 ± 0.1

13.3.4. UK (National Compliance and Assessment Service, NCAS)

The aim of the UK 1999 inter-laboratory comparison was to clarify differences in reported figures for both HTO and OBT in effluent samples. Tritium labelled sucrose, in which the tritium was present attached to carbon atoms, was added to water. The resultant solution contained approximately 300 Bq L⁻¹ of tritium, 25% of which was present as sucrose. Individual aliquots of this solution in sealed glass bottles were distributed to six participating laboratories for analysis of total tritium and OBT. The results from the laboratories are presented in Figure 65. Uncertainties are quoted to two standard deviations.

Without any defined OBT analytical methodology, the reliability of the result of this inter-comparison depended on the ability to measure the difference between the total tritium present in the sample and the tritium present in the form which distils at 100°C. OBT may have been underestimated due to the removal of low volatile OBT during distillation or overestimated due to the inclusion of exchangeable OBT. The method whereby water was driven off the effluent sample prior to combustion and analysis of the combustion products for tritium carried out thereafter gave reasonably consistent results for OBT.

The most practical way to determine OBT in a sample is to assume that all tritium remaining after the tissue free water tritium (TFWT) has been removed is OBT. The freeze-drying method is the most suitable for removing TFWT from environmental samples such as vegetables. A method that is more applicable to water samples is to analyze separate aliquots of a sample for total tritium and for tritiated water using the distillation method and then to calculate OBT as the difference between results.

13.4. CRL'S OBT EXPERIMENT TO EVALUATE THE CONTRIBUTION OF RESIDUAL WATER

An experiment was conducted at CRL to quantify the contribution of residual water to OBT concentrations after freeze-drying and oven-drying (55°C). Three vegetables (tomato, lettuce and beet) were tested (Table 60).

The results indicated that freeze-drying is not able to completely remove tissue free water from frozen vegetables, with the exception of leafy vegetables such as lettuce.

Figure 66 shows data used to validate the experimental freeze drying time of 3 days used at CRL. When the methods of freeze-drying and oven-drying were combined, more water was removed, but the contribution of the residual water (before oven-drying) to the OBT

concentration was less than 2%. Therefore, the measured non-exchangeable OBT concentrations are not significantly impacted by this residual water.

13.5. DISCUSSION

Following routine releases of HTO to air and water, OBT contributes to the total tritium dose to members of the public and to aquatic and terrestrial plants and animals. Even though OBT measurement and prediction are associated with high uncertainties, OBT cannot be ignored in tritium dose estimates.

Most OBT models have been developed to predict OBT concentrations in the environment guided by observed HTO and OBT concentrations in biota. Therefore, if measured OBT has a high uncertainty, predicted OBT concentrations should have a higher uncertainty. Observed concentrations in the environment, rather than model predictions, should be used as the starting point in the calculation of doses to members of the public. OBT measurements provide a better indication of the level of environmental tritium contamination than do HTO measurements because OBT is retained longer in environmental samples. However, OBT measurements require quality assurance to improve confidence and reliability.

Chalk River Laboratories have analyzed OBT in more than 2000 environmental samples since the 1980's and is very confident in its ability to analyze OBT in many environmental samples such as plant leaves, vegetables, animal tissues and soils. CRL is convinced that that measurements between laboratories should agree better, that a method of measuring OBT should be agreed on, and that all OBT concentrations should be reported in the same units (Bq L^{-1} combustion water or Bq kg^{-1} fresh weight).

To encourage QA of OBT measurements in environmental samples, an international OBT inter-comparison project was proposed by CRL (Canada) and CEA (France). The first international OBT workshop will be held in May 2012 in France. Also, three inter-comparison exercises will be conducted by both organizations.

14. QUALITY ASSURANCE OF MODELS

14.1. OVERVIEW

Models are simplifications of reality, and therefore always have some uncertainty associated with their application. The term uncertainty refers to a lack of knowledge or information about the models, parameters, constants, input data and beliefs/concepts [167]. After the Chernobyl accident, the need for robust environmental models for radiological assessment was recognized, and many international programs were started under the auspices of the IAEA, including EMRAS. “The overarching objective of the IAEA’s activities in environmental modelling is to enhance the capabilities of Member States to simulate radionuclide transfer in the environment and, thereby, to assess exposure levels of the public and in the environment in order to ensure an appropriate level of protection from the effects of ionizing radiation, associated with radionuclide releases and from existing radionuclides in the environment. The activities within the framework of the EMRAS II Programme emphasize on improvement of environmental transfer models for reducing associated uncertainties or developing new approaches to strengthen the evaluation of the radiological impact to man, as well as to flora and fauna, arising from radionuclides in the environment”⁹.

In this context, at the start of WG7, it was asked: “What is the robustness (uncertainty) accepted by your organization or regulatory body when modelling accidental tritium releases?” From the answers we concluded that conservatism is required but the amount of uncertainty is unspecified. Some participants simply answered “NO IDEA”.

The Fukushima accident highlighted the need for robust radiological assessment models for releases to the environment. Thus far, there is no internationally agreed upon guidance for the quality assurance of environmental models and for the acceptable uncertainty for practical applications. In the discussion about the proposed work of WG7, some suggestions were made that guidelines might be adopted from IAEA member states, such as the Environmental Protection Agency (EPA), USA [167], UK [395, 396] or others, such as the Asian Nuclear Safety Network (ANSN) [397]. For routine releases of tritium, arguments have been made, based on guidance recently released [274] and past tests in BIOMASS [398], that an acceptable prediction for operational applications would be less than a factor of 3 for the predicted to observed ratio. For accidental releases of tritium (and other radionuclides), such an expectation has not been determined, and our goal must be to consider the model robustness in terms of the potential radiological impact [395]. Considering the model’s uncertainty itself, a score of 1 for uncertainty less than a factor of 3, a score of 2 for an uncertainty between 3 and 10, and a score of 3 for an uncertainty greater than 10 can be assessed. Considering potential doses, a score of 1 for doses less than 20 $\mu\text{Sv year}^{-1}$ and a score of 3 for doses larger than 100 $\mu\text{Sv year}^{-1}$ can be assessed. Multiplying the scores for uncertainty and dose, the necessary actions that must be taken to improve modeling are indicated. In EMRAS I WG 2, a hypothetical tritium accident was analyzed for a release of 10 g of tritium [4]. The dose predictions for the HTO release covered a wide range including doses greater than the limit of 100 $\mu\text{Sv year}^{-1}$. Based on these results, a robust model with an uncertainty of about a factor of 3 and, at worst,, a factor of 6 is needed.

Because a tritium model must be combined with an atmospheric transport model, the overall uncertainty must increase. The environmental transport modeller is encouraged to use an

⁹ See <http://www-ns.iaea.org/projects/emras/emras2/default.asp>.

atmospheric transport model that satisfies the quality assurance requirements of its use. The Forum for Air Quality Modelling in Europe (FAIRMODE¹⁰) established in 2008 as a joint action of the European Environment Agency (EEA) and the European Commission's Joint Research Centre (JRC), have published “The application of models under the European Union's Air Quality Directive” [399]. Many suggestions from this report [399] can be applied to radionuclide transport models.

For interested readers, the considerable literature on quality assurance of environmental models addresses various arguments [400–402].

14.2. QUALITY ASSURANCE (QA) AND SENSITIVITY – UNCERTAINTY ANALYSIS (SU)

Quality assurance (QA) may be defined as protocols and guidelines to support the proper application of models. Important aims of QA are to ensure the use of the best practice, to build consensus among the various participants in the modelling process and to ensure that the expected accuracy and model performance are in accordance with the project objectives.

EPA guidance [167] provides recommendations for the effective development, evaluation, and use of models in environmental decision making once an environmental issue has been identified. These recommendations are drawn from Agency white papers, EPA Science Advisory Board reports, the National Research Council’s “Models in Environmental Regulatory Decision Making”, and peer-reviewed literature. For organizational simplicity, the recommendations are categorized into three sections: model development, model evaluation, and model application.

The guidance recommends the best practices to help determine when a model, despite its uncertainties, can be appropriately used to inform a decision. Specifically, it recommends that model developers and users:

- Subject their model to credible, objective peer review;
- Assess the quality of the data they use;
- Corroborate their model by evaluating the degree to which it corresponds to the system being modelled;
- Perform sensitivity and uncertainty analyses.

Sensitivity analysis evaluates the effect of changes in input values or assumptions on a model's results.

Uncertainty [395] analysis measures the lack of knowledge of the system under investigation, which, in radiation dose assessment terms, will determine how well doses of interest can be estimated. For example, how well are the parameter values in a calculation of dose known? When further investigations can reduce the uncertainty in these parameter values by increasing the accuracy and precision with which they are known, then the uncertainty is known as epistemic or so called Type B uncertainty [403]. Type B uncertainty applies to a parameter that is thought to have a well-defined value, but, due to inevitable experimental difficulties, there is some uncertainty about that value. In many dose assessment applications, a detailed knowledge of the processes involved is not essential and a simpler parametric

¹⁰ See <http://fairmode.ew.eea.europa.eu/>.

representation can be employed that captures the salient details. This adds modelling uncertainty by simplifying relationships but allows the average parameter value to represent the process adequately. For example, there are many potential transfer coefficients for a radionuclide between a cow's intake and milk production. These are determined by a multiplicity of physiological processes, but a single average value that encompasses all transfer processes can be determined by a suitable experiment. In principle, carrying out further investigations to improve knowledge can reduce uncertainties. However, uncertainty is not simply the absence of knowledge. Uncertainty can still exist in situations even after more information has become available. Also, new information can either decrease or increase perceived uncertainty by revealing the presence of complexities previously unknown or poorly understood. In other words, more knowledge does not necessarily imply less uncertainty. Though it may reveal uncertainties that were previously hidden, it may not help to resolve them. When conducted in combination, sensitivity and uncertainty analyses allow model users to be more informed about the confidence that can be placed in model results. A model's ability to support a decision becomes better known when information is available to assess these factors.

In order to succeed in building a useful model, many steps (adapted from [167]) must be followed:

- Problem Identification
 - What is the goal of the model?
 - Who will use it?
 - What types of decisions will it support?
 - What data are available to support the model?
- Conceptual Model
 - Alternative hypotheses
 - Assumptions
 - Uncertainties
 - Peer Review
- Constructed Model
 - Spatial/temporal resolution
 - Algorithm choice
 - Assumptions
 - Data availability/software tools
 - Quality assurance/quality control
 - Test scenarios
 - Corroboration with observations
 - Uncertainty/sensitivity
 - Peer review
- Model Use
 - Appropriateness of model for problem
 - Assumptions
 - Model extrapolation
 - Input data quality
 - Comparison with observations
 - Uncertainty/sensitivity analysis
 - Peer review

14.2.1. Model development

Model development includes confirming whether a model is a useful tool to address the problem, determining what type of model would be the most useful, and developing the appropriate model.

Model development can be viewed as a process with three main steps:

- (1) Specify the environmental problem (or set of issues) the model is intended to address and develop the conceptual model;
- (2) Evaluate or develop the model framework (develop the mathematical model);
- (3) Parameterize the model for the application.

For WG7, the purpose of the model is to provide a robust assessment for accident preparedness and management of potential tritium accidents. If the uncertainty is known and relatively small, the same model can be used for licensing purposes by increasing the predicted doses by a safety factor. Due to the large range of environmental conditions, the model must function at a process level. Use of the interaction matrix is essential in achieving this (see Section 3). Furthermore, a deeper analysis is needed of various processes that drive the dynamics of tritium in the environment. A review published in 1998 [74] must be updated.

The complexity of the model directly influences the final uncertainty and can limit the suitability of the model to address the problem of concern. Two general aspects must be considered:

- Model framework uncertainty, which is a function of the soundness of the model's underlying scientific foundations.
- Data uncertainty, which arises from measurement errors, analytical imprecision and limited sample size during collection and treatment of the data used to delimit the values of the model parameters.

These two types of uncertainty have a reciprocal relationship, with one increasing as the other decreases. Thus, as illustrated in Figure 67, an optimal level of complexity (the “point of minimum uncertainty”) exists for each model. As Figure 67 illustrates, as models become more complex to describe more physical processes, their performance tends to decrease, because they require many input variables, leading to larger data uncertainty. Because different models contain different types and ranges of uncertainty, it can be useful to conduct a sensitivity analysis early in model development to identify the relative importance of model parameters.

Model complexity can be constrained by eliminating parameters when sensitivity analyses show that they do not significantly affect the output and when there is no process-based rationale for including them. However, a variable of little significance in one application of a model may be more important in a different application. Hence, it is important to identify the efforts that are needed to adequately parameterize the model framework and support the application of a model by examining existing data and and/or field collection. The National Research Council (NRC) Committee on Models in the Regulatory Decision Process [404] recommended that models used in the regulatory process should be no more complicated than is necessary to inform the regulatory decision and that it is often preferable to omit capabilities that do not substantially improve the model performance.

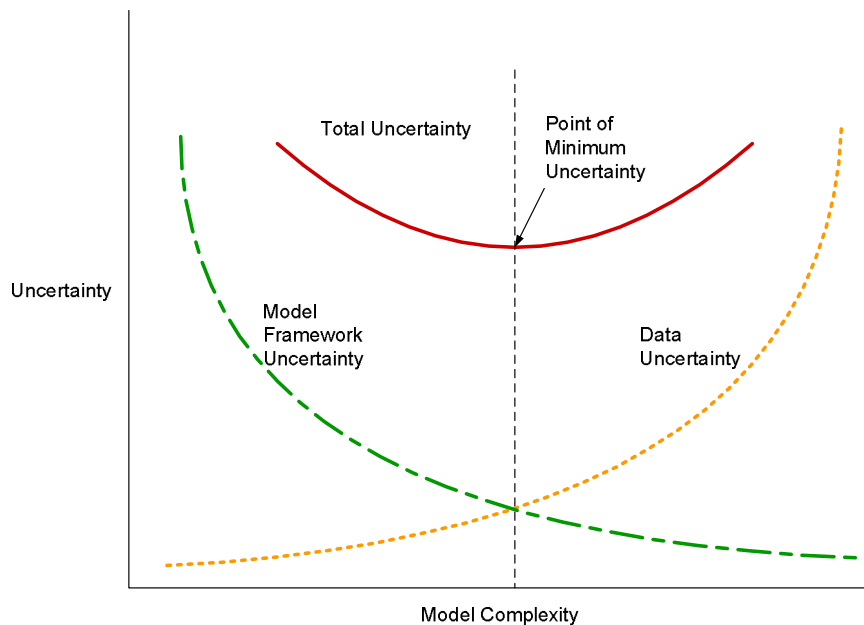


FIG. 67. Relationship between model framework uncertainty and data uncertainty and the combined effect on total model uncertainty (taken from [167]).

The accuracy, variability, and precision of input data used in the model are a major source of uncertainty:

- Accuracy refers to the closeness of a measured or computed value to its “true” value (the value obtained with perfect information). Due to natural heterogeneity and random variability (stochasticity) of many environmental systems, this “true” value exists as a distribution rather than a discrete value;
- Variability refers to differences attributable to true heterogeneity or diversity in model parameters. Because of variability, the “true” value of model parameters is often a function of the degree of spatial and temporal aggregation.
- Precision refers to the quality of being reproducible in outcome or performance. With models and other forms of quantitative information, precision often refers to the number of decimal places to which a number is computed. This is a measure of the “preciseness” or “exactness” of the model.

Modellers should always select the most appropriate data for use in modelling analyses. Whenever possible, all parameters should be directly measured in the system of interest.

For WG7, at the moment when this report was edited, a very complex model (SOLVEG-H3, see Section 11), a relatively simple one [405], and a series of intermediate models: UFOTRI [92], ETMOD [91], IFIN [269] were examined. An international coordinated research programme must use what is available to find a harmonized model with minimal uncertainty for practical application.

14.2.2. Model evaluation

The challenge of developing a model has been met when a model, despite its uncertainties, can be appropriately used to inform a decision. Model evaluation is the process of deciding whether and when a model is suitable for its intended purpose. It builds confidence in model applications and increases the understanding of model strengths and limitations. It involves peer review, corroboration of results with data and other information, quality assurance and quality control checks, uncertainty and sensitivity analyses, and other activities.

Model evaluation should not be confused with model validation, as “validated” means (a) proved to correspond exactly to reality or (b) demonstrated through experimental tests to make consistently accurate predictions. Because every model contains simplifications, the predictions derived from a model can never be completely accurate and a model can never correspond exactly to reality. Thus, some researchers assert that no model is ever truly “validated”; models can only be invalidated for a specific application. Accordingly, guidance [167] focuses on processes and techniques for model evaluation rather than model validation or invalidation.

“Verification” is another term commonly applied to the evaluation process, but model verification typically refers to verification of the computer code. Verification refers to activities that are designed to confirm that the mathematical framework embodied in the module is correct and that the computer code for a module is operating according to its intended design. Thus, results obtained compare favourably with those obtained using known analytical solutions or numerical solutions from simulators based on similar or identical mathematical frameworks.

In simple terms, model evaluation provides information to help answer four main questions [167]:

- (1) How have the principles of sound science been addressed during model development?
- (2) How is the choice of model supported by the quantity and quality of available data?
- (3) How closely does the model approximate the real system of interest?
- (4) How does the model perform the specified task while meeting the objectives set by QA project planning?

Regulatory models exhibit some fundamental characteristics:

- They are always constrained by computational limitations, assumptions, and knowledge gaps;
- They can never be completely “validated” in the traditional sense, but they can be “evaluated”;
- They are typically used to describe important, complex, and poorly characterized problems;
- They are best seen as tools providing input, as opposed to “truth generating machines”.

There are several “tools” or best practices to address these constraints:

- Data analysis: to evaluate or summarize input and model output data;
- Identifiability analysis: to expose inadequacies in the data or suggest improvements in the model structure;

- Parameter estimation: to quantify uncertain model parameters using model simulations and available output data;
- Sensitivity analysis: to determine which inputs are the most significant;
- Uncertainty analysis: to quantify output uncertainty by propagating sources of uncertainty through the model;
- Multi-model analysis: to evaluate the model uncertainty or generate combined predictions using many plausible models;
- Bayesian networks: to combine prior distributions of uncertainty with general knowledge and site-specific data to yield an updated (a posteriori) set of distributions.

The most used practical tools are: peer review of models; QA project planning, including data quality assessment; model corroboration (qualitative and/or quantitative evaluation of a model's accuracy and predictive capabilities); sensitivity and uncertainty analyses; and operational model evaluation. These tools and practices include both qualitative and quantitative techniques [167]:

Qualitative assessments: Some of the uncertainty in model predictions may arise from sources whose uncertainty cannot be quantified. Examples are uncertainties about the theory underlying the model, the manner in which that theory is mathematically expressed to represent the environmental components, and the theory being modelled. Subjective evaluation of experts may be needed to determine appropriate values for model parameters and inputs that cannot be directly observed or measured (e.g. air emissions estimates). Qualitative assessments are needed for these sources of uncertainty. These assessments may involve expert elicitation regarding the system's behaviour and comparison with model forecasts.

Quantitative assessments: The uncertainty in some sources — such as some model parameters and some input data — can be estimated through quantitative assessments involving statistical uncertainty and sensitivity analyses. These types of analyses can also be used to quantitatively describe how model estimates of current conditions may be expected to differ from comparable field observations. However, since model predictions are not directly observed, special care is needed when quantitatively comparing model predictions with field data.

Peer review provides the main mechanism for independent evaluation and review of environmental models. Peer review provides an independent, expert review of the evaluation; therefore, its purpose is two-fold:

- To evaluate whether the assumptions, methods, and conclusions derived from environmental models are based on sound scientific principles;
- To check the scientific appropriateness of a model used to inform a specific regulatory decision. (The latter objective is particularly important for secondary applications of existing models).

In the case of WG7, the peer review is accomplished through discussions at the meetings and by encouraging the modellers to publish results in top peer reviewed journals.

14.2.2.1. *Corroboration, sensitivity analysis and uncertainty analysis*

The question “How closely does the model approximate the real system of interest?” is unlikely to have a simple answer. In general, answering this question is not simply a matter of comparing model results and empirical data.

Three approaches are used to understand the uncertainties underlying the model:

- Model corroboration, which includes all quantitative and qualitative methods for evaluating the degree to which a model corresponds to reality;
- Sensitivity analysis, which involves studying how a change in model input values or assumptions affects its output or response;
- Uncertainty analysis, which investigates how a model might be affected by the lack of knowledge about a certain population or the real value of model parameters.

Model corroboration includes all quantitative and qualitative methods for evaluating the degree to which a model corresponds to reality [167]. Quantitative model corroboration uses statistics to estimate how closely the model results match measurements made in the real system. Qualitative corroboration activities may include expert elicitation to obtain beliefs about a system’s behaviour in a data-poor situation. Formal corroboration may involve formulation of hypothesis tests for model acceptance, tests on datasets independent of the calibration dataset, and quantitative testing criteria. Robustness is the capacity of a model to perform equally well across the full range of environmental conditions for which it was designed. Quantitative model corroboration methods are recommended for choosing among multiple models that are available for the same application.

Sensitivity analysis is recommended as the principal evaluation tool for characterizing the most and least important sources of uncertainty in environmental models.

Uncertainty analysis investigates the lack of knowledge about a certain population or the real value of model parameters. Uncertainty can sometimes be reduced through further study and by collecting additional data. EPA guidance [167] distinguishes uncertainty analysis from methods used to account for variability in input data and model parameters.

Although sensitivity and uncertainty analyses are closely related, sensitivity is algorithm-specific with respect to model “variables” and uncertainty is parameter-specific. Sensitivity analysis assesses the “sensitivity” of the model to specific parameters and uncertainty analysis assesses the “uncertainty” associated with parameter values. Both types of analyses are needed to understand the degree of confidence a user can place in the model results.

The National Research Council (NRC) Committee [404] pointed out that uncertainty analysis for regulatory environmental modelling involves communicating the uncertainties to policy makers, i.e. “Effective uncertainty communication requires a high level of interaction with the relevant decision makers to ensure that they have the necessary information about the nature and sources of uncertainty and their consequences. Thus, performing uncertainty analysis for environmental regulatory activities requires extensive discussion between analysts and decision makers” [404].

14.3. SOURCES OF UNCERTAINTY

14.3.1. Types of uncertainty

Uncertainties are inherent in all aspects of the modelling processes. Identifying those uncertainties that significantly influence predictions (either qualitatively or quantitatively) and communicating their importance is the key to successfully integrating information from models into the decision making process. For organizational simplicity [167], uncertainties that affect model quality are categorized as:

- Model framework uncertainty, which results from incomplete knowledge about factors that control the behaviour of the system being modelled, limitations in spatial or temporal resolution, and simplifications of the system.
- Model input uncertainty, which result from data measurement errors, inconsistencies between measured values and those used by the model (e.g. in their degree of aggregation/averaging), and parameter value uncertainty.
- Model niche uncertainty, which results from the use of a model outside the system for which it was originally developed and/or from developing a larger model by combining several existing models with different spatial or temporal scales.

The sources of uncertainty in predictions from models can be grouped into broad categories [395] as illustrated in Figure 68 and outlined here:

- *Measurement uncertainty* is the uncertainty (e.g. lack of precision, inaccuracy, sampling and analysis errors) in the field or laboratory data on which models are based. In addition human errors (e.g. incorrect or misapplied measuring techniques and systematic errors such as measurements taken on disturbed samples, because in situ measurements are impossible) contribute to measurement uncertainty. For WG7, a good example is the measurement of OBT which is potentially highly uncertain. The OBT definition is restricted to biogenic carbon-bound and buried tritium formed in living systems through natural environmental or biological processes from HTO (or HT via HTO). There is no internationally accepted measurement procedure for the extraction of exchangeable organic tritium. Moreover, the many chemical forms of OBT with their different temperature dependencies affect the combustion technique and increase the uncertainty of the measurement.
- *Parameter value uncertainty* is caused by not knowing the most appropriate values to select for the various parameters of a model. Data may not have been collected, or it may be too expensive and/or resource intensive to measure needed data. Different data sets may have conflicting values. Parameter value uncertainty can also arise when the parameters of a model are not closely related to measurable quantities; this can make the interpretation of available data difficult. Data used to derive a parameter may not represent the parameter due to scale and geometric effects. An example in WG7 is the exchange rate between air and leaf water. This lumped parameter has a large range of experimental values because many processes are involved (see Section 6).

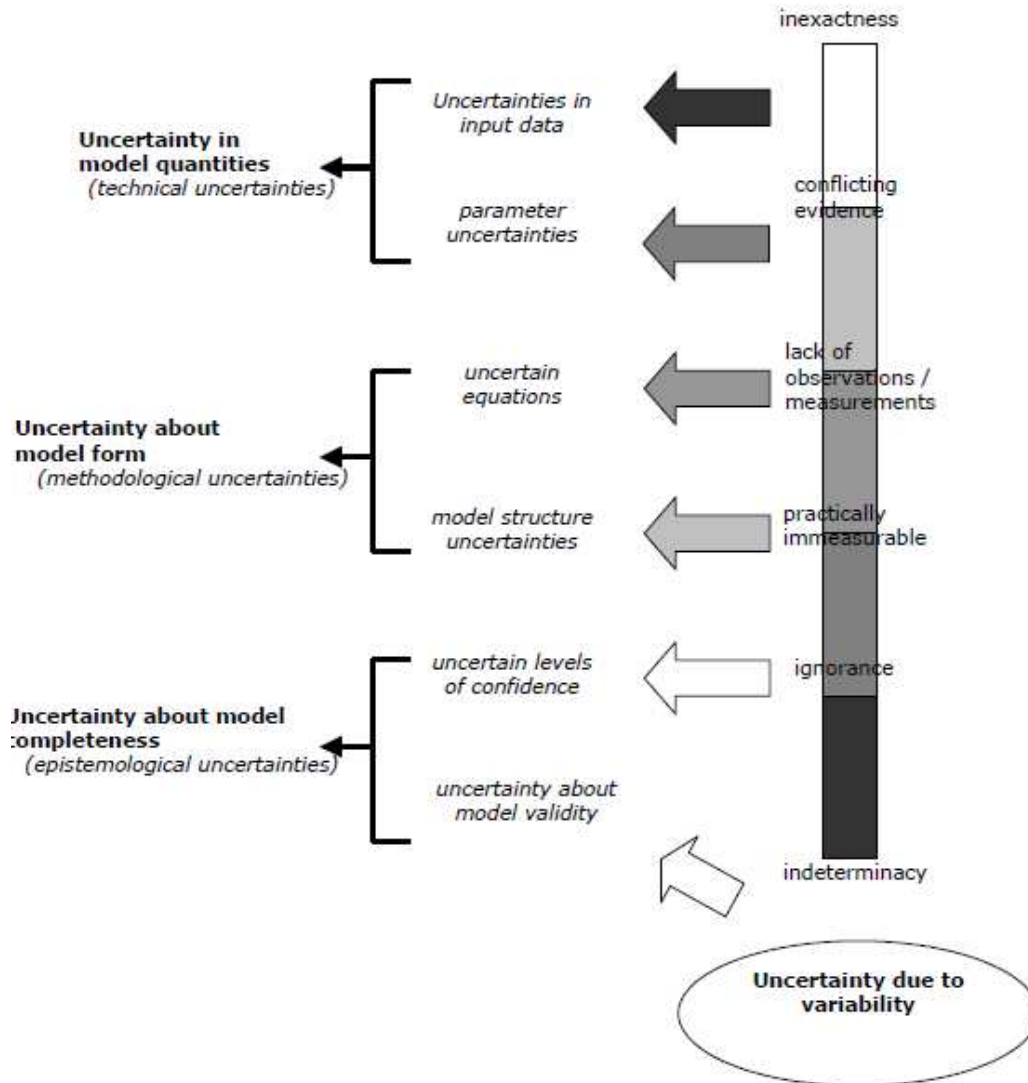


FIG. 68. A modellers' view of uncertainty (taken from [406]).

- *Conceptual modelling uncertainty* encompasses how well with the model coherently represents the various processes using available data. When a choice might exist between models, general considerations of simplicity, adequacy and underlying physical principles will govern the selection of an appropriate model. Model structural error is often overlooked when performing uncertainty analysis because the implicit assumption is that the model is a good 'fit' to the environment that it purports to represent. Many environmental models perform badly when compared with observations [407]. The conceptual model should be as complete and as appropriate to the scenario as possible, based on the information and data available, as well as on previous experience with similar types of problems. The formulation of the conceptual model can lead to uncertainty in a number of ways [408]:
- not all relevant pathways and processes may be included in the model;
 - the model may contain some pathways or processes that are not relevant;
 - the state of the system maybe poorly known so that the spatial variability and the future evolution of the system are likely to be poorly understood.

The Korean model [405] provides an example of conceptual uncertainty. The transfer of tritium between the OBT and HTO compartments of the plant body are modelled by two different pathways, with or without loss of OBT.

- *Computational (mathematical) uncertainty* arises from the representation of the selected model in computational terms. It includes the use of simplifying assumptions (because of an incomplete knowledge of the processes associated with the phenomena to be modelled), the inability to express many of the processes in exact mathematical terms, discretization (for spatial and temporal scales), and numerical methods of solution. For tritium, the spatial discretization in soil is of concern, due to the large gradient in the soil water pressure head and hydraulic conductivity near the surface. For accidental releases, temporal discretization must consider a small time step (10 minutes to half an hour) during the first few days post-accident to cope with changing meteorological conditions. Model structural error is ubiquitous and difficult to assess. Even if the conceptual model reflects reality, it may be poorly represented in computational terms and subject to structural error. The uncertainty in the models should be consistent with the effective observational error.
- *Scenario uncertainties* are those which cannot be adequately depicted in terms of chance or probability, but which can only be specified in terms of (a range of) possible outcomes. In dose assessment, this source of uncertainty includes the need to make assumptions about the habits of animals in the food chain and human behaviour. For WG7, the most relevant example is the variability of meteorological conditions and consequent influence on tritium transfer in crops. For an accidental release, actual meteorological data are available for use in calculations. For the prediction of consequences, predicted weather conditions must be used for at least the next 2–3 days based on the local forecast. Even the most advanced weather forecast provide the probable weather with quite large uncertainty.
- *Subjective uncertainty* arises from the reliance of the assessment team on expert (user) judgement at many stages of the assessment. This uncertainty can be due to a variety of reasons, such as lack of knowledge about current and future conditions, choice of conceptual model, and assumptions about data/parameter values (and distributions). The effect of subjective uncertainty is illustrated by the user interpretation exercise in BIOMOV5 II [409]. In this exercise, the same three scenarios and the same computer codes were provided to participants. For any set of calculations, the variation in the best estimates was larger than an order of magnitude, and most calculations showed an order of magnitude difference between best estimates and actual measured values. In this exercise, the choice of parameter values contributed the most to the user-induced variability, followed by scenario interpretation, and, to a lesser extent, to user error. The contribution due to code implementation was low [409].
- *Ignorance*: “Although not a manageable category of uncertainty, the recognition of ignorance allows for the fact that “we don't know what we don't know” and that there are inherent limitations to the reduction of uncertainty” [395]. In other terms we have:
 - Type III modelling error: processes are neglected because of ignorance of how the system works [410].

Tritium enters the life cycle, many aspects of which are not very well understood. For example, at this moment, there is no quantitative explanation of OBT formation in crops at night. In general, tritium models suffer from subjective ignorance due to incomplete documentation and insufficient use of information from other disciplines.

14.4. TECHNIQUES TO MANAGE UNCERTAINTIES

Because it is difficult to quantify uncertainty, in most cases the quantification of uncertainty is in itself uncertain. Uncertainty is, in part, socially constructed and its assessment includes subjective judgements. Thus, the management of uncertainty is not just a technical exercise [395]. Those carrying out such uncertainty assessments should consider a number of issues before starting:

- Who will be the recipient of the assessment?
- What decisions will be made based on the assessment? Will inclusion of uncertainty and variability improve those decisions?
- Will incorporation of uncertainty and variability improve the assessment?
- What are the major sources of uncertainty and variability? How will these be kept separate in the analysis?
- What are the time and resource implications of including uncertainty and variability? Is this effort justified?
- Are the necessary skills and experience available to assess the uncertainty?
- What methods of incorporating uncertainty and variability are to be used? Have the strengths and weaknesses of those methods and other potential methods been evaluated and compared?
- How will the results be communicated to the public and decision-makers?

To build confidence in an assessment and to assist the decision-making process, it is important that uncertainties are identified and managed appropriately. Indeed, the International Commission on Radiological Protection (ICRP) recommends that “uncertainty analysis should be an integral part of the dose or risk calculation process and that whenever possible, reported results should include ranges of possible values rather than a single point value” [411]. The ICRP goes on to note that the uncertainty analysis should fit the purpose of the assessment [411].

It is impossible to guarantee with any absolute certainty that the “correct” decision has been made. However, the probability of making an appropriate decision can be improved by identifying and managing the uncertainties.

The management of uncertainties has four main components [412]:

- Awareness: Uncertainties cannot be managed if they are not known about. A safety assessment should identify all major potential sources of uncertainty.
- Importance: Some uncertainties have significant effects on the safety case, whilst many others are unimportant. Before attempting to reduce uncertainties it is first necessary to determine whether the uncertainty has a significant effect on the overall outcome of the safety assessment. This can be accomplished using sensitivity analysis.
- Reduction: Having ascertained the importance of particular uncertainties, measures can then be undertaken to reduce them.
- Quantification: The effect of uncertainties on the final safety assessment needs to be quantified using uncertainty analysis. Some uncertainties are more difficult to quantify than others, but an attempt should be made to quantify the most important ones.

The relative importance of sources of uncertainty can vary from assessment to assessment and can be up to four orders of magnitude. It was found that:

- Uncertainty associated with predictions for a long term assessment of a waste repository can typically range between three and five orders of magnitude. For an accidental atmospheric tritium release, unknown weather conditions can contribute less than an order of magnitude uncertainty, but more research is needed.
- Uncertainty associated with conceptual, mathematical and computer models is generally less than two orders of magnitude [4];
- Uncertainty associated with the data/parameters sometimes exceeds an order of magnitude, but more research for tritium accidents is needed.

14.4.1. Management of scenario uncertainty

Scenarios are descriptions of alternative, but internally consistent, future changes and conditions. Future uncertainty is handled directly by describing alternative futures and allowing quantitative analysis and qualitative judgement. Scenarios do not predict the future; rather, the aim of a scenario is to identify salient changes, based on analysis of trends, within which variants are explored, to investigate the importance of particular sources of uncertainty. The emphasis is therefore on providing meaningful illustrations of future conditions to assist in the decision-making process [413]. For the treatment of scenario uncertainties, there is a need for a consistent approach for identifying the relevant assumptions and hypotheses. The IAEA's BIOMASS programme has recommended the use of a well defined methodology for "Reference Biospheres" (and associated exposed humans) for estimating radiation doses arising from long-term releases of radionuclides to the environment [414]. The main steps in the methodology can be applied to the purposes of WG7:

- Development and confirmation of the assessment context;
- Biosphere system identification and justification;
- Biosphere system description;
- Identification of representative exposed population groups, including hypothetical critical groups;
- Conceptual and mathematical model development for radionuclide migration and accumulation, and consequent radiation exposures;
- Calculation of assessment end-points (e.g. doses) and confirmation, normally by iteration of some or all of the above steps, of the characteristics of the hypothetical critical groups.

In WG7, hypothetical scenarios, coupled with site specific information and various sequences of meteorological data, are used for accident preparedness. The "Hypothetical Releases" [4] scenario, in which the transfer of tritium at the receptor was well defined but the meteorological conditions following an accidental release were not, was an interesting exercise. For licensing purposes, the scenario must represent the worst case, and the model must be run using a large selection of multi-year meteorological data. Because nuclear reactors may work for 40–60 years, studies must also include the influence of climate change as a source of uncertainty in the scenario.

14.4.2. Management of model uncertainty

Conceptual model uncertainty can be reduced through additional modelling studies and data collection which allow better defined conceptual models to be developed. Tools, such as *Interaction Matrices* and *Process Influence Diagrams*, provide a graphical representation of the conceptual model and its associated processes.

Certain measures can be taken to facilitate the assessment of conceptual model uncertainty. If models are described explicitly, including lists of assumptions, then a comparison may provide at least a qualitative understanding as to why various results differ and what the critical decisions are. Conceptual model uncertainty can be treated through a bias audit of all conceptual decisions. All alternative decisions can be considered, employed, or ruled out (for whatever reason), and estimates can be made of potential shifts, or biases, in the results that result from the adoption of these alternatives. The main objective of this audit is to review the modelling assumptions and provide a quantitative estimate of how well the results represent the assumptions. For each decision, there are at least two issues to be considered:

- How correct are the assumptions that are being made?
- How much impact would these have on the assessment results if they were shown/found to be incorrect?

The task to answer to these questions should lie with experts or expert groups. Because the information elicited from experts will be subjective, each expert should be asked to formulate his/her decision explicitly and include how confident s/he is in the decision.

Mathematical and computer model uncertainties, as well as conceptual model uncertainty, can be addressed through model verification, calibration and validation. Verification is achieved by solving test problems designed to show that the equations in the mathematical model are solved satisfactorily [415]. Calibration is performed by comparing model predictions with site-specific field observations and experimental measurements [415] (i.e. a set of site specific input data is used to compare model calculations and observations at a particular site).

Mathematical and computer model uncertainty can also be examined by, where possible, using a range of models and codes. For example, in the model complexity exercise in BIOMOVs II, a range of models of differing complexity calculated predictions for the same scenario [416]. For tritium, a model inter-comparison and blind test was carried out in BIOMOVs [267]. A detailed analysis of the conceptual models and parameters revealed a list of needed improvements, many of which still should be addressed. Other works with blind tests and model inter-comparisons have been done in the framework of the EMRAS I programme [4].

14.5. MANAGEMENT OF DATA/PARAMETER UNCERTAINTY

Uncertainty in the quality and accuracy of data and parameters can often be considerably reduced in radiological assessments, by collecting further field data and applying suitable quality assurance procedures during the collection and manipulation of the data. However, it is impossible to completely eliminate data and parameter uncertainty from safety assessments, especially when site characteristics can change over the timescales of the assessment so that the parameter values may no longer be appropriate.

Five approaches can be used to handle data/parameter uncertainty (these approaches can also be used to address scenario and model uncertainties) [412].

- Conservative/worse case: In the conservative approach, an attempt is made to choose parameter values that will result in an overestimation of the impact of tritium transfer. There is a danger that if conservative values are assigned to all parameters, the resulting overestimated prediction will become worthless and misleading. Also, in certain cases it becomes difficult to define and prove the worst (i.e. most conservative) value. Furthermore, it is not always obvious what is conservative for a particular combination of parameters, exposure pathways and radionuclides.

However, there can be times when the conservative approach can be useful. For example, in some cases it might be simpler and more pragmatic to take a conservative approach for certain aspects of the transfer than to model them in detail.

- Best estimate and what if: In the best estimate approach, a central (“the best estimate”) set of parameter values is used. It is often unclear how these values have been chosen because there can be a tendency to err on the side of conservatism when choosing them. This, obviously, is inconsistent with the normal meaning of “best estimate”. This kind of confusion can lead to serious problems when the results are explained. Furthermore, uncertainty/variability in parameter values is ignored.
- Sensitivity analysis: This allows the effect of perturbations in the values of input parameters to be investigated. Such perturbations could arise from data/parameter uncertainties but also from scenario and model uncertainties. The overall robustness of the transfer system to change in its parameter values (and changes in scenarios and models) can be assessed. This in turn encourages improvements to those aspects of the assessment that have the largest impact on model output. However, it must be recognised that different models may be sensitive to different parameters, depending upon the structure of the model.

The role of sensitivity analysis is very important [415]. Initially, the impact on the output of a single parameter or a few combinations of a few parameters should be considered. Different methods for varying parameter values can be used for this task, but the analysis should be structured carefully to ensure that the combinations that are chosen by the computer code are not physically unrealistic. In addition, the output from the exercise should be structured to preserve the information that determines the sensitive combinations and identifies the sensitive parameters.

- Probabilistic: With this approach, all uncertain and variable parameters are described by probability density functions (PDFs) that characterise their uncertainties and variability [415]. A rigorous mathematical approach based on the Monte Carlo method with random sampling techniques (such as Simple Random Sampling and Latin Hypercube Sampling [417]) is then used to analyse the parameter uncertainty and variability and generate PDFs for the results. Similarly, scenarios and conceptual models can be described by PDFs.

Difficulties with the probabilistic approach include:

- Requiring more computational effort and more man-hours to prepare the input and interpret the output than a deterministic approach;

- Being less understood by non-technical audiences than a deterministic approach;
- Needing to recognise correlations between parameters so that physically unrealistic combinations of parameter values cannot occur; and
- Needing to justify the chosen probability distributions for each sampled parameter.

More fundamentally, the use of probability theory may be inappropriate for the types of uncertainty that are to be addressed. Often it is the experts rather than the parameter values that are uncertain. Thus, the uncertainties are largely subjective and not well characterised by probabilities. Such problems are compounded by the fact that regulatory targets are usually expressed as deterministic rather than probabilistic numbers.

For tritium, a parameter uncertainty analysis was done for one scenario and one model, UFOTRI [418]. One finding was that correlations between some model parameters must be explicitly considered. Ranking each parameter's contribution to overall uncertainty revealed the important parameters. The scenario described a 1 hour release of atmospheric tritium in prescribed meteorological conditions. When the UFOTRI code was run with more variable meteorology, the ranking of the key parameters changed [68]. More examples can be found in the previous Tritium and Carbon WG [4] for dynamic scenarios. No definitive conclusions can be drawn regarding the uncertainties in the model predictions. However, rough estimates can be obtained from an overall assessment of the scatter in the predictions and the differences between predictions and observations. These suggest that the 95% confidence intervals on HTO and ^{14}C concentrations were about a factor of 10 shortly after the release. These intervals stayed roughly constant over time for the Mussel scenario [339], Pig scenario [273] and Potato scenario [419], but increased to a factor of 100 or higher later in time in the Soybean scenario [7] and at longer distances from the source in the Hypothetical scenario [4]. The confidence intervals were generally smaller for OBT than for HTO, reflecting the fact that, for the dynamic scenarios, HTO concentrations vary rapidly over time whereas OBT concentrations are integrated.

- Possibilistic/Fuzzy: This approach uses fuzzy set theory and is suitable for the treatment of non-stochastic (subjective) uncertainties. Possibility distributions (membership functions) for each parameter are combined to give a possibility distribution for a calculated result. The combination rules for possibilities are different from those for probabilities – minima and maxima are used in place of products and sums. Apart from these differences, the fuzzy approach can be undertaken in a similar manner to the probabilistic approach.

Uncertainties associated with scenarios, models and parameters were defined in terms of fuzzy membership functions derived through a series of interviews with experts, while variability was formulated through the use of PDFs based on available data sets. The exercise demonstrated the applicability of the approach and, in particular, its advantage in quantifying uncertainties based on expert opinion and in providing information on the dependence of assessment results on the level of conservatism.

14.6. MANAGEMENT OF SUBJECTIVE UNCERTAINTY

Subjective uncertainties can be managed in three main ways: (a) first, through the use of fuzzy set theory; (b) second, as suggested in BIOMOVs II [420], through the assessment of the same problem by two or more independent teams. (This approach has been used in a number of assessments of near surface disposal facilities, but unfortunately, up to now, none

have been published); and (c) third, through a systematic and transparent approach to the assessment. These methods should allow all subjective judgements to be documented, justified and quantified (as far as possible). A key requirement is model documentation.

User's Manual: The user's manual can often borrow heavily from the software requirements document which specifies all the software functions. The scope of the user's manual should take into account such issues as the level and sophistication of the intended user and the complexity of the interface. Online help can also serve this function if such help is provided by the code developers.

14.7. CONCLUSIONS

Once the scenarios and associated conceptual and mathematical models have been developed and implemented in computer codes and the associated data collated, two types of calculations can be undertaken to assess the impacts of tritium releases: deterministic and probabilistic. At the completion of the calculations, the results need to be collated and analysed. The results should be compared with calculation end-points that were identified when the assessment context was developed. When the results are analysed, it is important to recognise that there are a number of sources of associated uncertainty that must not be ignored (scenario, model, data/parameter, and subjective uncertainties). Because of this, the results should not be seen as absolute values, and any comparison with regulatory criteria and any subsequent decisions should be undertaken with this firmly in mind.

Different techniques are needed to manage different types of uncertainty. The uncertainty management process should provide a variety of useful insights including:

- An appreciation of the overall degree of variability and uncertainty and the confidence that can be placed in the analysis and its findings;
- An understanding of the key sources of variability and uncertainty and their impacts on the assessment;
- An understanding of the key assumptions and their impact on the assessment;
- an understanding of the unimportant assumptions and why they are unimportant;
- An understanding of the extent to which plausible alternative assumptions or models could affect any conclusions.

Once the results (and associated uncertainties) have been analysed, there is a need to determine the adequacy of the safety assessment. This should be based on reasonable assurance rather than on an absolute demonstration of compliance. If the assessment is found to be inadequate, further iteration of the entire process or parts of the process can be undertaken to improve its adequacy.

In conclusion, certain minimum standards are needed when reporting on model development and performance and to advance knowledge:

- Clear statement of the objectives of the model and who will be the end users of the model;
- Documentation of the nature (identity, provenance, quantity and quality) of the data used to drive, analyze and test the model;
- A strong rationale for the choice of model families and features (encompassing alternatives);

- Justification of the methods and criteria employed in calibration;
- A thorough analysis and testing of model performance given the resources and the demands of the application;
- A statement of model utility, assumptions, accuracy, limitations, and the need and potential for improvement.

When a complete report that meets the criteria listed above has been prepared, it should support informed criticism.

15. STATUS AND PERSPECTIVES OF ACCIDENTAL TRITIUM MODELLING

Although we know much about water behaviour in the environment, the sound prediction of tritium concentrations in environmental media after an accident must account for complex interactions between a number of factors that are subject to hourly, daily and annual fluctuations. Due to large uncertainties in the environmental conditions at the time of the accidental release, predictions are unavoidably associated with considerable uncertainty. At the beginning of EMRAS II WG7 activities, the goals for investigating the problems that must be solved to reliably model tritium transfer in the food chain following accidental releases to the atmosphere or to the aquatic environment were defined, as follows:

- To identify the main contributors to uncertainty;
- To identify the times of the year that will result in the highest exposures to tritium after an accidental release;
- To identify the important and sensitive parameters, bearing in mind hourly, daily and annual variations in parameters/processes;
- To explore how practical it is to determine those parameters and their values;
- To assess the achievable reliability of tritium modelling in practice under accidental field conditions;
- To clarify which phases of a tritium accident can be best handled by a model.

The present TECDOC only partially accomplishes these goals because of limited time and budget and the complexity of the task. For tritium washout, updated information is presented, providing all the necessary input to model an actual event. For aquatic food chain modelling, the WG7 report offers basic information and advice to solve a site specific task. For terrestrial modelling, much work is still needed before a final robust conceptual and operational model can be made available. Depending on interest and resources, the final goal can be attained in the next few years within the framework of MODARIA programme. Below, we summarize the plans in each participating institution.

IRSN (France) initially itemized the ongoing problems with sampling and measurement; evolution of the chemical form of tritium in the atmosphere, vegetation, soil and groundwater; quantification of dry and wet deposition; and quantification of organically bound tritium (OBT). The present TECDOC partially addresses these areas. The upgrades to the TOCATTA model [306] will include a finer time step than 1 day and will take into account plant physiology and local meteorology. The upgraded model still needs to be adapted to take account of large variations in radionuclide releases and weather fluctuations. An hourly time-step is required to simulate photosynthesis, including carbon-14 and tritium cycling, and simulation of water exchange. To evaluate the concentrations of ^{14}C and ^3H (HTO, OBT) in the different compartments of rural ecosystems, from the atmosphere to the groundwater *via* grassland, pasture –cow-milk pathway will be studied in the near future (Table 61).

TABLE 61. TIME SCHEDULE FOR TOCATTA UPGRADES

Upgrade	2011	2012	2013	2014
Measurements in air, rain water, grass, soil, soil unsaturated zone and ground water	X	X		
Measurements in cow milk			X	X
Model-measures comparison			X	X
Model adjustment and publications		X	X	X

For many years, AECL (Canada) has used the ETMOD model [91], which has been tested on many occasions. Some weak points include:

- (1) Predictions of plant tritium in ETMOD deviate from observations after ~72 hours post-accident; soil modelling in ETMOD needs to be updated.
- (2) Plant OBT translocation is not modelled. The model of OBT formation is needs to be improved.
- (3) Animal OBT is not modelled.

ETMOD will be merged with the CLASS (Canadian Land Surface scheme) + CTEM (Canadian Terrestrial Ecosystem Model) models. The CLASS model provides the carbon framework and soil water dynamics, while CTEM provides for carbon translocation. AECL needs to validate soil HTO processes and OBT formation. ETMOD can incorporate the validated animal module developed by IFIN-HH [312].

Because there are no Certified Reference Materials (CRMs) and no Standard OBT Procedures, AECL and CEA initiated a collaboration to improve OBT measurement . A 3 day workshop will be held in France (May 2012) on environmental tritium monitoring, OBT in environmental samples and plans for three inter-comparison exercises (2012–2015).

At JAEA (Japan), the development of the complex SOLVEG-H3 (C-14) model is continuing. The model has been used to study precipitation effects on OBT formation [421]. It was concluded that night-time wet deposition of HTO markedly increases OBT formation if the HTO concentration in rain exceeds the equilibrium concentration of the air HTO near the ground. HT deposition and conversion to HTO in soil was also studied [422], and the importance of root depth and root uptake was demonstrated. At this moment there are no plans for upgrades to the SOLVEG tritium model, but the model will be applied to soil organic carbon studies (in support of climate change studies).

At IFIN-HH (Romania), a project dedicated to tritium dynamics in agricultural crops has financing until the autumn of 2014. It will include:

- New approach for HTO uptake by crops from air and subsequent conversion to OBT (during daytime and night time);
- Analysis of the processes involved in root uptake of HTO;
- Completion of a multi-compartmental model for the late phase of a hypothetical tritium accident
- Analysis of the diurnal and seasonal patterns of the model predictions using the local meteorological data base;
- Sensitivity and uncertainty analysis, with an attempt to reduce the model complexity without reducing the predictive power (economical approach);
- New approaches for atmospheric dispersion and tritium washout, other than the Gaussian model;
- Human and non-human dose assessment for a hypothetical tritium accident.

APPENDIX I. INPUT DATA FOR MODELS OF FARM ANIMALS

TABLE 62. FRACTIONS OF HYDROGEN AND CARBON IN THE BASIC CONSTITUENTS OF FOOD [300, 423]

Food constituent	Free H	Organically bound H	Total organic H	C
Water	0.11	0	0	0
Carbohydrate	0.02	0.044	0.064	0.44
Protein	0.017	0.051	0.068	0.52
Lipids	0.003	0.117	0.12	0.77

TABLE 63. CARBON AND BOUND HYDROGEN (EXCHANGEABLE AND NON-EXCHANGEABLE) CONTENT OF ANIMAL FOODSTUFFS

Food class	C content (kg C kg ⁻¹ dm)	CV	Organic H content (kg H kg ⁻¹ dm)	CV	NE organic H content (kg H kg ⁻¹ dm)
Grasses	0.418	0.03	0.06	0.03	0.043
Hay	0.424	0.012	0.061	0.02	0.043
Silage	0.403	0.09	0.058	0.07	0.041
Roots	0.414	0.05	0.059	0.04	0.041
Concentrates	0.457	0.06	0.066	0.05	0.045
“Table scraps”	0.45	0.02	0.063	0.02	0.043

TABLE 64. TYPICAL HYDROGEN AND CARBON CONTENTS OF ANIMAL PRODUCTS (kg H or kg C per kg fw) [424]

Animal product	Free H	Organically bound H	Total organic H	C
Milk				
Cow	0.096	0.008	0.010	0.067
Sheep	0.090	0.014	0.016	0.107
Goat	0.095	0.009	0.010	0.070
Meat				
Beef	0.077	0.022	0.025	0.178
Veal	0.077	0.021	0.024	0.173
Mutton	0.074	0.026	0.029	0.203
Lamb	0.077	0.021	0.025	0.176
Goat	0.077	0.021	0.024	0.172
Pork	0.066	0.034	0.038	0.258
Hen	0.077	0.022	0.025	0.178
Chicken	0.080	0.019	0.22	0.155
Egg	0.074	0.018	0.021	0.142

TABLE 65. RUMINANT FEED PARAMETERS AND VALUES

Feed	dm ¹	D _{om} ²	MED ³ (kJ kg ⁻¹ fw)	MED ³ (kJ kg ⁻¹ dm)	q ⁴	K _m ⁵	K _l ⁶	K _g ⁷
Hay	0.86	0.592	7160	8326	0.45	0.66	0.577	0.357
Concentrates	0.88	0.815	10690	12148	0.64	0.74	0.657	0.528
Grain	0.88	0.87	11528	13100	0.715	0.75	0.667	0.564
Straw	0.88	0.84	1147	1303	0.302	0.6	0.525	0.241
Pasture	0.215	0.72	2181	10144	0.56	0.7	0.617	0.443
Upland pasture	0.376	0.51	2200	5851	0.344	0.65	0.5404	0.27432

¹ Dry matter; ² Organic matter digestibility; ³ Metabolisable energy density; ⁴ Metabolisability; ⁵ Efficiency for maintenance; ⁶ Efficiency for lactation; ⁷ Efficiency for growth.

APPENDIX II. TRITIUM DYNAMICS IN AN AQUATIC ENVIRONMENT FOR TROPICAL ENVIRONMENTS

II.1. OVERVIEW

In this appendix, an assessment of tritium accidents in an aquatic tropical environment that was requested by Working Group 7 (WG7) of the Project on Environmental Modeling for Radiation Safety (EMRAS II) is presented. Results were generated using computational models that run mathematical equations of environmental hydrodynamics and contaminant transport. Maps and graphics are shown below that enhance the main points discussed in the text.

The work describes the hydrodynamic circulation and transport of tritium (HTO) in the Ilha Grande Bay, where the operational Nuclear Power Plants of Brazil are situated. The objectives of the modeling approach were to:

- Describe the hydrodynamic circulation in the two horizontal directions with vertical averaging (2DH), considering different tide patterns on the model domain.
- Discuss aquatic processes that must be considered to assess the radiological consequences of tritium accidents in conjunction with aquatic environmental characteristics such as forcing features and climate.
- Assess the dispersion of the HTO plume in Ilha Grande Bay from an accidental release (LOCA) of 50% of the liquid tritium inventory from a hypothetical CANDU 6 reactor (see accident description in Section II.4.4).

II.2. STUDY AREA AND MODELLING SYSTEM

Figure 69 shows a map with the mesh discretization, composed of 1163 finite elements and 5403 knots, and the bathymetry of the modeled domain. The Ilha Grande Bay supplies water to nuclear plants from Itaorna beach; afterward the liquid wastes are discharged in another part of the bay (Piraquara de Fora). The modeled domain has a terrestrial outline and two external boundaries, called open boundary 1 and 2, placed respectively to the west and east of the bay.

The Database System for Environmental Hydrodynamics (SisBAHIA®) is a computational model applied to hydrodynamical circulation and advection-diffusion contaminant transport in natural water bodies under different meteorological, fluvial, lacustrine or oceanographic conditions that has been continuously developed by the Program on Coastal and Oceanographic Engineering of the Federal University of Rio de Janeiro since 1987. It runs using the FORTRAN programming language.

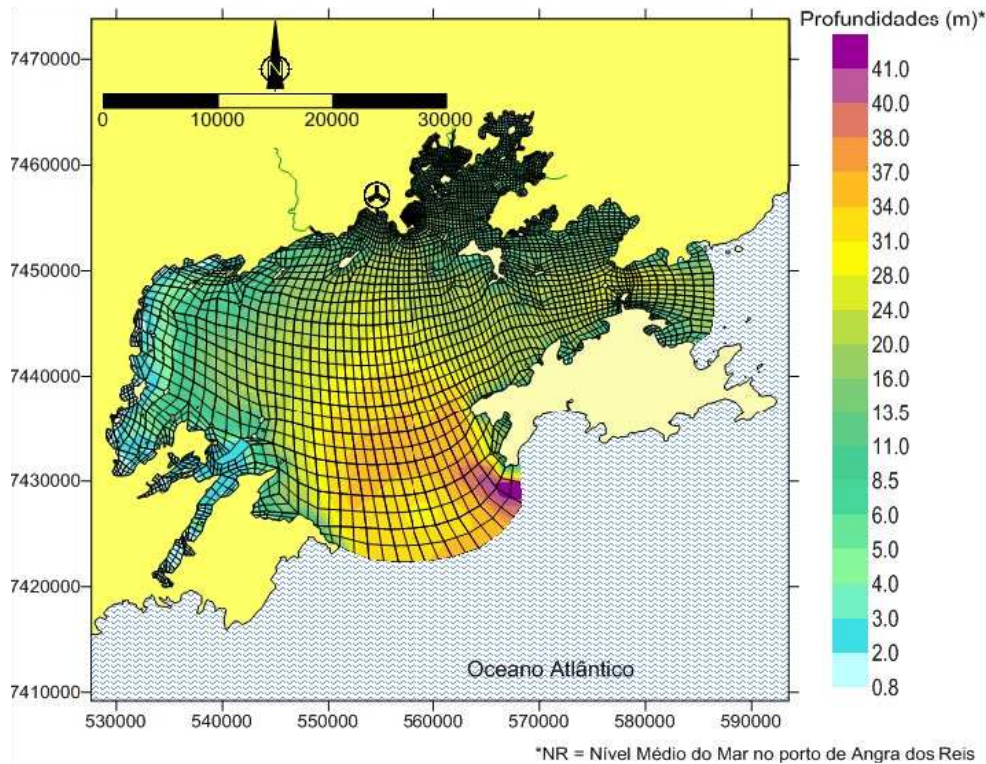


FIG. 69. Modelled domain of Ilha Grande Bay, illustrating the finite element discretization mesh and recent bathymetry with reference to mean seawater level in Angra dos Reis Harbour. The axes represent distances in meters. The radioactivity symbol shows the release area on the Nuclear Plant site.

II.2.1. Model formulation, uncertainty and reliability

The mathematical models that represent hydrodynamics and contaminant transport in water bodies are generally based on conceptual laws or principles expressed by differential equations. Numerical or Numerical-Analytical models translate mathematical equations into computational language (e.g. finite difference, finite element or probabilistic models) and have high predictive power with little loss of information. The uncertainty can be largely reduced by calibration and model validation. For these reasons, a tritium assessment should consider using hydrodynamic process-oriented numerical models instead of box-model hydrological models (with high uncertainties).

The main attributes of hydrodynamic models are:

- The FIST (filtered in space and time) hydrodynamic turbulence model is based on Large Eddy Simulation (LES) to simulate vortices;
- The model computes flow velocities either in three-dimensions (3D) or in two horizontal dimensions with vertical averaging (2DH);
- The spatial discretization is based on 4th order finite elements with two-quadratic squares or quadratic triangles or both;
- Sigma transformation is used for vertical discretization resulting in a finite element mesh;

- Processing time is 50 times faster than real time, i.e. 1 day of circulation is simulated in less than half hour.

The modeling of advection-diffusion contaminant transport can be performed by two different modules of the system according to Computational Fluid Dynamics (CFD) formulations. The Eulerian module works with fixed meshes as references, while the Lagrangean module uses adaptative meshes that accompany the movement of the particles of the pollutant.

The main characteristics of Eulerian Modules are:

- Suits simulating the dispersion of dissolved substances;
- Possible to apply to 2DH or to selected layers of 3D hydrodynamic output;
- Solves scale conflict with adaptative (changing) mesh only around the contaminant
- Processing is 5 to 8 times faster than FIST3D.

The main characteristics of Lagrangean Modules are:

- Suits the scale of contaminant spots that are small in comparison with the domain;
- Useful for practically any kind of kinetic reaction of contaminant decay or production;
- Computes the position of each particle when the contaminant is represented as a cloud with countless particles. Because the particle space position is continuous, scale conflict disappears;
- 1 day of real time takes only 1 minute of simulation because the gain is around 10 to 100 times faster than FIST3D.

With two approaches:

- Deterministic: useful to simulate liquid waste discharge along the coast, mixing in the water, and residence time mapping;
- Probabilistic: computed from N events or during some time interval T that permits, for instance, the evaluation of the probability that a contaminant discharge will create some spots with activity concentrations above the derived limits or other value previously defined.

A detailed description of the SisBAHIA® computational system is available in Portuguese¹¹. A technical reference, also in Portuguese, with all the mathematical equations and numerical formulations used by the modeling system, may also be downloaded. In the link “O que é?” (what is it ?) it is possible to find a discussion about the reliability and uncertainties of the model. the SisBAHIA® computational system has been used in a large number of applications and projects that can be seen in the corresponding link (“Aplicações-Projetos”). An English version of the system is underway.

II.2.2. About the user license of SisBAHIA®

The SisBAHIA® system is freely supplied for non-commercial applications through a technical cooperation contract or term agreement with the University Foundation (COPPETEC). Instructions are available on the page link “Como Obter o SisBAHIA” (how to

¹¹ See www.sisbahia.coppe.ufrj.br.

get SisBAHIA). Commercial use of SisBAHIA® can be made through the establishment of working programs provided for in the contract. This working program can include training courses.

The source codes of the post-processing interfaces, as well as the hydrodynamical and transport models, are programmed in FORTRAN and are available through an agreement of technical cooperation with the University.

II.3. MODELLING SCENARIOS

The modeling scenarios used the input data and boundary conditions described in the next section. A hypothetical accidental release of tritium during a LOCA event (without the core melting) in a CANDU6 reactor was proposed as the exercise. In a 1 hour period, half of the tritium inventory of a CANDU6 reactor was to have been released to Ilha Grande Bay at the same location as the planned discharge of the third Brazilian Nuclear Power Plant (under construction). A period of 1 year after the accident was simulated.

All the simulations assumed astronomical tide conditions, including spring and neap tide cycles, with enough time to reach steady-state equilibrium. The tritium transport was simulated in two different hydrodynamic scenarios. In the first, the three NPPs are immediately shut down after the LOCA event, so pumping and discharge of seawater ceases. IN the second, the other two PWR reactors (operating today) keep pumping and discharging water.

When HTO is assumed to behave conservatively, sedimentation and degradation are not of concern. Even radioactive decay is negligible ($< 10\%$) for the simulated period. Advective and turbulent diffusion are the only transport mechanisms responsible for HTO aquatic dispersion, which is the main process leading to tritium uptake by organisms in form of OBT.

II.4. INPUT DATA AND BOUNDARY CONDITIONS FOR SIMULATIONS

A brief description of the parameters used in model simulations is discussed below.

II.4.1. Bathymetry

The bathymetry of Ilha Grande Bay was defined through digitizing nautical charts published by the bureau of Hydrography and Navigation (DHN chart numbers 1607, 1633, 1637 and 23100) and adding the value of 0.68 cm to correct for the reduction level used for navigation that, in the present case, corresponds to the Mean Higher Low Water (MHLW). Thus, all depth values correspond to the mean level of the bay. These data were interpolated to generate a bathymetric map (Figure 69) in which a depth value was assigned for each mesh node.

TABLE 66. HARMONIC CONSTANTS SORTED BY SIGNIFICANCE OF AMPLITUDE (ANGRA DOS REIS HARBOR STATION, ILHA GRANDE BAY)

Name	Period (s)	Amplitude (m)	Phase (degrees)
M2	44714.16439359	0.2869	1.3799
S2	43200.00000000	0.1649	1.4396
O1	92949.62999305	0.0967	1.4692
M4	22357.08219679	0.0332	0.5664
K1	86164.09076147	0.0535	2.4888
K2	43082.04523752	0.0616	1.2908
N2	45570.05368141	0.0356	2.1349
MS4	21972.02140437	0.0165	2.0408
MN4	22569.02607322	0.0144	6.0327
Q1	96726.08402232	0.0270	1.0818
L2	43889.83274041	0.0164	1.6310
P1	86637.20458000	0.0171	2.2640
2N2	46459.34813490	0.0098	2.2611
M3	29809.44292906	0.0121	3.4137
MU2	46332.00000000	0.0155	1.7054

II.4.2. Astronomical tide

The propagation of tides on the open borders was simulated from the measurements of water levels inside the domain, which also determine the boundary conditions. To simulate circulations in the Ilha Grande Bay, synthetic tides generated from the harmonic constants from Angra dos Reis Harbor were modelled.

Tide heights at the boundaries were calculated in each time step, using the harmonic constants showed in Table 66 from Angra dos Reis. A time interval 30 days that contained spring and neap tide cycles was simulated. Figure 70 shows the tide elevation curves from Angra dos Reis that were used as boundary conditions for the performed simulations.

The positioning of open border 1 is almost perpendicular to the tide front that propagates on the coast mostly from west to east; the tide front is also perpendicular to open border 2, situated in a more sheltered zone. Thus, a phase lag between the two boundaries occurs so that the tide arrives first at border 1 and arrives sometime later at border 2. This difference is estimated to be about 600 s. During outflow, the boundary conditions are prescribed as the tide level oscillation. This was accomplished by using inverse modeling to estimate tide elevations on the borders, which are obtained by applying the harmonic constants from inside the domain (Table 66) and using the same overestimation produced by model results to correct the border values. This was done because there are no tide measurements from outside the domain to use for modeling. On the other hand, during discharge, the boundary condition adopted forced the flow to enter normal (90°) to the border.

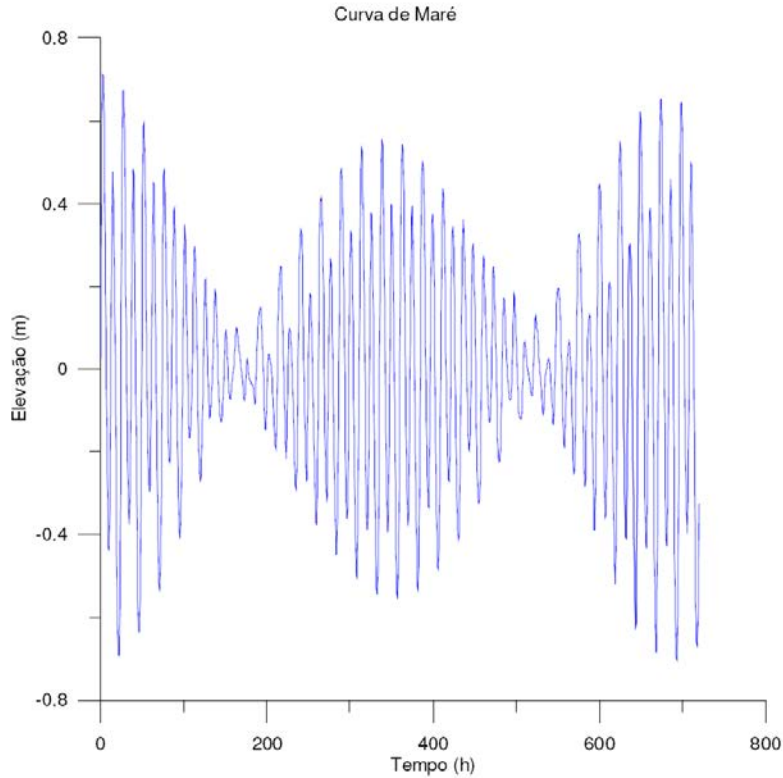


FIG. 70. Tide elevation curves for Angra dos Reis Harbor for 1 month, showing the forcing parameters, used to model Ilha Grande Bay, that are generated using the harmonic constants of Table 66.

II.4.3. River discharge

The watershed of the bay is characterized as an estuarine system where the mountains (Serra do Mar) are in direct contact with the sea and coastal plains are practically nonexistent. The majority of the land is poorly drained, and the rivers generally exhibit low average discharge. They originate at high elevations and fall steeply towards the sea but are only about 15 km long. Larger discharges occur during the summer. The most important river is the Mambucaba with a drainage basin of 592 km² that corresponds to 78% of the watershed area. The average discharge is 27.5 m³ s⁻¹ with high values between January and March, when the maximum discharges reach 157 m³ s⁻¹; smaller values occur between June and October, when the average and minimum discharges are respectively 14 and 10 m³ s⁻¹.

The Mambucaba River was used to dictate the boundary conditions for the terrestrial closed border. The value for all nodes was defined as zero, with exceptions of the Mambucaba River Discharge (see monthly discharges in Figure 71) and two other points (intake and discharge of seawater) that accounted for a total flux of 120 m³s⁻¹ (but only for the second scenario). The estimated discharge input values also accounted for the cross sectional areas of the river, intake point, and discharge point. Also considered was the effect of lateral friction on the closed borders that modifies the friction tension in the bottom; described by a sliding index (between 0 and 1), in the present case, the value was set to 0.7.

VAZÕES MÉDIAS MENSAIS DO RIO MAMBUCABA

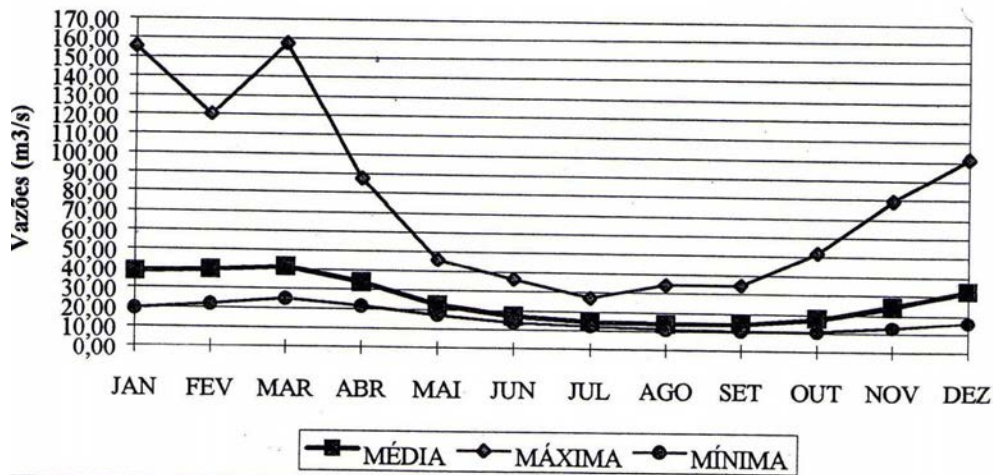


FIG. 71. Hydrograph of discharges from Mambucaba River.

TABLE 67. HYPOTHETICAL ACCIDENTAL TRITIUM RELEASE INTO ILHA GRANGE BAY

Discharge = $0.018 \text{ m}^3 \text{ s}^{-1}$ Pollutant	HTO initial concentration (Bq m^{-3})	Pollutant load (Bq s^{-1})	Concentration level 3H – seawater (Bq m^{-3})	Required dilution of source
3H	6.8×10^{10}	3.7×10^{12}	1.11×10^6	6×10^4

II.4.4. Postulated LOCA: HTO source and dispersion

The scenario outlined a hypothetical accidental tritium release into Ilha Grande Bay of 37 PBq of HTO in a volume of 66 m³ of coolant after a LOCA event. The waste was released onto concrete-covered ground around the plant producing a discharge of $0.018 \text{ m}^3 \text{ s}^{-1}$ of liquid wastes to Ilha Grande Bay lasting for 1 hour after the accident (Table 67).

Licensing restrictions limit the concentration of dissolved radioactive material or entrained noble gases released from the site to 1.11 MBq m^{-3} . This specification is provided to ensure that the concentration of radioactive materials released in liquid waste effluents from the site will be less than the concentration levels specified in 10 CFR 20 [404]. The release limits are applicable to the assessment and control of dose to the public. They are equivalent to radionuclide concentrations which, if inhaled or ingested continuously over the course of a year, would produce a total effective dose equivalent of 0.05 rem (50 millirem or 0.5 millisieverts).

II.5. HYDRODYNAMIC CIRCULATION

II.5.1. Results of hydrodynamic scenarios

The hydrodynamics of Ilha Grande Bay depend on the action of tides and winds, with rivers being of minor importance because of steep slopes, as mentioned above. The bay is very

shallow with relatively strong tide currents and frequent winds; the circulation pattern is mainly barotropic, i.e. the flow is produced mainly by differences in the position of the free surface, running from high to low waters. In this case, density gradients (baroclinic conditions) are not expected to greatly influence the hydrodynamics.

The inverse modeling used in the work, as explained above, showed no amplification on the order of 20% in the tide of Angra dos Reis Harbor. Thus, it was possible to calibrate the harmonic constants as an open boundary condition to model results according to measured records of tide propagation.

Good agreement (around 10%) was seen between the measured elevation (from Angra dos Reis Harbor) and the model results for the same observation point. The comparison was in better agreement during spring tides (Figure 72) than neap tides (Figure 73); this demonstrates success in reproducing the diurnal and semi-diurnal tide component. These components have the most effect on advective transport and so are important for simulating the aquatic dispersion of tritium.

There is an amplification of the tide wave once it propagates forward in the bay, with a small increase in the mean water level. This feature is a consequence of the reflection suffered by the tide wave as it enters the bay. The reflection is due to the stationary character of the tide in this estuary. The current reversals (or slacks, high-water and low-water) occur soon after the high tide (PM) and low tide (BM), respectively, as shown in Figure 74.

Modeled (2DH) velocity fields and directions of major currents that correspond to instances of flood stocking-tide (FST) and ebb stocking-tide (EST) are shown in Figures 75 and 76 (FST and EST occurrences for a neap tide, respectively) and Figures 77 and 78 (FST and EST instances for a spring tide, respectively).

Looking at the velocity fields, low current velocities dominate over most of Ilha Grande Bay, with average values on the order of 0.05 m s^{-1} and 0.1 m s^{-1} , respectively, for neap and spring tides. The current velocities simulated by the model are in good agreement with the data measured in the bay.

For both scenarios, the decision was made to work with patterns of average currents for tide cycles in neap and spring conditions. These types of currents make it easier to distinguish the accumulated effect of the recirculation caused by pumping and discharge operations. Figures 79 and 80 show residual current patterns for 1 day of neap and spring tides with diurnal inequalities (about 24.7 hours), respectively, for Scenario 1. Figures 81 and 82 show the same endpoints for Scenario 2, respectively, during neap and Spring tides. The residual currents shown here are eulerian, i.e. average values calculated for the time interval for fixed points.

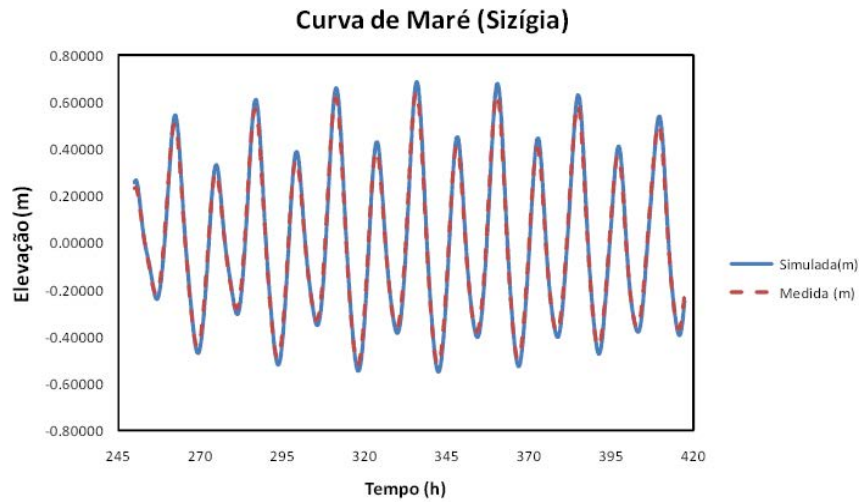


FIG. 72. Comparison of measured and simulated seawater levels for Spring tide after model calibration with Angra dos Reis Harbor Station.

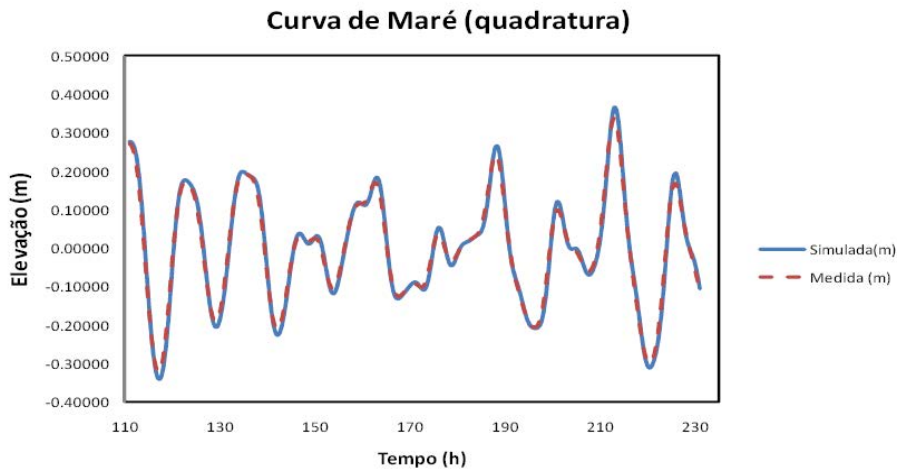


FIG. 73. Comparison of measured and simulated seawater levels for neap tide after model calibration with Angra dos Reis Harbor Station.

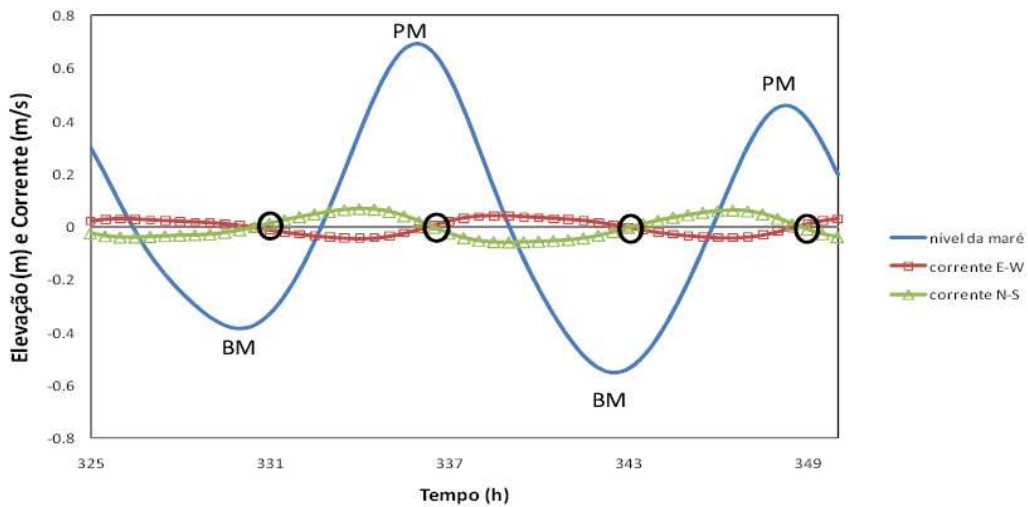


FIG. 74. Vertical (water level) and Horizontal (currents) Tide cycles in Ilha Grande Bay show the stationary behavior of the tide wave; Slacks (the reversal of flood and ebb currents) occur just after the high tide (PM) or low tide (BM).

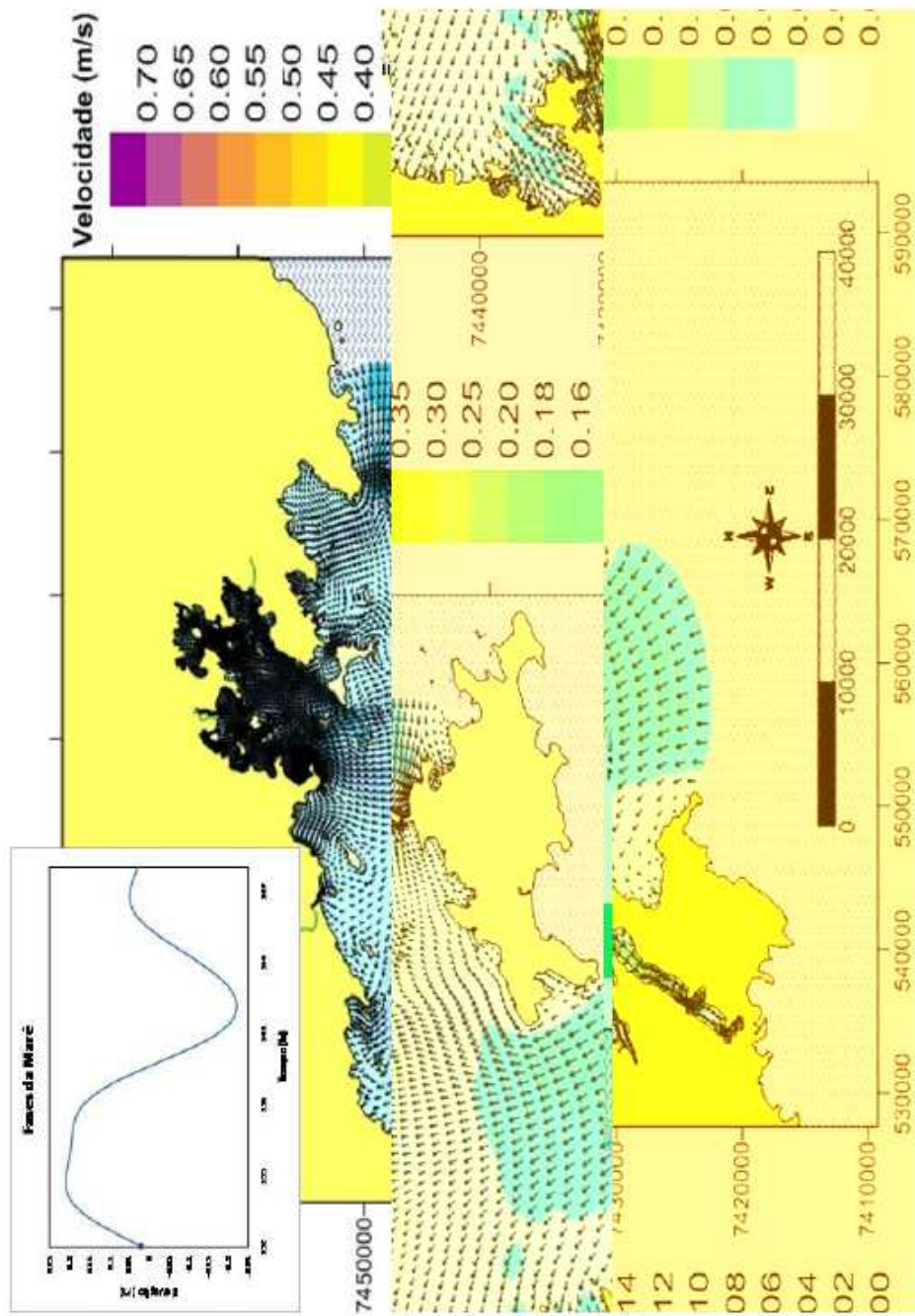


FIG. 75. Field velocities and current direction for the instance of flood stocking-tide (132 hours of simulation) in neap tide cycle.

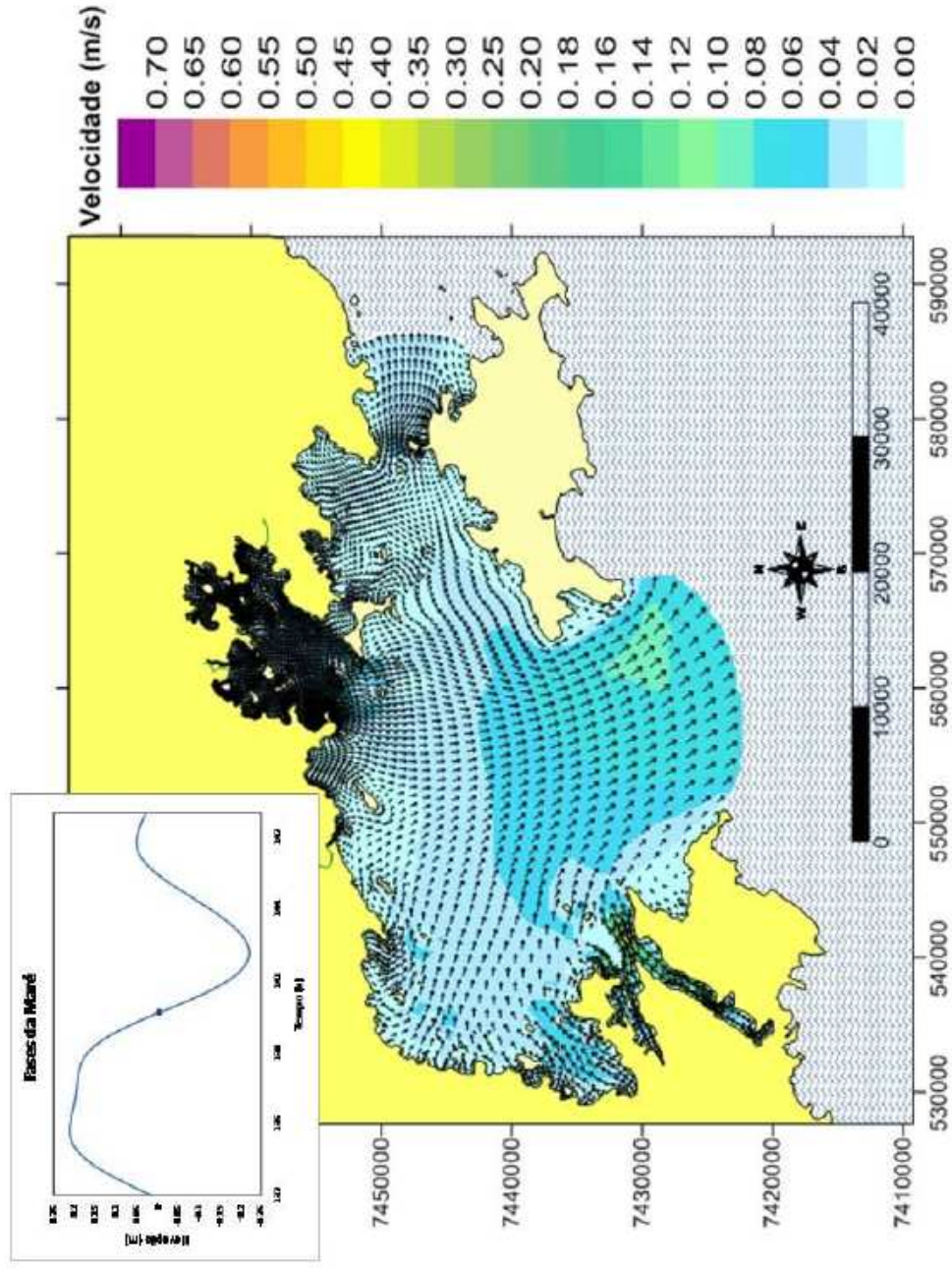


FIG. 76. Field velocities and current direction for the instance of ebb stocking-tide (140 hours of simulation) in neap tide cycle.

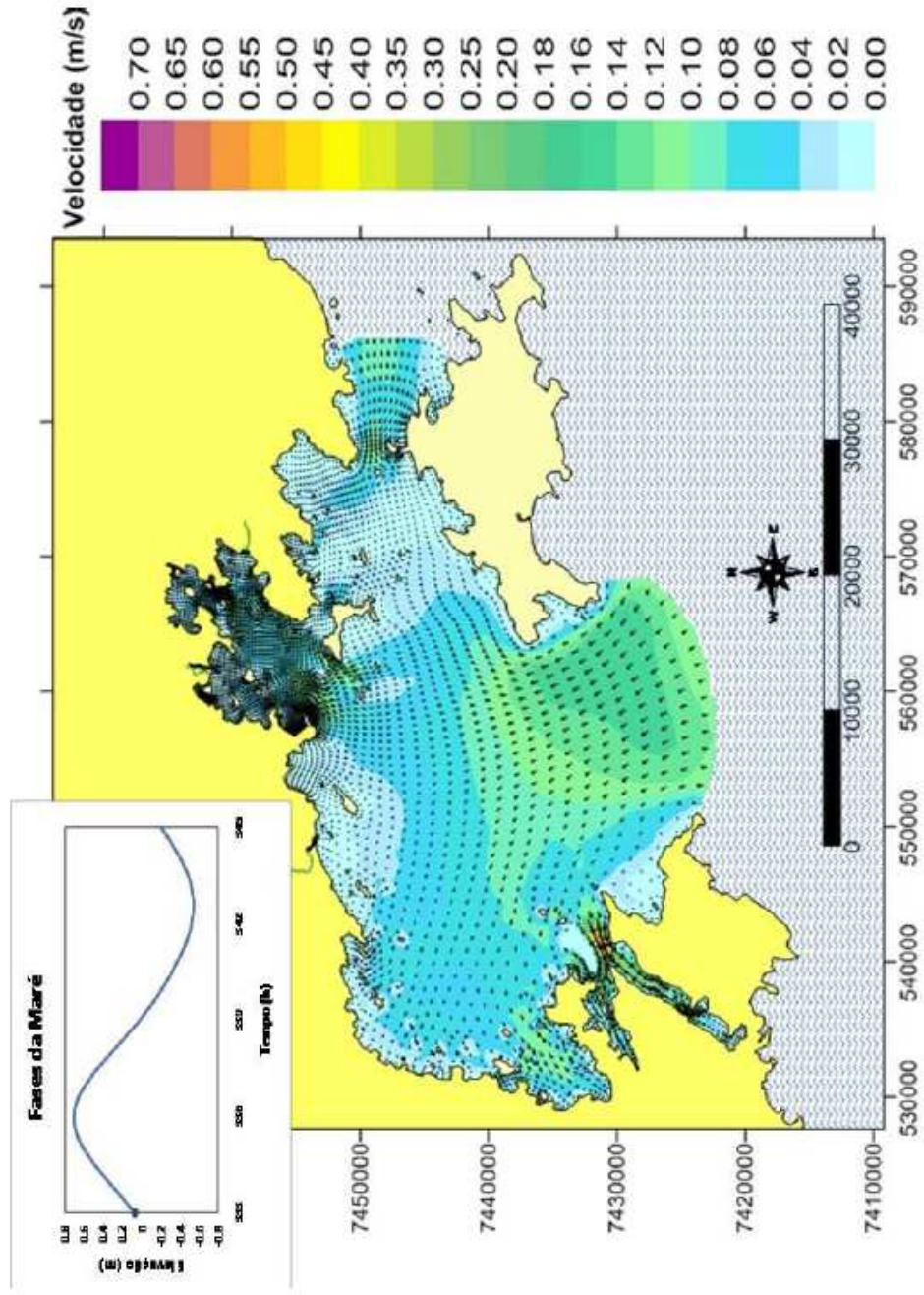


FIG. 77. Field velocities and current direction for the instance of flood stocking-tide (333 hours of simulation) in spring tide cycle.

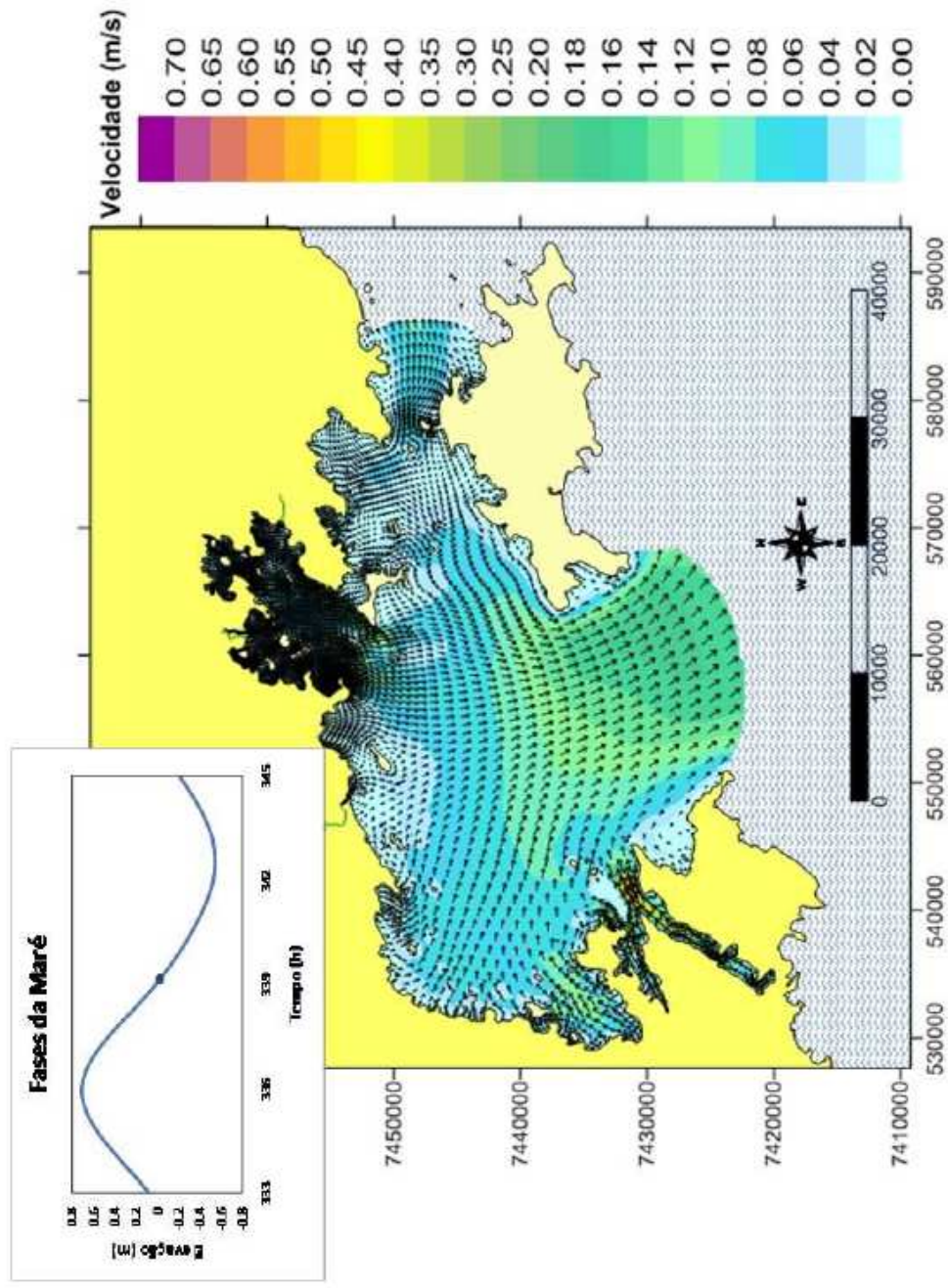


FIG. 78. Field velocities and current direction for the instance of ebb stocking-tide (339 hours of simulation) in spring tide cycle.

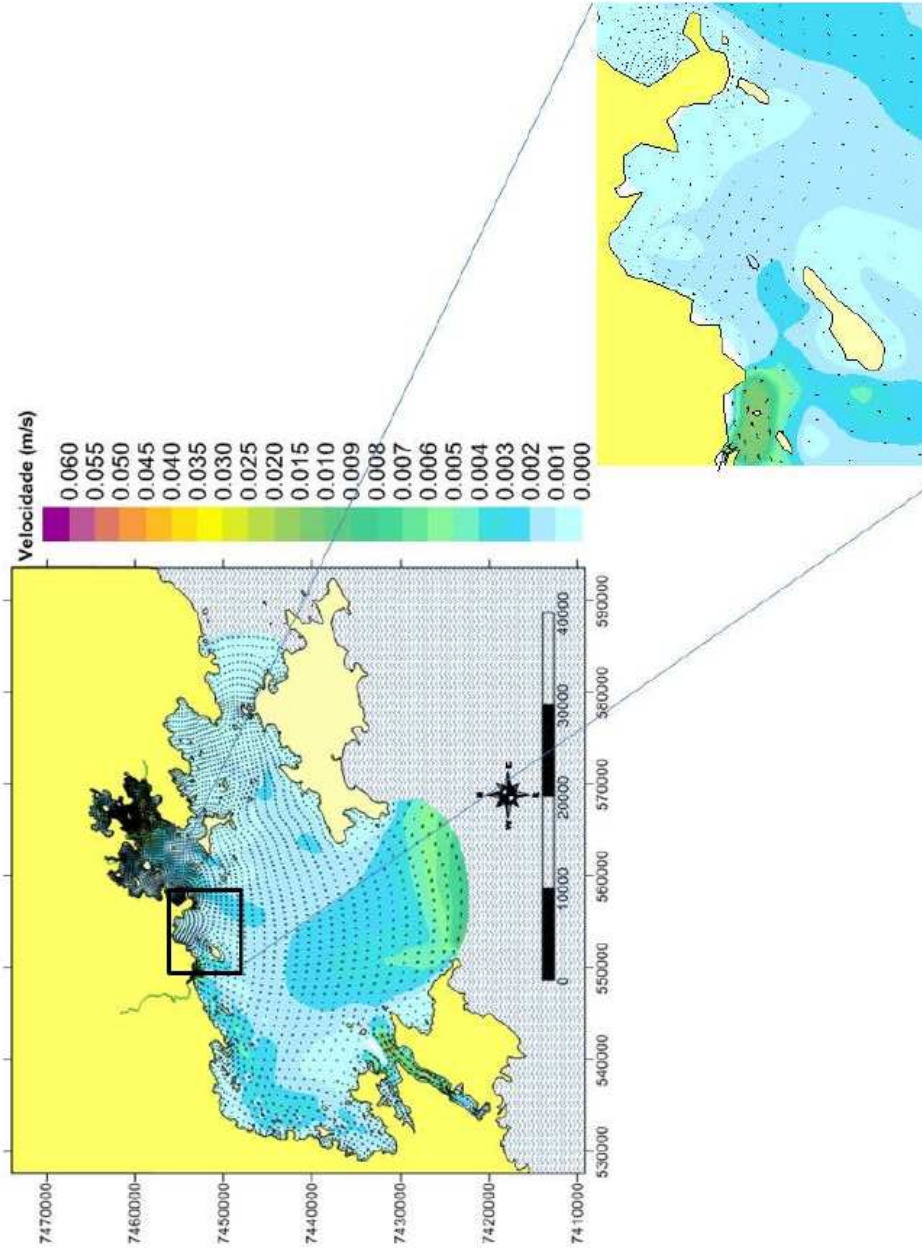


FIG. 79. Eulerian residual currents for 1 day of neap tide for Scenario 1. This period corresponds to the time interval between 124 and 148 hours of simulation.

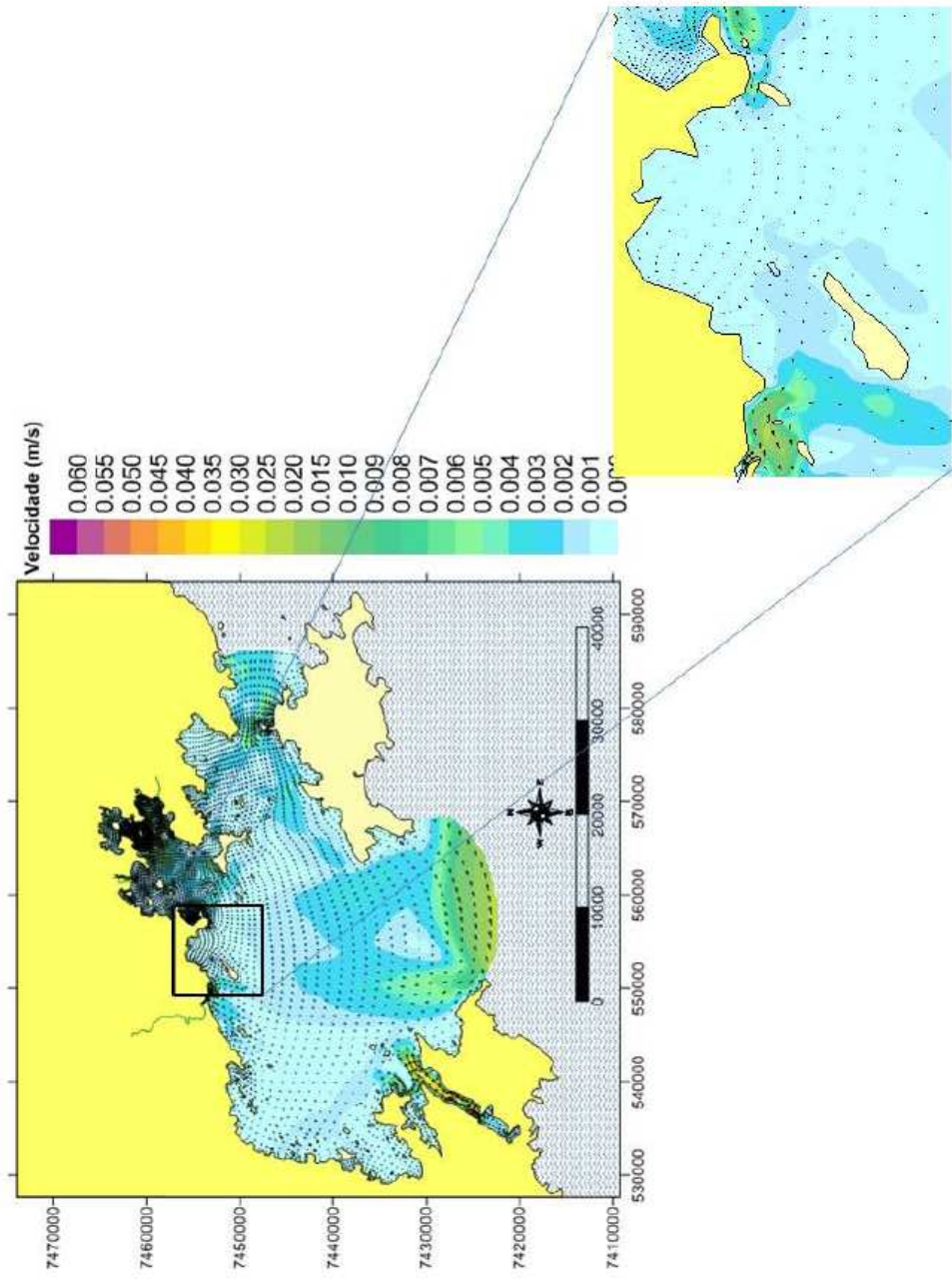


FIG. 80. Eulerian residual currents for 1 day of spring tide for Scenario 1. This period corresponds to the time interval between 324 and 348 hours of simulation.

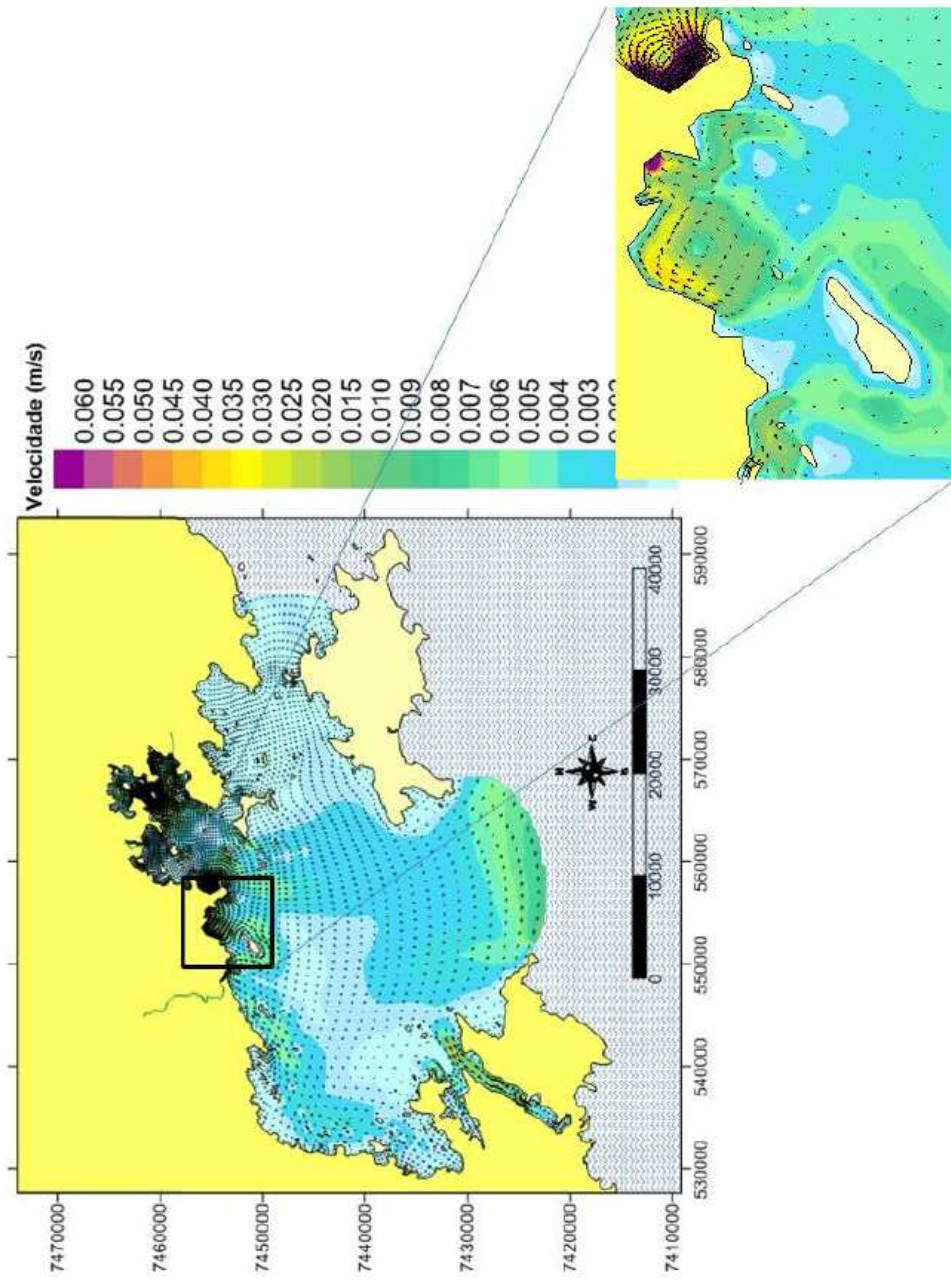


FIG. 81. Eulerian residual currents for 1 day of neap tide for Scenario 2. This period corresponds to the time interval between 124 and 148 hours of simulation.

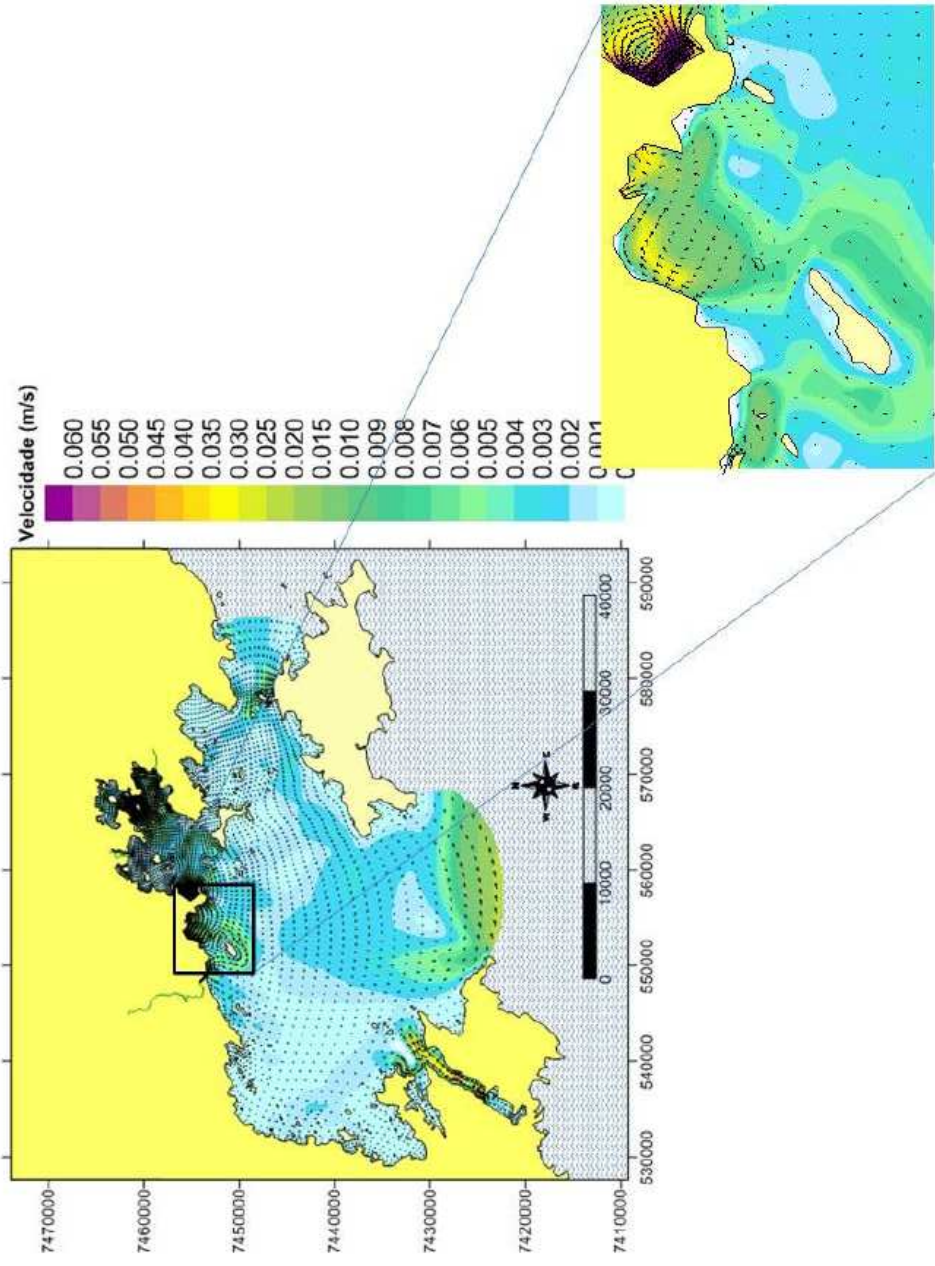


FIG. 82. Eulerian residual currents for 1 day of spring tide for Scenario 2. This period corresponds to the time interval between 324 and 348 hours of simulation.

The water intake and discharge of $120 \text{ m}^3 \text{ s}^{-1}$ influences the receiving contributions of the Mambucaba River from the west. Looking at the big picture, it is possible to observe that the velocity field at the open border 1 flows to the west during neap tide. In spring tide, a displacement of currents occurs towards the east close to the open border one that changes direction to inside the bay, when approaching the Big Island (Ilha Grande), due to the interaction with currents from Sepetiba Bay to the East. This pattern creates a large area of recirculation in the center-south portion of the estuary.

As expected, the scenario with intake and discharge (Scenario 2) completely changed the residual currents in the impact area. A belt was formed in the velocity field from the outlet of the Mambucaba River, Sandri Island was surrounded, and vortices formed near several beaches until the currents reached Itaorna. In addition, strong vortices formed in the discharge area along the coast. Velocities in the belt and vortices, however, are not particularly high, varying in general from 5 to 20 mm s^{-1} and only in some particular instances reaching values between 40 to 60 mm s^{-1} .

II.6. HTO TRANSPORT AND RADIOLOGICAL IMPACT

II.6.1. Results of hypothetical accidental tritium release

This sub-section shows the predicted dispersion of tritium in the period between 24 hours and 1 year after an accidental release into Ilha Grande Bay. If the concentration of radioactive material released from the site exceeds the reference levels mentioned in Section II.4.4, action must be taken immediately to bring the concentration to within regulatory limits. In the case of tritium in seawater, the limit is 1.11 MBq m^{-3} . At the end of the first day after the hypothetical accident, tritium concentrations of up to 1 GBq m^{-3} were predicted close to Itaorna beach, but the area of the highest concentration was limited in extent.

The dispersion of tritium in the bay was similar for the two scenarios on the whole. The differences were observed between the third and fourteenth day (Figures 83–88), the time in which water contaminated with concentrations above the regulatory limit spread over a maximum area more than 10 km in diameter. In the scenario with pumping and discharge operations (#2), the area occupied by such concentrations decreased more quickly during the time interval (Figures 83, 85 and 87) than in the first scenario (Figures 84, 86 and 88). Such a difference was caused by the removal of a large volume of contaminated water from the accident site and its dilution in the discharge area, a region with minimal tritium concentrations. As a result of the dilution promoted by keeping the other plants operating, it is predicted that the tritium regulatory limit will not be exceeded after the eleventh day for Scenario 2, while it will take sixteen days for this to occur in Scenario 1. Modelling results suggest, therefore, that increasing the pumping and discharging rates could be used immediately after an accident to accelerate the dilution.

Pumping and discharging operations would only be effective to manage the highest concentrations of the plume, however, because they did not affect the general distribution of the HTO plume in the bay. Plume evolution is presented for 1, 2 and 6 months (Figures 89–91) post-accident for Scenario 1; these results are quite similar to those of Scenario 2 for the same time periods. After 1 month (Figure 89), the plume reached its maximum spread in the bay, and concentrations on the order of 50 KBq m^{-3} were predicted in most locales. Because such concentrations are still very high and because the ingestion dose from organically bound tritium (OBT) in seafood is highly uncertain, it would be wise to suspend fishing activities in the whole bay for a minimum period of 60 days. After that, the concentrations are predicted to

decrease quickly. After 3 months (Figure 90), with the exception of Ribeira Bay where fishing restrictions could be maintained, predicted concentrations in the rest of the bay would be below the detection limit (DL) used by the environmental monitoring program (11 KBq m^{-3}). After 6 months (Figure 91), the tritium plume would be completely undetectable.

The behavior of tritium was assumed conservative because it behaves like a water molecule and remains in solution. For the simulation, radioactive decay was assumed negligible because the simulation time corresponded to less than 10% of tritium's half-life (12.6 years).

Finally, 1 year after the accident, the results of the modeling showed that that Ilha Grande Bay would have returned to its original state, i.e. concentrations would be the same as those predicted at steady-state from routine releases. It should be stressed that the equations of advective and diffusive transport used to model tritium dispersion use the Eulerian frame of reference.

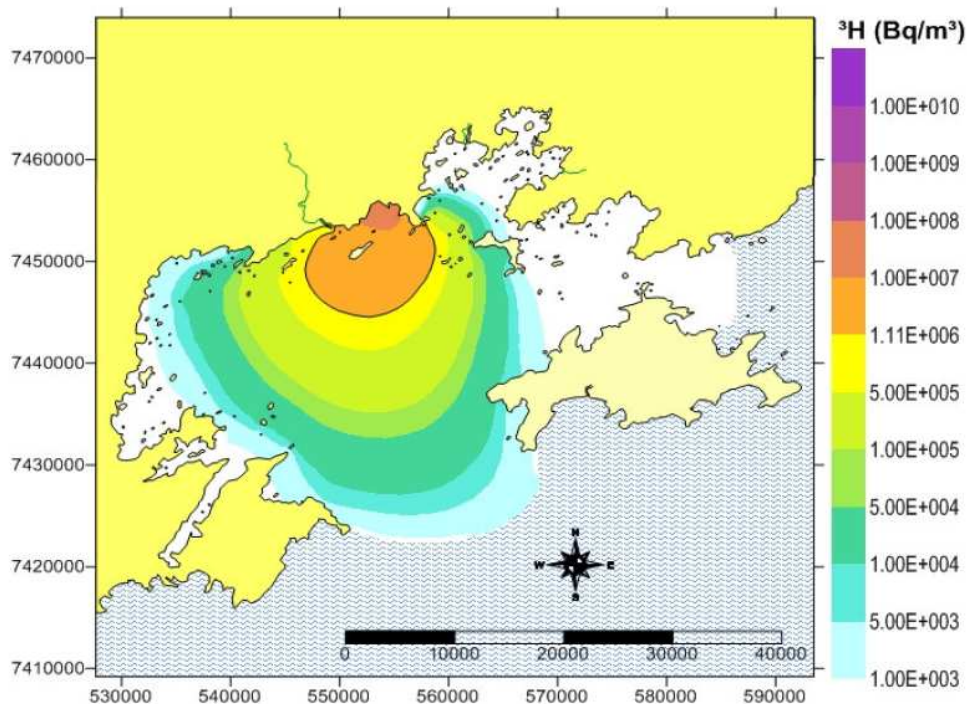


FIG. 83. Dispersion of the HTO plume 3 days post accident in Scenario 1.

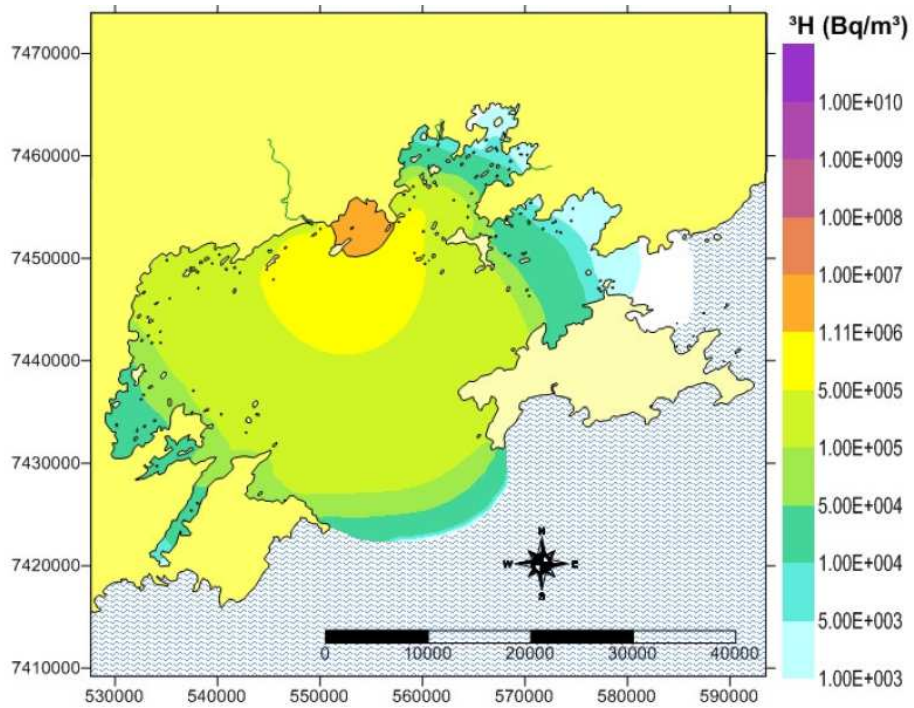


FIG. 84. Dispersion of the HTO plume 3 days post- accident in Scenario 2.

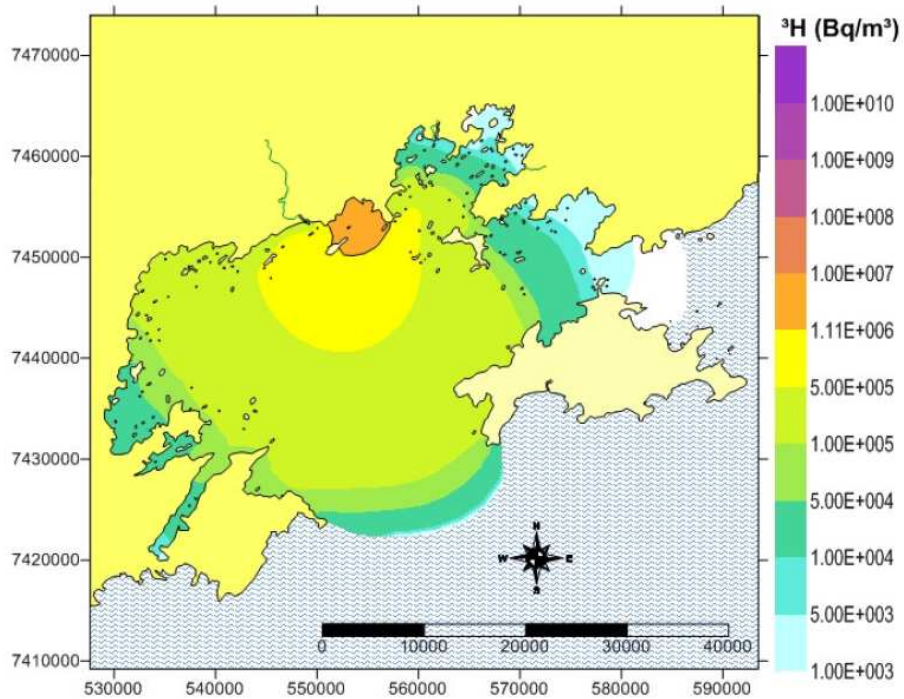


FIG. 85. Dispersion of the HTO plume 10 days post- accident in Scenario 1.

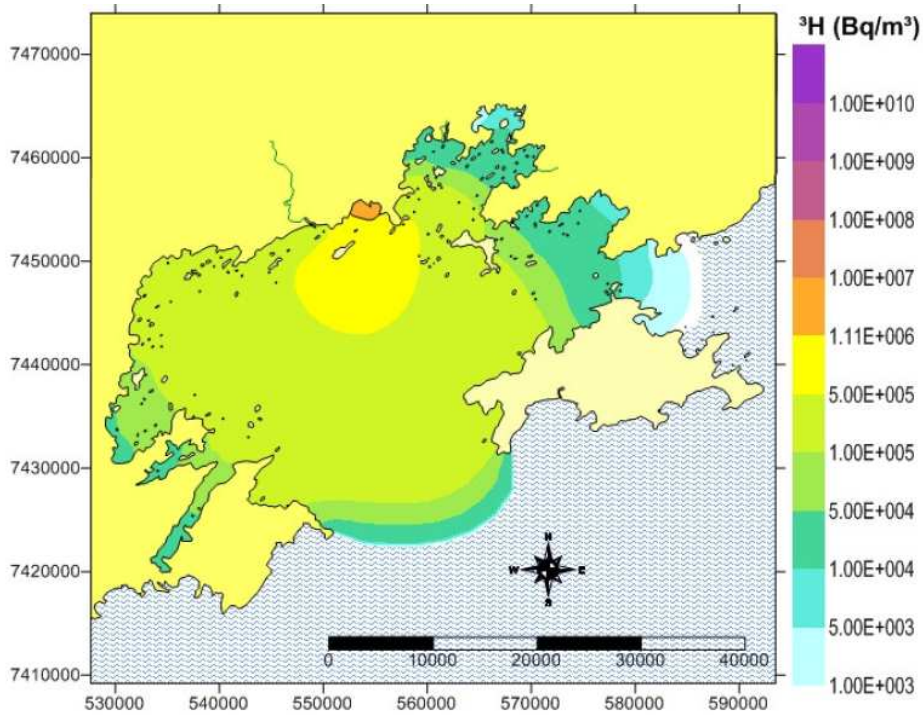


FIG. 86. Dispersion of the HTO plume 10 days post-accident in Scenario 2.

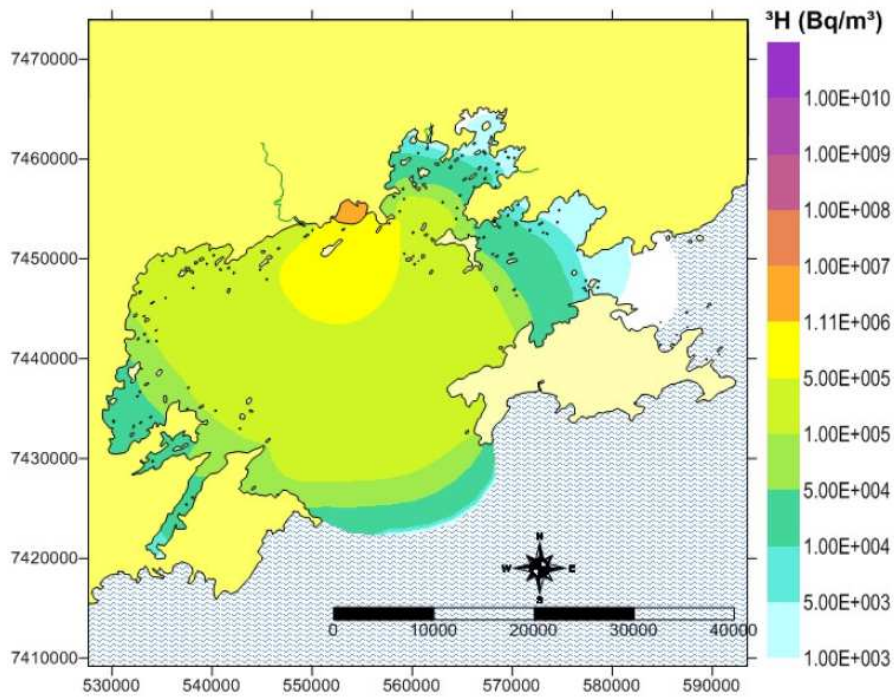


FIG. 87. Dispersion of the HTO plume 14 days post-accident in Scenario 1.

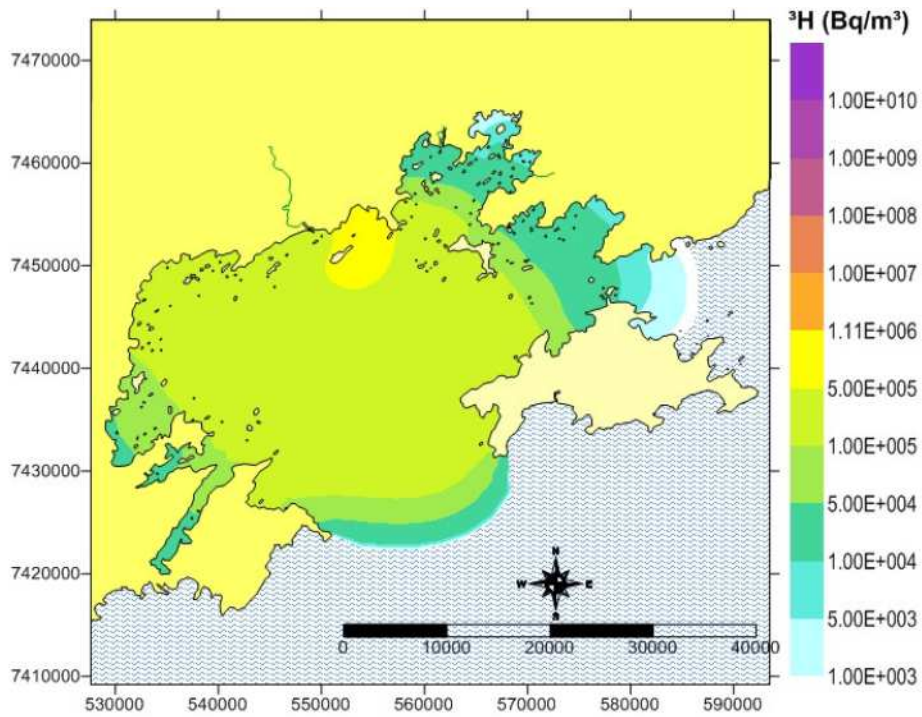


FIG. 88. Dispersion of the HTO plume 14 days post-accident in Scenario 2.

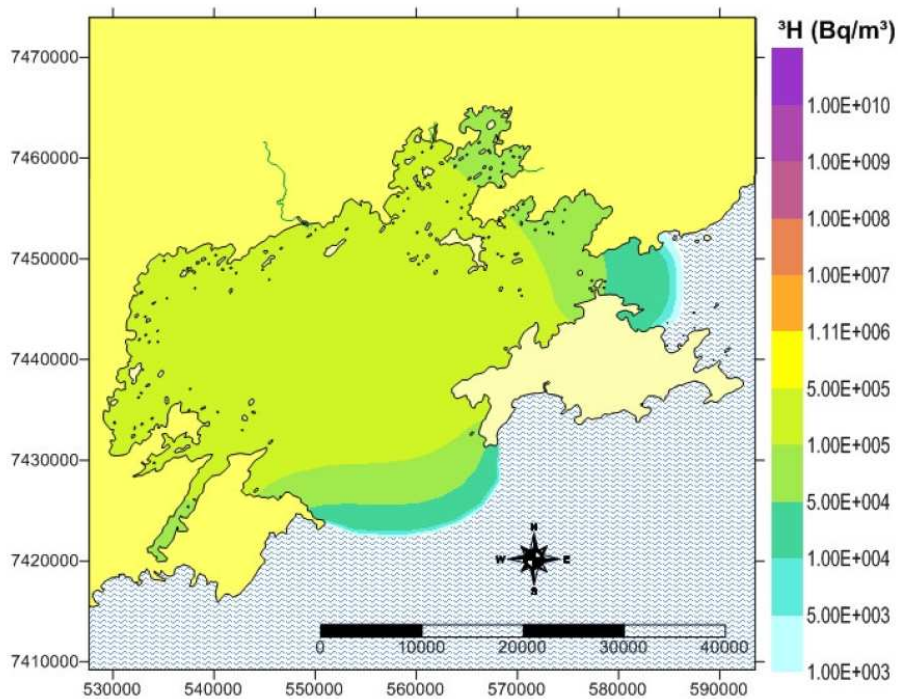


FIG. 89. Dispersion of the HTO plume 30 days post-accident in Scenario 1.

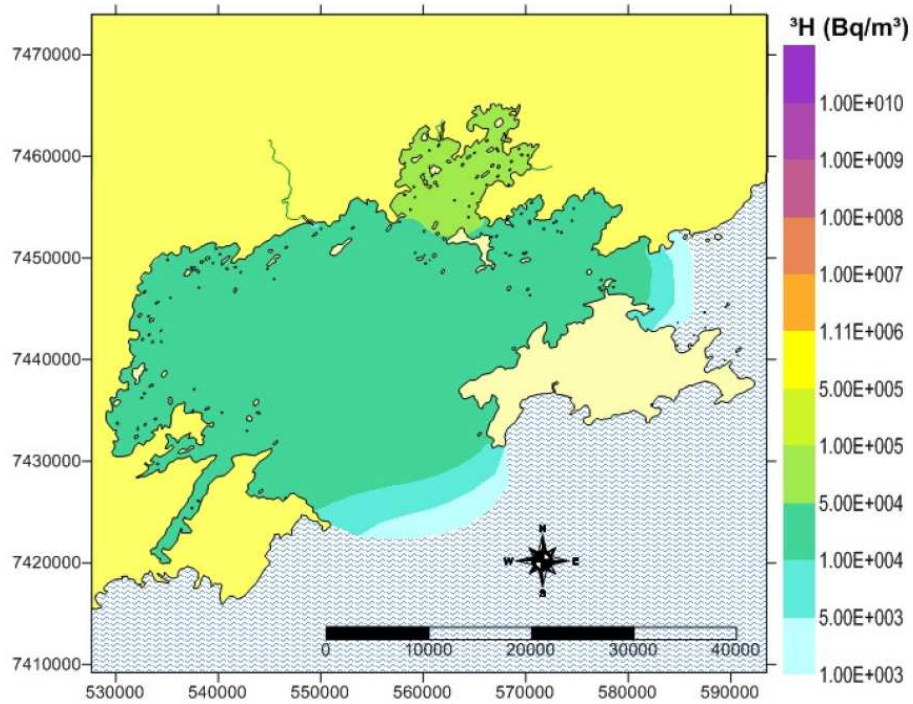


FIG. 90. Dispersion of the HTO plume 90 days post-accident in Scenario 1.

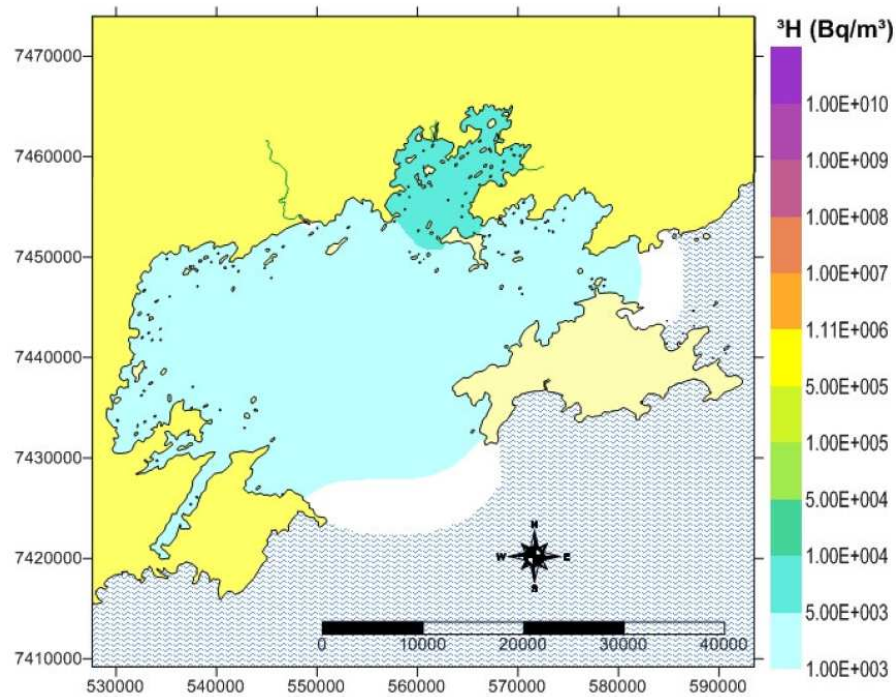


FIG. 91. Dispersion of the HTO plume 180 days post-accident in Scenario 1.

APPENDIX III. DEFINITION OF ORGANICALLY BOUND TRITIUM (OBT)

Definition¹²: OBT is carbon-bound and buried tritium formed in living systems through natural environmental or biological processes from HTO (or HT via HTO). Other types of organic tritium (e.g. tritiated methane, tritiated pump oil, radiochemicals and so on) should be called tritiated organics, which can exist in any chemical or physical form.

Notes:

- (1) Buried tritium is tritium that occupies exchangeable positions in large biomolecules in dry matter but that is not removed by rinsing with tritium-free water. Buried tritium therefore contributes to the OBT concentration in the traditional experimental determination of OBT. It is analogous to buried hydrogen in biochemistry.
- (2) OBT should not include tritium bound to sulphur, nitrogen or oxygen (exchangeable OBT) that can be removed by washing with tritium-free water. This fraction depends strongly on the HTO concentration in effect at the time of sampling and can exchange with water vapour during analysis. Inclusion of the exchangeable fraction would lead to measurements that are highly variable and difficult to interpret.
- (3) From an analytical perspective, OBT is the activity in dry biomatter that is not exchangeable with water. In measuring OBT concentrations, exchangeable OBT should first be removed by moderately drying the sample without decomposing the organic molecules, washing the residue repeatedly with tritium free water and then drying the material again. The OBT concentration can then be determined as the tritium activity in the dry sample. This is generally done by combusting the sample and determining the activity in the combustion water by liquid scintillation counting, or by analysing the sample by He-3 mass spectrometry. There are no generally accepted standard techniques for measuring OBT and the methods used should be documented when reporting results.
- (4) In the washing process, exchangeable tritium nuclei are removed and replaced by hydrogen nuclei, but exchangeable hydrogen nuclei are simply replaced by other hydrogen nuclei. Thus measurements of OBT do not reflect the specific activity of the non-exchangeable hydrogen. This specific activity can be estimated by dividing the measured concentration by the fraction of hydrogen nuclei in the dry sample that are non-exchangeable. For example, this fraction has been empirically determined to be 0.78 for leaf tissues, but different values may apply for other plant or animal materials. Care must be taken in comparing model predictions and experimental data that the same quantity (OBT concentration or specific activity of non-exchangeable hydrogen nuclei) is being considered.
- (5) OBT concentrations should be reported in units of Bq L⁻¹ of combustion water. This is the fundamental unit that can be converted, if necessary, to the specific activity of the non-exchangeable hydrogen nuclei. Use of Bq L⁻¹ makes it easy to compare concentrations in different media and to determine whether specific activity is depleted, preserved or enriched when tritium is transferred from one compartment to another.

¹² Definition of OBT proposed by the EMRAS I Tritium and C-14 Working Group [4].

- (6) OBT refers to organic tritium formed from HTO by natural processes in living organisms, or in materials such as soils or lake sediments that are derived from living material. Put another way, OBT is that organic tritium found in a normal diet that imparts a dose consistent with the ICRP ingestion dose coefficient for OBT. All other types of organic tritium, no matter how they form or how they appear in the environment, should be called tritiated organics and assigned their own dose coefficient for purposes of dose calculation.

REFERENCES

- [1] ADVISORY GROUP ON IONISING RADIATION, Review of risks from tritium, Report of the Independent Advisory Group on Ionising Radiation, Documents of the Health Protection Agency RCE4, Chilton: HPA, AGIR (2007).
- [2] GALERIU, D., MELINTESCU, A., Tritium, in Radionuclides in the environment, Edited by David A. Atwood, Copyright 2010, John Wiley & Sons Ltd., West Sussex, England, ISBN 978-0-47 (2010) 47–65.
- [3] DAVIS, P., GALERIU, D., Tritium in the environment, in Encyclopaedia of Sustainability Science and Technology, Editor-in-chief: Meyers, Robert A., Environmental Radioactivity and Ecotoxicology of Radioactive Substances, Editor Glen Bird, Springer (in press).
- [4] INTERNATIONAL ATOMIC ENERGY AGENCY, Modelling the environmental transfer of tritium and carbon-14 to biota and man, Report of the Tritium and Carbon-14 Working Group of EMRAS Theme 1, IAEA's Environmental Modelling for Radiation Safety (EMRAS) Programme 2003–2007, IAEA, Vienna (2008a). Available at: <http://www-ns.iaea.org/downloads/rw/projects/emras/draft-final-reports/emras-tritium-wg.pdf>
- [5] BOYER, C., VICHOT, L., FROMM, M., LOSSET, Y., TATIN-FROUXA, F., GUÉTAT, P., BADOT, P.M., Tritium in plants: A review of current knowledge, Environ. Exp. Bot. **67** (2009) 34–51.
- [6] VAN DIEPEN, C.A., DRIESSEN, P.M, VAN DER GOOT, E., GOUDRIAAN, J., HIJMANS, R.J., HOOIJER, A.A., VAN KEULEN, H., VAN KAPPEL, R.R., DE KONING, G.H.J., VAN KRAALINGEN, D.W.G., KROPFF, M.J., VAN LAAR, H.H., RAPPOLDT, C., PENNING DE VRIES, F.W.T., SPITTERS, C.J.T., SUPIT, I., VAN DER WAL, T., WOLF, J., Updated system description of the WOFOST crop growth simulation model as implemented in the Crop Growth Monitoring System applied by the European Commission, Editors I. Supit, E. van der Goot (2003).
- [7] INTERNATIONAL ATOMIC ENERGY AGENCY, Soybean scenario, Final report, IAEA's Environmental Modelling for Radiation Safety (EMRAS) Programme 2003–2007, IAEA, Vienna (2008b). Available at: <http://www-ns.iaea.org/downloads/rw/projects/emras/tritium/soybean-final.pdf>
- [8] DAVIS, P.A. LECLERC, E., GALERIU, D.C., MELINTESCU, A., KASHPAROV, V., PETERSON, S.-R., RAVI, P.M., SICLET, F., TAMPONET, C., Specific activity models and parameter values for tritium, ^{14}C and ^{36}Cl in: Quantification of Radionuclide Transfer in Terrestrial and Freshwater Environments for Radiological Assessments, IAEA-TECDOC-1616, IAEA, Vienna (2009).
- [9] BIOSPHERIC MODEL VALIDATION STUDY (BIOMOVS II), Development of a reference biosphere methodology for radioactive waste disposal. BIOMOVS II Technical Report No. 6. Stockholm, Sweden: BIOMOVS II Steering Committee, Swedish Radiation Protection Institute (1996a).
- [10] WATKINS, B.M., SMITH G.M., LITTLE, R.H., KESSLER, J., A Biosphere modelling methodology for dose assessments of the potential Yucca Mountain deep geological high level radioactive waste repository, Health Phys. **76** (1999) 355–367.
- [11] LIMER, L.M.C., SMITH, K., ALBRECHT, A., MARANG, L., NORRIS, S., SMITH, G.M., THORNE, M.C., XU, S., C-14 Long-Term Dose Assessment: Data Review, Scenario Development, and Model Comparison, Draft final report, version 2.0., 31 August 2011 (2011).

- [12] BELOT, Y., ROY, M., METIVIER, H., *Le TRITIUM de l'Environnement a l'Homme*, Insitut de Protection et de Surete Nucleaire, Les Edition de Physique, France, ISBN: 2-86883-275-X (1996) (in French).
- [13] YOKOYAMA, S., NOGUCHI, H., ICHIMASA, Y., ICHIMASA, M., FUKUTANI, S., Deposition of heavy water on soil and reemission to the atmosphere, *Fusion Eng. Des.* **42** (1998) 141–148.
- [14] YOKOYAMA, S., NOGUCHI, H., Development of dose assessment code for accidental tritium releases, Japan Atomic Energy Research Institute, Japan P-4b-227, International Radiation Protection Association (2002).
- [15] YOKOYAMA, S., NOGUCHI, H., ICHIMASA, Y., ICHIMASA, M., Re-emission of heavy water vapour from soil to the atmosphere, *J. Environ. Radioactiv.* **71** (2004) 201–213.
- [16] VANDECASTEELE, C.M., BAKER, S., FORSTEL, H., MUZINSKY, M., MILLAN, R., MADDOZ-ESCANDE, C., TORMOS, J., SAURAS, T., SCHULTE, E., COLLE, C., Interception, retention and translocation under greenhouse conditions of radiocaesium and radiostrontium from a simulated accidental source, *Sci. Total Environ.* **278** (2001) 199–214.
- [17] CHADWICK, R.C., CHAMBERLAIN, A.C., Field loss of radionuclides from grass, *Atmos. Environ.* **4** (1970) 51–56.
- [18] CHAMBERLAIN, AC., Interception and retention of radioactive aerosols by vegetation, *Atmos. Environ.* **4** (1970) 57–78.
- [19] KRAMER, P.J., Transpiration and the water economy of plants, In: *Plant Physiology: A treatise Vol.VII* (F.C. Steward, Ed.) Academic Press, New York (1959) 607–726.
- [20] SEINFELD, J.H., PANDIS, S.N., *Atmospheric Chemistry and Physics: From Air Pollution to Climate Change*, 2nd Edition, Wiley-interscience (2006).
- [21] ENGELMANN, R., The calculation of precipitation scavenging, D. Slade (Ed.), *Meteorology and Atomic Energy*, USAEC Report TID-24190 (1968) 208–221.
- [22] CHAMBERLAIN, A., EGGLETON, E., Washout of tritiated water vapour by rain, *Int. J. Air Water Pollut.* **8** (1964) 135–149.
- [23] INTERNATIONAL ATOMIC ENERGY AGENCY, *Atmospheric dispersion in nuclear power plant siting*, Safety Series No. 50-SG-S3, IAEA, Vienna (1980).
- [24] HARRIS, J., MILLER, D., FOSTER, D.W., Tritium recapture behavior at a nuclear power reactor due to airborne releases, *Health Phys.* **95** (2008) 203–212.
- [25] HIDEKI, T., MASAKI, O., Precipitation washout of tritiated water vapor from a nuclear reactor, *J. Environ. Radioactiv.* **34** (1997) 59–68.
- [26] INOUE, Y., IWAKURA, T., MIYAMOTO, K., Environmental aspects of tritium released into the atmosphere in the vicinity of nuclear facilities in Japan, *NIRS-M-52* (1985) 296–315.
- [27] PAPADOPOULOS, D., KÖNIG, L., LANGGUTH, K.-G., FARK, S., Contamination of precipitation due to tritium release into the atmosphere, *Radiat. Prot. Dosim.* **16** (1986) 95–100.
- [28] TADMOR, J., Deposition of ⁸⁵Kr and tritium deposition released from a nuclear fuel processing plant, *Health Phys.* **24** (1973) 37–42.
- [29] KÖLLÖ, Z., PALCSU, L., MAJOR, Z., L., P., MOLNÁR, M., RANGA, T., DOMBÓVÁRI, P., MANGA, L., Experimental investigation and modelling of tritium washout by precipitation in the area of the nuclear power plant of Paks, Hungary, *J. Environ. Radioactiv.* **102** (2011) 53–59.
- [30] HALES, J.M., Fundamentals of the theory of gaz scavenging by rain, *Atmos. Environ.* **6** (1972) 635–659.

- [31] BELOVODSKI, L.F., GAEVOY, V.K., GOLUBEV, A.V., KOSHELEVA, T.A., Tritium oxide wash-out by drops, *J. Environ. Radioactiv.* **36** (1997) 129–139.
- [32] BELOVODSKI, L.F., Washout of tritium oxide with precipitation from atmosphere, Technical Report (2010).
- [33] DAVIS, P., Tritium transfer parameters for the winter environment, *J. Environ. Radioactiv.* **36** (1997) 177–196.
- [34] KONIG, L.A., LANGGUTH, K.-G., PAGLIOSA, G., PAPADOPOULOS, D., RADZIWILL, A., SCHULTE, S., STRACK, S., Radiokologische Studien der Auswirkungen von Tritiumemissionen am Beispiel des KfK, Technical report, Report KfK 3715, Forschungszentrum Karlsruhe, Karlsruhe, Germany (1984) (in German).
- [35] GALERIU, D., DAVIS, P., WORKMAN, W., Tritium profiles in snowpacks, *J. Environ. Radioactiv.* **101** (2010) 869–874.
- [36] JUSTIO, J., Fog structure in clouds: their formation, optical properties and effects', HOBBS, P.V and DEEPAK, A, (Eds.) Academic Press (1981).
- [37] GIBB, R., CARSON, P., THOMPSON, W., The effect of fog on radionuclide deposition velocities, Canadian Nuclear Association, Annual Meeting (1997).
- [38] GOLUBEV, A., ALEINIKOV, A., GOLUBEVA, V., KHABIBULIN, M., GLAGOLEV, M., MISATYUK, S., MAVRIN, S., Studies of HT and HTO behavior in the vicinity of long-term emission source: Model, Experiment Intercomparison WM 03 Conference, Tucson, Arizona, USA (2003).
- [39] MELINTESCU, A., Processes and parameters in modelling dry and wet deposition of radionuclides, part of PhD thesis, PhD thesis, University of Bucharest, Romania (2002a) (in Romanian).
- [40] ATANASSOV, D., GALERIU, D., Rain scavenging of tritiated water vapour: A numerical eulerian stationary model, *J. Environ. Radiactiv.* **102** (2011) 43–52.
- [41] GOLUBEV, A., ALEINIKOV, A., GOLUBEVA, V., Studies of hto washout and deposition in the vicinity of emission source ii: model-experiment intercomparison, *Fusion Sci. Technol.* **41** (2002) 474–477.
- [42] HALES, J.M., Wet removal of pollutants from gaussian plumes: Basic linear equations and computational approaches, *J. Appl. Meteorol.* **41** (2002) 905–918.
- [43] BELOT, Y., Predicting the washout of tritiated water from atmospheric plumes for single rain events, Private report (2002).
- [44] OGRAM, G.L., Precipitation scavenging of tritiated water vapour (HTO), Technical report, Ontario Hydro research division, Canada (1985).
- [45] ELECTRIC POWER RESEARCH INSTITUT, Groundwater protection guidelines for nuclear powerplants, EPRI Final Report, Public edition 1016099, USA (2008). Available at:
http://www.powerreactorrrp.com/References/Groundwater/EPRI_Groundwater.pdf
- [46] PAINE, J.R., LEW, F., Project PRIME: Evaluation of Building Downwash Models Using Field and Wind Tunnel Data. Paper No. 4B.2, 10th Joint Conference on the Applications of Air Pollution Meteorology, Phoenix, AZ, USA (1998).
- [47] THOMPSON, R.S., Building Amplification Factors for Sources Near Buildings – A Wind-Tunnel Study, *Atmos. Environ. Part A-General Topics* **27** (1993) 2313–2325.
- [48] OLESEN, H.R., BERKOWICZ, R.B, KETZEL, M., LØFSTRØM, P., Validation of OML, AERMOD/PRIME and MISKAM using the Thompson wind tunnel data set for simple stack-building configurations, 6th International Conference on Urban Air Quality, March 27–29, 2007, Cyprus, (2007). Available at:
http://www2.dmu.dk/atmosphericenvironment/Docs/Using_Thompsons_data.pdf

- [49] HANNA, S. R., BRIGGS, G. A., HOSKER, R. P. J., Handbook on atmospheric diffusion National Oceanic and atmospheric administration, Oak Ridge, Tennessee (USA), Atmospheric Turbulence and Diffusion Lab. (1982).
- [50] HUNT, J.C.R., CARRUTHERS, D., BRITTER, R., DAISH, N.C., Dispersion from Accidental Releases in Urban Areas. No.ADMCL/2002/3, Atmospheric Dispersion Modelling Liaison Committee (2003).
- [51] BRITTER, R. E., HANNA, S.R., Flow and dispersion in urban areas, *Annu. Rev. Fluid Mech.* **35** (2003) 469–496.
- [52] KAKOSIMOS, K.E., HERTEL, O., KETZEL, M., BERKOWICZ R., Operational Street Pollution Model (OSPM) – a review of performed validation studies, and future prospects, *Environ. Chem.* **7** (2010) 485–503.
- [53] HUANG, H., SHEN, S., HARA, T., OKABAYASHI, K., OHBA, R., Development of Lagrangian/Eulerian hybrid atmospheric dispersion model around buildings, The Fifth International Symposium on Computational Wind Engineering (CWE2010), May 23–27, 2010, Chapel Hill, North Carolina, USA (2010). Available at:
ftp://ftp.atdd.noaa.gov/pub/cwe2010/Files/Papers/198_Huang.pdf
- [54] ULBRICH, C.W., Natural variations in the analytical form of the raindrop size distribution, *J. Climate Appl. Meteorol.* **22** (1983) 1764–1776.
- [55] MARSHALL, J., PALMER, D.V., The distribution of raindrops with size, *J. Meteorol.* **5** (1948) 165–166.
- [56] WILLIS, P.T., Functional Fits to Some Observed Drop Size Distributions and Parameterization of Rain, *J. Atmos.Sci.* **41** (1984) 1648–1661.
- [57] FEINGOLD, G., LEVIN, Z., The lognormal fit to raindrop spectra from frontal convective clouds in Israel, *Journal Climate Appl. Meteorol.* **25** (1986) 1346–1363.
- [58] ANDRONACHE, C., Diffusion and electric charge contributions to below-cloud wet removal of atmospheric ultra-fine aerosol particles, *J.Aerosol Sci.* **35** (2004) 1467–1482.
- [59] CERRO, C., CODINA, B., BECH, J., LORENTE, J., Modeling raindrop size distribution and z(r) relations in the western mediterranean area, *J. Appl. Meteorol.* **36** (1997) 1470–1479.
- [60] LOOSMORE, G.A., CEDERWALL, R.T., Precipitation scavenging of atmospheric aerosols for emergency response applications: testing an updated model with new real-time data, *Atmos. Environ.* **38** (2004) 993–1003.
- [61] PRUPPACHER, H.R., KLETT, J.D., *Microphysics of Clouds and Precipitation*, Kluwer Academic Publishers (1998).
- [62] UNDERWOOD, B., Review of deposition velocity and washout coefficient, Technical report, AEA Technology (2001).
- [63] ANDRONACHE, C., Estimated variability of below-cloud aerosol removal by rainfall for observed aerosol size distribution, *Atmos. Chem. Phys.* **3** (2003) 131–143.
- [64] PATRYL, L., GALERIU, D., ARMAND, P., Sensitivity analysis of rain characteristics on HTO concentration in drops, *Fusion Sci. Technol.* **60** (2011) 1228–1231.
- [65] TOKAY, A., SHORT, D.A., Evidence from tropical raindrop spectra of the origin of rain from stratiform versus convective clouds. *J. Appl. Meteorol.*, **35** (1996) 355–371.
- [66] MAKI M., KEENAN T.D., SASAKI, Y., NAKAMURA, K., Characteristics of the Raindrop Size Distribution in Tropical Continental Squall Lines Observed in Darwin, Australia, *J. Appl. Meteorol.* **40** (2001) 1393–1412.

- [67] TÄSCHNER, M., BUNNENBERG, C., GULDEN, W., Maximum permissible amounts of accidentally released tritium derived from an environmental experiment to meet dose limits for public exposure, *Fusion Technol.* **20** (1991) 58–64.
- [68] RASKOB, W., BARRY P., Importance and variability in processes relevant to environmental tritium ingestion dose models, *J. Environ. Radioactiv.* **36** (1997) S237–S251.
- [69] FEINHALS, J., BUNNENBERG, C., Laboratory investigations of HTO deposition to soils. *Fusion Technol.* **14** (1988) 1253–1257.
- [70] TÄSCHNER, M., BUNNENBERG, C., CAMUS, H., BELOT, Y., Investigations and modeling of tritium reemission from soil, *Fusion Technol.* **28** (1995) 976–981.
- [71] TÄSCHNER, M., BUNNENBERG, C., RASKOB, W., Measurements and modeling of tritium reemission rates after HTO deposition at sunrise and sunset, *J. Environ. Radioactiv.* **36** (1997) 219–235.
- [72] GARLAND, J.A., The absorption and evaporation of tritiated water vapor by soil and grassland, *Water Air Soil Pollut.* **13** (1980) 317–333.
- [73] RASKOB, W., Modeling of tritium behavior in the environment, *Fusion Technol.* **21** (1992) 636–644.
- [74] GALERIU, D., PAUNESCU, N., RASKOB, W., Review of processes and parameter uncertainties of present tritium modeling. RODOS (WG3)-TN(98)-07 (1998).
- [75] STULL, R.B., *An Introduction to Boundary Layer Meteorology*, Kluwer Academic Publishers (1988).
- [76] BOYBEYI, Z., *Mesoscale Atmospheric Dispersion*, WIT Press (2000).
- [77] DYER, A.J., HICKS, B.B., Flux-gradient relationships in the constant flux layer, *Quart. J. R. Meteor. Soc.* **96** (1970) 715–721.
- [78] KONDO, J., KANECHIKA, O., YASUDA, N., Heat and momentum transfer under strong stability in the atmospheric surface layer, *J. Atm. Sci.* **35** (1978) 1012–1021.
- [79] YASUDA, N., Turbulent diffusivity and diurnal variations in the atmospheric boundary layer, *Bound.-Lay. Meteor.* **43** (1988) 209–221.
- [80] KONDO, J., SAIGUSA, N., SATO, T., A parameterization of evaporation from bare soil surfaces, *J. Appl. Meteor.* **29** (1990) 385–389.
- [81] MAHFOUF, J.F., NOILHAN, J., Comparative study of various formulations of evaporation from bare soil using in situ data, *J. Appl. Meteor.* **30** (1991) 1354–1365.
- [82] TINDALL, J.A., KUNKEL, J.R., *Unsaturated zone hydrology for scientists and engineers*, Prentice-Hall Inc. (1999).
- [83] SUN, S.F., Moisture and heat transport in a soil layer forced by atmospheric conditions, M.S. thesis, University of Connecticut, USA (1982).
- [84] RUSSEL, S.B., OGRAM, G.L., Modeling elemental tritium deposition, conversion and reemission using Ontario Hydro's tritium dispersion code, *Fusion Technol.* **14** (1988) 1193–1198.
- [85] BELOT, Y., WATKINS, B.M., EDLUND, O., GALERIU, D., GUINOIS, G., GOLUBEV, A.V., MEURVILLE, C., RASKOB, W., TÄSCHNER, M., YAMAZAWA, H., Upward movement of tritium from contaminated groundwaters: a numerical analysis, *J. Environ. Radioact.* **84** (2005) 259–270.
- [86] YAMAZAWA, H., A one-dimensional dynamical soil-atmosphere tritiated water transport model, *Environ. Model. Softw.* **16** (2001) 739–751.
- [87] PENMAN, H.L., Gas and vapor movements in the soil: 1. The diffusion of vapors through porous solids, *J. Agr. Sci.* **30** (1940) 467–461.

- [88] MARSHALL, T.J., The diffusion of gases through porous media, *Eur. J. Soil Sci.* **10** (1959) 79–82.
- [89] MILLINGTON, R.J., Gas diffusion in porous media, *Science*. **130** (1959) 100-102.
- [90] MOLDRUP, P., OLESENA, T., KOMATSU, T., SCHJØNNING, P., ROLSTON, D.E., Tortuosity, diffusivity, and permeability in the soil liquid and gaseous phases, *Soil Sci. Soc. Am. J.* **65** (2001) 613–623.
- [91] RUSSELL, S.B., OGRAM, G.L., ETMOD: A New Environmental Tritium Model, *Fusion Technol.* **21** (1992) 645-650.
- [92] RASKOB, W., Description of the new version 4.0 of the tritium model UFOTRI including user guide, Report KfK-5194, Kernforschungszentrum Karlsruhe, Karlsruhe, Germany (1993).
- [93] JURY, W.A., HORTON, R., *Soil Physics*, John Wiley and Sons, Inc. (2004).
- [94] MUALEM, Y., New model for predicting hydraulic conductivity of unsaturated porous media, *Water Resour. Res.* **12** (1976) 513–522.
- [95] CLAPP, R., HORNBERGER, G., Empirical equations for some soil hydraulic properties. *Water Resour. Res.* **14** (1978) 601–604.
- [96] VAN GENUCHTEN, M.T., A closed-form equation for predicting the hydraulic conductivity of unsaturated soils, *Soil Sci. Soc. Am. J.* **44** (1980) 892–899.
- [97] ATARASHI, M., AMANO, H., ICHIMASA, M., ICHIMASA, Y., Deposition of D₂O from air to plant and soil during an experiment of D₂O vapor release into a vinyl house, *Fusion Eng. Des.* **42** (1998) 133–140.
- [98] CONRAD, R., SEILER, W., Decomposition of atmospheric hydrogen by soil microorganisms and soil enzymes, *Soil Biol. Biochem.* **13** (1981) 43–49.
- [99] CONRAD, R., WEIBER, M., SEILER, W., Kinetics and electron transport of soil hydrogenases catalyzing the oxidation of atmospheric hydrogen, *Soil Biol. Biochem.* **15** (1983) 167–173.
- [100] CONRAD, R., Soil microorganisms as controllers of atmospheric trace gases (H₂, CO, CH₄, OCS, N₂O, and NO), *Microbiol. Rev.* **60** (1996) 609–640.
- [101] GARLAND, J.A., COX, L.C., The absorption of tritium gas by English soils, plants and the sea, *Water Air Soil Pollut.* **14** (1980) 103–114.
- [102] YAMAZAWA, H., OTA, M., MORIIZUMI, J., Realistic and practical modeling of tritium deposition to bare soil, *Fusion Sci. and Technol.* **60** (2011) 1224–1227.
- [103] FALLON, R.D., Influences of pH, temperature, and moisture on gaseous tritium uptake in surface soils, *Appl. Environ. Microbiol.* **44** (1982b) 171–178.
- [104] OGRAM, G.L., SPENCER, F.S., BROWN, R.M., Field studies of HT behavior in the environment: 2. The interaction with soil, *Fusion Technol.* **14** (1988) 1170–1175.
- [105] ICHIMASA, M., ICHIMASA, M., AZUMA, Y., KOMURO, M., FUJITA, K., AKITA, Y., Oxidation of molecular tritium by surface soils, *J. Radiat. Res.* **29** (1988) 144–151.
- [106] ICHIMASA, M., SUZUKI, M., OBAYASHI, H., SAKUMA, Y., ICHIMASA, Y., In vitro determination of oxidation of atmospheric tritium gas in vegetation and soil in Ibaraki and Gifu, JAPAN, *J. Radiat. Res.* **40** (1999) 243–251.
- [107] MOMOSHIMA, N., NAGASATO, Y., TAKASHIMA, Y., Kinetic studies on oxidation of molecular tritium by soils, *Appl. Radiat. Isot.* **41** (1990) 655–660.
- [108] SMITH-DOWNEY N.V., RANDERSON, J.T., EILER, J.M., Temperature and moisture dependence of soil H₂ uptake measured in the laboratory, *Geophys. Res. Letters.* **33**, L14813 (2006).

- [109] OTA, M., YAMAZAWA, H., MORIIZUMI, J., IIDA, T., Measurement and modeling of oxidation rate of hydrogen isotopic gases by soil, *J. Environ. Radioactiv.* **97** (2007) 103–115.
- [110] OTA, M., YAMAZAWA, H., MORIIZUMI, J., IIDA, T., Measurement and modeling of the oxidation rate of hydrogen isotopic gases by soil, *J. Nucl. Sci. Technol. Suppl.* **6** (2008) 185–190.
- [111] KOMURO, M., ICHIMASA, Y., ICHIMASA, M., HT oxidation in soils in Ibaraki and isolation, identification of HT oxidizing soil bacteria, *Fusion Sci. Technol.* **41** (2002) 422–426.
- [112] MCFARLANE, J.C., ROGERS, R.D., BRADLEY JR., D.V., Tritium oxidation in surface soils. A survey of soils near five nuclear fuel reprocessing plants, *Environ. Sci. Technol.* **13** (1979) 607–608.
- [113] BELOT, Y., GUENOT, J., CAPUT, C., Emission of tritiated water formed at soil surface by oxidation of HT, *Fusion Technol.* **14** (1988) 1231–1234.
- [114] FOERSTEL, H., LEPA, K., TRIERWEILER, H., Re-emission of HTO into the atmosphere after HT/HTO conversion in the soil, *Fusion Technol.* **14** (1988) 1203–1208.
- [115] WIENER, B., TÄSCHNER, M., BUNNENBERG, C., HTO reemission from soil after HT deposition and dose consequences of HT releases, *Fusion Technol.* **14** (1988) 1247–1252.
- [116] SWEET, C.W., MURPHY, C.E., Oxidation of molecular tritium by intact soils, *Environ. Sci. Technol.* **12** (1981) 1485–1487.
- [117] SWEET, C.W., MURPHY, C.E., Tritium deposition in pine trees and soil from atmospheric releases of molecular tritium, *Environ. Sci. Technol.*, **18** (1984) 358–361.
- [118] FALLON, R.D., Molecular tritium uptake in southeastern U.S. soils, *Soil Biol. Biochem.* **14** (1982a) 553–556.
- [119] FÖRSTEL, H., Uptake of elementary tritium by the soil, *Radiation Protection Dosimetry* **16** (1986) 75–81.
- [120] DIABATÉ, S., HONIG, D., Conversion of molecular tritium to HTO and OBT in plants and soils, *Fusion Technol.* **14** (1988) 1235–1239.
- [121] TÄSCHNER, M., WIENER, B., BUNNENBERG, C., HT dispersion and deposition in soil after experimental releases of tritiated hydrogen, *Fusion Technol.* **14** (1988) 1264–1269.
- [122] NOGUCHI, H., MATSUI, T., MURATA, M., Tritium behavior observed in the Canadian HT release study, *Fusion Technol.* **14** (1988) 1187–1192.
- [123] SPENCER, F.S., OGRAM, G.L., BROWN, R.M., Field studies of HT behavior in the environment: 3. Tritium deposition and dynamics in vegetation, *Fusion Technol.* **14** (1988) 1176–1181.
- [124] DAVIS, P.A., GALERIU, D.C., SPENCER, F.S., AMIRO, B.D., Evolution of HTO concentrations in soil, vegetation and air during an experimental chronic HT release, *Fusion Technol.* **28** (1995) 833–839.
- [125] MCFARLANE, J.C., ROGERS, R.D., BRADLEY JR., D.V., Environmental tritium oxidation in surface soil, *Environ. Sci. Technol.* **12** (1978) 590–592.
- [126] AMANO, H., ATARASHI, M., NOGUCHI, H., YOKOYAMA, S., ICHIMASA, Y., ICHIMASA, M., Formation of organically bound tritium in plants during the 1994 chronic HT release experiment at Chalk River, *Fusion Technol.* **28** (1995) 803–808.
- [127] MELINTESCU, A., GALERIU, D., A versatile model for tritium transfer from atmosphere to plant and soil, *Radioprotection* **40** (2005) S437–S442.

- [128] ICHIMASA, M., WENG, C., ARA, T., ICHIMASA, Y., Organically bound deuterium in rice and soybean after exposure to heavy water vapor as a substitute for tritiated water, *Fusion Sci. Technol.* **41** (2002) 393–398.
- [129] ICHIMASA, M., MAEJIMA, T., SEINO, N., ARA, T., MASUKURA, A., NISHIHIRO, S., TAUCHI, H., ICHIMASA, Y., Organically bound deuterium in soybean exposed to atmospheric D₂O vapor as a substitute for HTO under different growth phase, *Proceedings of the International Symposium: Transfer of Radionuclides in Biosphere – Prediction and Assessment*, Mito, December 18–19, 2002, JAERI-Conf 2003-010 (2003) 226–232.
- [130] ICHIMASA, Y., SASAJIMA, E., MAKIHARA, H., TAUCHI, H., UDA, T., ICHIMASA, M., Uptake of Heavy Water and Loss by Tangerine in the Heavy Water Vapor Release Experiment in a Greenhouse as a Substitute for Tritiated Water, *Fusion Sci. Technol.* **48** (2005) 775–778.
- [131] ATARASHI, M., AMANO, H., ICHIMASA, M., KANEKO, M., ICHIMASA, Y., Uptake of heavy water vapor from atmosphere by plant leaves as a function of stomatal resistance, *Proceedings of International Meeting on Influence of Climatic Characteristics upon Behavior of Radioactive Elements*, Rokkasho, Aomori, Japan, October 14–16, 1997, Y. Ohmomo and N. Sakurai (Eds.), IES (1997) 236–242.
- [132] BALDOCCHI, D., Lecture 17 – Wind and Turbulence, Surface Boundary Layer: Theory and Principles Part II, Biometeorology Lab, ESPM and Atmospheric Science Center, University of California, Berkeley, USA (2010). Available at: <http://nature.berkeley.edu/biometlab/espm129/overheads/Lecture%2017%20ESPM%20129%20Wind%20and%20Turbulence,%20Part%20II%20overheads.pdf>
- [133] SCHUEPP, P., Tansley Review No. 59, Leaf Boundary Layers, *New Phytologist* **125** (1993) 477–507.
- [134] NIYOGI, D.S., ALAPATY, K., RAMAN, S., A photosynthesis-based dry deposition modelling approach, *Water Air Soil Poll.* **144** (2003) 171–194.
- [135] DAMOUR, G., SIMONEAU, T., COCHARD, H., URBAN, L., An overview of models of stomatal conductance at the leaf level, *Plant Cell Environ.* **33** (2010) 1419–1438.
- [136] JARVIS, P.G., The interpretation of the variations in leaf water potential and stomatal conductance found in canopies in the field, *Philos. T. R. Soc. B* **273** (1976) 593–610.
- [137] BALL, M.C., WOODROW, I.E., BERRY, J.A., A Model Predicting Stomatal Conductance and its Contribution to the Control of Photosynthesis under Different Environmental Conditions, *Progress in Photosynthesis Research* (ed. J. Biggins), Martinus Nijhoff Publishers, Dordrecht, Netherlands (1987) 221–224.
- [138] LEUNING, R., Modelling stomatal behaviour and photosynthesis of *Eucalyptus grandis*. *Australian J. Plant Physiol.* **17** (1990) 159–175.
- [139] COWAN, I.R., Stomatal behaviour and environment, *Adv. Bot. Res.* **4** (1977) 117–288.
- [140] GOUDRIAAN, J., VAN LAAR, H.H., VAN KEULEN, H., LOUWERSE, W., Photosynthesis, CO₂ and Plant Production, in *Wheat Growth and Modelling*, NATO ASI Series, Series A (W. Day and R.K. Atkin (Eds.)), Plenum Press, New York, USA (1985) 107–122.
- [141] JACOBS, C.M.J., Direct Impact of Atmospheric CO₂ Enrichment on Regional Transpiration, PhD. Thesis, Wageningen Agricultural University, The Netherlands, ISBN 90-5485-250-X (1994).

- [142] RONDA, R.J, DE BRUIN, H.A.R., HOLTSLAG, A.A.M., Representation of the canopy conductance in modeling the surface energy budget for low vegetation, *J. Appl. Meteorol.* **40** (2001) 1431–1444.
- [143] STEENEVELD, G.J., On Photosynthesis Parameters for the A-gs Surface Scheme for High Vegetation, PhD Thesis, Wageningen University, Meteorology and Air Quality Group, The Netherlands (2002).
- [144] MELINTESCU, A., GALERIU, D., Exchange velocity approach and the role of photosynthesis for tritium transfer from atmosphere to plants, *Fusion Sci. Technol.* **60** (2011a) 1179–1182.
- [145] FARQUHAR, G.D., VON CAEMMERER, S., BERRY, J.A., A biochemical model of photosynthetic CO₂ assimilation in leaves of C3 species, *Planta* **149** (1980) 78–90.
- [146] COLLATZ, G.J., BALL, J.T., GRIVET, C., BERRY, J.A., Physiological and environmental regulation of stomatal conductance, photosynthesis and transpiration: a model that includes a laminar boundary layer, *Agric. Forest Meteorol.* **54** (1991) 107–136.
- [147] COLLATZ, G.J., RIBAS-CARBO, M., BERRY, J.A., A coupled photosynthesis – stomatal conductance model for leaves of C4 plants, *Aust. J. Plant. Physiol.* **19** (1992) 519–538.
- [148] KIM, J., VERMA, S.B., Modeling canopy photosynthesis: scaling up from a leaf to canopy in a temperate grassland ecosystem, *Agric. For. Meteorol.* **57** (1991) 187–208.
- [149] DE PURY, D.G.G., FARQUHAR, G.D., Simple scaling of photosynthesis from leaves to canopies without the errors of big-leaf models, *Plant Cell Environ.* **20** (1997) 537–557.
- [150] THORNLEY, J.H.M., JOHNSON, I.R., *Plant and Crop Modelling: a mathematical approach to plant and crop physiology*, Clarendon Press, Oxford, UK, ISBN 0-19-854160-0 (1990) 669 pp.
- [151] GAO, Q., ZHAO, P., ZENG, X., CAI, X., SHEN, W., A model of stomatal conductance to quantify the relationship between leaf transpiration, microclimate and soil water stress, *Plant Cell Environ.* **25** (2002) 1373–1381.
- [152] BOOGAARD, H.L., VAN DIEPEN, C.A., ROETTER, R.P., CABRERA, J.M.C.A., VAN LAAR, H.H., User's Guide for the WOFOST 7.1 Crop Growth Simulation Model and WOFOST Control Center 1.5, Technical Document 52, DLO Winand Staring Centre, Wageningen, The Netherlands (1998).
- [153] MELINTESCU, A., GALERIU, D., MARICA, E., Using WOFOST crop model for data base derivation of tritium and terrestrial food chain modules in RODOS, *Radioprotection* **37** (2002) 1242–1246.
- [154] BALDOCCHI, D., A comparative study of mass and energy exchange over a closed (wheat) and an open (corn) canopy: I. The partitioning of available energy into latent and sensible heat exchange, *Agr. Forest Meteorol.* **67** (1994) 191–220.
- [155] CHOUDHURY, B., IDSO, S., An empirical model for stomatal resistance of wheat, *Agr. Forest Meteorol.* **36** (1985) 65–82.
- [156] VOS, J., GROENWOLD, J., Characteristics of photosynthesis and conductance of potato canopies and the effects of cultivars and transient drought, *Field Crop Res.* **20** (1989) 237–250.
- [157] SAUGIER, B., KATERJI, N., Some plant factors controlling evapotranspiration, *Agr. Forest Meteorol.* **54** (1991) 263–278.
- [158] OLIOSO, A., CARLSON, T.N., BRISSON, N., Simulation of diurnal transpiration and photosynthesis of a water stressed soybean crop, *Agr. Forest Meteorol.* **81** (1996) 41–59.

- [159] KNAPP, A.K., Gas exchange dynamics in C3 and C4 grasses: consequences of differences in stomatal conductance, *Ecology* **74** (1993) 113–123.
- [160] DIABATE, S., STRACK, S., Organically bound tritium in wheat after short-term exposure to atmospheric tritium under laboratory conditions, *J. Environ. Radioactiv.* **36** (1997) 157–175.
- [161] MOSES, V., CALVIN, M., Photosynthesis studies with tritiated water, *Biochim. Biophys. Acta* **33** (1959) 297–312.
- [162] THOMPSON, R.G., NELSON, C.D., Photosynthetic assimilation and translocation of ³H- and ¹⁴C-organic compounds after 3HHO and i4CO₂ were simultaneously offered to a primary leaf of soybean, *Can. J. Bot.* **49** (1971) 757–766.
- [163] ARAI, K., TAKEDA, H., IWAKURA, T., Studies on the tritium uptake in some edible plants and transfer to the rat, in *Tritium Radiobiology and Health Physics*, Chiba, Japan (1985) pp. 3549.
- [164] INDEKA, L., Incorporation of tritiated water from the atmosphere into aqueous and organic components of plants, in *Biological incorporation of Tritium*, Z. Jaworowski (Ed.), Central Laboratory for Radiological Protection, CLOR-115/D, Warsaw, Poland (1981) 21–27.
- [165] GALERIU, D., Transfer parameters for routine release of HTO, incorporation of OBT, Atomic Energy of Canada report, AECL 11052, COG -94-76 (1994).
- [166] CANADIAN STANDARD ASSOCIATION, Guidelines for calculating derived release limits for radioactive material in airborne and liquid effluents for normal operation of nuclear facilities. CSA N288.1, CSA Guideline N288.1-08, Canadian Standards Association, Mississauga (2008).
- [167] ENVIRONMENTAL PROTECTION AGENCY, Guidance on the Development, Evaluation, and Application of Environmental Models, EPA/100/K-09/003, March 2009 (2009).
- [168] BIOSPHERIC MODEL VALIDATION STUDY (BIOMOVS II), Tritium in the food chain, BIOMOVS II Technical Report No. 8, Stockholm, Sweden: BIOMOVS II Steering Committee, Swedish Radiation Protection Institute (1996b).
- [169] AUTORITE DE SURETE NUCLEAIRE, Livre blanc du Tritium (2010) (in French). Available at:
http://livre-blanc-tritium.asn.fr/fichiers/Tritium_livre_blanc_integral_web.pdf
- [170] CANADIAN NUCLEAR SAFETY COMMISSION, Tritium Studies (2010). Available at:
http://www.nuclearsafety.gc.ca/eng/readingroom/tritium/tritium_studies.cfm
- [171] STRACK, S., Personal communication (2010).
- [172] DIABATÉ, S., STRACK, S., Tritium Uptake in Wheat Plants after Short-Term Exposure to Atmospheric Tritium under Field Conditions, Personal communication (1998).
- [173] RASKOB, W., Test and Validation Studies Performed with UFOTRI and NORMTRI, FZK Report 7281, Karlsruhe, Germany (2007).
- [174] STRACK, S., DIABATÉ, S., RASKOB, W., Modellrechnungen zur Biokinetik von Tritium in Pflanzen, in: Winter, M. (Hrsg.), *Radioaktivität in Mensch und Umwelt*, 30. FS-Jahrestagung, 28.9. – 2.10.98, Lindau, Bd. II, S. 855-860, Köln: TueV Rheinland (1998) (in German).
- [175] RASKOB, W., DIABATÉ, S., STRACK, S., A new approach for modelling the formation and translocation of organically bound tritium in accident consequence assessment codes. *Int. Symposium on Ionization Radiation: Protection of the Natural Environment*, Stockholm, Sweden, May 20–24, 1996 (1996).

- [176] STRACK, S., DIABATÉ, S., RASKOB, W., Organically bound tritium in plants: insights gained by long-term experience in experimental and modelling research, *Fusion Sci. Technol.* **48** (2005) 767–770.
- [177] DIABATÉ, S., STRACK, S., PAUNESCU, N., Tritium uptake in green bean and potato plants after short-term exposure to atmospheric tritium, Preprint IFIN-HH/RB-53 (1998).
- [178] ICHIMASA, M., WENG, C., ARA, T., ICHIMASA, Y., Heavy water release experiment: transfer of heavy water to vegetation, Proceedings of the International Workshop on Environmental Behaviour and Biological Effects of Tritium. Kumatori, Osaka, Japan, 8–9 May 2000 (2001) 42–47.
- [179] ATARASHI-ANDOH, M., AMANO, H., KAKIUCHI, H., ICHIMASA, M., ICHIMASA, Y., Formation and retention of organically bound deuterium in rice in deuterium water release experiment. *Health Phys.* **82** (2002) 863–868.
- [180] ATARASHI-ANDOH, M., KUMAKURA, Y., AMANO, H., FUKU, M., Formation of Organically Bound Deuterium at Each Growing Stage of Rice, *Fusion Sci. Technol.* **48** (2005) 771–774.
- [181] CHOI, Y.H., LIM, K.M., LEE, W.Y., DIABATE', S., STRACK, S., Tissue free water tritium and organically bound tritium in the rice plant acutely exposed to atmospheric HTO vapor under semi-outdoor conditions, *J. Environ. Radioactiv.* **58** (2002) 67–85
- [182] CHOI, Y. H., LIM, K.M., LEE, W.Y., KANG, H.S., CHOI, H.J, LEE, H.S., DIABATE', S., STRACK, S., TFWT and OBT concentration in rice plants exposed to HTO vapor during daytime and nighttime at different seed-developing stages. *J. Korea Soc. Radiat. Prot.* **28** (2003) 9–18 (in Korean).
- [183] CHOI, Y.H., LIM, K.M., LEE, W.Y., PARK, H.G., CHOI, G.S., KEUM, D.K., LEE, H., KIM, S.B., LEE, C.W., Tritium levels in Chinese cabbage and radish plants exposed to HTO vapor at different growth stages, *J. Environ. Radioactiv.* **84** (2005) 79–94.
- [184] BEATON, D., DAVIS, P.A., KOTZER, T., Plant Respiratory Metabolism, Assimilate Transport and Organically Bound Tritium Formation, COG-01-081 (2001).
- [185] DAVIS, P.A., KIM, S.B., KOTZER, T.G., Mathematical model of OBT formation at night in edible parts of non-leafy vegetables, Report COG-01-79, CANDU Owners Group Inc., Toronto, ON (2002).
- [186] KIM, S.B., SCHEIER N.W., Organically Bound Tritium (OBT) formation in night experiments and modeling trials at CRL, Personal communication (2009).
- [187] KIM, S.B., OBT formation in night experiments and modeling trials at CRL, Third Meeting of International Atomic Energy Agency (IAEA)'s Environmental Modelling for Radiation Safety (EMRAS II) Programme 2009-2011, Working Group 7 "Tritium Accidents", Vienna, Austria, 25-29 January 2010 (2010a). Available at: <http://www-ns.iaea.org/downloads/rw/projects/emras/emras-two/first-technical-meeting/second-working-group-meeting/working-group-presentations/workgroup7-presentations/presentation-wg7-night-experiments-3rd-mtg.pdf>
- [188] BOYER, C., Etude des transferts du tritium atmospherique chez la laitue: etude cinetique, etat d'equilibre et integration du tritium sous forme organique lors d'une exposition atmospherique continue, PhD Thesis, Universite de Franche-Compte, France (2009) (in French).
- [189] KERSTIENS, G., Water transport in plant cuticles: an update, *J. Exp. Bot.* **57** (2006) 2493–2499.

- [190] SCHOENHERR, J., Characterization of aqueous pores in plant cuticles and permeation of ionic solutes, *J. Exp. Bot.*, **57** (2006) 2471–2491.
- [191] RIEDERER, M., SCHREIBER, L., Protecting against water loss: analysis of the barrier properties of plant cuticles, *J. Exp. Bot.* **52** (2001) 2023–2032.
- [192] MOMOSHIMA, N., KAKIUCHI, H., OKAI, T., YOKOYAMA, S., NOGUCHI, H., ATARASHI, M., AMANO, H., HISAMATSU, S., ICHIMASA, M., ICHIMASA, Y., MAEDA, Y., Uptake kinetics of deuteriated water vapor by plants: Experiments of D₂O release in a greenhouse as a substitute for tritiated water, *J. Radioanal. Nucl. Chem.* **239** (1999) 459–464.
- [193] THORNTON, P.E., Regional ecosystem simulation: combining surface- and satellite-based observations to study linkages between energy and mass budgets, Ph.D. Thesis, University of Montana, Missoula, MT, USA (1998) 200 pp.
- [194] ÁCS, F., On transpiration and soil moisture content sensitivity to soil hydrophysical data, *Bound.-Lay. Meteorol.* **115** (2005) 473–497.
- [195] BELJAARS, A.C., VITERBO, P., MILLER, M.J., BETTS, A.K., The anomalous rainfall over the United States during July 1993: Sensitivity to land surface parameterization and soil moisture anomalies, *Mon. Wea. Rev.* **124** (1996) 362–383.
- [196] BETTS, A.K., BALL, J.H., BELJAARS, A.C.M., MILLER, M.J., VITERBO, P.A., The land surface–atmosphere interaction: A review based on observational and global modeling perspectives, *J. Geophys. Res.*, **101** (1996) 7209–7225.
- [197] BOUWER, L.M., BIGGS T.W., AERTS, J.C.J.H., Estimates of spatial variation in evaporation using satellite-derived surface temperature and a water balance model, *Hydrol. Process.*, **22** (2008) 670–682.
- [198] GLEESON T., MARKLUND L., SMITH L., MANNING, A.H., Classifying the water table at regional to continental scales, *Geophys Res. Lett.*, **38** (2011) L05401.
- [199] WOOD, E.F., SIVAPALAN, M., BEVEN, K., BAND, L., Effects of spatial variability and scale with implications to hydrologic modelling, *J. Hydrol.* **102** (1988) 29–47.
- [200] SZILAGYI, J., JOZSA, J., Complementary relationship of evaporation and the mean annual water-energy balance, *Water Resour. Res.* **45**, W09201 (2009) 4 pp.
- [201] RIHANI, J.F., MAXWELL, R.M., CHOW, F.K., Coupling groundwater and land surface processes: Idealized simulations to identify effects of terrain and subsurface heterogeneity on land surface energy fluxes, *Water Resour. Res.* **46**, W12523 (2010) 14 pp.
- [202] SIVAPALAN, M., YAEGER, M.A., HARMAN, C.J., XU, X., TROCH, P.A., Functional model of water balance variability at the catchment scale: 1. Evidence of hydrologic similarity and space-time symmetry, *Water Resour. Res.* **47**, W02522, (2011) 18 pp.
- [203] FERGUSON, I.M., MAXWELL, R.M., Hydrologic and land–energy feedbacks of agricultural water management practices, *Environ. Res. Lett.* **6**, 014006 (2011).
- [204] ARRIGO, J.A.S., SALVUCCI, G.D., Investigation hydrologic scaling: Observed effects of heterogeneity and nonlocal processes across hillslope, watershed, and regional scales, *Water Resour. Res.*, **41**, W11417 (2005) 17 pp.
- [205] DECHARME, B., DOUVILLE, H., BOONE A., HABETS, F., NOILHAN, J., Impact of an Exponential Profile of Saturated Hydraulic Conductivity within the ISBA LSM: Simulations over the Rhône Basin, *J. Hydrometeorol.* **7** (2006) 61–80.

- [206] MILLY, P.C.D., DUNNE, K.A., On the Hydrologic Adjustment of Climate-Model Projections: The Potential Pitfall of Potential Evapotranspiration, *Earth Interact.* **15** (2011) 1–14.
- [207] MAXWELL, R.D., LUNDQUIST, J.K., MIROSHA, J.D., SMITH, S.G., WOODWARD, C.S., TOMPSON, A.F.B., Development of a Coupled Groundwater–Atmosphere Model, *Monthly Weather Review* **139** (2011) 96–116.
- [208] MILLY, P.C.D., Climate, soil water storage, and the average annual water balance, *Water Resour. Res.* **30** (1994) 2143–2156.
- [209] KIM, C.P., SALVUCCI, G.D., ENTEKHABI, D., Groundwater-surface water interaction and the climatic spatial patterns of hillslope hydrological response, *Hydrol. Earth Syst. Sci.* **3** (1999) 375–384.
- [210] THOMPSON, S.E., HARMAN, C.J., TROCH, P.A., BROOKS, P.D., SIVAPALAN, M., Spatial scale dependence of ecohydrologically mediated water balance partitioning: A synthesis framework for catchment ecohydrology, *Water Resour. Res.* **47**, W00J03 (2011) 20 pp.
- [211] MIGUEZ-MACHO G., FAN Y., WEAVER, C.P., WALKO, R., ROBOCK, A., Incorporating water table dynamics in climate modeling: 2. Formulation, validation, and soil moisture simulation, *J. Geophys. Res.* **112**, D13108 (2007) 16 pp.
- [212] MA, L., HOOGENBOOM, G., AHUJA, L.R., NIELSEN, D.C., ASCOUGH, J.C. II, Development and evaluation of the RZWQM-CROPGRO hybrid model for soybean production, *Agron. J.* **97** (2005) 1172–1182.
- [213] MA, L., AHUJA, L.R., BRUULSEMA, T.W., Quantifying and understanding plant nitrogen uptake for systems modeling, Kluwer Academic Publishers, Norwell, MA. (2009) 150 pp.
- [214] GASSMAN, P.W., Historical development and applications of the EPIC and APEX models, Edited by J. R. Williams, V. W. Benson, R. C. Izaurralde, L. M. Hauck, C. A. Jones, J. D. Atwood, J. R. Kiniry and J. D. Flowers, Iowa State University: Center for Agricultural and Rural Development (2005).
- [215] GASSMAN, P.W., WILLIAMS, J.R., WANG, X., SALEH, A., OSEI, E., HAUCK, L.M., IZAURRALDE, R.C., FLOWERS, J. D., The Agricultural Policy Environmental EXtender (APEX) Model: An Emerging Tool for Landscape and Watershed Environmental Analyses, Technical Report 09-TR 49, Center for Agricultural and Rural Development, Iowa State University, Ames, Iowa 50011-1070 (2009). Available at: www.card.iastate.edu
- [216] WANG X., HOFFMAN, D.W., WOLFE, J.E., WILLIAMS, J.R., FOX, W.E., The Agricultural Policy Environmental Extender (APEX) model: An emerging tool for landscape and watershed environmental analyses, *Transactions of the ASABE*, **52** (2009) 1181–1192.
- [217] FLANAGAN, D.C., ASCOUGH II, J.C., M.A. NEARING, M.A., LAFLEN, J.M., Chapter 7: The Water Erosion Prediction Project (WEPP) Model. In (R.S. Harmon and W.W. Doe III, (Eds.): *Landscape Erosion and Evolution Modeling*, Kluwer Academic Publishers, Norwell, MA (2001) 51 pp.
- [218] GATES, L.W., AMIP: The Atmospheric Model Intercomparison Project. *Bull. Amer. Meteor. Soc.* **73** (1992) 1962–1970.
- [219] PRENTICE, I.C., CRAMER, W., HARRISON, S.P., LEEMANS, R., MONSERUD, R.A., SOLOMON, A.M., A global biome model based on plant physiology and dominance, soil properties and climate, *J. Biogeogr.* **19** (1992) 117–134.

- [220] LIANG, X., LETTENMAIER, D.P., WOOD, E., BURGESS, S.J., A simple hydrologically based model of land surface water and energy fluxes for general circulation models. *J. Geophys. Res.* **99** (1994) 14415–14428.
- [221] FOLEY, J.A., PRENTICE, I.C., RAMANKUTTY, N., LEVIS, S., POLLARD, D., SITCH, S., HAXELTINE, A., An integrated biosphere model of land surface processes, terrestrial carbon balance, and vegetation dynamics (IBIS), *Global Biogeochem.Cy.* **10** (1996) 603–628.
- [222] HAXELTINE, A., PRENTICE, I.C., CRESWELL, I.D., A coupled carbon and water flux model to predict vegetation structure (BIOME2), *J. Veg. Sci.* **7** (1996) 651–666.
- [223] MILLY, P.C.D., SHMAKIN, A.B., Global Modeling of Land Water and Energy Balances. Part II: Land-Characteristic Contributions to Spatial Variability, *J. Hydrometeorol.* **3** (2002) 301–310.
- [224] POTTER, C., Predicting climate change effects on vegetation, soil thermal dynamics, and carbon cycling in ecosystems of interior Alaska, *Ecol. Model.* **175** (2004) 1–24.
- [225] SELLERS, P.J., Canopy reflectance, photosynthesis, and transpiration, *Int. J. Remote Sens.* **6** (1985) 1335–1372.
- [226] SELLERS, P.J., BERRY, J.A., COLLATZ, G.J., FIELD, C.B., HALL, F.G., Canopy reflectance, photosynthesis, and transpiration III. A reanalysis using improved leaf models and a new canopy integration scheme, *Remote Sens. Environ.* **42** (1992) 187–216.
- [227] SELLERS, P.J., LOS, S.O., TUCKER, C.J., JUSTICE, C.O., DAZLICH, D.A., COLLATZ, G.J., D.A. RANDALL, D.A., A revised land surface parameterization (SiB2) for atmospheric general circulation models. Part 2. The generation of global fields of terrestrial biophysical parameters from satellite data. *J. Clim.* **9** (1996) 706–737.
- [228] FARMER, D., SIVAPALAN, M., JOTHITYANGKOON, C., Climate, soil, and vegetation controls upon the variability of water balance in temperate and semiarid landscapes: Downward approach to water balance analysis, *Water Resour. Res.* **39**, 1035 (2003) 21 pp.
- [229] DALY, E., A. PORPORATO, A., 2006, Impact of hydroclimatic fluctuations on the soil water balance, *Water Resour. Res.* **42**, W06401 (2006).
- [230] MAHRT, L., PAN, H., A two-layer model of soil hydrology. *Bound.-Lay. Meteor.* **29** (1984) 1–20.
- [231] YANG, D., SUN F., LIU, Z., CONG, Z., NI, G., LEI, Z., Analyzing spatial and temporal variability of annual water-energy balance in nonhumid regions of China using the Budyko hypothesis, *Water Resour. Res.* **43** (2007) W04426.
- [232] CORNWELL, A.R., HARVEY, L.D.D., Soil moisture: a residual problem underlying AGCMs, *Clim. Change* **84** (2007) 313-336.
- [233] CORNWELL, A.R., HARVEY, L.D.D., Simulating AOGCM Soil Moisture Using an Off-Line Thornthwaite Potential Evapotranspiration–Based Land Surface Scheme. Part I: Control Runs, *J. Clim.* **21** (2008) 3097–3117.
- [234] GERRITS, A.M.J., SAVENIJE, H.H.G., VELING, E.J.M., PFISTER, L., Analytical derivation of the Budyko curve based on rainfall characteristics and a simple evaporation model, *Water Resour. Res.* **45** (2009) W04403.
- [235] EBEL, B.A., MIRUS B.B., First-order exchange coefficient coupling for simulating surface water–groundwater interactions: parameter sensitivity and consistency with a physics-based approach, *Hydrol. Process.* **23** (2009) 949–1959.

- [236] RODERICK, M.L., FARQUHAR, G.D., A simple framework for relating variations in runoff to variations in climatic conditions and catchment properties, *Water Resour. Res.* **47**, W00G07 (2011) 11 pp.
- [237] GATES, L.W., et al., An overview of the results of the Atmospheric Model Intercomparison Project (AMIP I), *Bull. Amer. Meteor. Soc.*, **80** (1999) 29–55.
- [238] DECHARME, B., DOUVILLE, H., Introduction of a sub-grid hydrology in the ISBA land surface model. *Clim. Dynam.* **26** (2006) 65–78.
- [239] GUETAT, P., ARMAND, P., Projet EdF/CIDEN. IV – Presentation du modele et des resultants de calcul pour le tritium. Rapport Technique SMQ.EEX52 RBC RTE QRCE 0064 B, CEA/DAM-Ile-de-France (2011).
- [240] OTA, M., NAGAI, H., Development and validation of a dynamical atmosphere–vegetation–soil HTO transport and OBT formation model, *J Environ. Radioactiv.* **102** (2011a) 813–823.
- [241] ARORA, V.K., Simulating energy and carbon fluxes over winter wheat using coupled land surface and terrestrial ecosystem models, *Agr. Forest Meteorol.* **118** (2003) 21–47.
- [242] MILLY, P.C.D. Sensitivity of greenhouse summer dryness to changes in plant rooting characteristics, *Geophys. Res. Lett.* **24** (1997) 269–271.
- [243] REICH, P.B., WALTERS, M.B., TJOELKER, M.G., VANDERKLEIN, D., BUSCHENA, C., Photosynthesis and respiration rates depend on leaf and root morphology and nitrogen concentration in nine boreal tree species differing in relative growth rate, *Funct. Ecol.* **12** (1998) 395–405.
- [244] FEDERER, C.A., VÖRÖSMARTY, C., FEKETE, B., Sensitivity of Annual Evaporation to Soil and Root Properties in Two Models of Contrasting Complexity, *J. Hydrometeorol.* **4** (2003) 1276–1290.
- [245] LÜDEKE M. K. B., BADECK, F.W., OTTO, R.D., HÄGER, C., DÖNGES, S., KINDERMANN, J., WÜRTH, G., LANG, T., JÄKEL, U., KLAUDIUS, A., RAMGE, P., HABERMEHL, S., KOHLMAIER, G.H., The Frankfurt Biosphere Model: a global process oriented model of seasonal and long-term CO₂ exchange between terrestrial ecosystems and the atmosphere. I. Model description and illustrative results for cold deciduous and boreal forests. *Clim. Res.* **4** (1994) 143–166.
- [246] IRVINE, J., LAW, B.E., ANTHONI, P.M., MEINZER, F.C., Water limitations to carbon exchange in old-growth and young ponderosa pine stands. *Tree Physiol.* **22** (2002) 189–196.
- [247] ARORA, V.K., BOER, G.J., A representation of variable root distribution in dynamic vegetation models, *Earth Interact.* **7**, Paper 6 (2003) 19 pp.
- [248] JACKSON, R.B., CANADELL, J., EHRINGER, J.R., MOONEY, H.A., SALA, O.E., SCHULZE, E.D., A global analysis of root distributions for terrestrial biomes, *Oecologia*, **108** (1996) 389–411.
- [249] XU, L., BALDOCCHI, D.D., Seasonal trends in photosynthetic parameters and stomatal conductance of blue oak (*Quercus douglasii*) under prolonged summer drought and high temperature, *Tree Physiol.* **23** (2003) 865–877.
- [250] MÉSZÁROS, R., SZINYEI, D., VINCZE, C., Effect of the soil wetness state on the stomatal ozone fluxes over Hungary, *Int. J. Environ. Pollut.* **36** (2009) 180–194.
- [251] HOWARD, P.J.A., HOWARD, D.M., Respiration of decomposing litter in relation to temperature and soil moisture, *Oikos* **33** (1979) 457–465.

- [252] LAVELLE, P., BLANCHART, E., MARTIN, S., MARTIN, A., BAROIS, S., TOUTAIN, F., SPAIN, A., SCHAEFER, R., A hierarchical model for decomposition in terrestrial ecosystems: Application to soils of the humid tropics. *Biotropica* **25** (1993) 130–150.
- [253] GHOLZ, H.L., WEDIN, D.A., SMITHERMAN, S.M., HARMON, M.E., PARTON, W.J., Long-term dynamics of pine and hardwood litter in contrasting environments: toward a global model of decomposition, *Global Change Biol.* **6** (2000) 751–765.
- [254] PAUL, K., Temperature and moisture effects on decomposition, in *Net Ecosystem Exchange*, Cooperative Research Centre for Greenhouse Accounting, edited by M.U.F. Kirschbaum and R. Mueller, Canberra, Australia (2001) pp. 95–102.
- [255] ORCHARD, V.A., COOK, F.J., Relationship between soil respiration and soil moisture, *Soil Biol. Biogeochem.* **15** (1983) 447–453.
- [256] SCHLENTNER, R.E., VAN CLEVE, K., Relationships between CO₂ evolution from soil, substrate temperature, and substrate moisture in four mature forests types in interior Alaska, *Can. J. For. Res.* **15** (1985) 97–106.
- [257] RYAN, M.G., Effects of climate change on plant respiration. *Ecol. Appl.* **1** (1991) 157–167.
- [258] ORCHARD, V.A., COOK, F.J., CORDEROY, D.M., Field and laboratory studies on the relationships between respiration and moisture for two soils of contrasting fertility status, *Pedobiologia*, **36** (1992) 21–33.
- [259] LLOYD, J., TAYLOR, J.A., On the temperature dependence of soil respiration, *Funct. Ecol.*, **8** (1994) 315–323.
- [260] KIRSCHBAUM, M.U.F., The temperature dependence of soil organic matter decomposition, and the effect of global warming on soil organic C storage. *Soil Biol. Biochem.* **27** (1995) 753–760.
- [261] AERTS, R., Climate, leaf litter chemistry and leaf litter decomposition in terrestrial ecosystems: a triangular relationship, *Oikos*, **79** (1997) 439–449.
- [262] SCHLESINGER, W.H., ANDREWS, J.A., Soil respiration and the global carbon cycle, *Biogeochemistry*, **4** (2000) 7–20.
- [263] SCHLESINGER, W.H., WINKLER, J.P., MEGONIGAL, J.P., Soils and the global carbon cycle, in *The Carbon Cycle*, Edited by T.M.L Wigley and D.S. Schimel, Cambridge University Press (2000) 93–101.
- [264] TJOELKER, M.G., OLEKSYN, J., REICH, P.B., Modelling respiration of vegetation: evidence for a general temperature-dependent Q₁₀. *Global Change Biol.* **7** (2001) 223–230.
- [265] LUKEN, J.O., BILLINGS, W.D., The influence of microtopographic heterogeneity on carbon dioxide efflux from a subarctic bog, *Holarct. Ecol.* **8** (1985) 306–312.
- [266] RAICH, J. W., TUFEKCIOGLU, A., Vegetation and soil respiration: Correlations and controls, *Biogeochemistry*, **48** (2000) 71–90.
- [267] BARRY, P.J., WATKINS, B.M., BELOT, Y., DAVIS, P.A., EDLUND, O., GALERIU, D., RASKOB, W., RUSSELL, S., TOGAWA, O., Intercomparison of model predictions of tritium concentrations in soil and foods following acute airborne HTO exposure, *J. Environ. Radioactiv.* **42** (1999) 191–207.
- [268] PATRYL, L., ARMAND, P., Key assumptions and modelling approaches of tritium models implemented in GAZAXI 2002 and, CERES, CEA report EOTP A-24100-01-01-AW-43 (2007). Available upon request to luc.patryl@cea.fr.

- [269] GALERIU, D., RASKOB, W., MELINTESCU, A., TURCANU, C., Model Description of the Tritium Food Chain and Dose Module FDMH in RODOS PV 4., RODOS (WG3)-TN(99)-54 (2000). Available at http://www.rodos.fzk.de/Documents/Public/CD1/Wg3_CD1_General/WG3_TN99_54.pdf
- [270] ENVIRONMENTAL PROTECTION AGENCY, Guiding Principles for Monte Carlo Analysis, EPA/630/R-97/001, Risk Assessment Forum, U.S. Environmental Protection Agency, Washington, D.C. 20460 (1997).
- [271] CHANG, J.C., HANNA, S.R., Technical descriptions and user's guide for the BOOT statistical model evaluation software package, Version 2.0, Technical report (2005).
- [272] COX, W., TIKVART, J., A statistical procedure for determining the best performing air quality simulation model, *Atmos. Environ.* **24A** (1990) 2387–2395.
- [273] INTERNATIONAL ATOMIC ENERGY AGENCY, Pig scenario, Final report, IAEA's Environmental Modelling for Radiation Safety (EMRAS) Programme 2003–2007, IAEA, Vienna (2008c). Available at: <http://www-ns.iaea.org/downloads/rw/projects/emras/tritium/pig-report-final.pdf>
- [274] INTERNATIONAL ATOMIC ENERGY AGENCY, Handbook of parameter values for the prediction of radionuclide transfer in terrestrial and freshwater environments, Technical Reports Series No. 472, IAEA, Vienna (2010).
- [275] VAN DEN HOEK, J., TENHAVE, M.H.J., The metabolism of tritium and water in the lactating dairy cow, *Health Phys.* **44** (1983) 127–133.
- [276] VAN DEN HOEK, J., TENHAVE, M.H.J., GERBER, G.B., KIRCHMANN, R., The transfer of tritium-labelled organic material from grass into cow milk. *Radiat. Res.* **103** (1985) 105–113.
- [277] VAN DEN HOEK, J., Tritium metabolism in animals, *Radiat. Prot. Dosim.* **16** (1986) 117–121.
- [278] FREER, M., Sheep nutrition (Animal nutrition), CABI Publishing, ISBN 9780851995953, New York, USA (2002).
- [279] PETERSON, S.R., Historical Doses from Tritiated Water and Tritiated Hydrogen Gas Released to the Atmosphere from Lawrence Livermore National Laboratory (LLNL) – Part 1. Description of Tritium Dose Model (DCART) for Chronic Releases from LLNL, UCRL-TR-205083 (2004).
- [280] MÜLLER, H., PRÖHL, G., ECOSYS-87: A Dynamic Model for Assessing Radiological Consequences of Nuclear Accidents, *Health Phys.* **64** (1993) 232–252.
- [281] MULLEN, A.L., MOGHISSI, A.A., WAWERNA, J.C., MITCHELL, B.A., BRETTHAUER, E.W., Tritium Retention by Cows and Steers and Transfer to Milk, Ecological research series, EPA-600/3-77-076, Environmental Monitoring and Support Laboratory, Las Vegas, Nevada, USA (1977).
- [282] POTTER, G.D., VATTUONE, G.M., MCINTYRE, D.R., Metabolism of tritiated water in the dairy cow, *Health Phys.* **22** (1972) 405–409.
- [283] THORNE, M.C., GOULD, L.J., KELLY, M., Review of Data Suitable for Food Chain Modelling of ^{14}C , ^3H and ^{35}S in Animals, AEA Technology Report to the Food Standards Agency, AEAT/ERRA-0359, Issue 1 (2001).
- [284] GALERIU, D., CROUT, N.M.J., MELINTESCU, A., BERESFORD, N.A., PETERSON, S.R., VAN HESS, M., A Metabolic Derivation of Tritium Transfer Factors in Animal Products, *Radiat. Environ. Biophys.* **40** (2001) 325–334.
- [285] GALERIU, D., MELINTESCU, A., SLAVNICU, D., GHEORGHIU, D., SIMIONOV, V., Accidental release of tritiated water – toward a better radiological assessment, *Radioprotection* **44** (2009a) 177–183.

- [286] HIGGINS, N.A., SHAW, P.V., HAYWOOD, S.M., TRIF – A dynamic environmental model for predicting the consequence of atmospheric releases of tritium, Report NRPB-R278, National Radiological Protection Board, Chilton, UK (1995).
- [287] SMITH, G.M., ROBINSON, P.C., STENHOUSE, M.J., H-3 Food chain Modelling Following Short Term Release to Atmosphere, INTERA Environmental Division report IE3947-1, INTERA, Henley-on-Thames (1995).
- [288] WATKINS, B.M., ROBINSON, P.C., SMITH, G.M., Update of Models for Assessing Short-Term Atmospheric Releases of C-14 and Tritium in the Light of New Information and Experimental Data, Quantisci – MAFF-5044-1 (1998).
- [289] MAUL, P.R., WATSON, C.E., THORNE, M.C., Probabilistic Modelling of C-14 and H-3 Uptake by Crops and Animals, Quintessa report QRS-1264A-1, Version 3.0, September 2005 (2005).
- [290] TAMPONNET, C., Modelling Tritium and Carbon 14 in the environment: A biomass-oriented approach, *Radioprotection* **40** (2005) S713–S719.
- [291] SHEPPARD, S.C., CIFFROY, P., SICLET, F., DAMOIS, C., SHEPPARD, M.I., STEPHENSON, M., Conceptual approaches for the development of dynamic specific activity models of ^{14}C transfer from surface water to humans, *J. Environ. Radioactiv.* **87** (2006a) 32–51
- [292] SHEPPARD, S.C., SHEPPARD, M.I., SICLET, F., Parameterization of a dynamic specific activity model of ^{14}C transfer from surface water-to-humans, *J. Environ. Radioactiv.* **87** (2006b) 15–31.
- [293] TAKEDA, H., Metabolic and dosimetric study to estimate an annual limit on intake for organic tritium, *Fusion Technol.* **28** (1995) 964–969.
- [294] CROUT, N.M.J., MAYES, R.W., BERESFORD, N.A., LAMB, C.S., HOWARD, B.J., A metabolic approach to simulating the dynamics of C-14, H-3 and S-35 in sheep tissues, *Radiat. Environ. Biophys.* **36** (1998) 243–250.
- [295] THORNE, M., Parameterization of animal models, Report MTA/P0022/2003-1, Mike Thorne and Associates Ltd., Halifax (2003).
- [296] GALERIU, D., MELINTESCU, A., BERESFORD, N.A., CROUT, N.M.J., TAKEDA, H., ^{14}C and tritium dynamics in wild mammals: a metabolic model, *Radioprotection* **40** (2005a) S351–S357.
- [297] JONES, J.H., JACKSON, D., A review of data on C-14 and development of a model of the environmental transport of C-14, Report ANS 513-1 (1986).
- [298] MELINTESCU A, GALERIU, D., Energy metabolism used as a tool to model the transfer of ^{14}C and ^3H in animals, *Radiat. Environ. Biophys.* **49** (2010) 657–672.
- [299] GALERIU, D., BERESFORD, N.A., CROUT, N.M.J., MELINTESCU, A., TAKEDA, H., Biological and Carbon half-time in farm and wild animals, IUR Waste Task Force Meeting “Radiocology and Waste”, 27–28 February 2003, Merlewood, Cumbria, UK (2003).
- [300] MCDONALD, P., EDWARDS, R.A., GREENHALGH, J.F.D., MORGAN, C.A., *Animal nutrition*, 5th edn., Longman Scientific & Technical, Harlow, UK (1995).
- [301] WEST, G.B., BROWN, J.H., ENQUIST, B.J., A general model for ontogenetic growth, *Nature* **413** (2001) 628–631.
- [302] BERESFORD, N.A., BROADLEY, M.R., HOWARD, B.J., BARNETT, C.L., WHITE, P.J., Estimating radionuclide transfer to wild species—data requirements and availability for terrestrial ecosystems, *J. Radiol. Prot.* **24** (2004) A89–A103.
- [303] MAKARIEVA, A.M., GORSHKOV, V.G., BAI-LIAN, L., Ontogenetic growth: models and theory, *Ecol. Model.* **176** (2004) 15–26.

- [304] CIFFROY, P., SICLET, F., DAMOIS, C., LUCK, M., A dynamic model for assessing radiological consequences of tritium routinely released in rivers, Parameterisation and uncertainty/sensitivity analysis, *J. Environ. Radioactiv.* **83** (2005) 9–48.
- [305] CIFFROY, P., SICLET, F., DAMOIS, C., LUCK, M., A dynamic model for assessing radiological consequences of tritium routinely released in rivers. Application to the Loire River, *J. Environ. Radioactiv.* **90** (2006) 110–139.
- [306] LE DIZES, S., Modélisation du transfert de Tritium issu de rejets atmosphériques dans les systèmes agricole et anthropique. Rapport IRSN/DEI/SECRE/2004-030; Modélisation du transfert de Carbone 14 dans l'environnement, Rapport IRSN/DEI/SECRE/2004-029 (2004) (in French).
- [307] KIRCHMANN, R., RÉMY, J., CHARLES, P., KOCH, G., VAN DEN HOEK, J., Distribution et incorporation du tritium dans les organes de ruminant, paper IAEA-SM-172/81, Environmental behaviour of radionuclides released in the nuclear industry, IAEA, Vienna (1973) 385–402 (in French).
- [308] VAN HESS, M., Personal communication (2000).
- [309] SAITO, M., A Modified three-Compartment Model for Tritium Metabolism in man. *Radiat. Prot. Dosim.* **42** (1992) 17–24.
- [310] WALKE, R., THORNE, M., EMRAS Model Comparisons: Adaptation of PRISM H-3 Model to Partition Excretion, QRS-3004B-TN1, Version 1.0 (2007).
- [311] MELINTESCU, A., GALERIU, D., Tritium transfer in pigs – a model test, *Fusion Sci. Technol.* **54** (2008) 269–272.
- [312] GALERIU, D., MELINTESCU, A., BERESFORD, N.A., TAKEDA, H., CROUT, N.M.J., The Dynamic transfer of ^3H and ^{14}C in mammals – a proposed generic model, *Radiat. Environ. Biophys.* **48** (2009b) 29–45.
- [313] GALERIU, D., MELINTESCU, A., Personal communication (2002).
- [314] MELINTESCU, A., Revision of experimental tritium data for farm animals, Contract CERES 73 /2001, Internal report (2002b). Available at: <http://www-ns.iaea.org/downloads/rw/projects/emras/emras-two/first-technical-meeting/fourth-working-group-meeting/working-group-presentations/workgroup7-presentations/presentation-4th-wg7-farm-animals.pdf>
- [315] GALERIU, D., MELINTESCU, A model approach for tritium dynamics in wild animals and birds”, *Radioprotection*, **46** (2011) S445–S451.
- [316] TEDESCHI, L., O’CANNAS, A., FOX, D.G., Development and Evaluation of Nutrition Models for Domesticated Small Ruminants: The SRNS (2008).
- [317] VAN MILGEN, J., NOBLET, J., VALANCOGNE, A., DUBOIS, S., DOURMAD, J.Y., InraPorc: un modèle pour analyser les performances et évaluer les stratégies alimentaires chez le porc en croissance, *Journées de la Recherche Porcine en France* **37** (2005) 291–298 (in French).
- [318] GOUS, R.M., MORAN Jr, E.T., STILBORN, H.R., BRADFORD, G.D., EMMANS, G.C., Evaluation of the parameters needed to describe the overall growth, the chemical growth, and the growth of feathers and breast muscles of broilers, *Poult. Sci.* **78** (1999) 812–821.
- [319] LOPEZ, G., DE LANGE, K., LEESON S., Partitioning of Retained Energy in Broilers and Birds with Intermediate Growth Rate. *Poultry Sci.* **86** (2007) 2162–2171.
- [320] NAGAI, H., Incorporation of CO₂ exchange processes into a multiplayer atmosphere-soil-vegetation model, *J. Appl. Meteorol.* **44** (2005) 1574–1592.
- [321] KONDO, J., SAIGUSA, N., Modeling the evaporation from bare soil with a formula for vaporization in the soil pores, *J. Meteorol. Soc. Jpn.* **72** (1994) 413–421.

- [322] LEUNING, R., A critical appraisal of a combined stomatal-photosynthesis model for C₃ plants, *Plant Cell Environ.* **18** (1995) 339–355.
- [323] DIABATE, S., STRACK, S., Organically bound tritium, *Health Phys.* **65** (1993) 698–712.
- [324] SERVAITES, J.C., GEIGER, D.R., Effects of light intensity and oxygen on photosynthesis and translocation in sugar beet, *Plant Physiol.* **54** (1974) 575–578.
- [325] FONDY, B., GEIGER, D.R., Diurnal pattern of translocation and carbohydrate metabolism in source leaves of *Beta vulgaris L.*, *Plant Physiol.* **70** (1982) 671–676.
- [326] INTERNATIONAL ATOMIC ENERGY AGENCY, Testing of Models for Predicting the Behaviour of Radionuclides in Freshwater Systems and Coastal Areas, Report of the Aquatic Working Group of EMRAS Theme 1, IAEA's Environmental Modelling for Radiation Safety (EMRAS) Programme 2003–2007, IAEA, Vienna (2008d). Available at: <http://www-ns.iaea.org/downloads/rw/projects/emras/final-reports/aquatic-tecdoc-final.pdf>
- [327] GOUTAL, N., LUCK, M., BOYER, P., MONTE, L., SICLET, F., ANGELI, G., Assessment, validation and intercomparison of operational models for predicting tritium migration from routine discharges of nuclear power plants: the case of Loire River, *J. Environ. Radioactiv.* **99** (2008) 367–382.
- [328] ZHELEZNYAK, M., DONTCHITS, G., DZJUBA, N., GIGINYAK, V., LYASHENKO, G., MARINETS, A., TKALICH, P., RIVTOX – One dimensional model for the simulation of the transport of radionuclides in a network of river channels, RODOS Report WG4-TN(97)05, Forschungszentrum Karlsruhe, Germany (2003). Available at: <http://www.rodos.fzk.de/Documents/Public/HandbookV6/Volume3/RIVTOX.pdf>
- [329] HELING, R., LEPICARD, S., MADERICH, V., SHERSHAKOV, V., MUNGOV, G., CATSAROS, N., POPOV, A., POSEIDON Final Report (1 October- 30 September 2000) IC15-CT98-0210. 15 November 2000, NRG Report no. P26072/00.55075/P (2000).
- [330] GALERIU, D., HELING, R., MELINTESCU, A., The dynamic of tritium – including OBT – in the aquatic food chain, *Fusion Sci. Technol.* **48** (2005b) 779-782.
- [331] MELINTESCU, A., GALERIU, D., Dynamic model for tritium transfer in an aquatic food chain, *Radiat. Environ. Biophys.* **50** (2011b) 459–473.
- [332] TURNER, A., MILLWARD, G.E., STEMP, M., Distribution of tritium in estuarine waters: the role of organic matter, *J. Environ. Radioactiv.* **100** (2009) 890–895.
- [333] HUNT, G.J., BAILEY, T.A., JENKINSON, S.B., LEONARD, K.S., Enhancement of tritium concentrations on uptake by marine biota: experience from UK coastal waters, *J. Radiol. Prot.* **30** (2010) 73–83.
- [334] MARANG, L., SICLET, F., LUCK, M., MARO, D., TENAILLEAU, L., JEAN-BAPTISTE, P., FOURRÉ, E., FONTUGNE, M., Modelling tritium flux from water to atmosphere: application to the Loire river, *J. Environ. Radioactiv.* **102** (2011) 244-251.
- [335] GONTIER, G., SICLET, F., Le tritium organique dans les écosystèmes d'eau douce: évolution à long terme dans l'environnement des Centres Nucléaires de Production d'Electricité français, *Radioprotection* **46** (2011) 457–491 (in French).

- [336] BOOKHOUT, T.A., WHITE, G.C., A simulation model of tritium kinetics in a freshwater marsh, Project completion report no. 487X, Ohio Cooperative Wildlife Research Unit, The Ohio State University, United States Department of the Interior, Contract no. A-038-OHIO (1976). Available at: https://kb.osu.edu/dspace/bitstream/handle/1811/36345/OH_WRC_487X.pdf
- [337] HELING, R., KOZIY, L., BULGAKOV, V., A dynamical approach for the uptake of radionuclides in the marine organisms for the POSEIDON model system, *Radioprotection* **37** (2002) C1-833-C1-838.
- [338] HELING, R., GALERIU, D., Modification of LAKECO-B for ^3H , Report P20874/02.55114/INRG (2002).
- [339] INTERNATIONAL ATOMIC ENERGY AGENCY, Mussel uptake scenario, Final report, IAEA's Environmental Modelling for Radiation Safety (EMRAS) Programme 2003–2007, IAEA, Vienna (2008e). Available at: <http://www-ns.iaea.org/downloads/rw/projects/emras/tritium/mussel-uptake-final.pdf>
- [340] YANKOVICH, T.L., KIM, S.B., BAUMGAERTNER, F., GALERIU, D., MELINTESCU, A., MIYAMOTO, K., SAITO, M., SICLET, F., DAVIS, P., Measured and modelled tritium concentrations in freshwater Barnes mussels (*Elliptio complanata*) exposed to an abrupt increase in ambient tritium levels, *J. Environ. Radioactiv.* **102** (2011) 1879–1700.
- [341] SICLET, F., Personal communication (2009).
- [342] RIOU, J., Modèle d'écosystème phytoplanctonique marin sur le littoral nord-breton (Manche occidentale), PhD Thesis, Institut National Polytechnique de Toulouse, France (1990) 430 pp (in French).
- [343] JORGENSEN, S.E., Handbook of Environmental Data and Ecological Parameters, International Society of Ecological Modelling, First Edition, Pergamon Press (1979).
- [344] KIRCHMANN, R., BONOTTO, S., SOMAN, S.D., KRISHNAMOORTHY, T.M., IYENGAR, T.S., MOGHISSI, A.A., Transfer and incorporation of tritium in aquatic organisms, In Proceedings of the International Symposium on the Behaviour of Tritium in the Environment, 16–20 October 1978, San Francisco, IAEA, Vienna (1979) 187–204.
- [345] HERB, W.R., STEFAN, H.G., Seasonal growth of submersed macrophytes in lakes: The effects of biomass density and light competition, *Ecol. Model.* **193** (2006) 560–574.
- [346] HAKANSON, L., BOULION, V.V., Empirical and dynamical models to predict the cover, biomass and production of macrophytes in lakes, *Ecol. Model.* **151** (2002) 213–243.
- [347] FRANCO, A.R., FERREIRA, J.G., NOBRE, A.M., Development of a growth model for penaeid shrimp, *Aquaculture* **259** (2006) 268–277.
- [348] RAY, S., BEREC, L., STRASKRABA, M., JORGENSEN, S.E., Optimization of energy and implications of body sizes of phytoplankton and zooplankton in an aquatic ecosystem model, *Ecol. Model.* **140** (2001) 219–234.
- [349] HELING, R., Off site emergency planning support, The validation of the lake ecosystem model LAKEKO KEMA, Report 40901-NUC-95-9113 (1995).
- [350] BEAUGELIN-SEILLER, K., BOYER, P., GARNIER-LAPLACE, J., ADAM, C., Casteaur: A simple tool to assess the transfer of radionuclides in waterways, *Health Phys.* **83** (2002) 539–542.
- [351] SUKHOTIN, A.A., ABELE, D., POERTNER, H.-O., Growth, metabolism and lipid peroxidation in *Mytilus edulis*: age and size effects, *Mar. Ecol. Prog. Ser.* **226** (2002) 223–234.

- [352] HEAN, R.L., CACHO, O.J., A growth model for giant clams *Tridacna crocea* and *T. derasa* Ecol. Model. **163** (2003) 87–100.
- [353] BREY, T., An empirical model for estimating aquatic invertebrate respiration. Method. Ecol. Evol. **1** (2010) 92–101.
- [354] OIKAWA, S., ITAZAWA, Y., Relationship between summated tissue respiration and body size in a marine teleost, the porgy *Pagrus major*, Fisheries Sci. **69** (2003) 687–694.
- [355] HANSON, P.C., JOHNSON, T.B., SCHINDLER, D.E., KITCHELL, J.F., Fish Bioenergetics 3.0. WISCU-T-97-001, University of Wisconsin Sea Grant Institute, Center for Limnology, USA (1997).
- [356] BAJER, P.G., WHITLEDGE, G.W., HAYWARD, R.S., Widespread consumption-dependent systematic error in fish bioenergetics models and its implications, Can. J. Fish Aquat. Sci. **61** (2004) 2158–2167.
- [357] CHIPPS, S.R., WAHL, D.H., Bioenergetics Modeling in the 21st century: reviewing new insights and revisiting old constraints, T. Am. Fish Soc. **137** (2008) 298–313.
- [358] MCCUBBIN, D., LEONARD, K.S., BAILEY, T.A., WILLIAMS, J., TOSSELL, P., Incorporation of organic tritium (^3H) by marine organisms and sediment in the Severn Estuary/Bristol Channel (UK), Mar. Poll. Bull. **42** (2001) 852–63.
- [359] WILLIAMS, J.L., RUSS, R.M., MCCUBBIN, D., KNOWLES, J.F., An overview of tritium behaviour in the Severn Estuary (UK), J. Radiol. Prot. **21** (2001) 337–344.
- [360] ABRIL, G., ETCHEBER, H., DELILLE, B., FRANKIGNOULLE, M., BORGES, A., Carbonate dissolution in the turbid and eutrophic Loire estuary, Mar. Ecol.-Prog. Ser. **259** (2003) 129–138.
- [361] ABRIL, G., NOGUEIRA, M., ETCHEBER, H., CABEÇADAS, G., LEMAIRE, E., BROGUEIRA, M.J., Behaviour of organic carbon in nine contrasting European estuaries, Estuar. Coast. Shelf S., **54** (2002) 241–262.
- [362] PELTZER, E.T., HAYWARD, N.A., Spatial and temporal variability of total organic carbon along 140°W in the Equatorial Pacific Ocean in 1992, Deep-Sea Research II, **43** (1996) 1155–1180.
- [363] STRACK, S., KIRCHMANN, R., BONOTTO, S., Radioactive contamination of the marine environment: Uptake and distribution of ^3H in *Dunaliella bioculata*, Helgoland Mar. Res. **33** (1980) 153–163.
- [364] INTERNATIONAL COMMISSION ON RADIOLOGICAL PROTECTION, Environmental Protection: the Concept and Use of Reference Animals and Plants, ICRP 1548, Publication 108, Annals of the ICRP 38 (4-6), Elsevier (2008).
- [365] RODGERS, D.W., Tritium dynamics in juvenile rainbow trout, *Salmo gairdneri*, Health Phys. **50** (1986) 89–98.
- [366] KIM, S.B., Personal communication (2010b).
- [367] PARK, R.A., CLOUGH, J.S., AQUATOX (RELEASE 3) Modelling environmental fate and ecological effects in aquatic ecosystems, Volume 2: Technical Documentation, Environmental Protection Agency USA, EPA-823-R-09-004 August 2009 (2009). Available at: http://www.epa.gov/waterscience/models/aquatox/technical/aquatox_release_3_technical_doc.pdf
- [368] TYLER, J.A., BOLDUC, M.B., Individual Variation in Bioenergetic Rates of Young-of-Year Rainbow Trout, T. Am. Fish Soc. **137** (2008) 314–323.
- [369] MURRAY, J., BURT, J.R., The composition of fish, Ministry of Technology, Torry research station, Torry advisory note 38 (2001). Available at: http://www.fao.org/wairdocs/tan/x5916e/x5916e00.htm#Accompanying_Notes

- [370] RAILSBACK, S.F., ROSE, K.A., Bioenergetics modeling of stream trout growth: temperature and food consumption effects, *T. Am. Fish Soc.* **128** (1999) 241–256.
- [371] RAND, P.S., STEWART, D.J., SEELBACH, P.W., JONES, M., WEDGE, L.R., Modeling steelhead population energetics in Lakes Michigan and Ontario, *T. Am. Fish Soc.* **122** (1993) 977–1001.
- [372] MELINTESCU, A., GALERIU, D., KIM, S.B., Tritium dynamics in large fish – a model test, *Radioprotection*, **46** (2011) S431–S436.
- [373] MEGREY, B.A., ROSE, K.A., KLUMB, R.A., HAY, D.E., WERNER, F.E., ESLINGER, D.L., SMITH, S.L., A bioenergetics-based population dynamics model of Pacific herring (*Clupea harengus pallasii*) coupled to a lower trophic level nutrient–phytoplankton–zooplankton model: Description, calibration, and sensitivity analysis, *Ecol. Model.* **202** (2007) 196–210.
- [374] ENVIRONMENTAL AGENCY, Potential for Bio-accumulation of Organically Bound Tritium in the Environment: Review of Monitoring Data, National Compliance Assessment Service Technical Report, NCAS/TR/2000/026 (2001).
- [375] BAUMGÄRTNER, F., DONHÄRL, W., Non-exchangeable organically bound tritium (OBT): its real nature, *Anal. Bioanal. Chem.* **379** (2004) 204–209.
- [376] BAUMGÄRTNER, F., Accumulative tritium transfer from water into biosystems, *Fusion Sci. Technol.* **48** (2005) 787–790.
- [377] KIM, S.B., WORKMAN, W.J.G., DAVIS, P.A., Experimental Investigation of Buried Tritium in Plant and Animal tissues, *Fusion Sci. Technol.* **54** (2008) 257–260.
- [378] WARE, A., ALLOTT, R.W., Review of methods for the Analysis of Total Tritium and Organically Bound Tritium, NCAS/TR/99/003 (1999).
- [379] WORKMAN, W.J.G., KIM S.B., KOTZER T.G., Inter-laboratory comparison of organically bound tritium measurements in environmental samples, *Fusion Sci. Technol.* **48** (2005) 763–766.
- [380] BAGLAN, N., ALANIC, G., LE MEIGNEN, R, POINTURIER, F., A follow up of the decrease of non exchangeable organically bound tritium levels in the surroundings of a nuclear research center, *J. Environ. Radioactiv.* **102** (2011) 695–702.
- [381] POINTURIER, F., BAGLAN N., ALANIC, G., A method for the determination of low-level organic-bound tritium activities in environmental samples, *Appl. Radiat. Isotopes*, **61** (2004) 293–298.
- [382] COSSONNET, C., NEIVA MARQUES, A.M., GURRIARAN, R., Experience acquired on environmental sample combustion for organically bound tritium, *Appl. Radiat. Isotopes*, **67** (2009) 809–811.
- [383] JEAN-BAPTISTE, P., FOURRE, E., DAPOIGNY, A., BAUMIER, D., BAGLAN, N., ALANIC, G., ³He mass spectrometry for very low-level measurement of organic tritium in environmental samples, *J. Environ. Radioactiv.* **101** (2010) 185–190.
- [384] WASSENAAR, L.I., HOBSON, K.A., Improved method for determining the stable-hydrogen isotopic composition (δD) of complex organic materials of environmental interest, *Environ. Sci. Technol.* **34** (2000) 2354–2360.
- [385] CURRIE, L.A., Limits for Qualitative Detection and Quantitative Determination, *Anal. Chem.* **40** (1968) 586–593.
- [386] PALOMO, M., PENALVER, A., AGUILAR, C., BORRULL, F., Tritium activity levels in environmental water samples from different origins, *Appl. Radiat. Isotopes* **65** (2007) 1048–1056.

- [387] STANGA, D., CASSETTE, P., Improved method of measurement for tritiated water standardization by internal gas proportional counting, *Appl. Radiat. Isotopes*, **64** (2006) 160–162.
- [388] SCHOENHOFER, F., KRALIK, C., Scintillations; Optimization of Liquid Scintillation Measurements of Environmental Tritium, *Radioactiv. Radiochem.* **10** (1999) 14–17.
- [389] KIM, M-A., BAUMGÄRTNER, F., Equilibrium and non-equilibrium partition of tritium between organics and tissue water of different biological systems, *Appl. Radiat. Isotopes*, **45** (1994) 353–360.
- [390] FUMA, S., INOUE, Y., Simplified and Sensitive Analysis of Organically Bound Tritium in Tree Rings to Retrospect Environment Tritium Levels, *Appl. Radiat. Isotopes* **46** (1995) 991–997.
- [391] KIM, S.B., DAVIS, P.A., OBT/HTO Ratios in Plants, COG report, COG-06-3053 (2007).
- [392] HISAMATSU, S., KATSUMATA, T., TAKIZAWA, Y., INOUE, Y., ISOGAI, K., KIM, J. M., KATAGIRI, H., TAKASHIMA, Y., KAJI, T., NAGATANI, F., UENO, K., ITOH, M., Inter-laboratory comparison of low-level organic tritium measurement in environmental samples, *Radioisotopes*, **39** (1990) 457–463.
- [393] BAGLAN, N., ANSOBORLO, E., COSSONNET, C., FOUHAL, L., FOURRE, E., HENRY, A., KIM, S.B., MOKILI, M., OLIVIER, A., GRANIER, G., Assessment and interpretation of a round robin exercise for organically bound tritium determination, LSC 2008, advances in liquid scintillation spectrometry, In: Eikenberg, J. et al., (Eds.), *Radiocarbon*, The University of Arizona, Tucson, Arizona, USA (2009) 229–240.
- [394] POINTURIER, F., BAGLAN N., ALANIC, G., CHIAPPINI, R., Determination of organically bound tritium background level in biological samples from a wide area in the south-west of France, *J. Environ. Radioactiv.* **68** (2003) 171–189.
- [395] NATIONAL DOSE ASSESSMENT WORKING GROUP, An Overview of Uncertainty in Radiological Assessments, NDAWG/1/2005, Subgroup on Uncertainty and Variability (2005).
- [396] NATIONAL DOSE ASSESSMENT WORKING GROUP, Overview of Radiological Assessments Models – Key Gaps and Uncertainties, NDAWG/2/2006, NDAWG Modelling Sub-group (2006).
- [397] ASIAN NUCLEAR SAFETY NETWORK, Notes for Lectures on the Safety Assessment of Near Surface Low and Intermediate Level Radioactive Waste Disposal Facilities (2004). Available at: www.ansn.org/ansn.org/Common/Documents/apmd/asia280p24.pdf
- [398] INTERNATIONAL ATOMIC ENERGY AGENCY, Modelling the environmental transport of tritium in the vicinity of long term atmospheric and sub-surface sources, Report of the Tritium Working Group of the Biosphere Modelling and Assessment (BIOMASS) Programme, Theme 3, IAEA, Vienna (2003a). Available at: http://www-pub.iaea.org/MTCD/publications/PDF/Biomass3_web.pdf
- [399] EUROPEAN ENVIRONMENT AGENCY, The application of models under the European Union's Air Quality Directive, EEA Technical Report No 10/2011, Copenhagen, Denmark, ISBN 978-92-9213-223-1 (2011).
- [400] BEVEN, K., Environmental modeling: An uncertain future? –Techniques for uncertainty estimation in environmental prediction, Taylor & Francis Ltd., London (2008).

- [401] JAKEMAN, A.J., LETCHER, R.A., NORTON, J.P., Ten iterative steps in development and evaluation of environmental models, *Environ. Modell. Softw.* **21** (2006) 602–614
- [402] WARMINK, J.J., JANSSEN, J.A.E.B., BOOIJ, M.J., M.S. KROL, M.S., Identification and classification of uncertainties in the application of environmental models, *Environ. Modell. Softw.* **25** (2010) 1518–1527.
- [403] INTERNATIONAL ATOMIC ENERGY AGENCY, Evaluating the reliability of predictions made using environmental transfer models, Safety Series No. 100, IAEA, Vienna (1989).
- [404] NATIONAL RESEARCH COUNCIL, Models in Environmental Regulatory Decision Making, National Academies Press, Washington DC (2007).
- [405] KEUM, D.K., LEE, H.S., KANG, H.S., JUN, I., CHOI, Y.H., LEE, C.W., Prediction of tritium level in agricultural plants after short term exposure to HTO vapor and its comparison with experimental results, *Health Phys.* **90** (2006) 42–55.
- [406] VAN ASSELT, M.B.A., Uncertainty in Decision Support: From Problem to Challenge, ICIS working paper I99-E006, International Centre for Integrative Studies (ICIS), University of Maastricht, The Netherlands (1999).
- [407] BEVEN, K., Towards a coherent philosophy for modelling the environment, *Proceedings of Mathematical, Physical & Engineering Sciences*, **458** The Royal Society (2002) 2465–2484.
- [408] BIOSPHERIC MODEL VALIDATION STUDY (BIOMOVS II), Guidelines for Uncertainty Analysis, BIOMOVS II Technical Report No. 1, Stockholm, Sweden: BIOMOVS II Steering Committee, Swedish Radiation Protection Institute (1993).
- [409] BIOSPHERIC MODEL VALIDATION STUDY (BIOMOVS II), Uncertainty and Validation: Effect of User Interpretation on Uncertainty Estimates, BIOMOVS II Technical Report No. 7, Stockholm, Sweden: BIOMOVS II Steering Committee, Swedish Radiation Protection Institute (1996c).
- [410] BEVEN, K., Towards integrated environmental models of everywhere: uncertainty, data and modelling as a learning process, *Hydrol. Earth Syst. Sci.* **11** (2007) 460–467.
- [411] INTERNATIONAL COMMISSION ON RADIOLOGICAL PROTECTION, Radiation Protection Recommendations as Applied to the Disposal of Longlived Solid Radioactive Waste, ICRP Publication 81, Pergamon Press (1998).
- [412] SAVAGE, D. (Ed.), The Scientific and Regulatory Basis for the Geological Disposal of Radioactive Waste, John Wiley & Sons Ltd. (1995).
- [413] WATTS, L., CLEMENTS, L., EGAN, M., CHAPMAN, N., KANE, P., THORNE, M., Development of Scenarios within a Systematic Assessment Framework for the Drigg Post-Closure Safety Case, In: Scenario Development Methods and Practices, Proceedings of a NEA Workshop on Scenario Development, Madrid, 10–12 May 1999, Nuclear Energy Agency, Organisation for Economic Co-operation and Development, Paris (2001) 133–144.
- [414] INTERNATIONAL ATOMIC ENERGY AGENCY, “Reference Biospheres” for solid radioactive waste disposal, Report of BIOMASS Theme 1 of the BIOSphere Modelling and ASSESSment (BIOMASS) Programme, IAEA, Vienna (2003b). Available at:
http://www-pub.iaea.org/MTCD/Publications/PDF/Biomass6_web.pdf
- [415] INTERNATIONAL ATOMIC ENERGY AGENCY, Safety assessment for near surface disposal of radioactive waste, Safety Standard Series No. WS-G-1.1, IAEA, Vienna (1999).

- [416] BIOSPHERIC MODEL VALIDATION STUDY (BIOMOVS II), Uncertainty and Validation: Effect of Model Complexity on Uncertainty Estimates, BIOMOVS II Technical Report No. 16, Stockholm, Sweden: BIOMOVS II Steering Committee, Swedish Radiation Protection Institute (1996d).
- [417] IMAN, R., SHORTENCARRIER, M., A FORTRAN 77 Program and User's Guide for the Generation of Latin Hypercube and Random Samples for Use with Computer Models, Albuquerque, NM: Sandia National Laboratory, NUREG/CR-3624, SAND83-2365 (1984).
- [418] GALERIU, D., DAVIS, P., CHOUHAN, S., RASKOB, W., Uncertainty and sensitivity analysis for the environmental tritium code UFOTRI, *Fus. Technol.* **28** (1995) 853–858.
- [419] INTERNATIONAL ATOMIC ENERGY AGENCY, Potato scenario, Final report, IAEA's Environmental Modelling for Radiation Safety (EMRAS) Programme 2003–2007, IAEA, Vienna (2008f). Available at: <http://www-ns.iaea.org/downloads/rw/projects/emras/tritium/potato-report-final.pdf>
- [420] BIOSPHERIC MODEL VALIDATION STUDY (BIOMOVS II), An Overview of the BIOMOVS II Study and its Findings, BIOMOVS II Technical Report No. 17, Stockholm, Sweden: BIOMOVS II Steering Committee, Swedish Radiation Protection Institute (1996e).
- [421] OTA, M., NAGAI, H., HTO transport and OBT formation after nighttime wet deposition of atmospheric HTO onto land surface, *Radioprotection* **46** (2011b) S417–S422.
- [422] OTA, M., NAGAI, H., KOARASHI, J., Importance of root HTO uptake in controlling land-surface tritium dynamics after an-acute HT deposition: A numerical experiment, *J. Environ. Radioactiv.* **109** (2012) 94–102.
- [423] STOICA, I., (Ed.), Animal nutrition and feeding, CORAL-SANIVET, Bucharest (1997) (in Romanian).
- [424] GEIGY, Geigy Scientific Tables, Units of measurement, body fluids, composition of the body, nutrition. Vol 1, 8th Edition, Basel, Switzerland, Ciba-Geigy Ltd (1981).

LIST OF ABBREVIATIONS

ATP	adenosine tri-phosphate
BAF	building amplification factor
BED	body energy density
BH	bound hydrogen
BURN	Biological Uptake model of RadioNuclides model
BWB	Ball-Woodrow-Berry model
CF	concentration factor
CFD	computational fluid dynamics (formulations)
CLR	carbon loss rate
CMOs	conceptual model objects
CRMs	certified reference materials
DAF	days after flowering
DOC	dissolved organic carbon
DOT	dissolved organic tritium
DSD	drop size distribution
DVS	development stage
EBW	empty body weight (kg)
ED	energy density
ETP	evapotranspiration
FAM	fast approximate models
FB	fractional bias
FBM	Frankfurt Biosphere Model
FBR	field (for active animals) metabolic rate
FCM	fully computational models
FDMH	food dose module tritium
FEPs	features, events and processes
FIST	filtered in space and time (hydrodynamic turbulence model)
HB	building height
HR	relative humidity
HT	tritiated hydrogen/gas
HTO	tritiated water
IMs	interaction matrices
IPCC	Intergovernmental Panel on Climate Change
LAI	leaf area index

LES	large Eddy simulation
LL	lower layer (soil)
LOD	limit of detection
LSC	liquid scintillation counter
LSS	land surface schemes
MAGENTC	MAmmal GENERIC model for transfer of Tritium and Carbon
MG	geometric mean bias
MS	mass spectrometry
NE	non-exchangeable (OBT)
NMSE	normalized mean square errors
OBD	organically bound deuterium
OBT	organically bound tritium
ODEs	off-diagonal elements
PDFs	probability density functions
PF	ParFlow (popular hydrological module)
PFT	plant functional type
P/O	predicted and observed results
QA	quality assurance
QC	quality control
RBC	red blood cells
RGR	relative growth rate
RZWQM	root zone water quality model
SA	specific activity
SAR	specific activity ratio
SMR	specific metabolic rate
SVAT	soil-vegetation-atmosphere transport
TJ	Thornley-Johnson leaf-level photosynthesis model
TLI	translocation index
TFWD	tissue free water deuterium
TFWT	tissue free water tritium
UL	upper layer (soil)
VG	geometric variance
VPD	vapour pressure deficit
WG7	Working Group 7 “Tritium Accidents” of the IAEA’s EMRAS II Programme
WRF	weather research forecast system

CONTRIBUTORS TO DRAFTING AND REVIEW

Atarashi-Andoh, M.	Japan Atomic Energy Agency, Japan
Berkovskyy, V.	International Atomic Energy Agency
Cortes, P.	ITER Organization, France
Davis, P.	Consultant, Canada
Duran, J.	VÚJE Inc. – Engineering, Design and Research Organization, Slovakia
Galeriu, D.	National Institute of Physics and Nuclear Engineering “Horia Hulubei”, Romania
Guetat, P.	Commissariat à l'Energie Atomique, France
Kim, S.B.	Atomic Energy of Canada Limited, Canada
Korolevych, V.	Atomic Energy of Canada Limited, Canada
Lamego Simões Filho, F.	Instituto de Engenharia Nuclear, Brazil
Le Dizès, S.	Institut de Radioprotection et de Sûreté Nucléaire, France
Melintescu, A.	National Institute of Physics and Nuclear Engineering “Horia Hulubei”, Romania
Nagai, H.	Japan Atomic Energy Agency, Japan
Ota, M.	Japan Atomic Energy Agency, Japan
Patryl, L.	Commissariat à l'Energie Atomique, France
Peterson, S.-R.,	Consultant, Canada
Siclet, F.	Electricité de France, France
Strack, S.	Karlsruhe Institute of Technology, Germany

LIST OF PARTICIPANTS

Amado, V.	Autoridad Regulatoria Nuclear, Argentina
Atarashi-Andoh, M.	Japan Atomic Energy Agency, Japan
Baigazinov, Z.	Institute of Radiation Safety and Ecology, Kazakhstan
Baumgärtner, F.	Technische Universität München, Germany
Berkovskyy, V.	International Atomic Energy Agency
Blixt Buhr, A.	Vattenfall Power Consultant AB, Sweden
Chouhan, S.	Atomic Energy of Canada Limited, Canada
Cortes, P.	ITER Organization, France
Coughlin, D.	Sellafield Limited, United Kingdom
Curti, A.	Autoridad Regulatoria Nuclear, Argentina
Dale, P.	Scottish Environment Protection Agency, United Kingdom
Damdinsuren, T.	Nuclear Energy Agency, Mongolia
Duran, J.	VÚJE Inc. – Engineering, Design and Research Organization, Slovakia
El Kadi Abderrezzak, K.	Electricité de France, France
Farfan, E.	Savannah River National Laboratory, United States of America
Galeriu, D.	National Institute of Physics and Nuclear Engineering “Horia Hulubei”, Romania
Guetat, P.	Commissariat à l'Energie Atomique, France
Horyna, J.	State Office for Nuclear Safety, Czech Republic
Iseli, M.	ITER Organization, France
Jaunet, P.	Autorité de Sûreté Nucléaire, France
Jurkin, D.	Technische Universität München, Germany
Keum, D.-K.	Korea Atomic Energy Research Institute, Republic of Korea
Kim, S.B.	Atomic Energy of Canada Limited, Canada
Korolevych, V.	Atomic Energy of Canada Limited, Canada
Kovalenko, G.	Ukrainian Scientific Research Institute of Ecological Problems, Ukraine
Lamego Simões Filho, F.	Instituto de Engenharia Nuclear, Brazil
Latouche, G.	Canadian Nuclear Safety Commission, Canada
Le Dizès, S.	Institut de Radioprotection et de Sûreté Nucléaire, France
Lee, P.	Savannah River National Laboratory, United States of America
Lukashenko, S.	National Nuclear Center, Republic of Kazakhstan
Malátová, I.	National Radiation Protection Institute, Czech Republic
Marang, L.	Electricité de France, France
Maro, D.	Institut de Radioprotection et de Sûreté Nucléaire, France

Melintescu, A.	National Institute of Physics and Nuclear Engineering “Horia Hulubei”, Romania
Mihok, S.	Canadian Nuclear Safety Commission, Canada
Momoshima, N.	Kyushu University, Japan
Nagai, H.	Japan Atomic Energy Agency, Japan
Nies, H.	International Atomic Energy Agency
Nsouli, B.	Lebanese Atomic Energy Commission, Lebanon
Ota, M.	Japan Atomic Energy Agency, Japan
Patryl, L.	Commissariat à l'Energie Atomique, France
Patterson, A.	Bruce Power, Canada
Popescu, I.	Societatea Nationala Nuclearelectrica S.A., Romania
Raskob, W.	Karlsruhe Institute of Technology, Germany
Ravi, P.M.	Bhabha Atomic Research Centre, India
Sazykina, T.	Scientific and Production Association (SPA) “Typhoon”, Russian Federation
Siclet, F.	Electricité de France, France
Simionov, V.	Societatea Nationala Nuclearelectrica S.A., Romania
Simpkins, A.	Dade Moeller and Associates, United States of America
Strack, S.	Karlsruhe Institute of Technology, Germany
Sugihara, S.	Kyushu University, Japan
Sundell-Bergman, S.	Swedish University of Agricultural Science, Sweden
Takahashi, T.	Kyoto University Research Reactor Institute, Japan
Umata, T.	University of Occupational and Environmental Health, Japan
Vichot, L.	Commissariat à l'Energie Atomique, France
Yankovich, T.	Saskatchewan Research Council, Canada

EMRAS II Technical Meetings, IAEA Headquarters, Vienna

Vienna, Austria: 19–23 January 2009, 25–29 January 2010, 24–28 January 2011

Interim Working Group Meetings, EMRAS II, Working Group 7

Chatou, France: 28–29 September 2009
Aix-en-Provence, France: 6–9 September 2010
Bucharest, Romania: 12–15 September 2011

Consultants Meetings

Vienna, Austria: 30 November – 2 December 2011



IAEA

International Atomic Energy Agency

No. 23

ORDERING LOCALLY

In the following countries, IAEA priced publications may be purchased from the sources listed below or from major local booksellers.

Orders for unpriced publications should be made directly to the IAEA. The contact details are given at the end of this list.

AUSTRALIA

DA Information Services

648 Whitehorse Road, Mitcham, VIC 3132, AUSTRALIA

Telephone: +61 3 9210 7777 • Fax: +61 3 9210 7788

Email: books@dadirect.com.au • Web site: <http://www.dadirect.com.au>

BELGIUM

Jean de Lannoy

Avenue du Roi 202, 1190 Brussels, BELGIUM

Telephone: +32 2 5384 308 • Fax: +32 2 5380 841

Email: jean.de.lannoy@euronet.be • Web site: <http://www.jean-de-lannoy.be>

CANADA

Renouf Publishing Co. Ltd.

5369 Canotek Road, Ottawa, ON K1J 9J3, CANADA

Telephone: +1 613 745 2665 • Fax: +1 643 745 7660

Email: order@renoufbooks.com • Web site: <http://www.renoufbooks.com>

Bernan Associates

4501 Forbes Blvd., Suite 200, Lanham, MD 20706-4391, USA

Telephone: +1 800 865 3457 • Fax: +1 800 865 3450

Email: orders@bernan.com • Web site: <http://www.bernan.com>

CZECH REPUBLIC

Suweco CZ, spol. S.r.o.

Klecakova 347, 180 21 Prague 9, CZECH REPUBLIC

Telephone: +420 242 459 202 • Fax: +420 242 459 203

Email: nakup@suweco.cz • Web site: <http://www.suweco.cz>

FINLAND

Akateeminen Kirjakauppa

PO Box 128 (Keskuskatu 1), 00101 Helsinki, FINLAND

Telephone: +358 9 121 41 • Fax: +358 9 121 4450

Email: akatilaus@akateeminen.com • Web site: <http://www.akateeminen.com>

FRANCE

Form-Edit

5 rue Janssen, PO Box 25, 75921 Paris CEDEX, FRANCE

Telephone: +33 1 42 01 49 49 • Fax: +33 1 42 01 90 90

Email: fabien.boucard@formedit.fr • Web site: <http://www.formedit.fr>

Lavoisier SAS

14 rue de Provigny, 94236 Cachan CEDEX, FRANCE

Telephone: +33 1 47 40 67 00 • Fax: +33 1 47 40 67 02

Email: livres@lavoisier.fr • Web site: <http://www.lavoisier.fr>

L'Appel du livre

99 rue de Charonne, 75011 Paris, FRANCE

Telephone: +33 1 43 07 50 80 • Fax: +33 1 43 07 50 80

Email: livres@appeldulivre.fr • Web site: <http://www.appeldulivre.fr>

GERMANY

Goethe Buchhandlung Teubig GmbH

Schweitzer Fachinformationen

Willstätterstrasse 15, 40549 Düsseldorf, GERMANY

Telephone: +49 (0) 211 49 8740 • Fax: +49 (0) 211 49 87428

Email: s.dehaan@schweitzer-online.de • Web site: <http://www.goethebuch.de>

HUNGARY

Librotade Ltd., Book Import

PF 126, 1656 Budapest, HUNGARY

Telephone: +36 1 257 7777 • Fax: +36 1 257 7472

Email: books@librotade.hu • Web site: <http://www.librotade.hu>

INDIA

Allied Publishers

1st Floor, Dubash House, 15, J.N. Heredi Marg, Ballard Estate, Mumbai 400001, INDIA
Telephone: +91 22 2261 7926/27 • Fax: +91 22 2261 7928
Email: alliedpl@vsnl.com • Web site: <http://www.alliedpublishers.com>

Bookwell

3/79 Nirankari, Delhi 110009, INDIA
Telephone: +91 11 2760 1283/4536
Email: bkwell@nde.vsnl.net.in • Web site: <http://www.bookwellindia.com>

ITALY

Libreria Scientifica "AEIOU"

Via Vincenzo Maria Coronelli 6, 20146 Milan, ITALY
Telephone: +39 02 48 95 45 52 • Fax: +39 02 48 95 45 48
Email: info@libreriaaeiou.eu • Web site: <http://www.libreriaaeiou.eu>

JAPAN

Maruzen Co., Ltd.

1-9-18 Kaigan, Minato-ku, Tokyo 105-0022, JAPAN
Telephone: +81 3 6367 6047 • Fax: +81 3 6367 6160
Email: journal@maruzen.co.jp • Web site: <http://maruzen.co.jp>

NETHERLANDS

Martinus Nijhoff International

Koraalrood 50, Postbus 1853, 2700 CZ Zoetermeer, NETHERLANDS
Telephone: +31 793 684 400 • Fax: +31 793 615 698
Email: info@nijhoff.nl • Web site: <http://www.nijhoff.nl>

Swets Information Services Ltd.

PO Box 26, 2300 AA Leiden
Dellaertweg 9b, 2316 WZ Leiden, NETHERLANDS
Telephone: +31 88 4679 387 • Fax: +31 88 4679 388
Email: tbeysens@nl.swets.com • Web site: <http://www.swets.com>

SLOVENIA

Cankarjeva Založba dd

Kopitarjeva 2, 1515 Ljubljana, SLOVENIA
Telephone: +386 1 432 31 44 • Fax: +386 1 230 14 35
Email: import.books@cankarjeva-z.si • Web site: http://www.mladinska.com/cankarjeva_zalozba

SPAIN

Diaz de Santos, S.A.

Librerias Bookshop • Departamento de pedidos
Calle Albasanz 2, esquina Hermanos Garcia Noblejas 21, 28037 Madrid, SPAIN
Telephone: +34 917 43 48 90 • Fax: +34 917 43 4023
Email: compras@diazdesantos.es • Web site: <http://www.diazdesantos.es>

UNITED KINGDOM

The Stationery Office Ltd. (TSO)

PO Box 29, Norwich, Norfolk, NR3 1PD, UNITED KINGDOM
Telephone: +44 870 600 5552
Email (orders): books.orders@tso.co.uk • (enquiries): book.enquiries@tso.co.uk • Web site: <http://www.tso.co.uk>

UNITED STATES OF AMERICA

Bernan Associates

4501 Forbes Blvd., Suite 200, Lanham, MD 20706-4391, USA
Telephone: +1 800 865 3457 • Fax: +1 800 865 3450
Email: orders@bernan.com • Web site: <http://www.bernan.com>

Renouf Publishing Co. Ltd.

812 Proctor Avenue, Ogdensburg, NY 13669, USA
Telephone: +1 888 551 7470 • Fax: +1 888 551 7471
Email: orders@renoufbooks.com • Web site: <http://www.renoufbooks.com>

United Nations

300 East 42nd Street, IN-919J, New York, NY 1001, USA
Telephone: +1 212 963 8302 • Fax: 1 212 963 3489
Email: publications@un.org • Web site: <http://www.unp.un.org>

Orders for both priced and unpriced publications may be addressed directly to:

IAEA Publishing Section, Marketing and Sales Unit, International Atomic Energy Agency
Vienna International Centre, PO Box 100, 1400 Vienna, Austria
Telephone: +43 1 2600 22529 or 22488 • Fax: +43 1 2600 29302
Email: sales.publications@iaea.org • Web site: <http://www.iaea.org/books>

International Atomic Energy Agency
Vienna
ISBN 978-92-0-102814-3
ISSN 1011-4289